NOAA Atlas NESDIS 1

WORLD OCEAN ATLAS 1994
VOLUME 1: NUTRIENTS

Washington, D.C.
March 1994

U.S. DEPARTMENT OF COMMERCE
National Oceanic and Atmospheric Administration
National Environmental Satellite, Data, and Information Service

NOAA Atlas NESDIS 1

WORLD OCEAN ATLAS 1994
VOLUME 1: NUTRIENTS

Margarita E. Conkright
Sydney Levitus
Timothy P. Boyer
National Oceanographic Data Center
Ocean Climate Laboratory

Washington, D.C.
March 1994

U.S. DEPARTMENT OF COMMERCE
Ronald H. Brown, Secretary

National Oceanic and Atmospheric Administration
D. James Baker, Under Secretary

National Environmental Satellite, Data, and Information Service
Robert S. Winokur, Assistant Administrator

National Oceanographic Data Center
User Services

This publication, as well as detailed information about NODC data holdings, products, and services, is available from the:

National Oceanographic Data Center
User Services Branch
NOAA/NESDIS E/OC21
1825 Connecticut Avenue, NW
Washington, DC 20235

Telephone: (202) 606-4549
Fax: (202) 606-4586
Omnet: NODC.WDCA
Internet: services@nodc.noaa.gov

Contents

List of Tables

List of Figures

APPENDIX C

APPENDIX D

APPENDIX E

APPENDIX F

APPENDIX G

APPENDIX H

APPENDIX I

APPENDIX J

APPENDIX K

APPENDIX L

APPENDIX M

Preface

This atlas continues and extends an earlier work entitled *Climatological Atlas of the World Ocean* (Levitus, 1982). This earlier work has proven to be of great utility to the international oceanographic, climate research and operational communities. In particular, the objectively analyzed fields of temperature and salinity have been used in a variety of ways. These include use as boundary and/or initial conditions in numerical ocean circulation models, for verification of numerical simulations of the ocean, as a form of "sea truth" for satellite measurements such as altimetric observations of sea surface height, and for planning oceanographic expeditions. We have expanded this earlier work to include chemical parameters such as phosphate, nitrate, and silicate because: 1) our belief that a comprehensive set of objectively analyzed parameter fields describing the state of the ocean, based on all existing oceanographic data, should be available as a matter of course to the international research community and 2) the immediate, compelling need for such analyses to study the role of biogeochemical cycles in determining how the earth's climate system works. For example, it is well known that the amount of carbon dioxide in the earth's atmosphere is expected to double during the next century. Regardless of one's scientific and/or political view of a possible "enhanced greenhouse warming" due to the increase of carbon dioxide, it is a necessity that the international scientific community have access to the most complete historical oceanographic data bases to study this problem, as well as other scientific and environmental problems.

The production of global analyses of oceanographic data is a major undertaking. Such work benefits from the input of many individuals and organizations. We have tried to structure the data sets and analyses that constitute this atlas in such a way as to encourage feedback from experts around the world who have knowledge that can improve future atlases. The production of works like this atlas series is becoming easier because of advances in computer hardware and software. These include: 1) the development of relatively inexpensive but powerful workstations that can be dedicated to data processing and analysis and 2) the development of high resolution printers and interactive graphics software that minimize the need for expensive, time consuming manual drafting and photographic processing. Because of the substantial increase in the historical oceanographic data bases expected over the next several years, the Ocean Climate Laboratory plans to update and expand this atlas series on a relatively frequent basis that is determined by the accession of significant amounts of new data. We plan to publish volumes that focus on derived quantities, higher resolution analyses, and additional parameters such as chlorophyll, primary production, and plankton taxa and biomass.

The objective analyses in this atlas, and data on which they are based, are being made available internationally without restriction on various magnetic media as well as CD-ROMs. This is to insure the widest possible distribution.

In each acknowledgement section of this atlas series we have expressed our view that undertaking such an atlas series as this is only possible through international cooperation of scientists, data managers, and scientific administrators throughout the international community. I would also like to thank my co-authors, colleagues, and staff from the Ocean Climate Laboratory of NODC for their dedication to the project leading to publication of this atlas series. Their integrity and thoroughness have made possible this multi-volume atlas series. Oceanography is a field of increasing specialization. It is my belief that the development of national and international oceanographic data archives is best performed by scientists who are actively working with the historical data. Margarita Conkright and Tim Boyer deserve particular thanks.

Sydney Levitus
Director, Ocean Climate Laboratory
National Oceanographic Data Center
Washington, D.C.
March, 1994

Acknowledgements

The establishment of a research group at the National Oceanographic Data Center to focus on the preparation of research quality oceanographic data sets and their objective analyses sets has been made possible by a grant from the NOAA Climate and Global Change Program. Substantial amounts of historical oceanographic data used in this study were located and digitized (Data Archaeology and Rescue projects) with funding from the NOAA Climate and Global Change Program, the NOAA Environmental Services Data and Information Management Program, the National Science Foundation, and the Office of Naval Research.

The work described in this atlas was made possible by scientists, technicians, ships' crew, data managers, and science administrators from the international scientific community. This atlas represents the results of several different research/data management projects of the NODC Ocean Climate Laboratory at the National Oceanographic Data Center (NODC), Washington, D.C. The products in this atlas are all based on the master oceanographic data archives maintained by NODC/WDC-A as well as data acquired as a result of the NODC Data Archaeology and Rescue (NODAR) project and the IODE/IOC Global Oceanographic Data Archaeology and Rescue (GODAR) project. These archives and data sets exist because scientists of the international scientific community have submitted their data to national and regional data centers. In turn, these centers have submitted data to the World Data Center system established under the International Council of Scientific Unions and the Intergovernmental Oceanographic Commission. This atlas and similar works would not exist without these international efforts. In particular we would like to thank data managers at these centers and the administrators and staff of these international organizations. The archiving of oceanographic data at international data centers means that the substantial expenditures in human and capital resources devoted to oceanographic measurement programs will be fully exploited, both for present and future scientific studies.

Although many data managers from the international community have been instrumental in the building of global oceanographic data bases, we would like to thank in particular Harry Dooley of the International Council for Exploration of the Sea, Osamu Yamada, Director of the Japanese Oceanographic Data Center, Yuri Sychev of the Russian National Oceanographic Data Center, Hou Wen-Feng of the Chinese National Oceanographic Data Center, Shin Tani formerly of the Japanese Oceanographic Data Center, and Ronald Wilson of the Marine Environmental Data Service, Canada.

Jeff Burney provided excellent system administration and programming support. Daphne Johnson provided invaluable assistance in unpacking numerous data sets used in this project and preparing figures. Robert Gelfeld was instrumental in the acquisition of numerous data sets as part of the NODAR and GODAR Projects. Grigory Isayev, Linda Stathoplos and Richard Abram helped with technical editing of the manuscript. Our colleagues at NODC/WDC-A provided support for various data management projects related to this atlas. Jennifer Campbell helped in preparing the manuscript for publication. The support of Gregory Withee and Bruce Douglas, former and present directors of NODC is appreciated. Management support by Dave Goodrich of the NOAA Office of Global Programs is appreciated.

We also would like to thank Eric Shulenberger, Lois Codispoti, Alan Longhurst, Arnold Mantyla, Glen Harrison and Peter Jones for reviewing the manuscript version of this atlas and providing comments that have led to substantial improvements in the text.

The data sets and products represented by this atlas are distributed internationally without restriction in accordance with U.S. Climate and Global Change as well as ICSU/IOC data management policies in support of Global Change Research.

WORLD OCEAN ATLAS, 1994: VOLUME 1, NUTRIENTS

Margarita E. Conkright, Sydney Levitus, and Timothy P. Boyer
National Oceanographic Data Center
Washington, D.C.

ABSTRACT

This atlas contains maps of phosphate, nitrate and silicate at selected standard levels of the world ocean on a one-degree grid. The fields used to generate these maps were computed by objective analyses of historical data. Maps for all-data annual compositing periods are presented. Data distribution maps are presented for various compositing periods. Basin zonal averages and basin volume averages are computed from these objectively analyzed fields and presented in the form of figures and tables.

1. INTRODUCTION

The format of this atlas, as well as some of the text, follow Levitus (1982). This atlas is an analysis of all historical phosphate, nitrate and silicate data available from the National Oceanographic Data Center (NODC), Washington, D.C. plus data gathered as a result of two data management projects: the NODC Oceanographic Data Archaeology and Rescue (NODAR) project and the Intergovernmental Oceanographic Commission (IOC) Global Oceanographic Data Archaeology and Rescue (GODAR) project. Data used here have been analyzed in a consistent, objective manner at standard oceanographic analysis levels on a one-degree latitude-longitude grid between the surface and ocean bottom or to a maximum depth of 3000m. The procedures used are similar, but not identical to, the analyses presented by Levitus (1982). Annual analyses have been computed for phosphate, nitrate, and silicate. The present analyses and statistical information are primarily intended for use in the study of the role of the world ocean as part of the earth's climate system.

Objective analyses shown in this atlas are limited by the nature of the data base (non-synoptic, scattered in space), characteristics of the objective analysis techniques, and the grid used. These limitations and characteristics will be discussed below.

Because of the lack of data, we are forced to examine the annual cycle by compositing all data regardless of the time or year of observation. In some areas quality control is made difficult by the limited number of data. Data may exist in an area for only one season, thus precluding any representative annual analysis. In some areas there may be a reasonable spatial distribution of data points on which to base an analysis, but there may be only a few, or perhaps only one datum in each one-degree square.

Other investigators have used the NODC nutrient archive for global studies. One example being the work of Kamykowski and Zentara (1985, 1989) who studied the patterns of distribution of nitrate and silicate in the world ocean.

2. DATA AND DATA DISTRIBUTION

Data sources and quality control procedures are described below. Because quality control procedures are so important, a technical report has been prepared fully describing these procedures (Conkright *et al.*, 1994).

2.1 Data sources

The Station Data used in this project were obtained from the National Oceanographic Data Center (NODC), Washington, D.C. and represent all the data available in the Oceanographic Station Data (SD) file as of the first

quarter of 1993 (NODC, 1993), plus data gathered as a result of the NODAR and GODAR projects (Levitus *et al.*, 1994a) that have not yet been archived in the NODC digital archives.

Figures 1-7 and Table 1 show the global distributions of nutrient measurements as a function of time at selected depths. Shown in these figures are the number of observed data points that occur in the depth range centered around each standard level. The depth range for the sea surface is 0-5 m. At all other standard levels, the depth range is defined as the region between the midpoints of the standard level being considered and the adjacent standard levels above and below. Appendices A, E and I show the geographic distribution of historical phosphate, nitrate and silicate observations as a function of depth.

One must understand our terms "standard level data" and "observed level data" to understand the various data distribution and summary figures and tables we present in this atlas. We refer to the actual measured value of an oceanographic parameter *in situ* as an "observation," and to the depth at which such a measurement was made as "observed level depth." We may refer to such data as "observed level data." Before the advent of oceanographic instrumentation that measure at high frequencies in the vertical, oceanographers often attempted to make measurements at selected "standard levels" in the water column. Sverdrup *et al.* (1942) presented the suggestions of the International Association of Physical Oceanography (IAPSO) as to which depths oceanographic measurements should be made or interpolated to for analysis. Different nations or institutions have "supersets" of standard level observation (e.g. NODC, 1993). For many purposes, including here, observed level data are interpolated to standard observation levels, if they do not occur exactly at a standard observation level. In contrast to Levitus (1982), we have used counts of "observed level values" wherever possible when summarizing the historical data used in this atlas. The distinction may seem minor, but in fact the criteria used to determine whether observed level data are suitable for use in interpolating to standard levels are not trivial. For example, one does not wish to use an observed level value at 5000 m depth to determine an interpolated standard level value at 20 m depth. Section 3.1 discusses this further.

2.2 Data quality control

Quality control of the data is a major task whose difficulty is directly related to the lack of data (in some areas) upon which to base statistical checks. Consequently certain empirical criteria were applied, and as part of the last processing step, subjective judgment was used. Individual data, and in some cases entire profiles or cruises, have been flagged because these data produced features that were judged to be non-representative or in error. As part of our work, we will make available both observed level profiles as well as standard level profiles with various quality control flags applied. Our knowledge of the variability of the world ocean now includes a greater appreciation and understanding of the ubiquity of eddies, rings, and lenses in some parts of the world ocean as well as interannual and interdecadal variability of water mass properties. Therefore, we have simply flagged data, not eliminated them. Thus individual investigators can make their own decision regarding the representativeness or correctness of the data. Investigators studying the distribution of features such as eddies will be interested in those data that we may regard as unrepresentative for our purpose here.

2.2a Duplicate elimination

Because data are received from many sources, all data files were checked for the presence of exact replicates. Approximately 20,000 Station Data profiles in the NODC Station Data File were found to be exact replicates of other profiles in this file. All but one profile from each set of replicate profiles were eliminated as the first step of our processing. All data sets used that were not part of the NODC Station Data file were checked for duplicates against the NODC Station Data file.

2.2b Range checking

Range checking was performed on all data as a first error check to eliminate the relatively few data that seemed to be grossly in error. Range checks were prepared for individual regions of the world ocean in contrast to Levitus' (1982) use of one range check for the entire world ocean for each parameter. Future work will include ranges for different basins by individual seasons. Conkright *et al.* (1994) detail the quality control procedures and include tables showing the ranges we selected for each basin.

2.2c Statistical checks

Statistical checks were performed to eliminate outliers as follows. All data for each parameter (irrespective of seasons), at each standard level, were averaged by

five-degree squares to produce a record of the number of observations, mean, and standard deviation in each square. Below 50 m depth, a three-standard-deviation criterion was used to flag data and eliminate individual observations from further use in our objective analyses. Above 50 m depth, a five-standard-deviation criterion was used in five-degree squares that contained any land area. In selected five-degrees squares that came close to land areas, a four-standard-deviation check was used. In all other squares a three-standard-deviation criterion was used with the following exceptions. For those data that occurred at or deeper than the standard level depth in the one-degree square in which the profile was observed, a four standard deviation criteria was used. For those data in a one-degree square that were measured at a depth deeper than the depth of any adjacent one-degree square, a four-standard-deviation check was used. The reason for the weaker criterion in coastal and near-coastal regions is the exceptionally large variability in the coastal five-degree square statistics for some parameters. Frequency distributions of some parameters in some coastal regions are observed to be skewed or bimodal. Thus to avoid eliminating possibly good data in highly variable environments, the standard deviation criteria were weakened.

The total number of nutrient measurements in each cast, as well as the total number of observations exceeding the criterion, were recorded. If more than two observations in a cast were found to exceed the standard deviation criterion, then the entire cast was eliminated. This check was imposed after tests indicated that surface data from particular casts (which upon inspection appeared to be erroneous) were being eliminated but deeper data were not. Other situations were found where erroneous data from the deeper portion of a cast were eliminated, while near-surface data from the same cast were not eliminated because of larger natural variability in surface layers. One reason for this was the decrease of number of observations with depth and the resulting change in sample statistics. The standard deviation check was applied twice to the data set.

In summary, first the five-degree square statistics were computed, and the elimination procedure described above was used to provide a preliminary data set. Next, new five-degree-square statistics were computed from this preliminary data set and used with the same statistical check to produce a new, "clean" data set. The reason for applying the statistical check twice was to eliminate, in the first round, any grossly erroneous or non-representative data from the data set that would artificially increase the variances. The second check then should be more effective in eliminating smaller, but probably still erroneous or non-representative observations.

2.2d Subjective elimination of data

The data were averaged by one-degree squares for input to the objective analysis program. After initial objective analyses were computed, the input set of one-degree means still contained suspicious data contributing to unrealistic distributions, yielding intense bull's-eyes or gradients. Examination of these features indicated that some of them were due to particular oceanographic cruises. In such cases data from an entire cruise were eliminated from further use by setting a flag on each profile from that cruise.

2.2e Representativeness of the data

Another quality control issue is data representativeness. The general paucity of data forces us to composite all historical data to produce "climatological" fields. In a given one-degree square, there may be data from a month or season of one particular year, while in the same or a nearby square there may be data from an entirely different year. If there is large seasonal or interannual variability in a region where scattered sampling in time has occurred, then one can expect the analysis to reflect this. Because the observations are scattered non-randomly with respect to time, except for a few limited areas, the results cannot, in a strict sense, be considered a true long-term climatological average.

We present smoothed analyses of historical means, based (in certain areas) on relatively few observations. We believe, however, that useful information about the oceans can be gained through our procedures and that the large-scale features are representative of the real ocean. We believe that, if a hypothetical global synoptic set of ocean data (temperature, salinity, oxygen or nutrients) existed, and one were to smooth this data to the same degree as we have smoothed the historical means overall, the large-scale features would be similar to our results. Some differences would certainly occur because of interannual to decadal-scale variability. As more data are added to the historical archives, we will be able to evaluate this variability on basin and gyre scales following the studies of Levitus (1989a,b,c; 1990) and Levitus *et al.* (1994b).

To clarify discussions of the amount of available data, quality control techniques, and representativeness of the data, the reader should examine in detail the maps showing

the distribution of data (Appendices A, E and I). These maps are provided to give the reader a quick, simple way of examining the historical data distributions. Basically, the data diminish in number with increasing depth and latitude. In the upper ocean, the all-data annual mean distributions are quite good for defining large-scale features, but for the seasonal periods, the data base is inadequate. Figs. 1, 3 and 5 show the possible bias in using an all-season database to examine properties which have a strong seasonal signal, particularly in the upper 200 m of the water column. For example, most expeditions to high latitudes are in the summer season, so a bias towards low nutrient values (due to uptake by phytoplankton) is expected when compositing these data. With respect to the deep ocean, in some areas the distribution of observations may be adequate for some diagnostic computations but inadequate for other purposes. Obviously if an isolated deep basin or some region of the deep ocean has only one observation, then no horizontal gradient computations are meaningful. However, useful information is provided by the observation in the computation of other quantities (e.g., a volumetric mean over a major ocean basin).

3. DATA PROCESSING PROCEDURES

3.1 Vertical interpolation to standard levels

Vertical interpolation of observed level data to standard levels followed procedures in UNESCO (1991). These procedures are in part based on the work of Reiniger and Ross (1968). Four observed level values surrounding the standard level values were used, two values from above the standard level and two values below the standard level. Paired parabolas were generated via Lagrangian interpolation. A reference curve was fitted to the four data points and used to define unacceptable interpolations caused by "overshooting" in the interpolation. When a spurious extremum could not be eliminated using this technique, linear interpolation was used. When there were too few data points above or below the standard level exists to apply the Reiniger and Ross technique, we used a three-point Lagrangian interpolation. If three points were not available (either two above and one below or vice-versa), we used linear interpolation. In the event that an observation occurred exactly at the depth of a standard level, then a direct substitution is made. Table 2 provides the range of acceptable distances for which observed level data can be used for interpolation to a standard level. The criteria were a function of depth. The criteria for the "outside" points are the same used by NODC in their three-point Lagrangian interpolation and by Levitus (1982). The criteria for the "inner" points was much more restrictive and results in fewer standard level data values compared to the NODC and Levitus (1982) criteria. Future criteria might depend on the geographic location of the profile as well as the time of year.

The data summaries in Table 1 and all other such counts represent the observed level data. These are counts of observed level data that occur within a depth interval around each standard level. This differs from the statistics presented by Levitus (1982) who presented counts of the interpolated standard level data.

3.2 Methods of analysis

3.2a Overview

An objective analysis scheme of the type described by Barnes (1973) was used to produce the fields shown in this atlas. This scheme had its origins in the work of Cressman (1959) and Barnes (1964). The Barnes (1973) scheme requires only one "correction" to the first-guess field at each grid point in comparison to the successive correction method of Cressman (1959) and Barnes (1964). For completeness we derive the weight function and response function for the procedures per Barnes (1964) and then per Barnes (1973).

Inputs to the analysis scheme were observed one-degree square means of data at standard levels (for whatever period and parameter analyzed) and a first-guess value for each square. For instance, one-degree square means for our annual analysis were computed using all available data regardless of date of observation.

Analysis was the same for all standard depth levels. Each one-degree square value was defined as being representative of its square. The 360x180 gridpoints are located at the intersection of half-degree lines of latitude and longitude. An influence radius was then specified. At those grid points where there was an observed mean value, the difference between the mean and the first-guess field was computed. Next, a correction to the first-guess value at all gridpoints was computed as a distance-weighted mean of all gridpoint difference values that lie within the area around the gridpoint defined by the influence radius. Mathematically, the correction factor derived by Barnes

(1964) is given by the expression

$$C_{i,j} = \frac{\sum_{s=1}^{n} W_s Q_s}{\sum_{s=1}^{n} W_s} \qquad (1)$$

in which

$C_{i,j}$ = **the correction factor at gridpoint coordinates (i,j)**

$(i_s j)$ = **coordinates of a gridpoint in the east-west and north-south directions, respectively**

n = **the number of observations that fall within the area around the point i,j defined by the influence radius**

Q_s = **the difference between the observed mean and the first guess at the ^{Sth} point in the influence area**

W_s = $\exp(-E\, r^2 R^{-2})$ **for** $r < R$

W_s = **0 for** $r > R$

r = **distance of the observation from the gridpoint**

R = **influence radius**

E = **4**

The derivation of the weight function, W_s, will be presented in the following section. At each gridpoint we computed an analyzed value $G_{i,j}$ as the sum of the first guess, $F_{i,j}$ and the correction $C_{i,j}$. The expression for this is

$$G_{i,j} = F_{i,j} + C_{i,j} \qquad (2)$$

If there were no data points within the area defined by the influence radius, then the correction was zero, the first-guess field was left unchanged, and the analyzed value was simply the first-guess value. This correction procedure was applied at all gridpoints to produce an analyzed field. The resulting field was first smoothed with a median filter (Tukey, 1974; Rabiner *et al.*, 1975) and then smoothed with a five-point smoother of the type described by Shuman (1957).

The analysis scheme is based on the work of several researchers analyzing meteorological data. Bergthorsson and Doos (1955) computed corrections to a first-guess field using various techniques: one assumed that the difference between a first-guess value and an analyzed value at a gridpoint was the same as the difference between an observation and a first-guess value at a nearby observing station. All the observed differences in an area surrounding the gridpoint were then averaged and added to the gridpoint first guess value to produce an analyzed value. Cressman (1959) applied a distance-related weight function to each observation used in the correction in order to give more weight to observations that occur closest to the gridpoint. In addition, Cressman introduced the method of performing several iterations of the analysis scheme using the analysis produced in each iteration as the first-guess field for the next iteration. He also suggested starting the analysis with a relatively large influence radius and decreasing it with successive iterations so as to analyze smaller scale phenomena with each pass.

Sasaki (1960) introduced a weight function that was specifically related to the density of observations, and Barnes (1964, 1973) extended the work of Sasaki. The weight function of Barnes (1973) has been used here. The derivation of the weight function we used which we present for completeness, follows the work of Barnes (1973).

The objective analysis scheme we used is in common use by the mesoscale meteorological community. Several studies of objective analysis techniques have been made. Achtemeier (1987) examined the "concept of varying influence radii for a successive corrections objective analysis scheme." Seaman (1983) compared the "objective analysis accuracies of statistical interpolation and successive correction schemes." Smith and Leslie (1984) performed an "error determination of a successive correction type objective analysis scheme." Smith *et al.* (1986) made "a comparison of errors in objectively analyzed fields for uniform and non-uniform station distribution."

3.2b Derivation of Barnes' (1964) weight function

The principle upon which Barnes' (1964) weight function is derived is that "the two-dimensional distribution of an atmospheric variable can be represented by the summation of an infinite number of independent harmonic waves, that is, by a Fourier integral representation." If f(x,y) is the variable, then in polar coordinates (r,θ), a smoothed or

filtered function g(x,y) can be defined:

$$g(x,y) = \frac{1}{2\pi}\int_0^{2\pi}\int_0^{\infty}\eta f(x+r\cos\theta, y+r\sin\theta)\, d\left(\frac{r^2}{4K}\right)d\theta \qquad (3)$$

in which r is the radial distance from a gridpoint whose coordinates are (x,y). The weight function is defined as

$$\eta = \exp(-r^2/4K) \qquad (4)$$

which resembles the Gaussian distribution. The shape of the weight function is determined by the value of K, which depends on the distribution of data. The determination of K follows.

The weight function has the property that

$$\frac{1}{2\pi}\int_0^{2\pi}\int_0^{\infty}\eta\, d\left(\frac{r^2}{4K}\right)d\theta = 1. \qquad (5)$$

This property is desirable because in the continuous case (3) the application of the weight function to the distribution f(x,y) will not change the mean of the distribution. However, in the discrete case (1), we only sum the contributions to within the distance R. This introduces an error in the evaluation of the filtered function, because the condition given by (5) does not apply. The error can be pre-determined and set to a reasonably small value in the following manner. If one carries out the integration in (5) with respect to θ, the remaining integral can be rewritten as

$$\int_0^{R}\eta\, d\left(\frac{r^2}{4K}\right) + \int_R^{\infty}\eta\, d\left(\frac{r^2}{4K}\right) = 1. \qquad (6)$$

Defining the second integral as ε yields

$$\int_0^{R}\exp\left(-\frac{r^2}{4K}\right)d\left(\frac{r^2}{4K}\right) = 1 - \epsilon. \qquad (7)$$

in which

$$\epsilon = \exp(-R^2/4K) \ .$$

Levitus (1982) chose ε = 0.02, which implies with respect to (6) the representation of 98 percent of the influence of any data around the gridpoint in the area defined by the influence radius, R. In terms of the weight function used in the evaluation of (1) this choice leads to a value of E=4 since

$$E = R^2/4K = -\ln \epsilon \ .$$

The choice of ε and the specification of R determine the shape of the weight function.

Barnes (1964) proposed using this scheme in an iterative fashion similar to Cressman (1959). Levitus (1982) used a four iteration scheme with a variable influence radius for each pass.

3.2c Derivation of Barnes' (1964) response function

It is desirable to know the response of a data set to the interpolation procedure applied to it. Following Barnes (1964) we let

$$f(x) = A \sin(ax) \qquad (8)$$

in which $a = 2\pi/\lambda$ with λ being the wavelength of a particular Fourier component, and substitute this function into equation (3) along with the expression for η in equation (4). Then

$$g(x) = D\,(A \sin(ax)) = D\, f(x) \qquad (9)$$

in which

$$D = \exp(-\pi^2R^2/4\lambda^2)$$

D is the response function for one application of the analysis. The phase of each Fourier component is not changed by the interpolation procedure. The results of an analysis pass are used as the first guess for the next analysis pass in an iterative fashion. The response

function after N iterations as derived by Barnes (1964) is

$$g_N(x) = f(x)D \sum (1-D)^{N-1} \qquad (10)$$

Equation (10) differs trivially from that given by Barnes. The difference is due to the fact that our first-guess field was defined as a zonal average, annual mean, or seasonal mean, whereas Barnes used the first application of the analysis as a first guess. Barnes (1964) also showed that applying the analysis scheme in an iterative fashion will result in convergence of the analyzed field to the observed data field. However, it is not desirable to approach the observed data too closely, because at least seven or eight gridpoints are needed to represent a Fourier component.

The response function given in (10) is useful in two ways: it is informative to know what Fourier components make up the analyses, and the computer programs used in generating the analyses can be checked for correctness by comparison with (10).

3.2d Derivation of Barnes' (1973) weight function

Barnes (1973) showed how a nearly equivalent analysis (with respect to the response function) could be performed with just one iteration, assuming a first-guess field is provided. We use this one-pass scheme in our present analysis. Derivation of the weight function for this scheme is provided (below) after the derivation of the response function in the following section. Following Barnes (1973), equation (9) can be rewritten as

$$g_0(x,y) = D_0 f(x,y) \qquad (11)$$

The subscript nought denotes the first pass through the data with weight function

$$\eta_0 = \exp(-r^2/4K_0) \qquad (12)$$

Using the results of the initial analysis as a first guess for the second iteration through the data, we add the residual field of the second pass analysis pass to the first guess provided by the first iteration. We write this as

$$g_1(x,y) = g_0(x,y) + [f(x,y) - g_0(x,y)] D_1 \qquad (13)$$

where D_1 is the response resulting from application of the weight function

$$\eta_1 = \exp(-r^2/4k_1); \quad k_1 = \gamma k_0 \text{ and } \gamma > 0 \qquad (14)$$

$$D_1 = \exp(-a^2k_1) = \exp(-a^2k_0) = D_0^{\gamma} \qquad (15)$$

Substituting (15) and (11) into (13) yields

$$g_1(x,y) = f(x,y)D_0 (1 + D_0^{\gamma-1} - D_0^{\gamma}) \qquad (16)$$

The new response function is

$$D' = D_0 (1 + D_0^{\gamma-1} - D_0^{\gamma}) \qquad (17)$$

The value $k_1 = \gamma k_0$ is chosen to produce a desired response function. In our analyses a value of $k_1 = 0.8$ was used. This choice leads to the response function given in Table 3.

There are several advantages of a one-pass interpolation analysis. The saving of computer time is an obvious advantage. A more important advantage is that statistical analysis of the analyzed fields becomes much simpler.

3.2e Choice of response function

The distribution of observations (Appendices A, E, I) at different depths, are not regularly distributed in space or by season. At one extreme, regions exist in which every one-degree square contains data and no interpolation needs to be performed. At the other extreme are regions in which few data exist. Thus with variable data spacing the average separation distance between gridpoints containing data is a function of geographical position and averaging period. However, if we computed and used a different average separation distance for each parameter at each depth and each averaging period, we would be generating analyses in which the wavelengths of observed phenomena might differ from one depth level to another and from one season to another. We chose instead to use a fixed influence radius of 555 km which allows us to analyze each parameter at every depth and season in exactly the same way.

Inspection of (1) shows that the difference between the

analyzed field and the first-guess at any gridpoint is proportional to the sum of the weighted differences between the observed mean and first guess at all gridpoints containing data within the influence area.

The reason for using the five-point smoother and the median smoother is that our data are not evenly distributed in space. As the analysis moves from regions containing data to regions devoid of data, small-scale discontinuities may develop. The five-point and median smoothers are used to eliminate these discontinuities. The five-point smoother does not affect the phase of the waves in the data.

At gridpoints where no observed data points fall within the influence area, one could expand the influence radius until some minimum number of data points were found. We did not use this procedure, because it implies an analysis with different maximum length scales in different regions, and we wish to minimize differences.

The response function for the analyses presented in this atlas is given in Table 3. The response function represents the smoothing inherent in the objective analysis described above plus the effects of one smoothing of the five-point smoother and one application of a five-point median smoother.

3.2f First-guess field determination

There are gaps in the data coverage and, in some parts of the world ocean, there exist adjacent basins whose water mass properties are individually nearly homogeneous but have distinct basin-to basin differences. Spurious features can be created when an influence area extends over two basins of this nature. Our choice of first-guess field attempts to minimize the creation of these features.

To provide a first-guess field for the annual analysis at any standard level, we first zonally averaged the observed data in each one-degree latitude belt by individual ocean basins. In the work of Levitus (1982), the Mediterranean and Red Seas were treated as individual basins and the Venezuela Basin and the Sulu Sea were treated as individual basins below their sill depths. The Norwegian Sea and Arctic Ocean were treated separately below the sill depth of the Greenland-Iceland-Shetland ridge. In the present work, additional basins have also been defined.

To avoid the problem of the influence region extending across land or sills to adjacent basins, the objective analysis program uses basin "identifiers" to avoid the use of data from adjacent basins. Table 4 lists these basins and the depth at which no exchange of information between basins is allowed during the objective analysis of data, i.e., "depths of mutual exclusion." Some regions are nearly, but not completely, isolated topographically. Because some of these nearly isolated basins have water mass properties that are different from surrounding basins, we have chosen to treat these as isolated basins as well. Not all such basins have been identified because of the complicated structure of the sea floor.

The zonal average computed at every one-degree belt in every individual ocean basin was used as the first guess for all one-degree squares in the belt. The reason for computing a separate first guess in each individual basin can be explained with the aid of equations (l) and (2). We have at any grid point (i,j) an analyzed value as defined by

$$G_{i,j} = F_{i,j} + \frac{\sum_{s=1}^{n} (W_s Q_s)}{\sum_{s=1}^{n} (W_s)} \qquad (18)$$

For simplicity, we discuss the case in which only one observed data point falls within the influence area. The coordinates of this point will be denoted by i',j' on our grid. If we let $OB_{i,j}$ denote the observed one-degree square mean at this point, then (18) becomes

$$G_{i,j} = F_{i,j} + (OB_{i',j'} - FG_{i',j'}) \qquad (19)$$

Thus, for this case the difference between the analyzed point and the first-guess at point (i,j) is assumed to equal the first-guess at the point (i',j'). If the observed mean at a gridpoint is equal to the first-guess at that gridpoint, then the correction is obviously zero, and this gridpoint will affect no other gridpoint. For situations where we have adjacent basins with individually nearly homogeneous properties (those not identified in Table 4), then defining a separate first-guess field for each basin means that the observed means in each basin are closer to their first-guess field than if this separation of basins had not been performed. Thus when the influence area extends across basins the corrections are relatively small.

One advantage of producing "global" fields for a particular compositing period (even though some regions are data void) is that such analyses can be modified by investigators for use in modelling studies. For example, England (1992) noted that the salinity distribution

produced by Levitus (1982) for the Antarctic is too low (due to a lack of winter data for the Southern Hemisphere) to allow for the formation of Antarctic Intermediate Water in an ocean general circulation model. By increasing the salinity of the "observed" field the model was able to produce this water mass.

3.3 Comments on the choice of objective analysis procedures

Optimum interpolation (Gandin, 1963) has been used by some investigators to objectively analyze oceanographic data. We recognize the power of this technique but have chosen not to use it to produce analyzed fields. As described by Gandin (1963), optimum interpolation is used to analyze synoptic data using statistics based on historical data. In particular, second-order statistics such as correlation functions are used to estimate the distribution of first order parameters such as means. We attempt to map most fields in this atlas based on relatively sparse data sets. By necessity we must composite all data regardless of the year of observation, to have enough data to produce a global hemispheric, or regional analysis for a particular month, season, or even yearly. Because of the paucity of data, we prefer not to use an analysis scheme that is based on second order statistics. In addition, as Gandin has also noted, there are two limiting cases associated with optimum interpolation. The first is when a data distribution is dense. In this case the choice of interpolation scheme makes little difference. The second case is when data are sparse. In this case an analyses scheme based on second order statistics is of questionable value.

For additional information on objective analysis, see Thiebaux and Pedder (1987) and Daley (1991).

3.4 Choice of spatial grid

We use the one-degree grid of Levitus (1982) which is based on the ocean topography defined by Smith *et al.,* (1966) as our spatial grid. We desire to build a set of climatological analyses that are identical in all respects for all parameters including relatively data sparse parameters such as nutrients. This provides investigators with a consistent set of analyses to work with. As more data are received at NODC/WDC-A, we will be able to produce higher resolution climatologies for certain parameters.

4. RESULTS

4.1 Annual mean nutrient parameters at standard levels

4.1a Explanation of standard level figures

All figures showing standard level analyses in this atlas series use similar symbols for displaying information. Continents are indicated as solid - black areas. Ocean areas shallower than the standard depth level being displayed are gray. Negative regions are dot stippled. Gridpoints for which there were less than three one-degree-square values available to "correct" the first-guess are indicated by an X. Dashed lines represent non-standard contours. "H" and "L" indicate locations of the absolute maximum and minimum of the entire field. All figures were computer drafted. As a result some contours are not labelled. For clarity we use dark lines for every fourth or fifth contour in the standard level fields.

4.1b Standard level analyses

We discuss major features in the distribution of phosphate, nitrate and silicate. A more thorough description of the annual mean distribution of nutrients is given by Levitus *et al.* (1993). Data used in Levitus *et al.* (1993) was compiled by J. Reid and A. Mantyla (Scripps Institution of Oceanography) based on a subset of the NODC Station Data file and additional data. The data have been used in several papers addressing circulation and nutrient distributions (Mantyla and Reid, 1983; Reid, 1981). Kamykoski and Zentara (1985, 1989) describe results obtained using NODC archived nutrient data.

Global distributions of annual mean phosphate, nitrate and silicate at standard analysis levels are presented in Appendices B, F, and J respectively. Levitus *et al.* (1993) and the figures in this atlas show similar major oceanographic features. Generally, surface waters have high nutrient content in colder latitudes and depletion in lower latitudes (except the upwelling areas along the western coasts of Africa and Peru).

The highest near surface concentrations for all three nutrients are found in Antarctic waters. The highest nitrate and silicate content are found in the Southern Ocean (0-100 m for nitrate, 0-500 m for silicate). High nutrient concentrations in the Antarctic are due to upwelling and upward mixing of deeper water (Olson, 1980) combined

with insufficient diatom growth to deplete available nutrients (Nelson and Gordon, 1982). Upwelling occurs primarily at the center of the divergent cyclonic gyres in the Weddell and Ross Seas (Gordon, 1971).

Appendices B, F, and J show that the subarctic Pacific also has high nutrient concentrations. The Bering Sea has high phosphate concentrations and high nitrate concentrations are found off the coasts of Kamchatka and Alaska. The subarctic Atlantic and (generally) the surface waters of the Atlantic have a lower nutrient content than the Pacific. Below 600 m the highest silicate concentrations are in the subarctic Pacific between Kamchatka and the Alaskan coast. The northeastern Pacific basin has a cyclonic gyre in the Gulf of Alaska (Uda, 1963), a region of divergence of surface waters and therefore characteristically high in nutrients due to entrainment of deep water, especially in the center of the gyre (Anderson *et al.*, 1969; Reid, 1962). High nutrient concentrations in these areas indicates incomplete biological utilization of available nutrients. Wheeler and Kokkinakis (1990) analyzed nitrate distribution in the subarctic Pacific and proposed two mechanisms that would maintain high concentrations: high grazing pressure (reduces phytoplankton standing stock) and rapid ammonia recycling. Other factors which could explain high nitrate concentrations are primary production limitation by low concentrations of available iron (Martin and Gordon, 1988; Martin *et al.*, 1989), nitrification, and a slow rate of nitrate removal by phytoplankton (Dugdale *et al.*, 1992).

Upwelling occurs along the equatorial African coast and depletion or near depletion of nutrients there is the result of high primary productivity (Friederich and Codispoti, 1979; Codispoti, 1983). In the Pacific, incomplete utilization of nutrients in surface equatorial waters could be due to failure of phytoplankton to adapt to high light and high nutrients (Dugdale *et al.*, 1992; Wilkerson and Dugdale, 1992) and/or control by grazing (Cullen *et al.*, 1992; Minas *et al.*, 1986; Walsh, 1977).

Subtropical gyres contain very low nutrient content in surface waters and are the least productive waters in the world (Blackburn, 1981). The source of nutrients to these gyres is either vertical eddy diffusion or horizontal advection from surrounding waters (Eppley *et al.*, 1979; Reid *et al.*, 1978). The North Indian Ocean gyre is much more complex and different in many respects to those in the Atlantic and Pacific Oceans and therefore does not have the nutrient depletion observed in the Southern Indian Ocean subtropical gyre. Rather, high nutrients concentrations are observed in the Bay of Bengal and the Arabian Sea as a result of monsoon driven circulation (Reid *et al.*, 1978). The South Indian Ocean subtropical gyre has low nutrient concentrations. The vertical extent of nutrient depletion within that gyre varies for the three nutrients.

High nutrient concentrations are found in the deep North Pacific because of deep circulation patterns. Nutrients in Pacific deep waters come partly from North Atlantic deep waters and Antarctic abyssal waters (Mantyla and Reid, 1983; Reid and Lynn, 1971; Broecker and Li, 1970). Those waters are also older and so have accumulated more remineralized plant material (ie. Broecker and Peng, 1982).

4.2 Basin zonal averages

Basin (per Fig. 8 and Levitus 1982) zonal averages were computed: Appendices C, G, and K show basin zonal averages of phosphate, nitrate and silicate respectively, 0-500 m (upper panel) and 0-3000 m (bottom panel).

4.2a Annual global zonal means for phosphate, nitrate, and silicate

Global nutrient distributions (Figs. C1, G1, and K1) show major features in common: mid-latitudes have two tongues of low nutrient waters separated by a broad (15°S-15°N) maximum centered about the equator, with a relative minimum at the equator. The subtropical low nutrient tongues extend to about 1000 m for phosphate and nitrate, and deeper for silicate. A phosphate and nitrate maximum is found between 500-1000 m in the equatorial region; this maximum is not evident for silicate. Silicate increases with depth throughout this region. Relatively high values for all nutrients are found in the Antarctic region. The front-like feature centered near 60°N represent low nutrient Atlantic waters next to high nutrient Pacific waters. There is considerable similarity between phosphate and nitrate distributions, which can be attributed to control by physical processes such as circulation, advection, upwelling and downwelling and to gross similarities in biogeochemical cycling, particularly in oxygenated waters. The differences can be ascribed mainly to those differences in their chemical pathways within the water column and sediments.

4.2b Nutrient zonal means in the Pacific Ocean

Pacific Ocean zonal averages of phosphate, nitrate and silicate in the Pacific Ocean are presented in Figs. C2, G2 and K2. Between the Antarctic Divergence and the

Antarctic Convergence (approx. 70°S-60°S), phosphate and nitrate content remains fairly uniform, but silicate decreases sharply. Uniform nitrate distributions could be a result of preferential use of ammonia by primary producers (Olson, 1980) and upward mixing of nitrate (Holm-Hansen, 1985). Upward mixing could also account for the phosphate uniformity. The decrease in silicate is probably due to removal of silicate by diatoms and silicoflagellates sinking out of the euphotic zone (Holm-Hansen, 1985).

North of 60°S, waters below 200 m are dominated by Antarctic Intermediate Water (AAIW) north of 60°S. These waters form a downward trending tongue (starting at 200 m) and move northward into the Pacific Ocean along potential density surfaces (Reid, 1965). These are relatively nutrient-poor and oxygen-rich waters (Levitus and Boyer, 1994), suggesting little remineralization of nutrients, since the oxidation of plant material consumes oxygen (Redfield *et al.*, 1963). Holm-Hansen *et al.* (1977) have suggested that in-situ remineralization of nutrients is not essential to primary production in these waters, since upwelling of deep water provides a continuous supply of nutrients.

Equatorial Pacific zonal mean is dominated by divergence of surface waters at or near the equator where nutrient-rich waters from below keeps the surface layer thin (Armstrong, 1965) with a very steep underlying vertical gradient. Phosphate and nitrate concentrations increase sharply with depth below equatorial surface waters, whereas silicate does not increase until about 100 m.

The downward tongues at mid-latitudes (Figs. C2 and G2 for phosphate and nitrate) represent the subtropical gyres, which characteristically have low nutrient concentrations at depth (due to downwelling of nutrient-poor surface waters (Reid, 1962)). There are several differences in nutrient distribution between the subtropical South and North Pacific. The low phosphate and nitrate tongue in the South Pacific (50°S to 20°S) extends downward to about 1000 m, compared to the North Pacific mid-latitude tongue which only extends to about 800 m. Waters between 40°N and 60°N have high nutrient content and sharp vertical changes of all three nutrients in the upper 200 m. The most pronounced changes with depth occur in silicate. Phosphate and nitrate content within the gyres changes more markedly with depth in the North Pacific than in the South Pacific due to intrusion of North Pacific Intermediate Water (NPIW). A mid-depth maximum is associated with NPIW, and has a broad tongue of high phosphate and nitrate values from 300 m in the subarctic to below 1000 m at the equator.

Pacific deeper waters show a gradual decrease in phosphate and nitrate from north to south. Silicate differs from nitrate and phosphate in that there is a sharp increase in the silicate concentration below 1000 m. The highest Pacific silicate concentrations are between 1000 and 4000 m. Regeneration of phosphate and nitrate occurs mainly in the upper 1000 m, but silicate dissolution continues below 1000 m. Increasing silicate concentration with depth clearly suggest the continual dissolution of diatom tests below the depth at which regeneration of nitrate and phosphate occurs; this silicate could also come from upward advection of deeper, high silicate water.

4.2c Nutrient zonal means in the Atlantic Ocean

Atlantic phosphate, nitrate and silicate zonal averages are shown in Figs. C3, G3 and I3. Phosphate and nitrate remain fairly constant in the upper waters of the Southern Ocean. Silicate shows a near continuous increase with depth south of about 55°S, similar to Nelson and Gordon (1982). High surface silicate is presumed to result from remineralization of diatoms (Nelson and Gordon, 1982; Edmond *et al.*, 1979) and/or upward mixing of deep waters. About 18-58% of silicate redissolves in the upper 100 m (Nelson and Gordon, 1982).

Mid-latitudes and subtropics have two tongues of increasing nutrient content with depth, associated with the North and South Atlantic anticyclonic gyres (Tchernia, 1980). The South Atlantic gyre extends deeper (about 1000 m) than the North Atlantic gyre (about 700 m), as reflected in the nutrient content of these waters. These areas of convergence are shallower in the Atlantic than in the Pacific. South Atlantic subtropical waters have a higher nutrient content than the North Atlantic. Nutrient concentrations in the southern high latitudes are almost twice those in the North Atlantic.

Highest Atlantic phosphate and nitrate concentrations are found in an intermediate layer at the equator, between 400-1000 m. Below 1000 m, there is a gradual increase in nutrient concentration from north to south. Nutrient distributions in Atlantic intermediate and deeper waters can be traced to different water masses and to the difference in chemical pathway of the nutrients. Antarctic Intermediate Water (AAIW) extends to about 15°N between 1000 and 1500 m. A layer of minimum phosphate, nitrate and silicate concentrations extends southward beneath the AAIW: this is North Atlantic Deep Water (NADW) which can be traced (at 1500-4000 m) as a southerly tongue. Nutrient depletion of these waters reflects the near surface origin of deep and bottom waters

in the North Atlantic (Mantyla and Reid, 1983).

Antarctic Bottom Water (AABW) extends northward along the Atlantic bottom to near the equator. This water mass is only distinct based on silicate concentrations which decreases from south to north as water is trapped in the basins and mixes with overlying lower silica content water.

4.2d Nutrient zonal means in the Indian Ocean

Indian Ocean zonal averages (Figs. C4, G4, K4) closely resemble those of the South Pacific. Indian Ocean surface waters show depletion or near depletion of nutrients in the tropical and subtropical waters, and enrichment of nutrients in the southern high latitudes and the North Indian Ocean.

The downward tongue centered around 30°S is associated with the subtropical gyre and is seen down to about 1000 m for phosphate and nitrate and almost to the bottom for silicate. Equatorial Indian surface waters also show nutrient depletion. Depletion of nutrients extends deeper for nitrate and silicate than for phosphate.

North Indian subsurface waters have high phosphate and nitrate. This is an area of low oxygen (Levitus and Boyer, 1994c), consistent with consumption of oxygen during nutrient regeneration. Below 1000 m, there are pockets of low nitrate associated with low oxygen content. Indian Ocean waters show areas of denitrification, which leads to the formation of nitrite and nitrogenous gas in low oxygen waters (Naqui *et al.*, 1982). This could cause the local nitrate minimum.

The nutrient content in the South Indian Ocean below 1000 m is fairly uniform except for a nitrate minimum below 2000 m (centered around 30°S). Indian Ocean deep waters derive partly from North Atlantic and Antarctic waters (Reid and Lynn, 1972; Broecker and Li, 1970). Nutrient content of deep waters is characteristic of the Circumpolar Deep Water which moves northward into the Indian Ocean. Similar to the Pacific Ocean, there is enrichment of nutrients from south to north as high nutrient southern waters move north and up. In addition, the Bay of Bengal sediment fan serves as a major nutrient source North Indian Ocean bottom waters (Broecker *et al.*, 1980).

4.3 Basin mean profiles and volume means

Area-weighted basin means of nutrient parameters have been computed for the world ocean, for each major ocean basin and for the northern and southern hemisphere portions of these basins and are presented as a function of depth in Appendices D, H, and L. These means and associated standard errors are also presented in tabular form in the same appendices. The area and volume of each standard level over which the means are computed are given in Appendix M. The percentage contribution that each standard level contributes to the volume of each basin is given, as well as the number of independent points used in the standard error computation. Basin volume-weighted means and the total volume in each basin are also presented in Appendix M. Of course one can construct and display the basin-wide averages in a number of ways to serve various purposes. The tabulations allow users to graph the information and perform computations in any desired format.

The formula for defining an area weighted mean of some parameter X over the N ocean one-degree squares in a particular region or basin is

$$\overline{X_N} = \frac{\Sigma_{n=1}^{N} X_n A_n}{\Sigma_{n=1}^{N} A_n} \qquad (20)$$

in which X_n represents the value of the parameter at the n^{th} one-degree square of the region, and A_n represents the area of the n^{th} one-degree square in the region. The computation of volume means uses formula (20) with the volume V_n replacing the area element A_n. The volume of a one-degree square box at any particular standard level is defined as follows. Excluding the sea surface and deepest standard level occurring at any one-degree square water column, the depth range Δz_k, through which a volume is computed for any standard level (denoted by k), is given as

$$\Delta z_k = 0.5\ [z_{k+1} - z_{k-1}] \qquad (21)$$

in which z_{k+1} is the depth of the first standard level deeper than standard level k, and z_{k-1} is the depth of the first standard level shallower than standard level k. The volume of the sea surface standard level is taken over the 0-5 m depth interval. The depth range through which a volume is computed for the deepest standard level is given as

$$\Delta z_k = 0.5\ [z_k - z_{k-1}]\ . \qquad (22)$$

The standard error (S.E.) of each basin mean is computed as follows. The area-weighted root-mean-square deviation of all gridpoint values is computed (denoted as σ). The total area of the standard level within the basin is computed and divided by the area defined by the influence radius of the objective analysis. This area is given as πR^2 in which R=555 km. The quotient yields a value, N_I, which is used as the number of independent points in estimating the standard error as

$$\text{S.E.} = \sigma/(N_I)^{1/2} \quad . \qquad (23)$$

Appendices D, H and L illustrate the basin mean profiles for the Globe, Pacific, Atlantic and Indian Oceans. Several features standout: (a) The Pacific Ocean is enriched in all three nutrients relative to the Indian and Atlantic Oceans; (b) the Atlantic Ocean is lowest in nutrients; (c) surface layers show a depletion of all three nutrients, followed by an increase with depth until maxima are reached (the exception is silicate, which shows a near continuous increase with depth). The depth of maximum concentration varies from nutrient to nutrient and basin to basin.

Figures D2, H2 and L2 show Pacific Ocean nutrient distributions. The maximum for phosphate is located around 1000 m for the North Pacific and phosphate decreases slightly below this depth. In contrast, a nitrate maximum is found at 1400 m with concentrations decreasing slightly below 1400 m. Silicate differs noticeably from the other two nutrients in its continuous increase in concentration with depth. A silicate maximum is clearly seen in the North Pacific at about 3000 m depth. The contrast between the nutrient distribution in the North and South Pacific is quite clear in all three figures.

The Atlantic nutrient profiles (Figs. D3, H3 and L3) show pronounced nitrate and phosphate maxima at about 1000 m, at the oxygen minimum layer (Broecker, 1974; Redfield *et al*, 1963). Deeper, concentrations are fairly uniform, although they increase slightly near the bottom. As in GEOSECS data (Bainbridge, 1976; Craig *et al.*, 1981; Spencer *et al.*, 1982, Sharp, 1983), the nitrate maximum is found at about the same depths in the North and South Atlantic, with the South Atlantic having a slightly broader maximum. Sharp's (1983) secondary maximum in the South Atlantic was not found with our data set. Even though our data include the GEOSECS data, some of the differences could be a result of the averaging during the objective analysis, or of the inclusion of more data.

Below the maxima, nitrate and phosphate maxima show up at around 2500 m in the South, but not in the North, Atlantic. Silicate profiles suggest a continual increase in diatom dissolution with depth in both Atlantic basins. A sharp increase in silicate below 4500 m in the South Atlantic is probably due to Antarctic Bottom Water.

Pacific and Atlantic Oceans nutrient distributions differ in the nitrate and phosphate minima found in the South Atlantic, in the enrichment of the South Atlantic compared to the North Atlantic (opposite of the Pacific situation), and in the sharp increase of silicate found in the South Atlantic. The difference in the nutrient distributions in the deep waters of these two oceans is related to their deep-water circulation and the age of the deep waters. Atlantic deeper waters, being younger, are lower in nutrients than the deep Pacific water masses.

The Indian Ocean profiles are shown in Figs. D4, H4 and L4. The North Indian Ocean is clearly enriched in nutrients relative to the South Indian Ocean.

5. SUMMARY

In the preceding sections we have described the results of a project to objectively analyze all historical nutrient data archived at the National Oceanographic Data Center, Washington, D.C., plus additional data gathered as a result of the NODC and IOC data archaeology and rescue projects which have not yet been incorporated into the NODC archive.

One advantage of the analyses techniques used in this atlas is that we know the amount of smoothing by objective analyses as given by the response function in Table 3. We believe this to be an important parameter in constructing, and describing a climatology of any geophysical parameter. Particularly when computing anomalies from a standard climatology, it is important that the synoptic field be smoothed to the same extent as the climatology to prevent generation of spurious anomalies simply through differences in smoothing. A second reason is that purely diagnostic computations require a minimum of seven or eight gridpoints to represent any Fourier component with accuracy. Higher order derivatives will require more smoothing.

We have attempted to create objectively analyzed fields and data sets that can be used as a "black box." For those users who wish to make their own choices, all the data used in our analyses are available both at standard depth levels as well as observed depth levels. The results

presented in this atlas show some features that are suspect and may be due to nonrepresentative or incorrect data that were not eliminated by the quality control techniques used. Although we have attempted to eliminate as many of these features as possible some obviously remain. Some may eventually turn out not to be artifacts but rather to represent real features, as yet undescribed.

6. FUTURE WORK

The acquisition of additional data will allow a decription of the nutrient seasonal cycle. Our analyses will be updated when justified by additional observations.

Improvement in our quality control procedures are a priority. This first attempt at using such procedures is part of an iterative process which will be updated and improved as more data are incorporated into the files. The methods developed apply to open ocean waters only and ignore the coastal regions. Future work will include developing ranges for each season, in each basin, as a function of depth, and the geographic expansion of the range definition process to include coastal regions and some of the major inland seas such as the Mediterranean, Baltic and Black Sea. In addition, we will improve the interpolation scheme by narrowing the acceptable distance between "inside" and "outside" values.

7. REFERENCES

Achtemeier, G.L., 1987: On the concept of varying influence radii for a successive corrections objective analysis. *Monthly Weather Review,* 11, 1761-1771.

Anderson, G.C., T.R. Parsons and K. Stephens, 1969: Nitrate distribution in the subartic Northeast Pacific Ocean. *Deep-Sea Res.*, 16, 329-334.

Armstrong, F.J.A., 1965: Silicon. In: *Chemical Oceanography* , J.P. Riley and G. Skirrow (Eds), Academic Press, London, pp. 409-432.

Bainbridge, A. E., 1976: *Geosecs Atlantic Expedition,* Vol. 2, National Science Foundation, Washington, D.C., 198 pp.

Barnes, S.L., 1973: *Mesoscale objective map analysis using weighted time series observations.* NOAA Technical Memorandum ERL NSSL-62, 60 pp.

_____ , 1964: A technique for maximizing details in numerical weather map analysis. *J. App. Meteor.*, 3, 396-409.

Bergthorsson, P., and B. Doos, 1955: Numerical Weather map analysis. *Tellus*, 7, 329-340.

Blackburn, M. 1981: Low latitude gyral regions. In: *Analysis of Marine Ecosystems,* A.R. Longhurst (Ed), Academic Press, London, pp.3-30.

Broecker W.S., 1974: *Chemical Oceanography*. Harcourt Brace Jovanovich, New York.

_____ and T. Peng, 1982: *Tracers in the Sea.* Columbia University, New York, pp.

_____ , J.R. Toggweiler and T. Takahashi, 1980: The Bay of Bengal - a major nutrient source for the deep Indian Ocean. *Earth Planet. Sci. Lett.,* 49, 506-512.

_____ and Y. Li, 1970: Interchange of water between the major oceans. *Deep-Sea Res.,* 25(18), 3545-3552.

Codispoti, L.A., 1983: Nitrogen in upwelling systems. In: *Nitrogen in the marine environment.* Academic Press, London, pp. 513-564.

Conkright, M.E., T.P. Boyer, and S. Levitus, 1994: *Quality Control and Processing of Historical Nutrient Data.* NOAA Technical Report. (In press).

Craig, H., W.S. Broecker and D. Spencer, 1981: GEOSECS Pacific Expedition, Vol. 4, Sections and Profiles. U.S. Government Printing Office, Washington, D.C.

Cressman, G.P., 1959: An operational objective analysis scheme. *Mon. Wea. Rev.*, 87, 329-340.

Cullen J.J., M.R. Lewis, C.O. Davis and R.T. Barber, 1992: Photosynthetic characteristics and estimated growth rates indicate grazing is the proximate control of primary production in the equatorial Pacific. *J. Geophys. Res.,* 97(C1), 639-654.

Daley, R., 1991: *Atmospheric Data Analysis.* Cambridge University Press, Cambridge, 457 pp.

Dugdale R.C., F.P. Wilkerson, R.T. Barber and F.P. Chavez, 1992: Estimating new production in the equatorial Pacific Ocean at 150°W. *J. Geophys. Res.,* 97(C1), 681-686.

Edmond J.M., S.S. Jacobs, A.L. Gordon, A.W. Mantyla and R.F. Weiss, 1979: Water column anomalies in dissolved silica over opaline pelagic sediments and the origin of the deep silica maximum. *J. Geophys. Res.*, 84(C12), 7809-7826.

England, M.H., 1992: On the formation of Antarctic Intermediate and Bottom Water in Ocean general circulation models. *J. Phys. Oceanogr.*, 22, 918-926.

Eppley R.W., E.H. Renger and W.G. Harrison, 1979: Nitrate and phytoplankton production in Southern California coastal waters. *Limnol. Oceanogr.*, 24(3), 483-494.

Friederich G.E. and L.A. Codispoti, 1979: On some factors influencing dissolved silicon distribution over the Northwest African Shelf. *J. Mar. Res.*, 37(2): 337-353.

Gandin, L.S., 1963: *Objective Analysis of Meteorological fields.* Gidrometeorol Izdat, Leningrad (translation by Israel program for Scientific Translations), Jerusalem, 1966, 242 pp.

Gordon A.L., 1971: Oceanography of Antarctic waters. In: *Antarctic oceanology.* J.L. Reid (Ed), Antarctic Research Series, pp.169-203.

Holm-Hansen O., 1985: Nutrient cycles in Antarctic marine ecosystems. In: *Antarctic Nutrient Cycles and Food Webs.* W.R. Siegfried, P.R. Condy and R.L. Cuhel (Eds), Springer-Verlag, Berlin, pp. 61-100.

_____, S.Z. El-Sayed, G.S. FranceshiniI and R.L. Cuhel, 1977: Primary production and factors controlling phytoplankton growth in the Southern Ocean. In: *Adaptations within Antarctic ecosystems.* G. Llano (Ed), Gulf Publ. Co., Houston, Texas, pp. 11-50.

Kamykowski D. and S.J. Zentara, 1989: Circumpolar plant nutrient covariation in the Southern Ocean: patterns and processes. *Mar. Ecol. Prog. Ser.*, 58, 101-111.

_____ and S.J. Zentara, 1985: Nitrate and silicic acid in the world ocean: patterns and processes. *Mar. Ecol. Prog. Ser.*, 26, 47-59.

Levitus, S., 1990: Interpentadal variability of Steric Sea Level and Geopotential Thickness of the North Atlantic Ocean 1970-74 Versus 1955-59. *J. Geophys. Res.*, 95, 5233-5238.

_____, 1989a: Interpentadal Variability of Temperature and Salinity at Intermediate Depths of the North Atlantic Ocean, 1970-74 Versus 1955-59. *J. Geophys. Res.*, 94, 6091-6131.

_____, 1989b: Interpentadal Variability of Salinity in the Upper 150 m of the North Atlantic Ocean, 1970-74 versus 1955-59. *J. Geophys. Res.*, 94, 9679-9685.

_____, 1989c: Interpentadal Variability of Temperature and Salinity in the Deep North Atlantic, 1970-74 versus 1955-59. *J. Geophys. Res.*, 94, 16125-16131.

_____, 1982: *Climatological Atlas of the World Ocean.* NOAA Professional Paper No. 13, U.S. Gov. Printing Office, 173 pp.

_____, R. Gelfeld, T. Boyer, and D. Johnson, 1994a: *Results of the NODC and IOC Oceanographic Data Archaeology and Rescue Projects: Report 1.* Key to Oceanographic Records Documentation No. 19, NODC, Washington, D.C., 73 pp.

_____, J. Antonov, X. Zhou, H. Dooley, K. Selemenov, and V. Tereschenkov, 1994b: Decadal-Scale Variability of the North Atlantic Ocean. Accepted by National Academy of Sciences for publication in "*Natural Climate Variability on Decade-to-Century Time Scales.*" (In preparation).

_____ and T.P. Boyer, 1994c: *World Ocean Atlas, 1993: Volume 2, Oxygen.* NOAA Atlas Series. In preparation.

_____ , M.E. Conkright, J.L. Reid, R. Najjar, and A. Mantyla, 1993: Distribution of nitrate, phosphate and silicate in the world ocean. *Prog. Oceanogr.,* 31, 245-273.

Mantyla A.W. and J.L. Reid, 1983: Abyssal characteristics of the World Ocean waters. *Deep-Sea Res.,* 30(8A), 805-833.

Martin, J.H., R.M. Gordon and S.E. Fitzwater, 1989: VERTEX: Phytoplankton/iron studies in the Gulf of Alaska. *Deep-Sea Res.,* 36, 649-680.

_____ and R.M. Gordon, 1988: Northeast Pacific iron distributions in relation to phytoplankton producticity. *Deep-Sea Res.,* 35, 177-196.

Minas H.J., B. Coste, P. Le Corre, M. Minas and P. Raimbault, 1991: Biological and geochemical signatures associated with the water circulation through the Strait of Gibraltar and in the western Alboran Sea. *J. Geophys. Res.,* 96(C5), 8755-8771.

Naqvi S.W.A., R.J. Noronha and C.V. Gangadhara Reddy, 1982: Denitrification in the Arabian Sea. *Deep-Sea Res.,* 29, 459-469.

Nelson D.M. and L.I. Gordon, 1982: Production and pelagic dissolution of biogenic silica in the Southern Ocean. *Geochim. Cosmochim. Acta,* 46, 491-501.

NODC, 1993: *NODC User's Guide.* National Oceanic and Atmospheric Administration, Washington, D.C. Key to Oceanographic Records Documentation No. 18, NODC, Washington, D.C.

Olson R.J., 1980: Nitrate and ammonium uptake in Antarctic waters. *Limnol. Oceanogr.,* 25, 1064-1074.

Rabiner, L.R., M.R. Sambur and C. E. Schmidt, 1975: Applications of a nonlinear smoothing algorithm to speech processing. *IEEE Trans. on Acoustics, Speech and Signal Processing,* Vol. Assp-23, pp. 552-557.

Redfield A.C., B.H. Ketchum and F.A. Richards, 1963: The influence of organisms on the composition of seawater. In: *The Sea, Volume 2: The Composition of Sea Water Comparative and Descriptive Oceanography,* M.N. Hill (Ed.), Robert E. Krieger Publishing Company, Florida, pp. 26-77.

Reid J.L., 1981: On the mid-depth circulation of the world ocean. *Evolution of Physical Oceanography,* B.A. Warren and C. Wunsch (Eds), MIT Press, Cambridge, Massachusetts, pp.70-111.

_____ , 1965: *Intermediate waters of the Pacific Ocean. (Number 2).* The Johns Hopkins press, Baltimore, 85 pp.

_____ , 1962: On circulation, phosphate-phosphorus content, and zooplankton volumes in the upper part of the Pacific Ocean. *Limnol. Oceanagr.,* 7(3), 287-306.

_____ ; E. Brinton, A. Fleminger, E.L. Venrick and J.A. McGowan, 1978: Ocean circulation and marine life. In: Henry Charnock and Sir George Deacon (Eds), *Advances in Oceanography,* Plenum Press, New York, pp. 65-130.

_____ and R.J. Lynn, 1971: On the influence of the Norwegian-Greenland and Weddell seas upon the bottom waters of the Indian and Pacific oceans. *Deep-Sea Res.,* 18, 1063-1088.

Reiniger, R.F. and C.F. Ross, 1968: A method of interpolation with application to oceanographic data. *Deep-Sea Res.,* 9, 185-193.

Sasaki, Y., 1960: *An objective analysis for determining initial conditions for the primitive equations.* Ref. 60-1 6T, Atmospheric Research Lab., Univ. of Oklahoma Research Institute, Norman, 23 pp.

Seaman, R.S., 1983. Objective analysis accuracies of statistical interpolation and successive correction schemes. *Australian Meteor. Mag.*, 31, 225-240.

Sharp, J.H., 1983: The distributions of inorganic nitrogen and dissolved and particulate organic nitrogen in the sea. In: *Nitrogen in the Marine Environment,* Academic Press, London, pp. 1-35.

Shuman, F.G., 1957: Numerical methods in weather prediction: II. Smoothing and filtering. *Mon. Wea. Rev.*, 85, 357-361.

Smith, D.R., M.E. Pumphry, J.T. Snow, 1986: A comparison of errors in objectively analyzed fields for uniform and nonuniform station distribution. *J. Atm. Oceanic Tech.*, 3, 84-97.

_____ and F. Leslie, 1984: Error determination of a successive correction type objective analysis scheme. J. Atm. Oceanic *Tech.*, 1, 121-130.

Smith, S.M., H.W. Menard and G. Sharman, 1966: *Worldwide ocean depths and continental elevations.* SIO Ref. G5-8, Scripps Institution of Oceanography, Univ. of California, La Jolla, 17 pp.

Spencer D., W.S. Broecker, H. Craig and R.F. Weiss, 1982: *GEOSECS Indian Expedition, Vol. 6, Sections and Profiles.* U.S. Government Printing Office, Washington, D.C.

Sverdrup, H.U., M.W. Johnson and R.H. Fleming, 1942: *The Oceans.* Prentice Hall Inc., New Jersey, 1087 pp.

Tchernia, P., 1980: *Descriptive Regional Oceanography.* Pergamon press, New York, 253 pp.

Thiebaux, H.J. and M.A. Pedder, 1987: *Spatial Objective Analysis: with applications in atmospheric science.* Academic Press, London, 299 pp.

Tukey, J.W., 1974: Nonlinear (nonsuperposable) methods for smoothing data, In: *Cong. Rec.*, 1974 EASCON, 673 pp.

Uda M., 1963: Oceanography of the subarctic Pacific Ocean. *J. Fish. Res. Bd. Can.*, 20, 119-179.

UNESCO, 1991: *Processing of Oceanographic Station Data.* Imprimerie des Presses Unibversitaires de France, Vendome, pp. 138 pp.

Walsh J.J., 1977: A biological sketchbook for an eastern boundary current. In: *The Sea.* E.D. Goldberg, I.H. McCave, J.J. O'Brien and J.H. Steele (Eds), Wiley (Interscience), New York, 6, pp.923-968.

Wheeler P.A. and S.A. Kokkinakis, 1990: Ammonium recycling limits nitrate use in the oceanic subarctic Pacific. *Limnol. Oceanogr.*, 35(6), 1267-1278.

Wilkerson F.P. and R.C. Dugdale, 1992: Measurements of nitrogen productivity in the Equatorial Pacific. *J. Geophys. Res.*, 97, (C1), 669-679.

Table 1. Distribution with depth of the number of one-degree squares of ocean (Ocean ODSQS), the total number (N) of phosphate, nitrate and silicate observations; and the number of one-degree squares (ODSQS) containing observations of phosphate, nitrate and silicate.

	Depth (m)	Ocean (ODSQS)	Phosphate		Nitrate		Silicate	
			N	ODSQS	N	ODSQS	N	ODSQS
1	0	42164	171064	18512	61817	9170	80235	14082
2	10	42054	168059	18353	59932	8928	78118	13798
3	20	41936	160780	18353	58209	8962	75952	13857
4	30	41809	154897	18306	55275	8985	73067	13878
5	50	41244	142542	18062	50016	9028	67301	13759
6	75	40945	119044	17331	41246	8676	58810	13130
7	100	40327	104199	16638	37764	8637	51515	12585
8	125	40169	84319	15535	31500	8340	41385	11535
9	150	39858	82344	15581	31059	8475	41534	11570
10	200	39255	63436	13451	24670	7226	31783	9562
11	250	39058	75696	15714	27861	8571	37940	11639
12	300	38623	67493	15044	25174	8153	33176	10989
13	400	38272	55279	13687	21255	7348	26673	9761
14	500	37849	47157	12143	18297	6566	23206	8775
15	600	37579	28066	9291	11183	5175	15020	6625
16	700	37352	19776	7797	8432	4372	11462	5667
17	800	37059	17627	6816	7006	3801	9592	4911
18	900	36879	42755	12524	14345	6713	21361	9416
19	1000	36493	35632	10991	12030	5881	17516	7956
20	1100	36315	27786	9878	10738	5504	13941	7054
21	1200	36057	19795	7994	8077	4429	10070	5542
22	1300	35862	16621	7555	7219	4316	9260	5221
23	1400	35716	14067	6461	6134	3747	7803	4602
24	1500	35405	9965	5265	4640	3014	6178	3863
25	1750	34914	5170	3240	3172	2067	3992	2633
26	2000	33856	19692	8880	7200	4421	10996	6566
27	2500	32077	12767	7135	5985	3829	8692	5516
28	3000	29188	9826	5891	4838	3277	6942	4602
29	3500	25089	7641	4705	3940	2699	5549	3729
30	4000	19718	5581	3562	3074	2135	4213	2893
31	4500	12856	3456	2314	2083	1478	2803	1943
32	5000	6883	1635	1185	1105	828	1471	1060
33	5500	1847	569	418	389	289	511	375

Table 2. Acceptable distances for "inside" and "outside" values used in the Reiniger-Ross scheme for interpolating observed level data to standard levels

Standard Levels	Standard Depths	Acceptable distances for inside values	Acceptable distances for outside values
1	0	5	200
2	10	50	200
3	20	50	200
4	30	50	200
5	50	50	200
6	75	50	200
7	100	50	200
8	125	50	200
9	150	50	200
10	200	50	200
11	250	100	200
12	300	100	200
13	400	100	200
14	500	100	400
15	600	100	400
16	700	100	400
17	800	100	400
18	900	200	400
19	1000	200	400
20	1100	200	400
21	1200	200	400
22	1300	200	1000
23	1400	200	1000
24	1500	200	1000
25	1750	200	1000
26	2000	1000	1000
27	2500	1000	1000
28	3000	1000	1000
29	3500	1000	1000
30	4000	1000	1000
31	4500	1000	1000
32	5000	1000	1000
33	5500	1000	1000

Table 3. Response function of the objective analysis scheme as a function of wavelength.

Wavelength*	Response Function
360ΔX	0.999
180ΔX	0.997
120ΔX	0.994
90ΔX	0.989
72ΔX	0.983
60ΔX	0.976
45ΔX	0.957
40ΔX	0.946
36ΔX	0.934
30ΔX	0.907
24ΔX	0.857
20ΔX	0.801
18ΔX	0.759
15ΔX	0.671
12ΔX	0.532
10ΔX	0.397
9ΔX	0.315
8ΔX	0.226
6ΔX	0.059
5ΔX	0.019
4ΔX	2.23×10^{-3}
3ΔX	1.90×10^{-4}
2ΔX	5.30×10^{-7}

* For $\Delta X = 111$ km

Table 4. Basin identifiers and depths of "mutual exclusion" used in this study

Basin	Depth (m)	Basin	Depth (m)
Atlantic Ocean	---*	Pacific Ocean	---*
Indian Ocean	---*	Mediterranean Sea	---*
Baltic Sea	0	Black Sea	0
Red Sea	0	Persian Gulf	0
Hudson Bay	0	Southern Ocean	---*
Arctic Ocean (Bering)	0	Sea of Japan	125
Kara Sea	200	Sulu Sea	500
Arctic Ocean (Atlantic)	600	Baffin Bay	700
East Mediterranean	1000	West Mediterranean	1000
Sea of Oshkotsk	1300	Banda Sea	1400
Caribbean Sea	1400	Andaman Basin	2000
North Caribbean	2000	Gulf of Mexico	2000
Beaufort Sea	3000	South China Sea	3000
Barent Sea	3000	Celebes Sea	3000
Aleutian Basin	3000	Fiji Basin	3500
North American Basin	3500	West European Basin	3500
Southeast Indian Basin	3500	Coral Sea	3500
East Indian Ocean	3500	Central Indian Ocean	3500
Southwest Atlantic	3500	East South Atlantic	3500
Southeast Pacific	3500	Guatemala Basin	3500
East Caroline Basin	4000	Marianas Basin	4000
Phillipine Sea	4000	Arabian Sea	4000
Chile Basin	4000	Somali Basin	4000
Mascarine Basin	4500	Guinea Basin	4500
Croset Basin	4500	Brazil Basin	4500
Argentine Basin	4500	Tasman Sea	4500

*Basins marked with a dash can interact with each other except certain areas such as the Isthmus of Panama

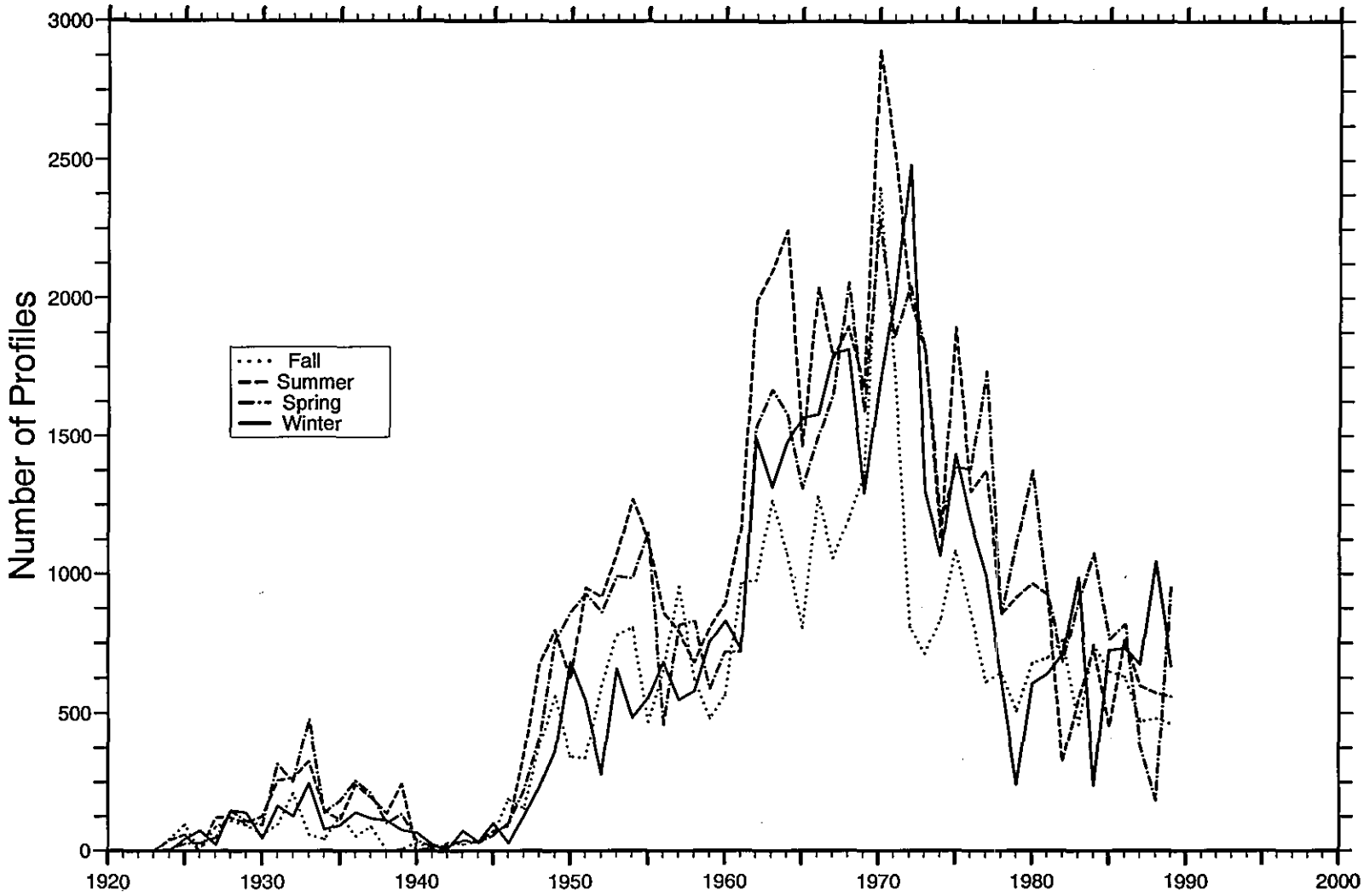

Figure 1. Time series of the number of phosphate profiles as a function of year for each season

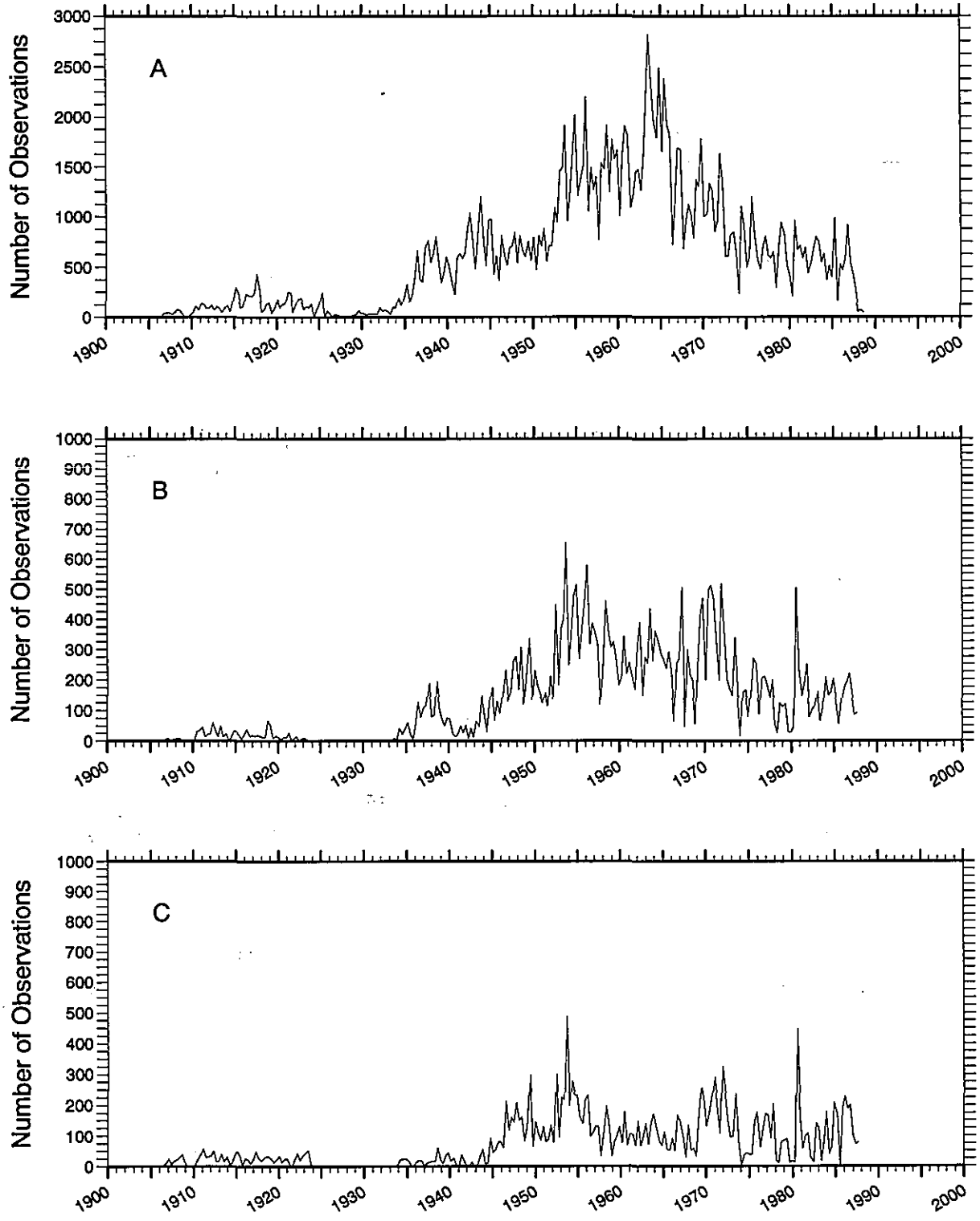

Figure 2. Time series of the number of phosphate observations as a function of year A) at the sea surface, B) at 1000 m, C) at 2000 m

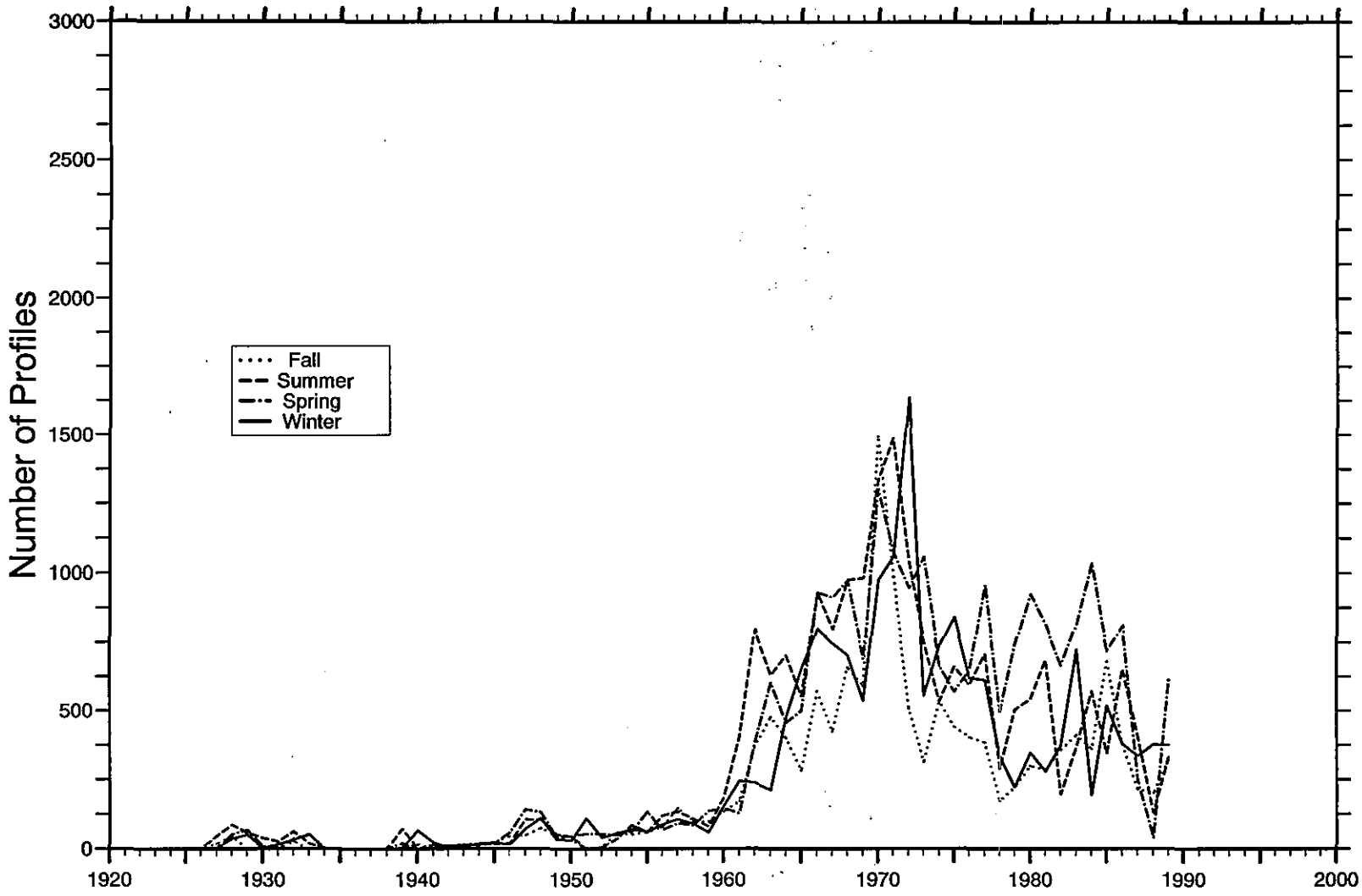

Figure 3. Time series of the number of nitrate profiles as a function of year for each season

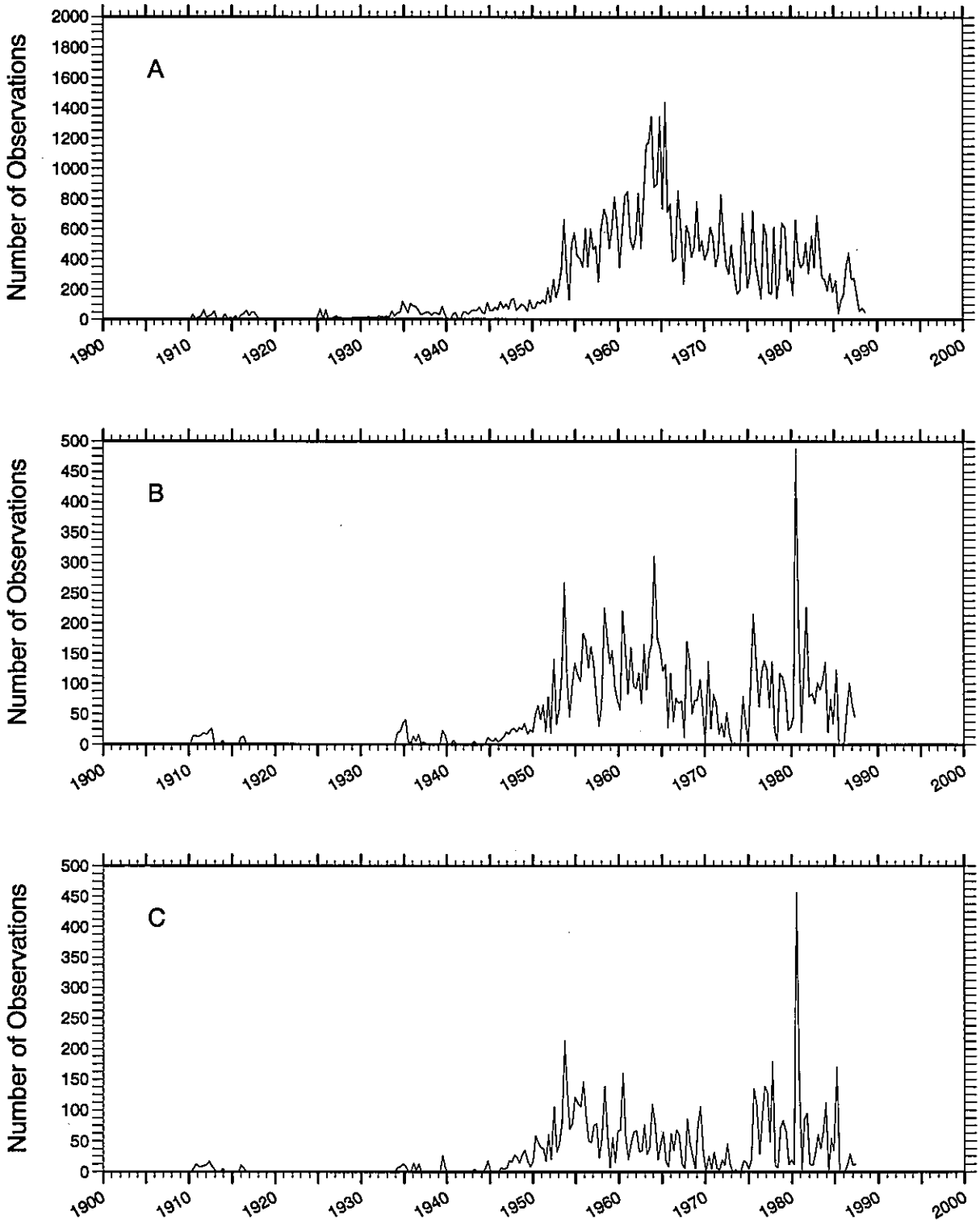

Figure 4. Time series of the number of nitrate observations as a function of year A) at the sea surface, B) at 1000 m, C) at 2000 m

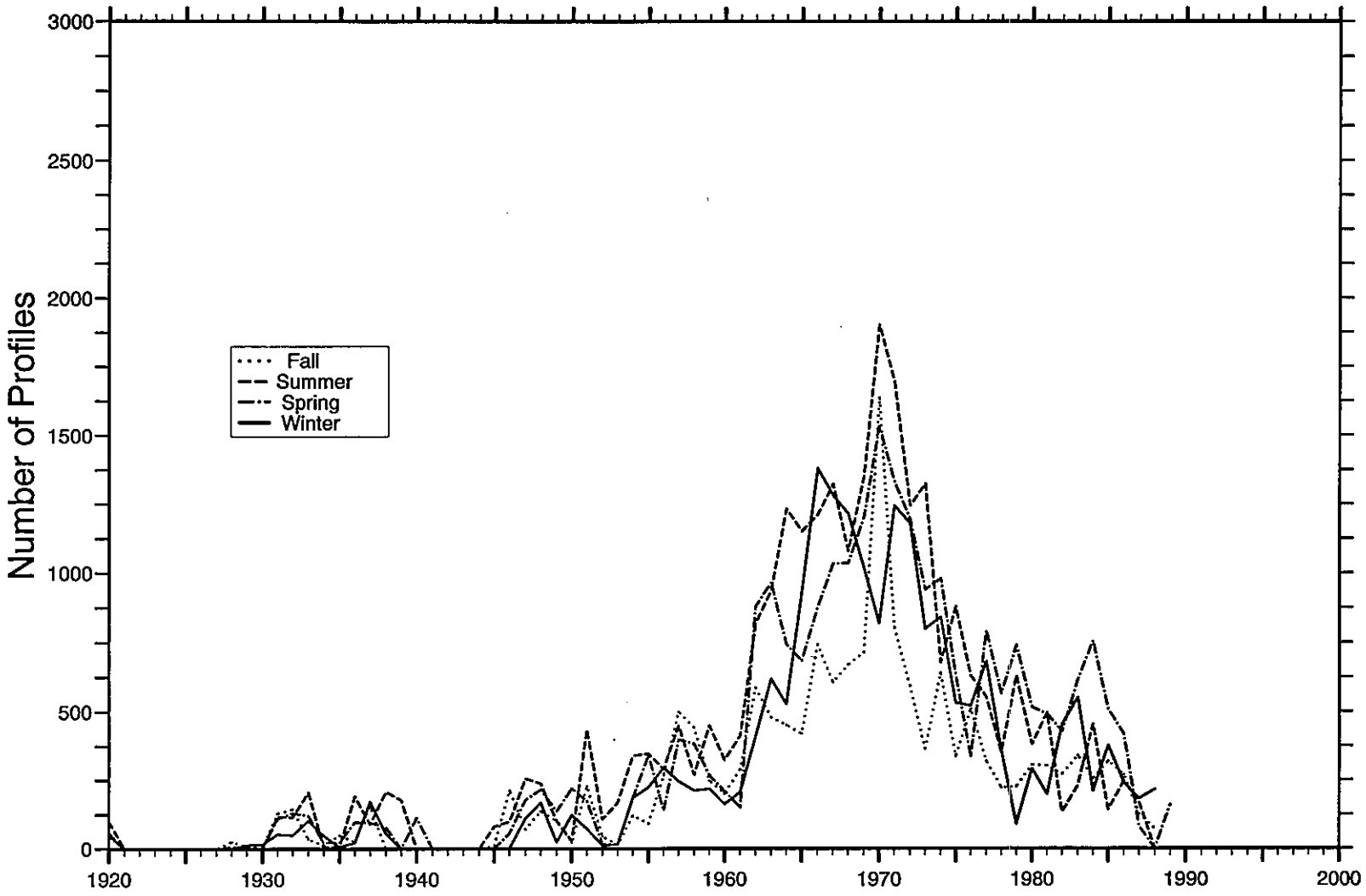

Figure 5. Time series of the number of silicate profiles as a function of year for each season

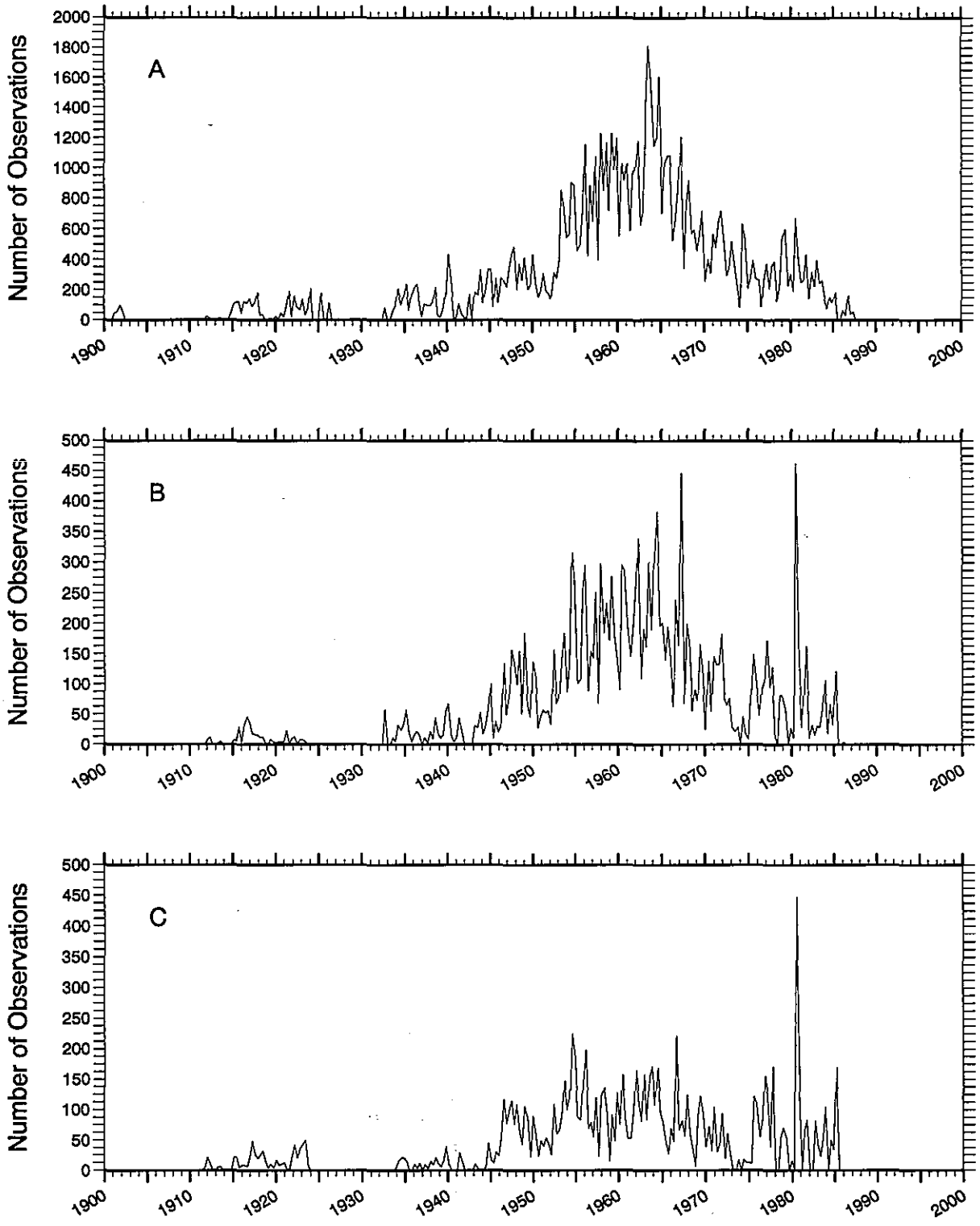

Figure 6. Time series of the number of silicate observations as a function of year A) at the sea surface, B) at 1000 m, C) at 2000 m

Fig. 7a Distribution of phosphate observations as a function of depth for the globe and Northern and Southern Hemispheres

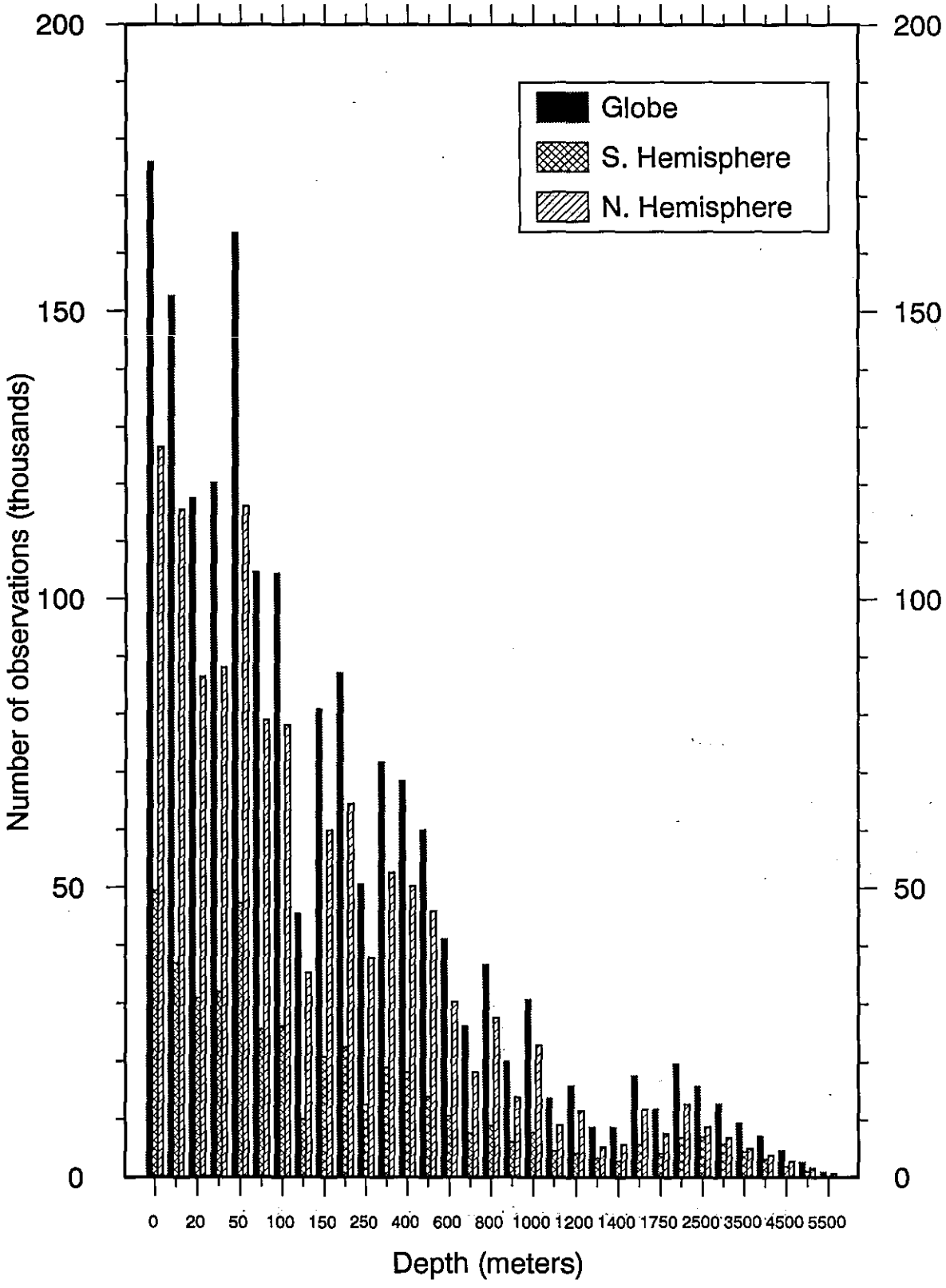

Fig. 7b Distribution of nitrate observations as a function of depth for the globe and Northern and Southern Hemispheres

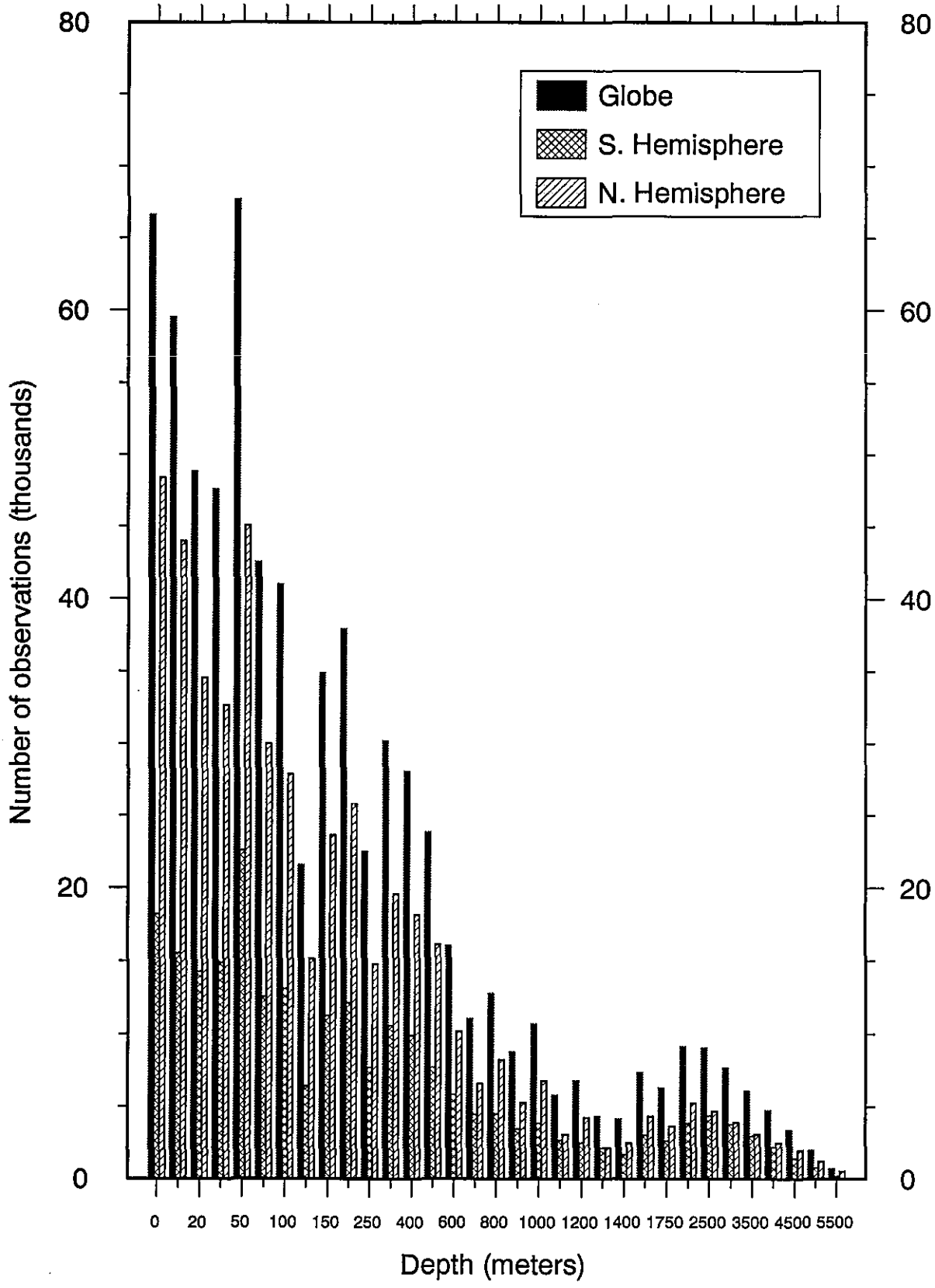

Fig. 7c Distribution of silicate observations as a function of depth for the globe and Northern and Southern Hemispheres

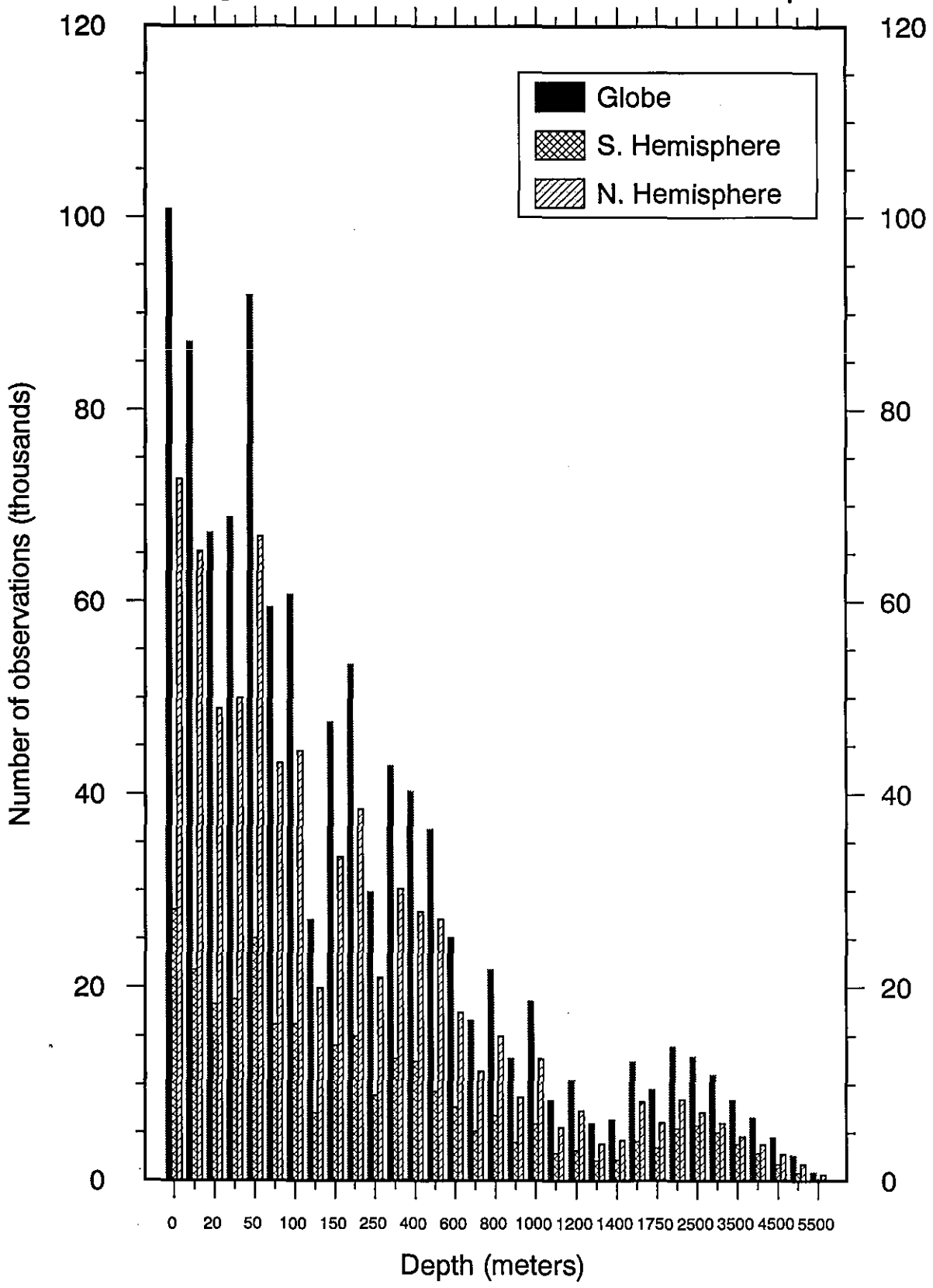

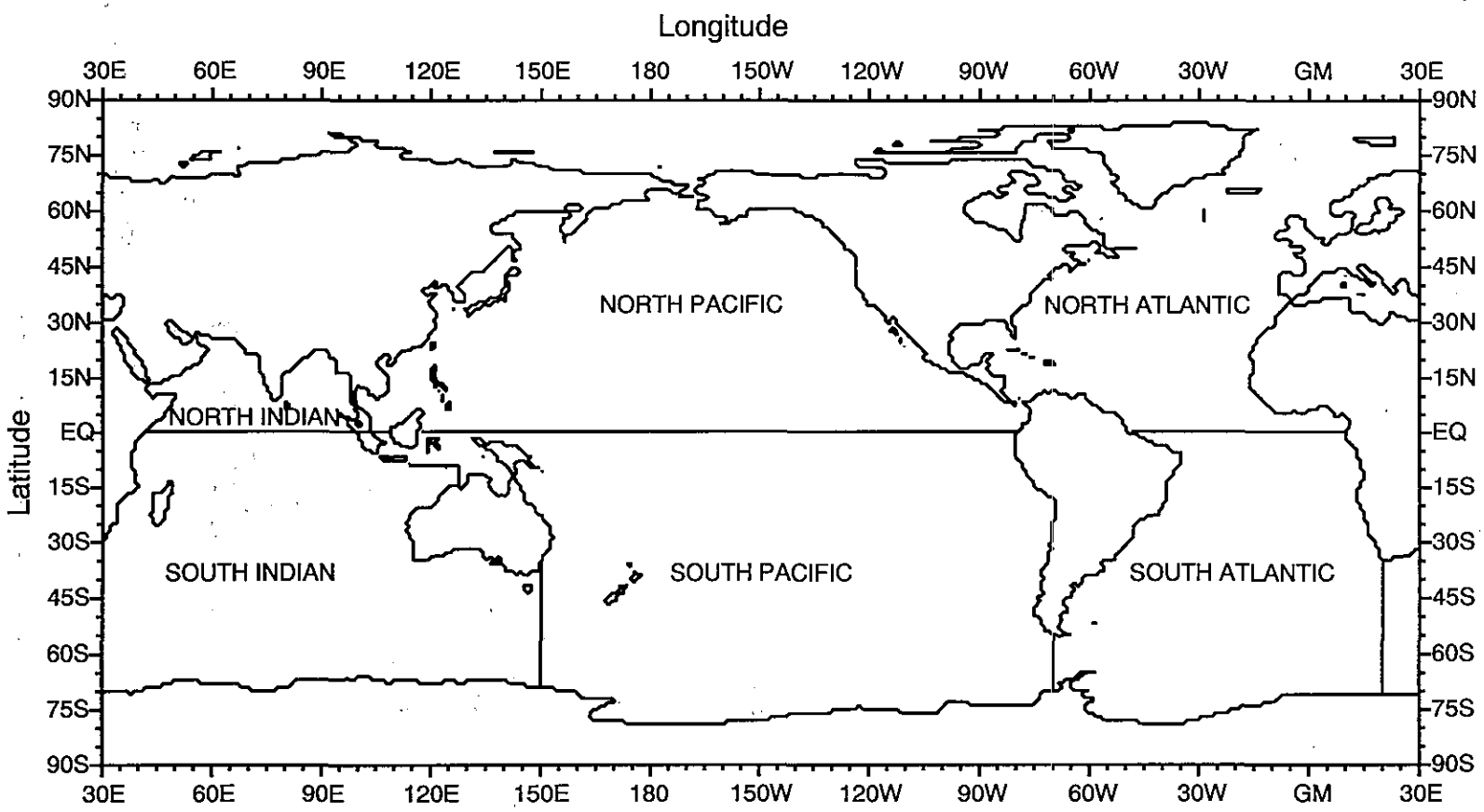

Fig 8. Division of world ocean into individual basins.

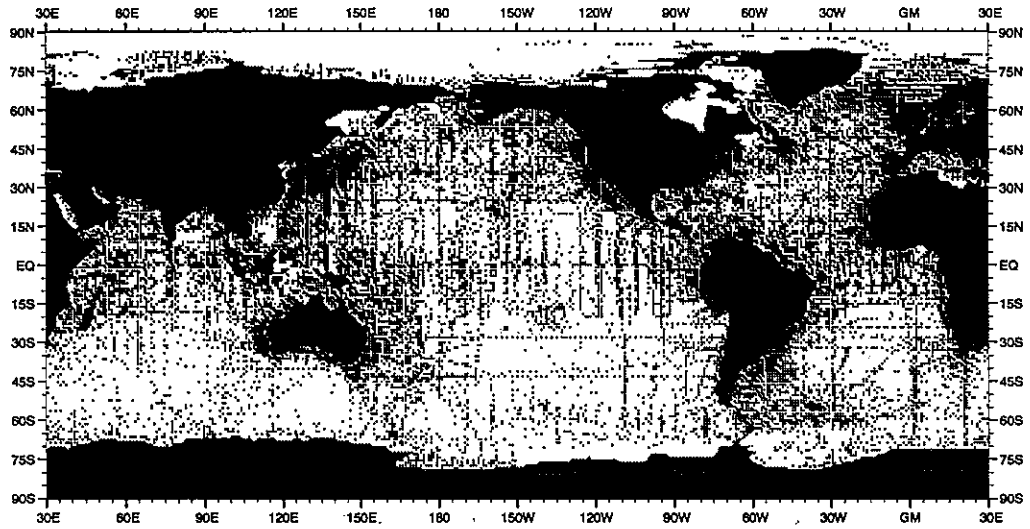

Fig. A1 Distribution of phosphate observations at the surface

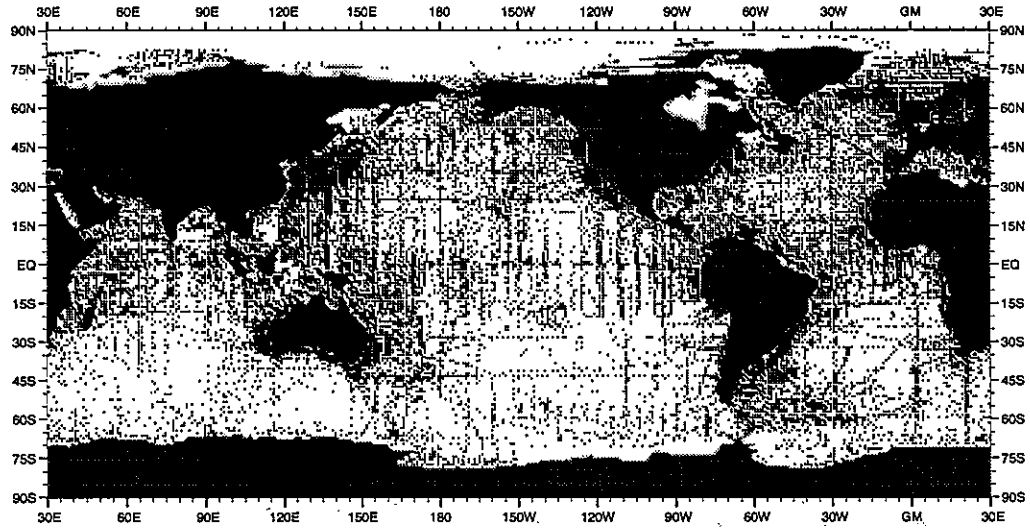

Fig. A2 Distribution of phosphate observations at 30 m depth

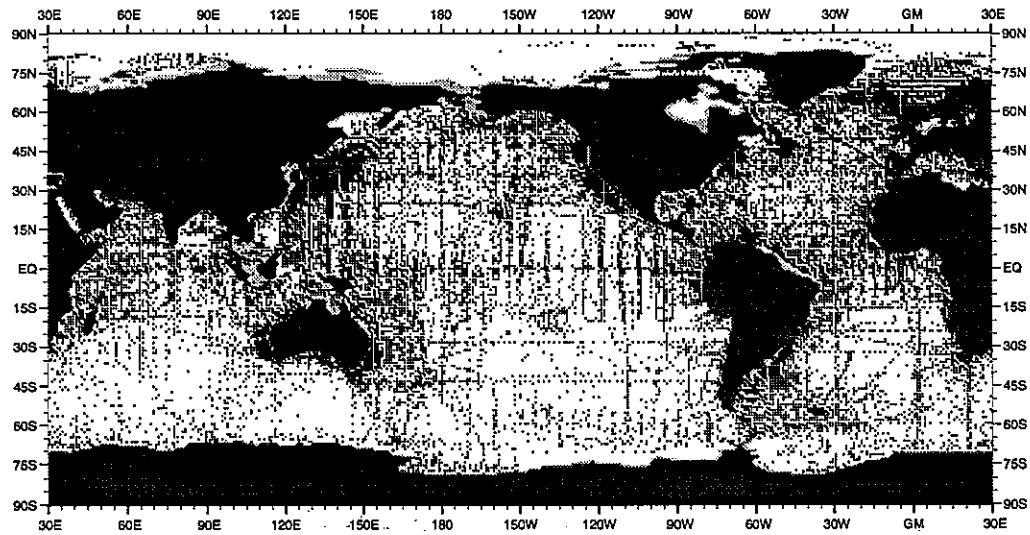

Fig. A3 Distribution of phosphate observations at 50 m depth

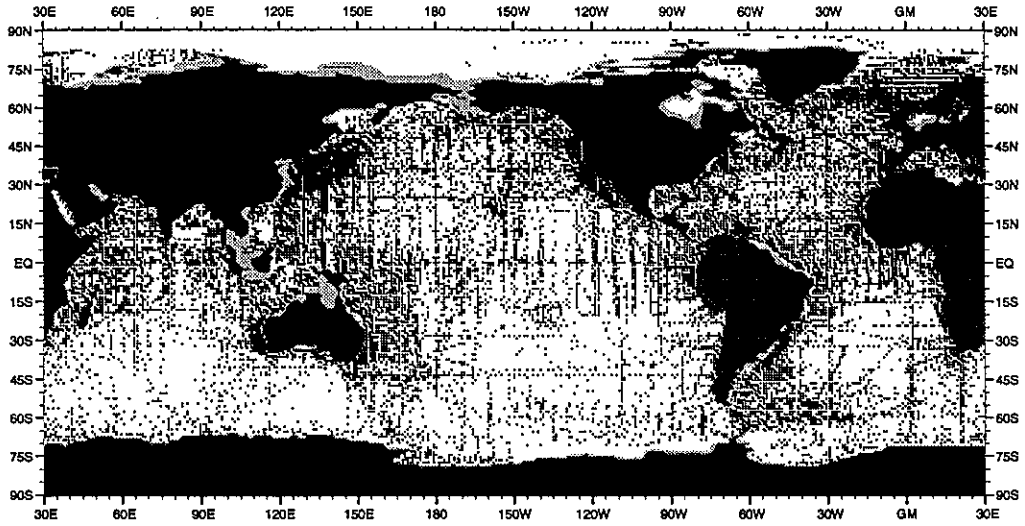

Fig. A4 Distribution of phosphate observations at 75 m depth

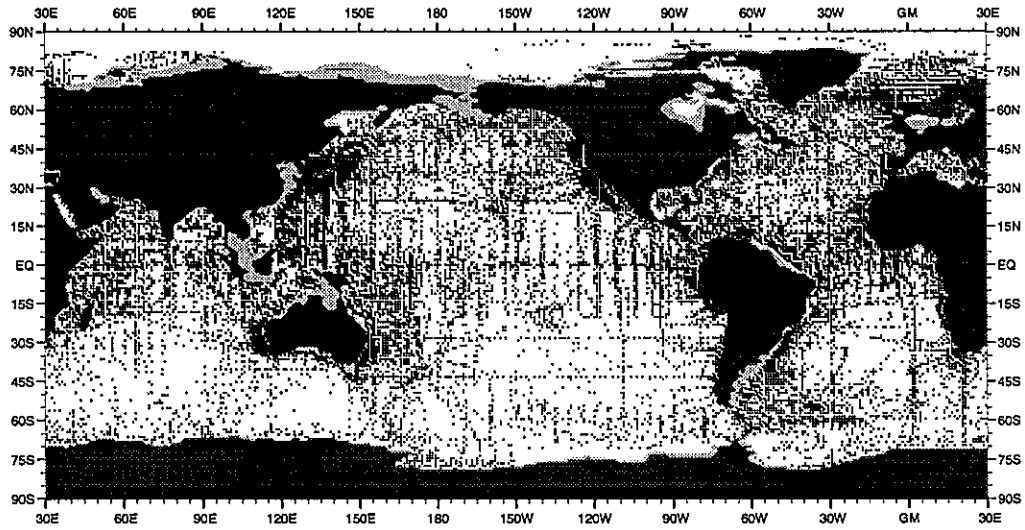

Fig. A5 Distribution of phosphate observations at 100 m depth

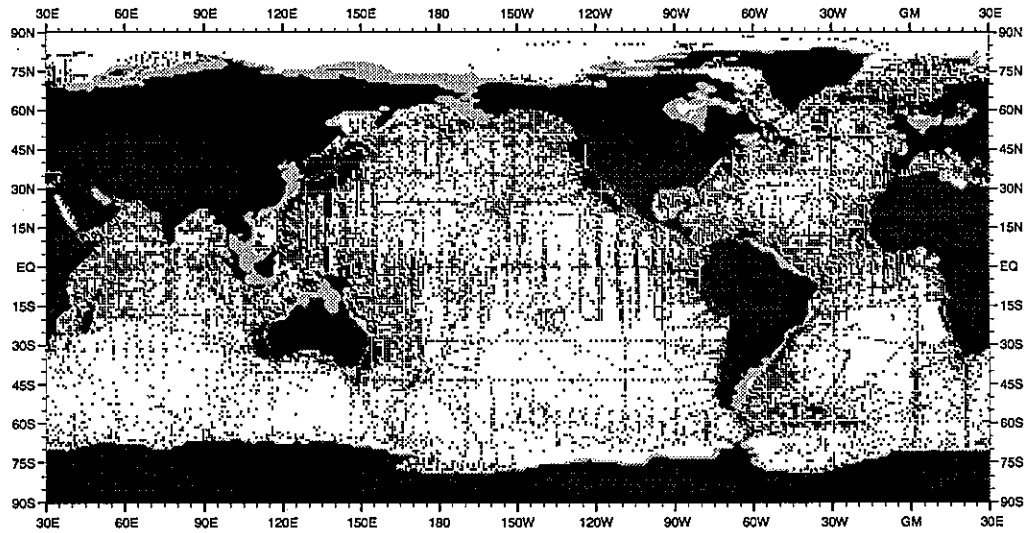

Fig. A6 Distribution of phosphate observations at 125 m depth

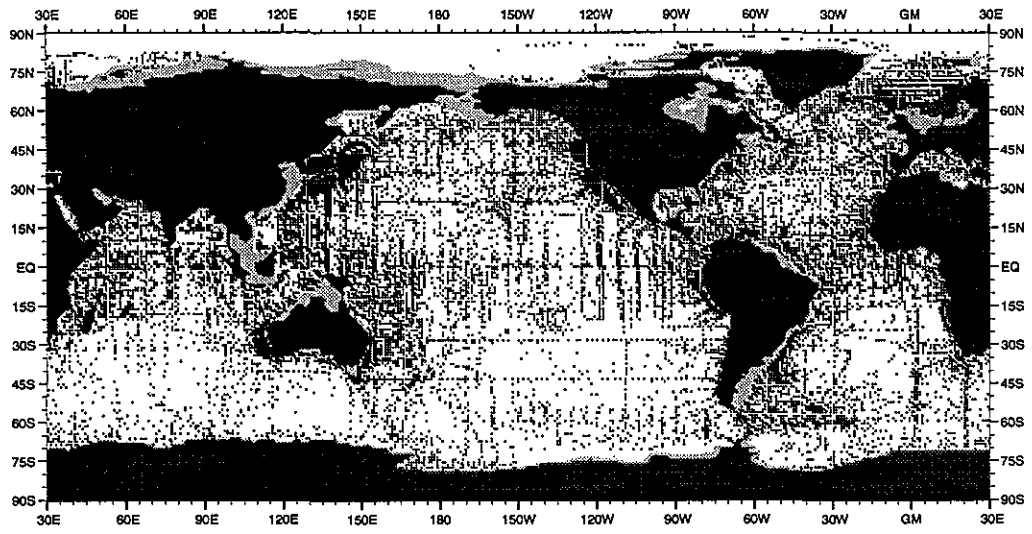

Fig. A7 Distribution of phosphate observations at 150 m depth

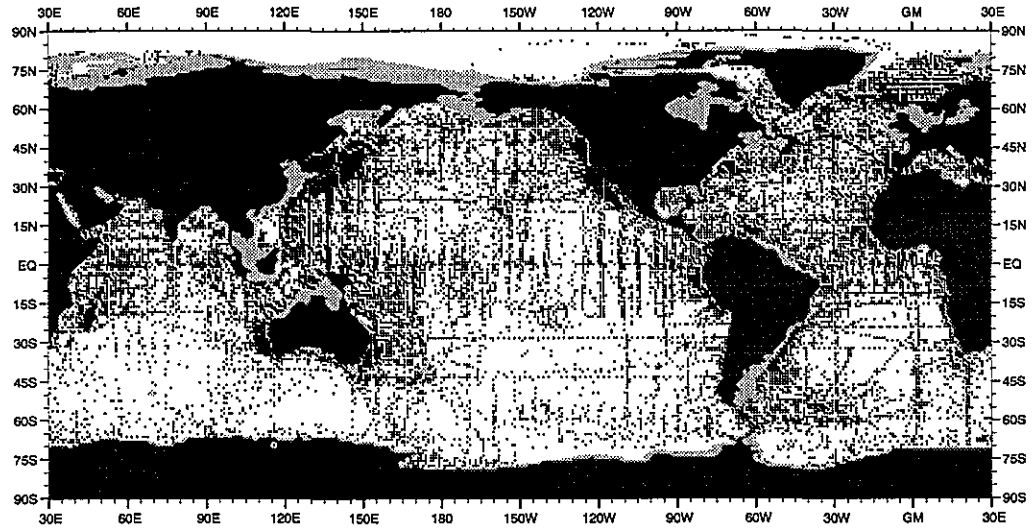

Fig. A8 Distribution of phosphate observations at 250 m depth

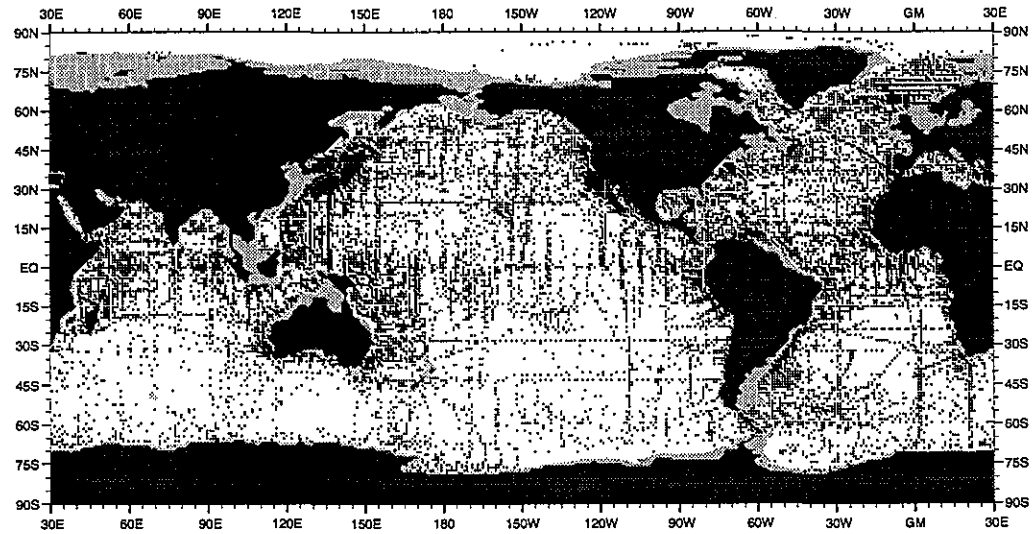

Fig. A9 Distribution of phosphate observations at 400 m depth

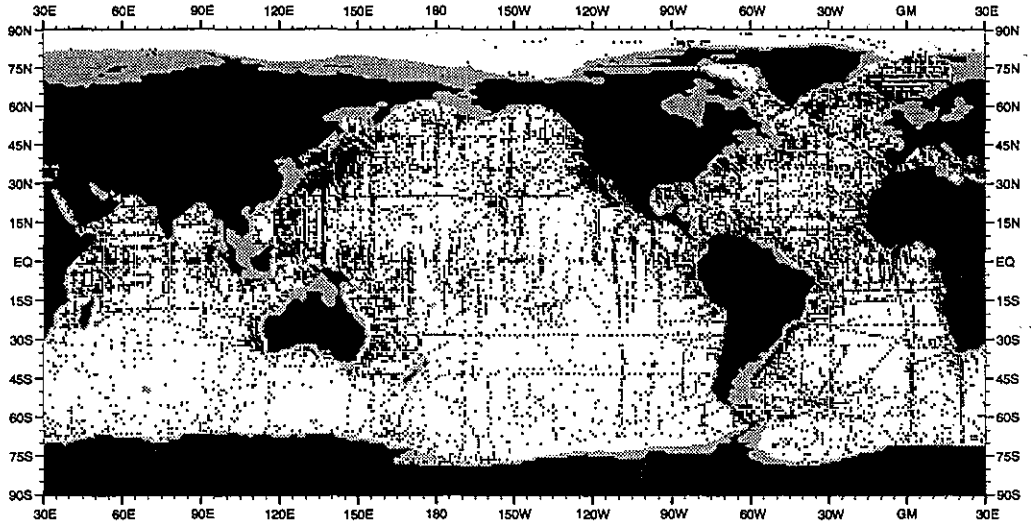

Fig. A10 Distribution of phosphate observations at 500 m depth

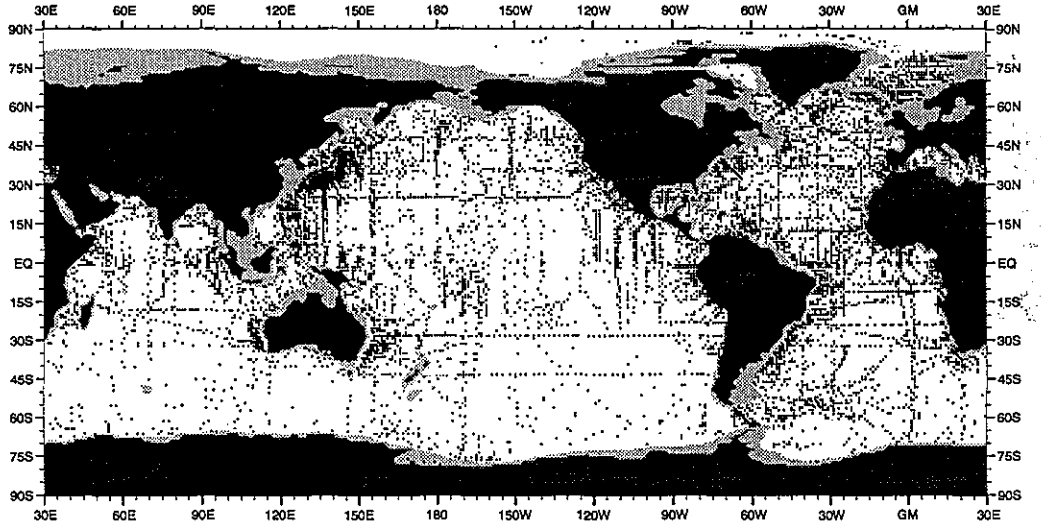

Fig. A11 Distribution of phosphate observations at 700 m depth

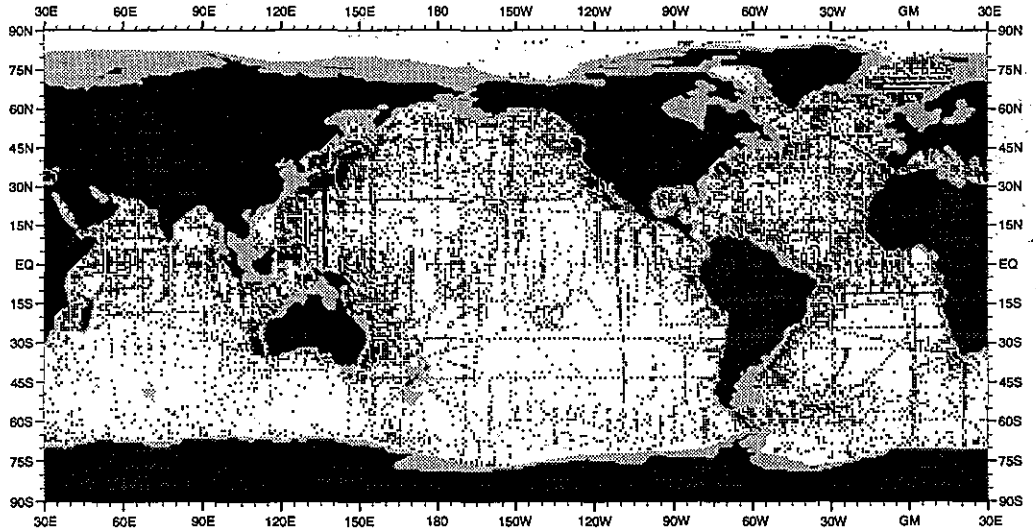

Fig. A12 Distribution of phosphate observations at 900 m depth

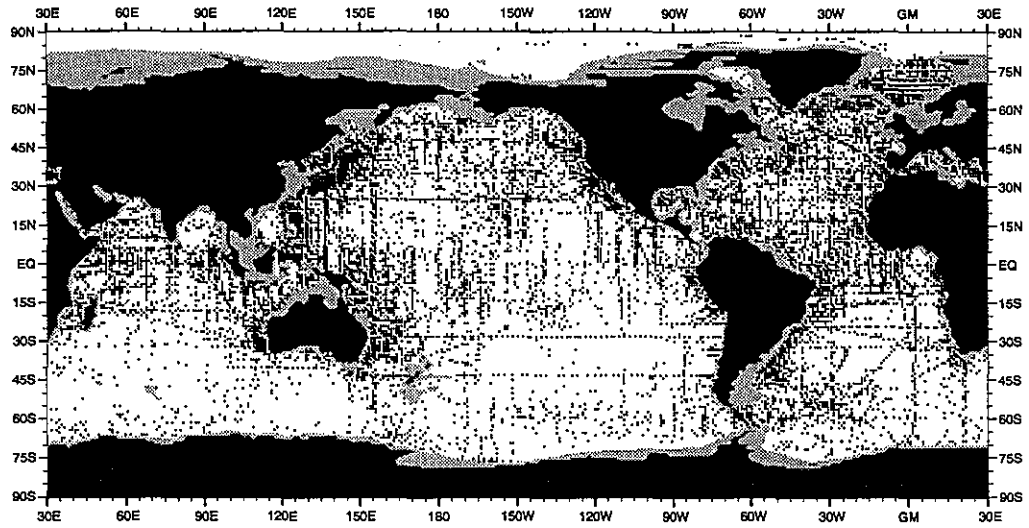

Fig. A13 Distribution of phosphate observations at 1000 m depth

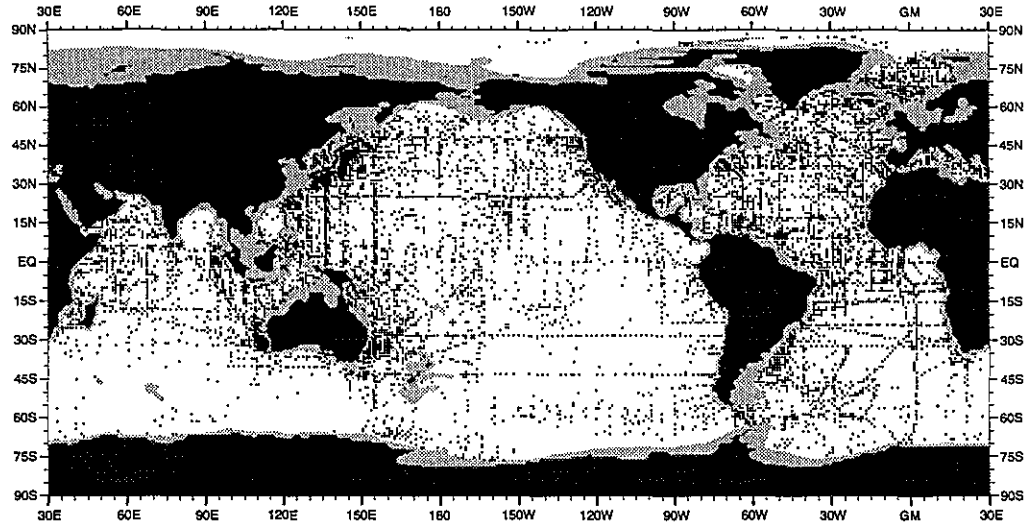

Fig. A14 Distribution of phosphate observations at 1200 m depth

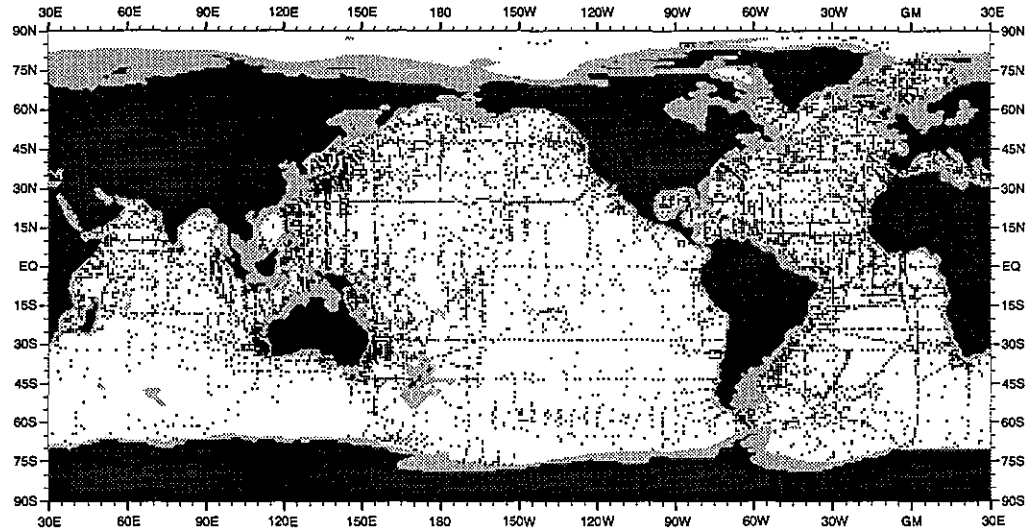

Fig. A15 Distribution of phosphate observations at 1300 m depth

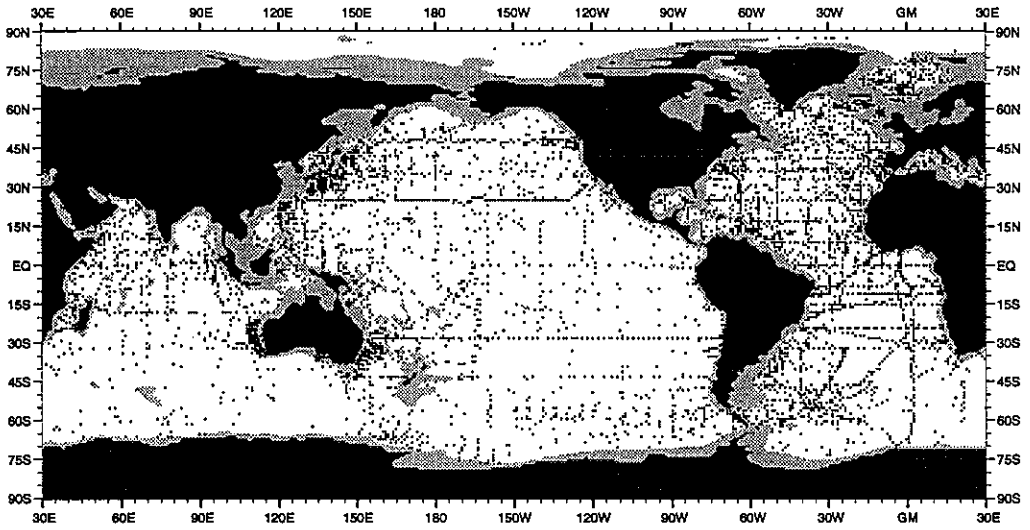

Fig. A16 Distribution of phosphate observations at 1500 m depth

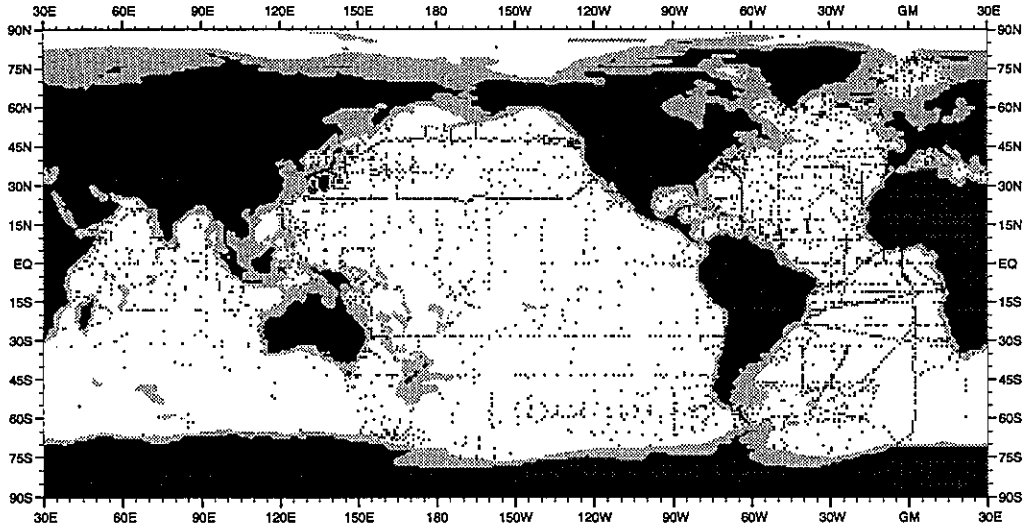

Fig. A17 Distribution of phosphate observations at 1750 m depth

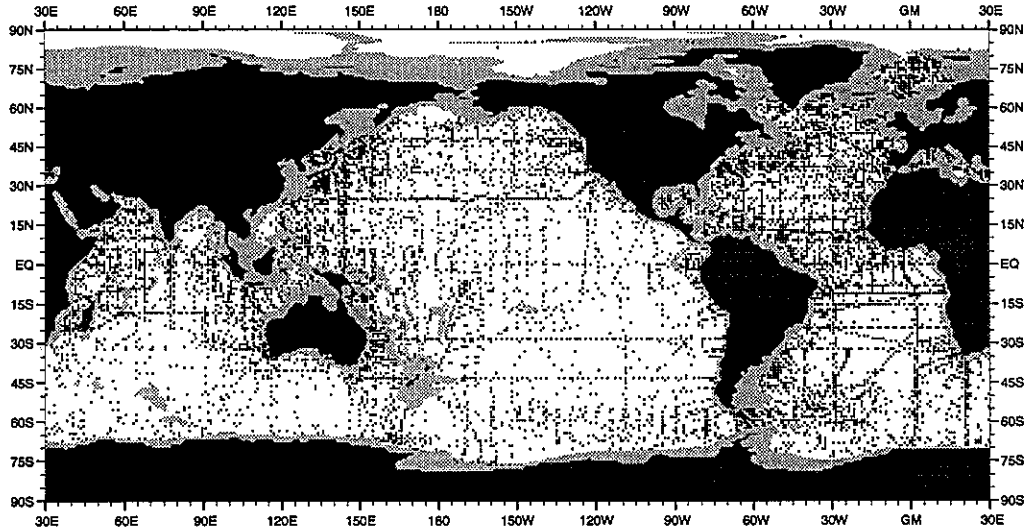

Fig. A18 Distribution of phosphate observations at 2000 m depth

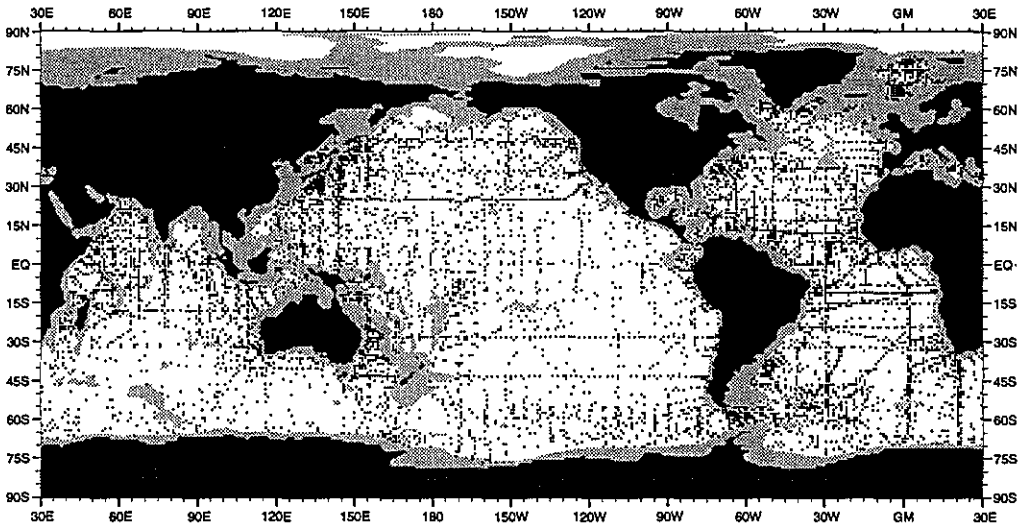

Fig. A19 Distribution of phosphate observations at 2500 m depth

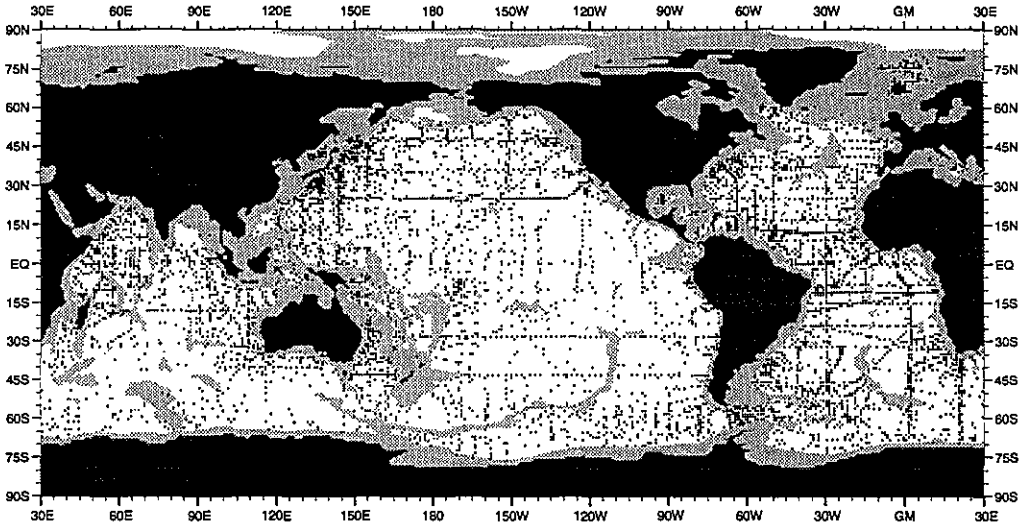

Fig. A20 Distribution of phosphate observations at 3000 m depth

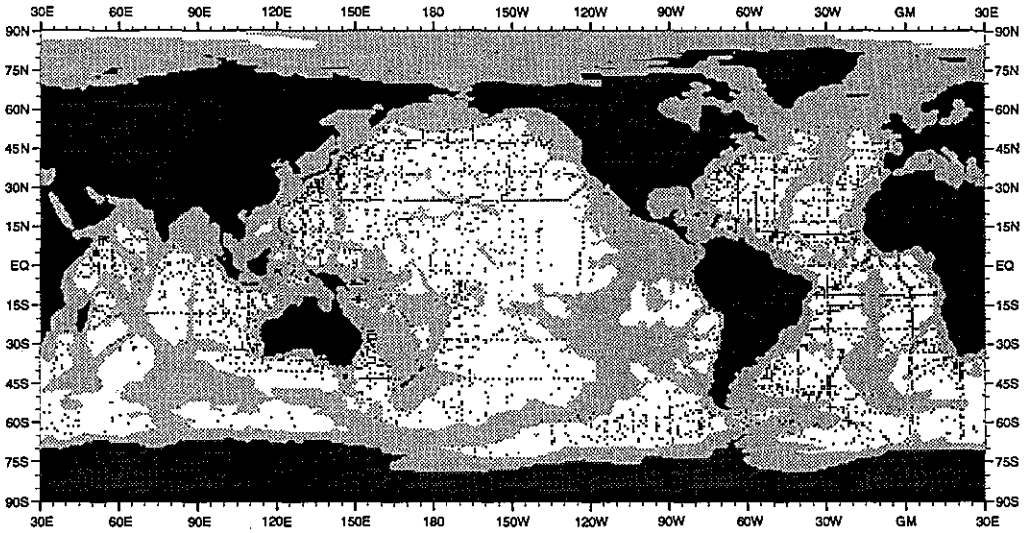

Fig. A21 Distribution of phosphate observations at 4000 m depth

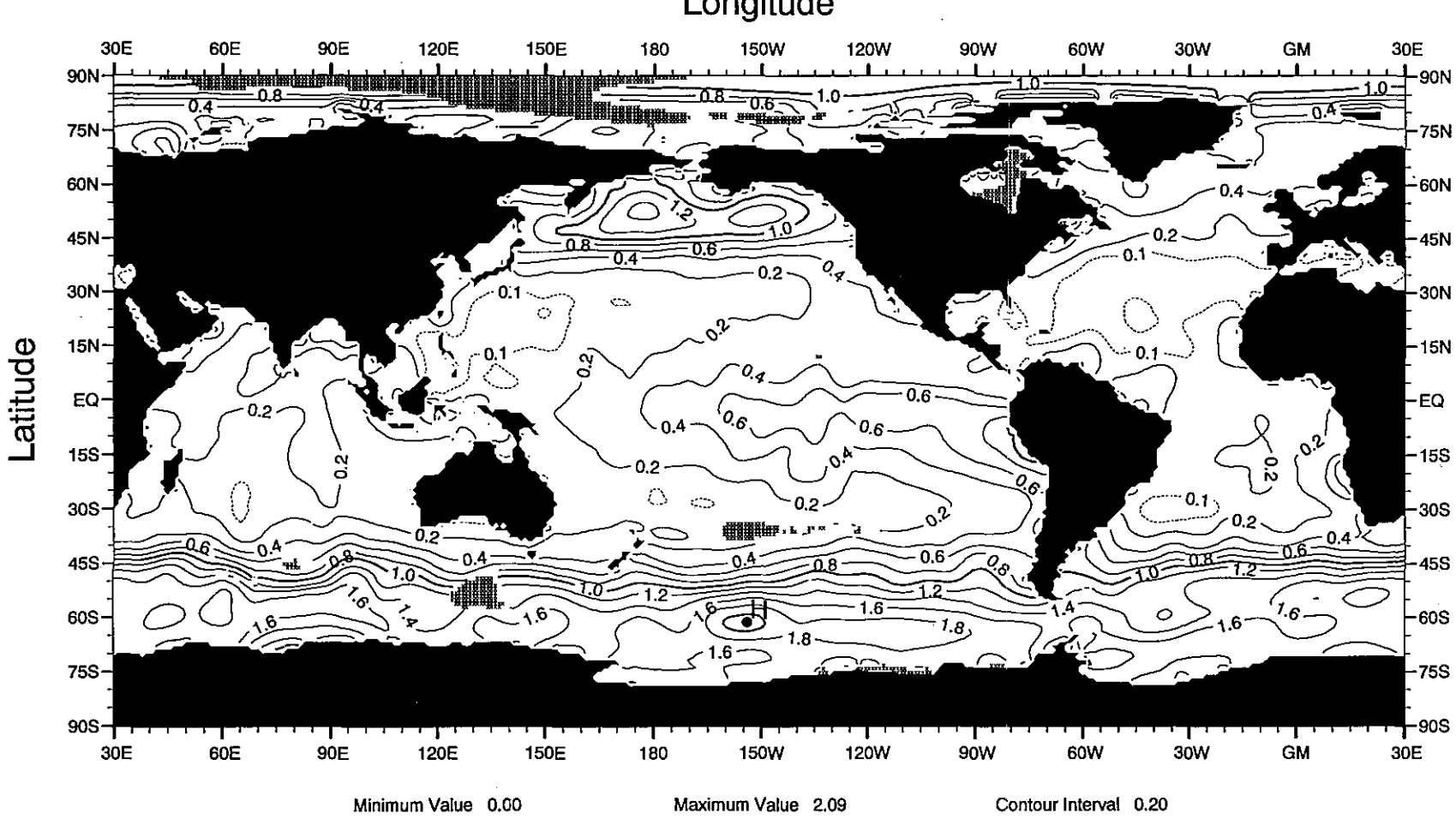

Fig. B1 Annual mean phosphate (μM) at the surface

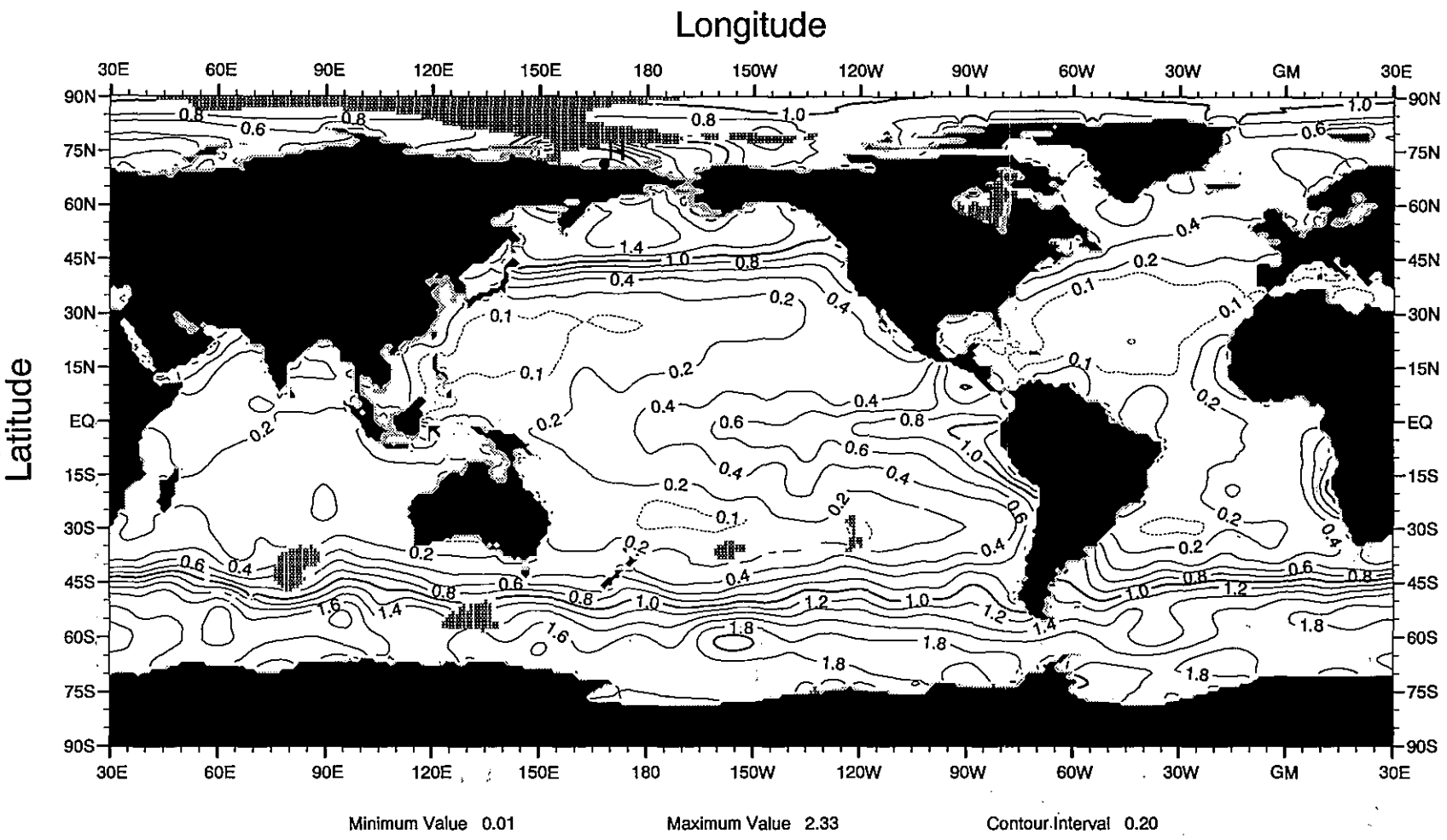

Fig. B2 Annual mean phosphate (μM) at 30 m depth

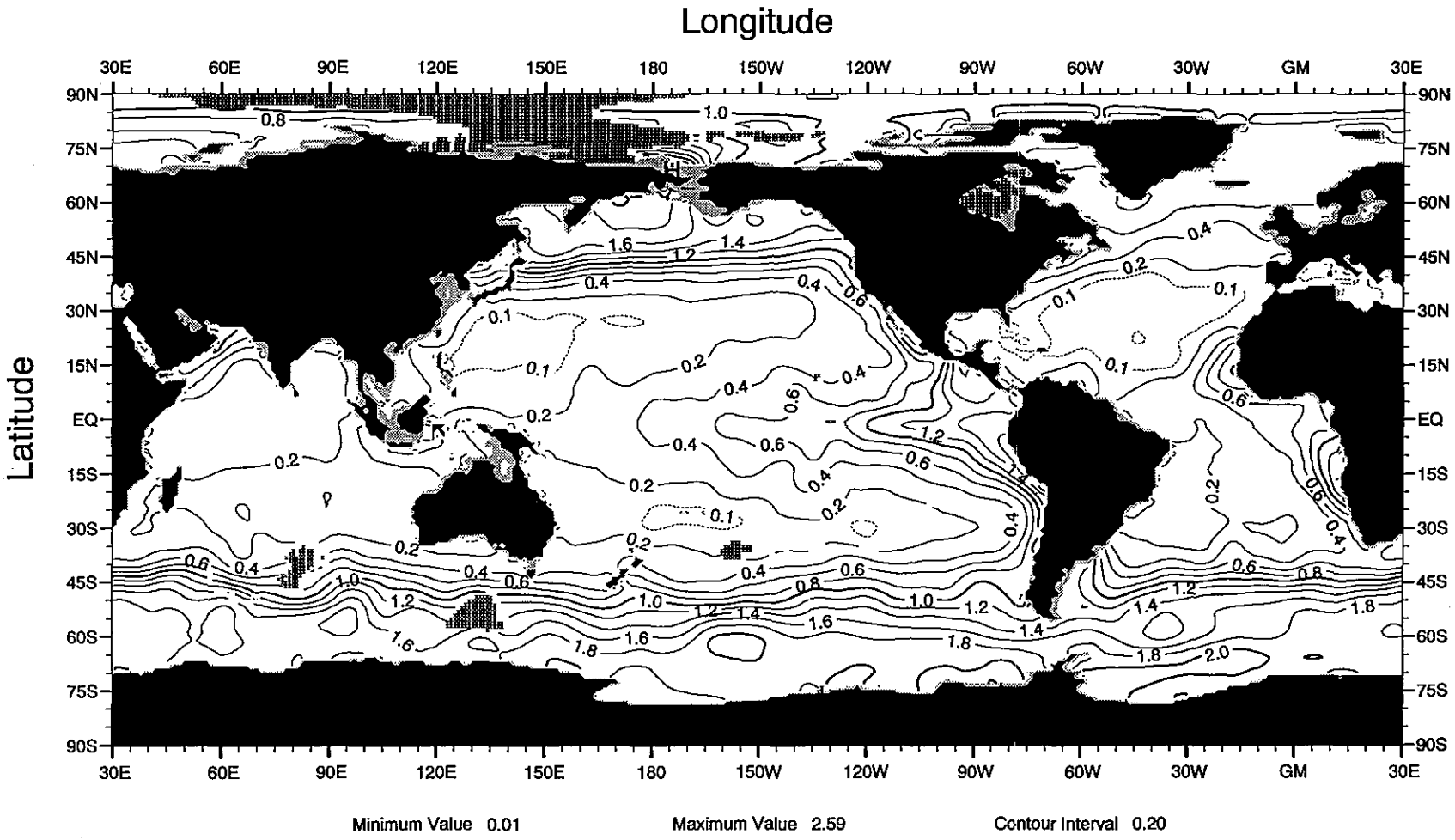

Fig. B3 Annual mean phosphate (μM) at 50 m depth

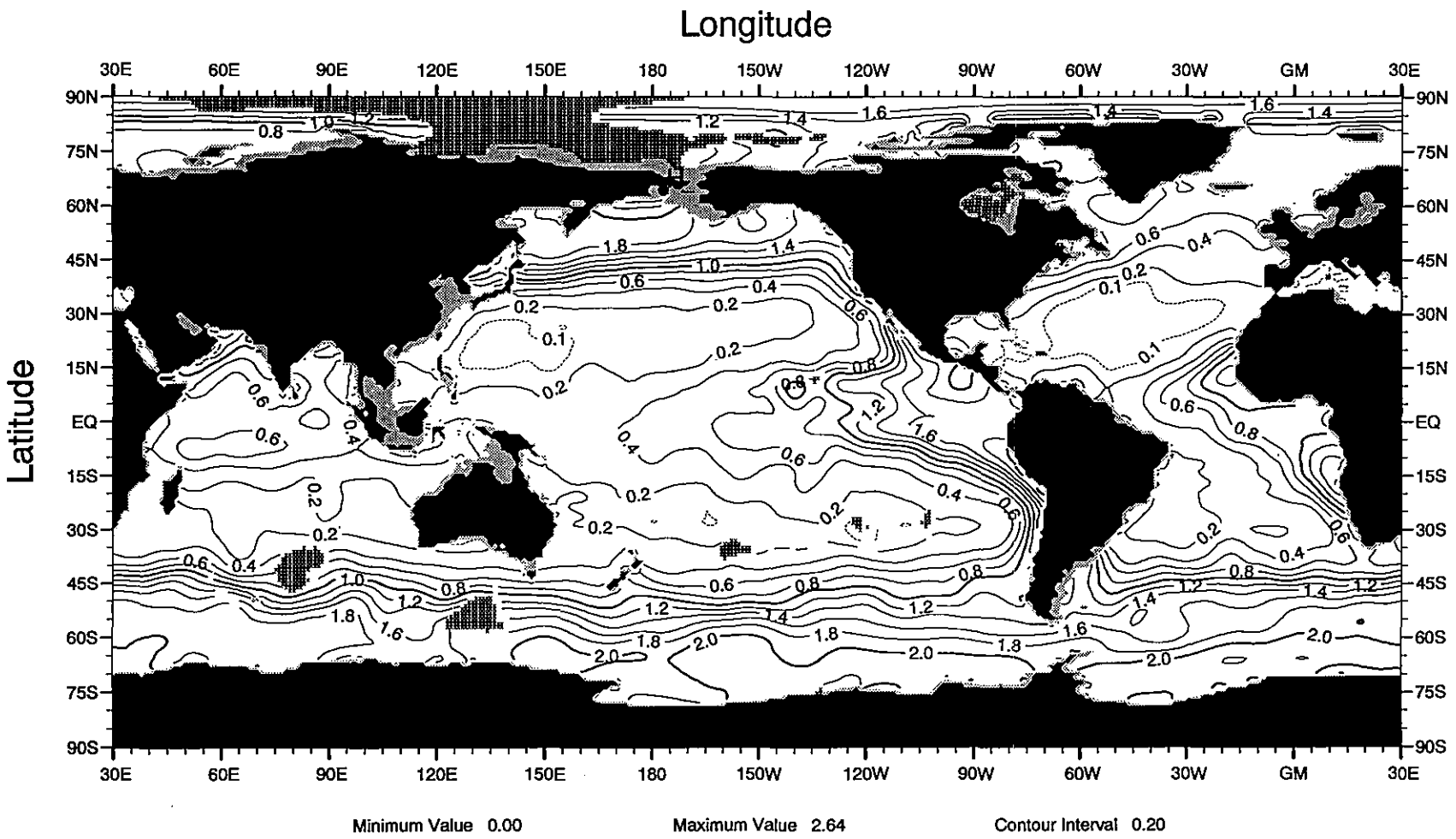

Fig. B4 Annual mean phosphate (μM) at 75 m depth

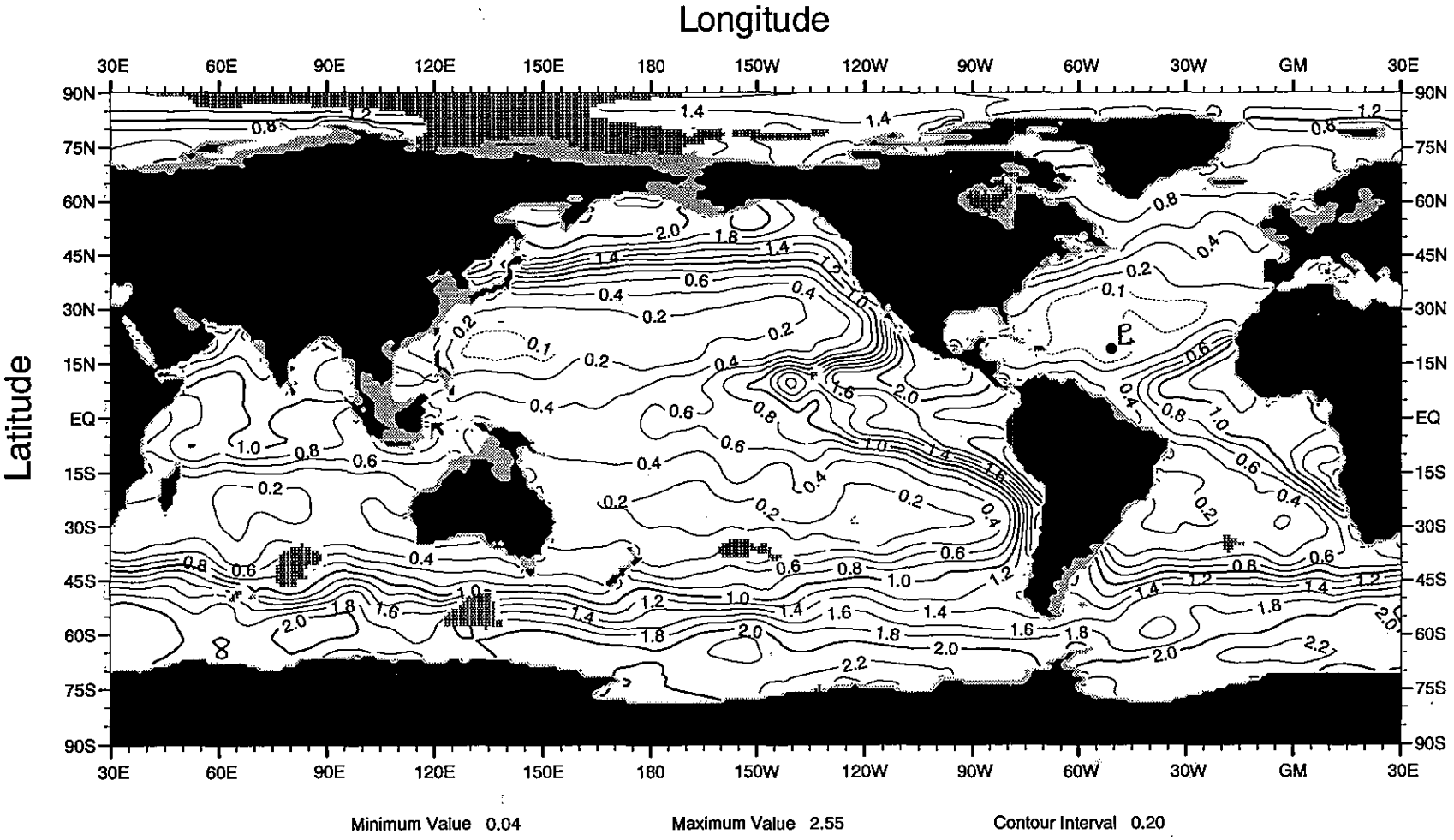

Fig. B5 Annual mean phosphate (μM) at 100 m depth

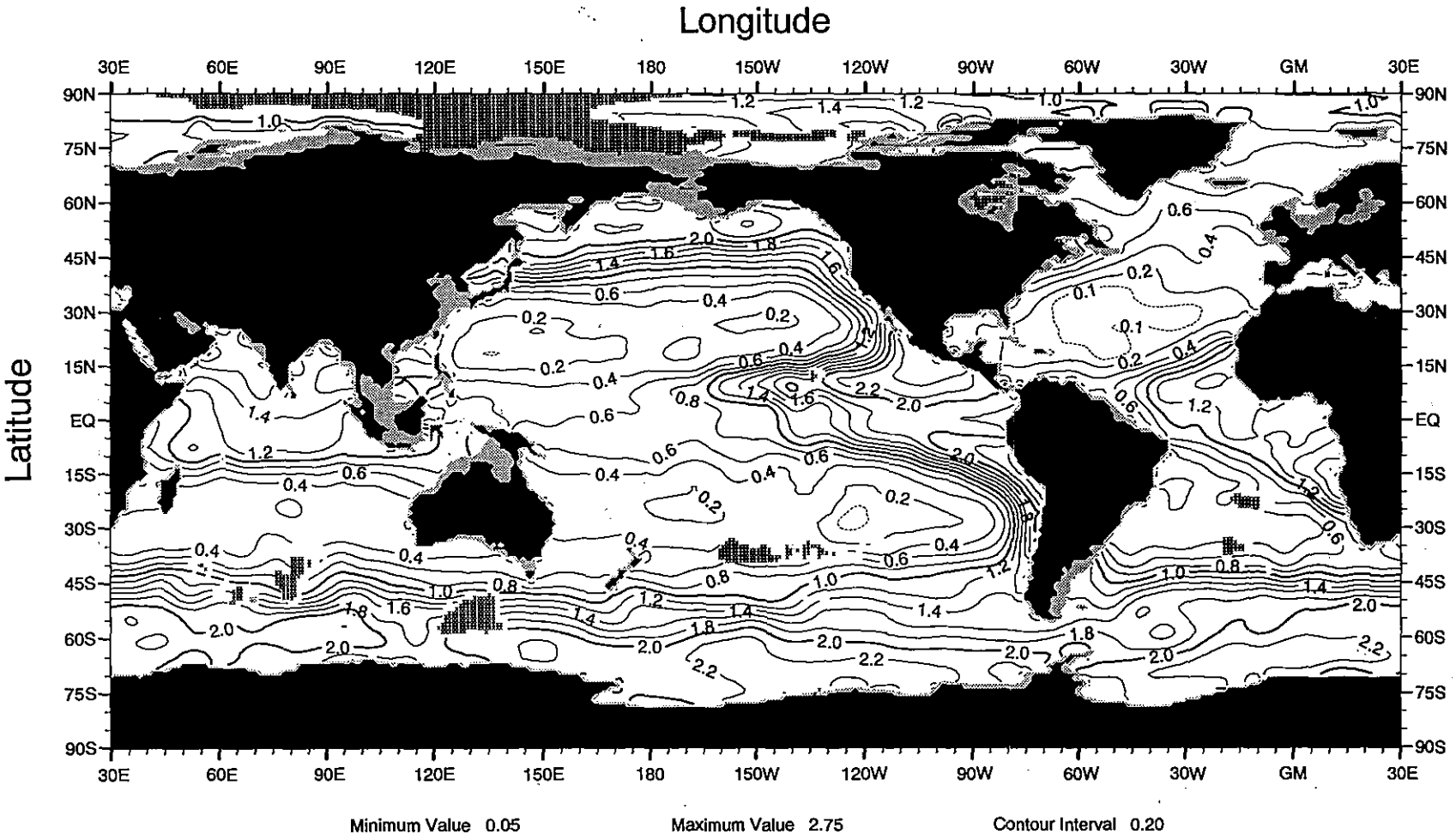

Fig. B6 Annual mean phosphate (μM) at 125 m depth

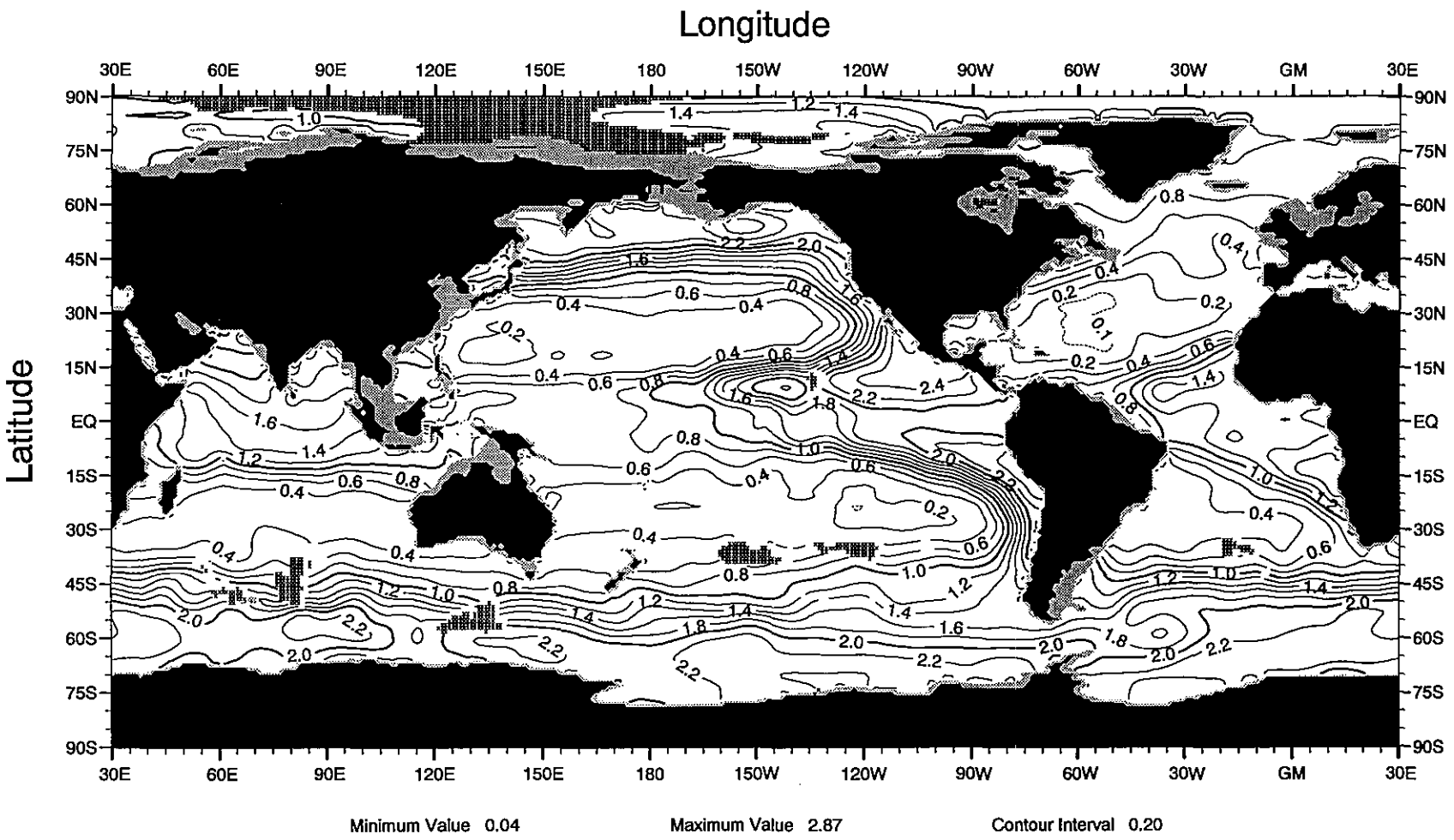

Fig. B7 Annual mean phosphate (μM) at 150 m depth

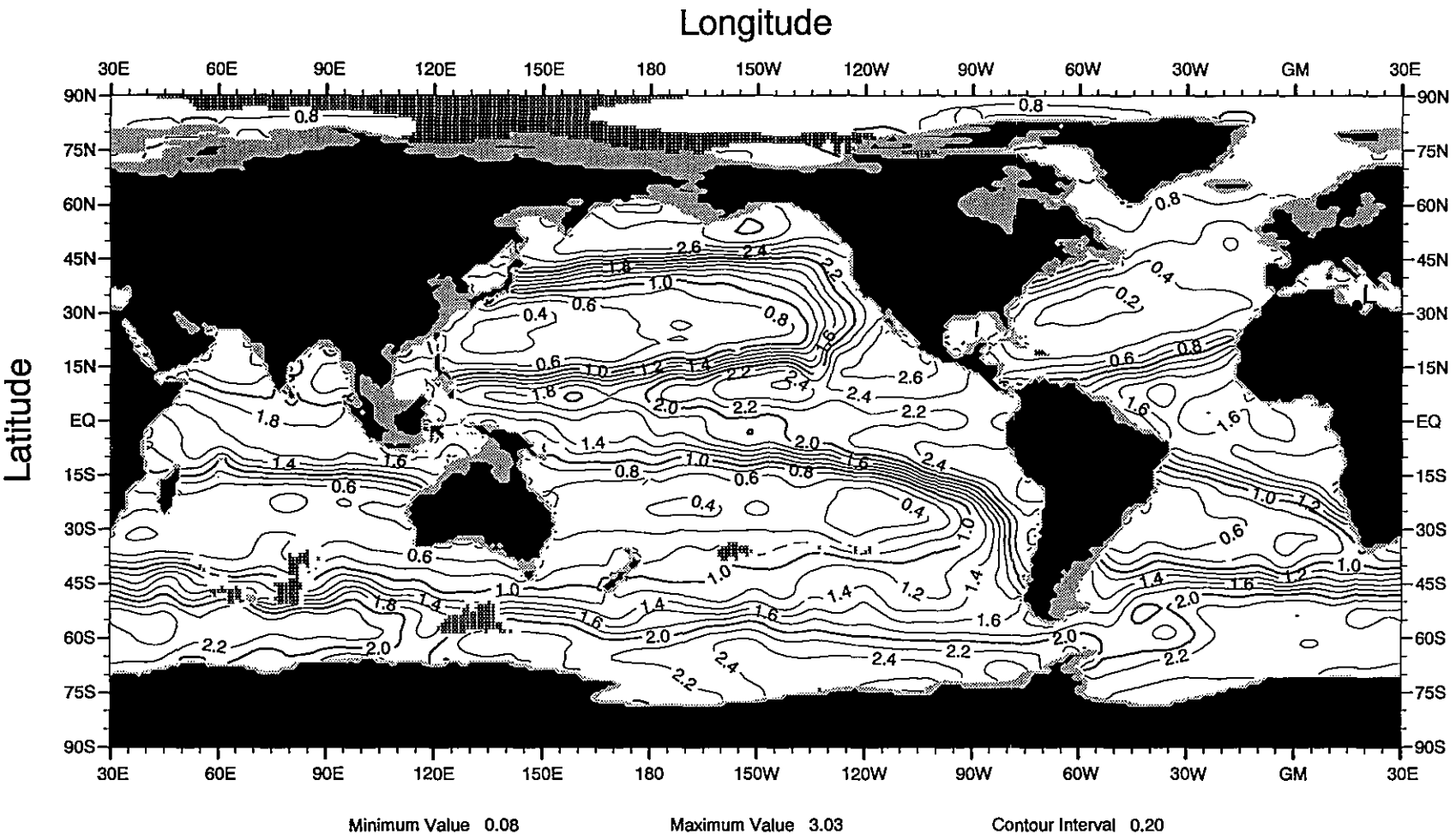

Fig. B8 Annual mean phosphate (μM) at 250 m depth

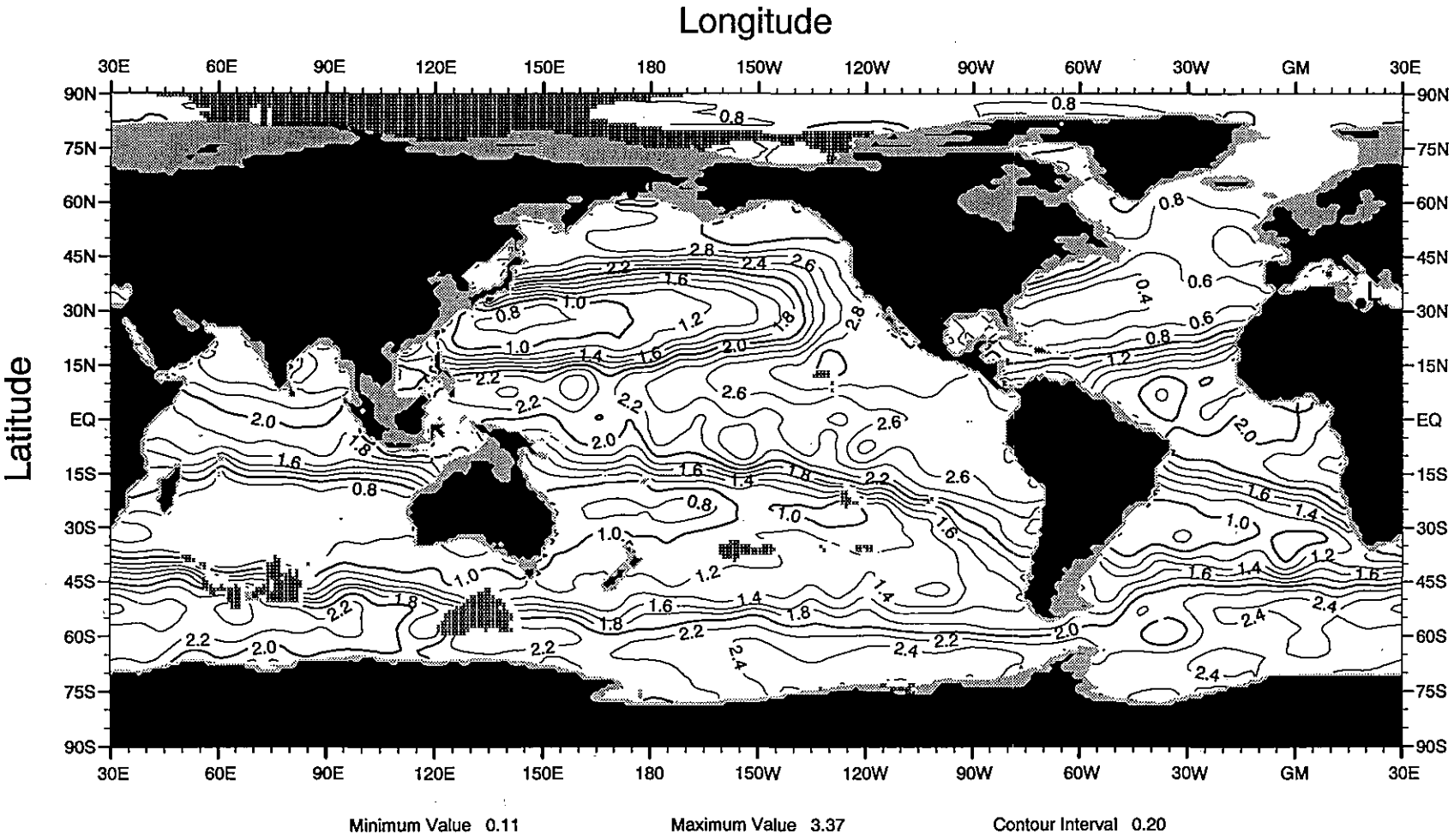

Fig. B9 Annual mean phosphate (μM) at 400 m depth

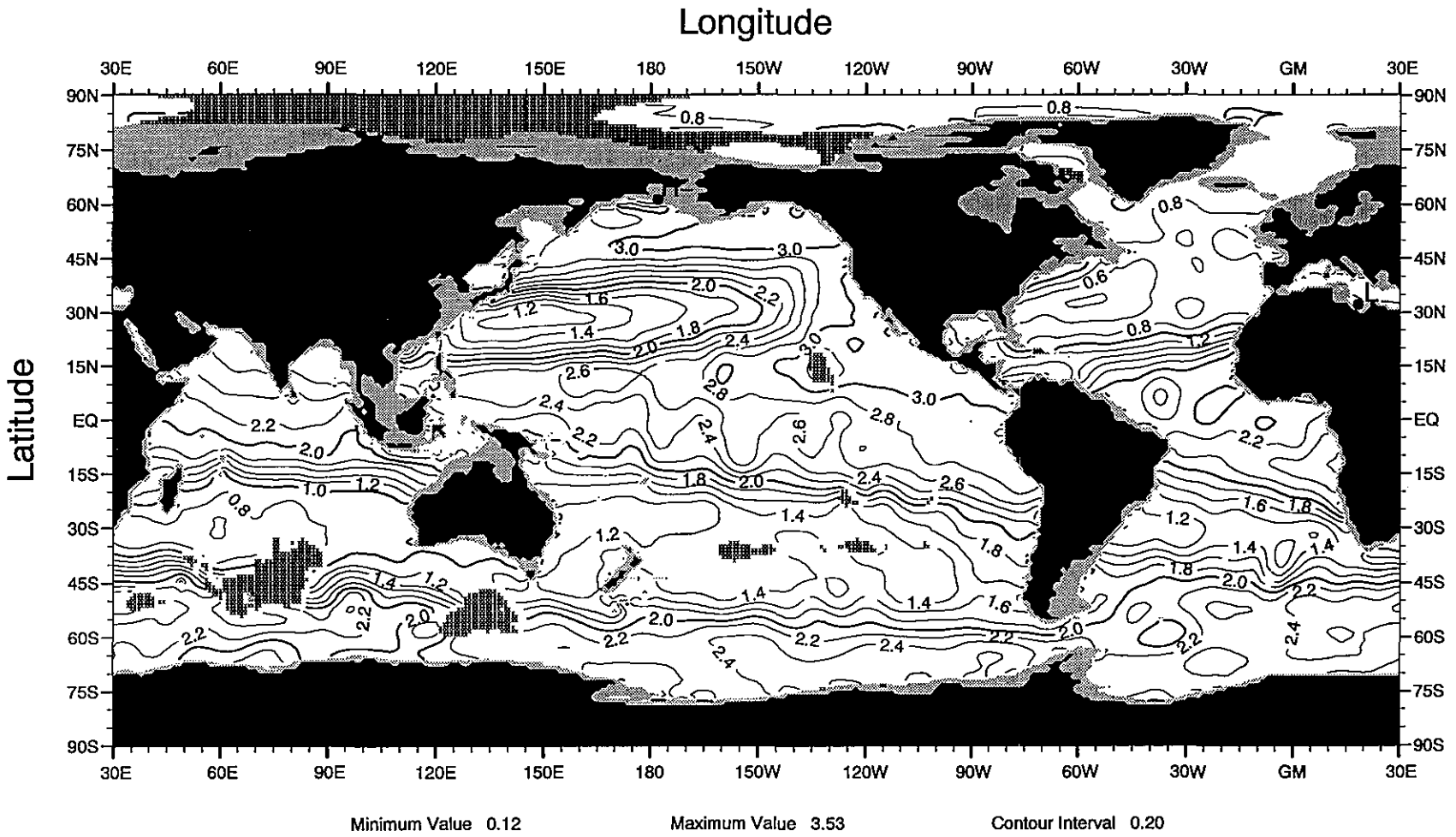

Fig. B10 Annual mean phosphate (μM) at 500 m depth

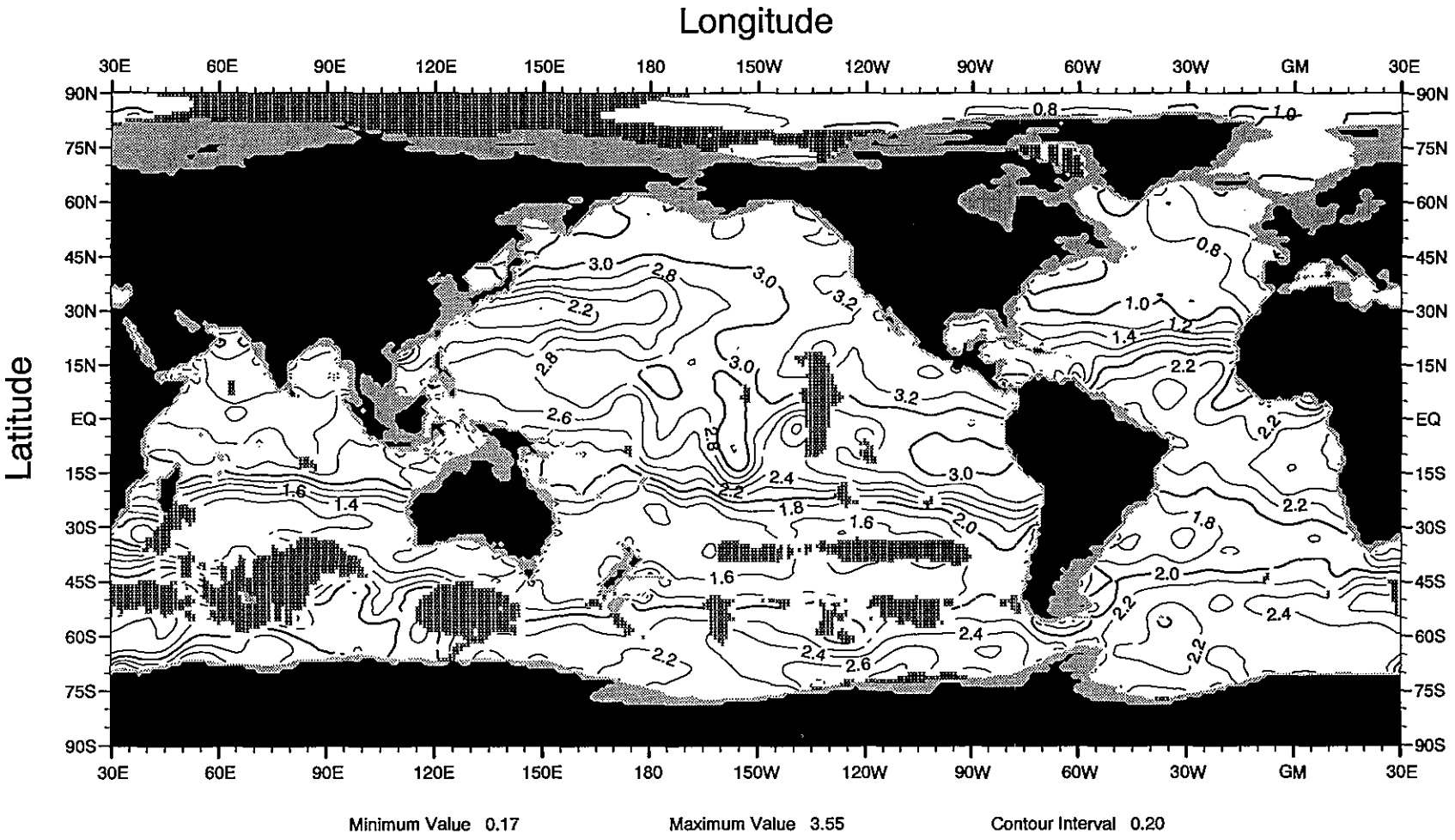

Fig. B11 Annual mean phosphate (μM) at 700 m depth

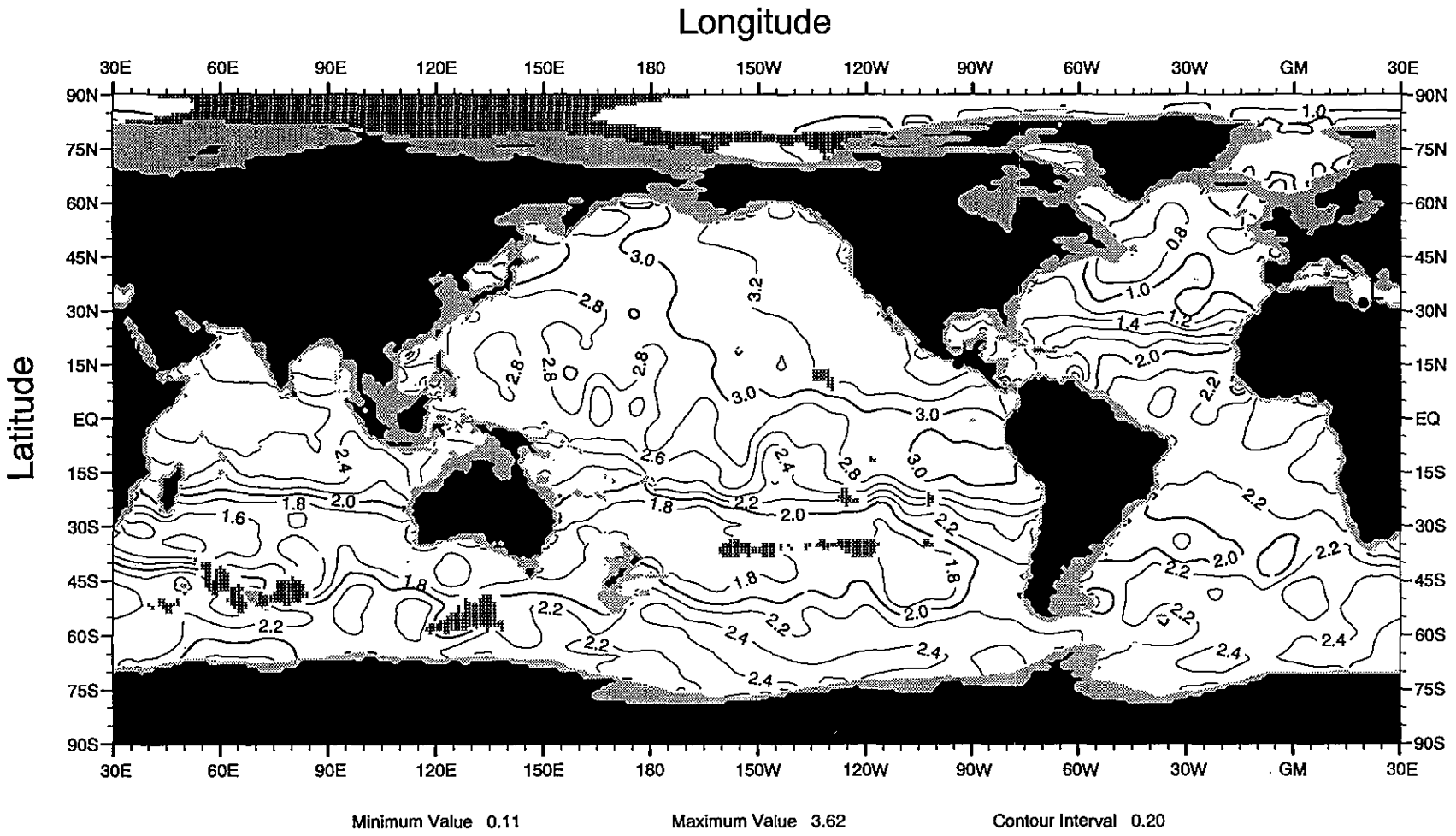

Fig. B12 Annual mean phosphate (μM) at 900 m depth

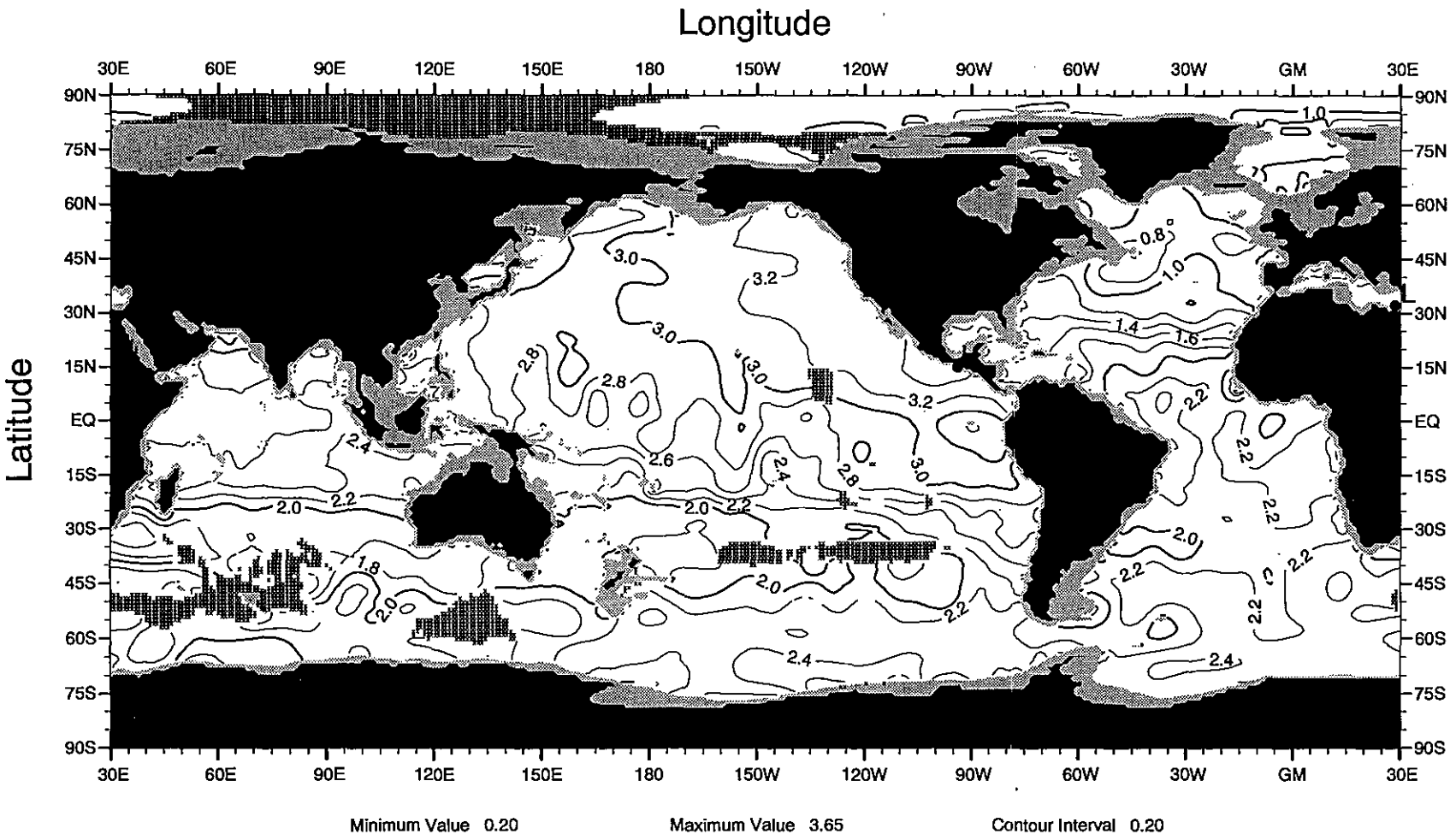

Fig. B13 Annual mean phosphate (μM) at 1000 m depth

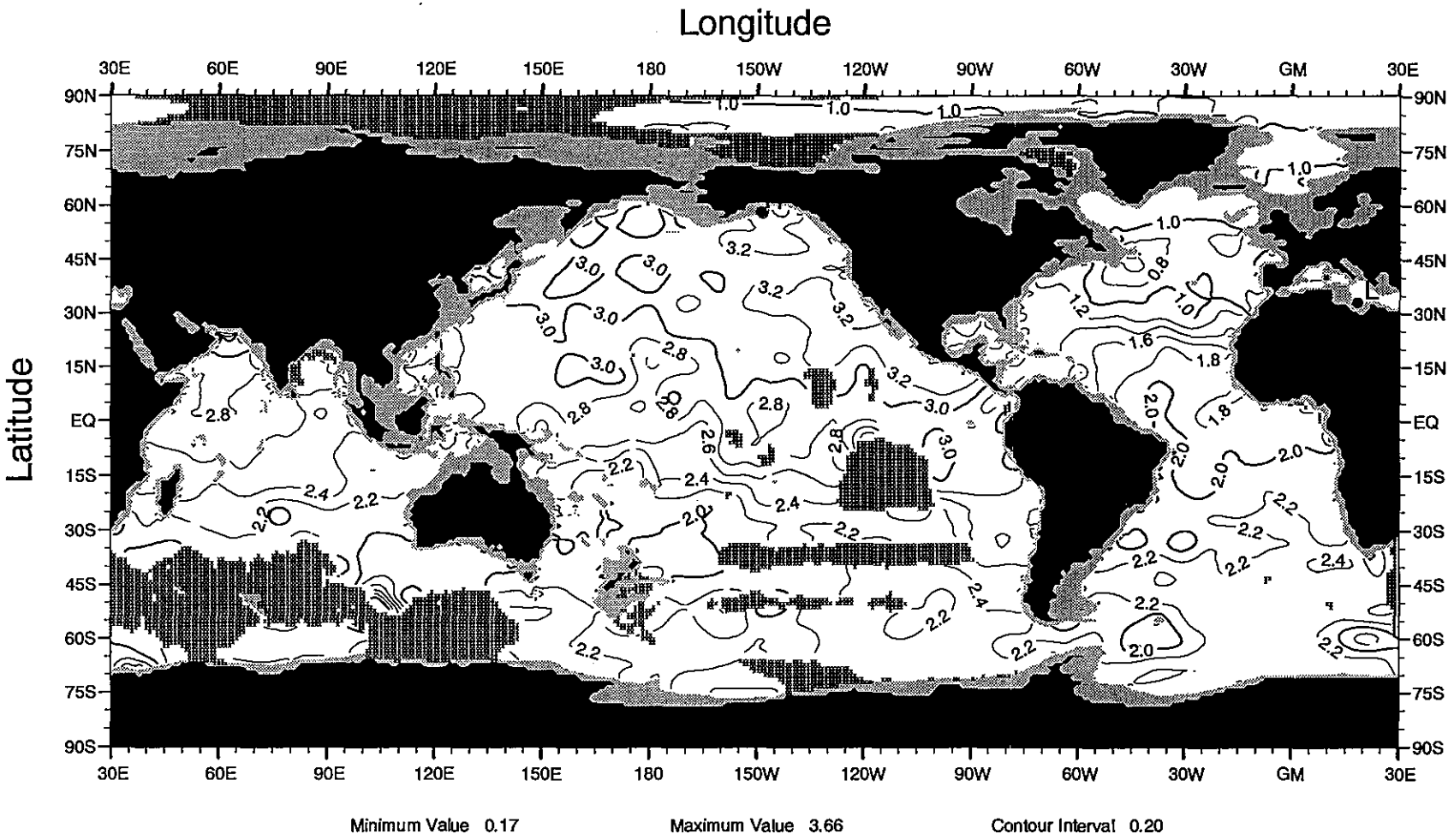

Fig. B14 Annual mean phosphate (μM) at 1200 m depth

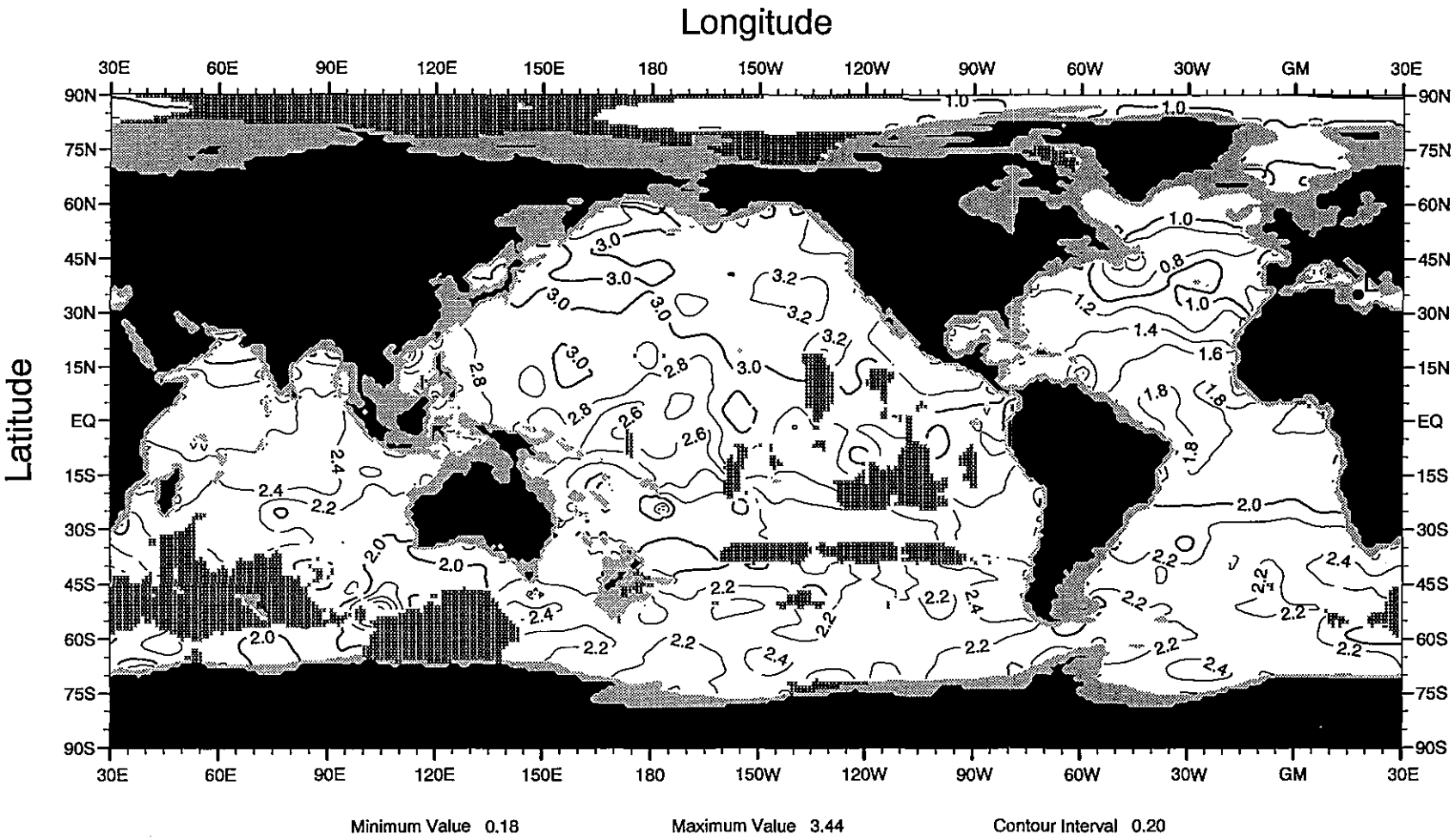

Fig. B15 Annual mean phosphate (μM) at 1300 m depth

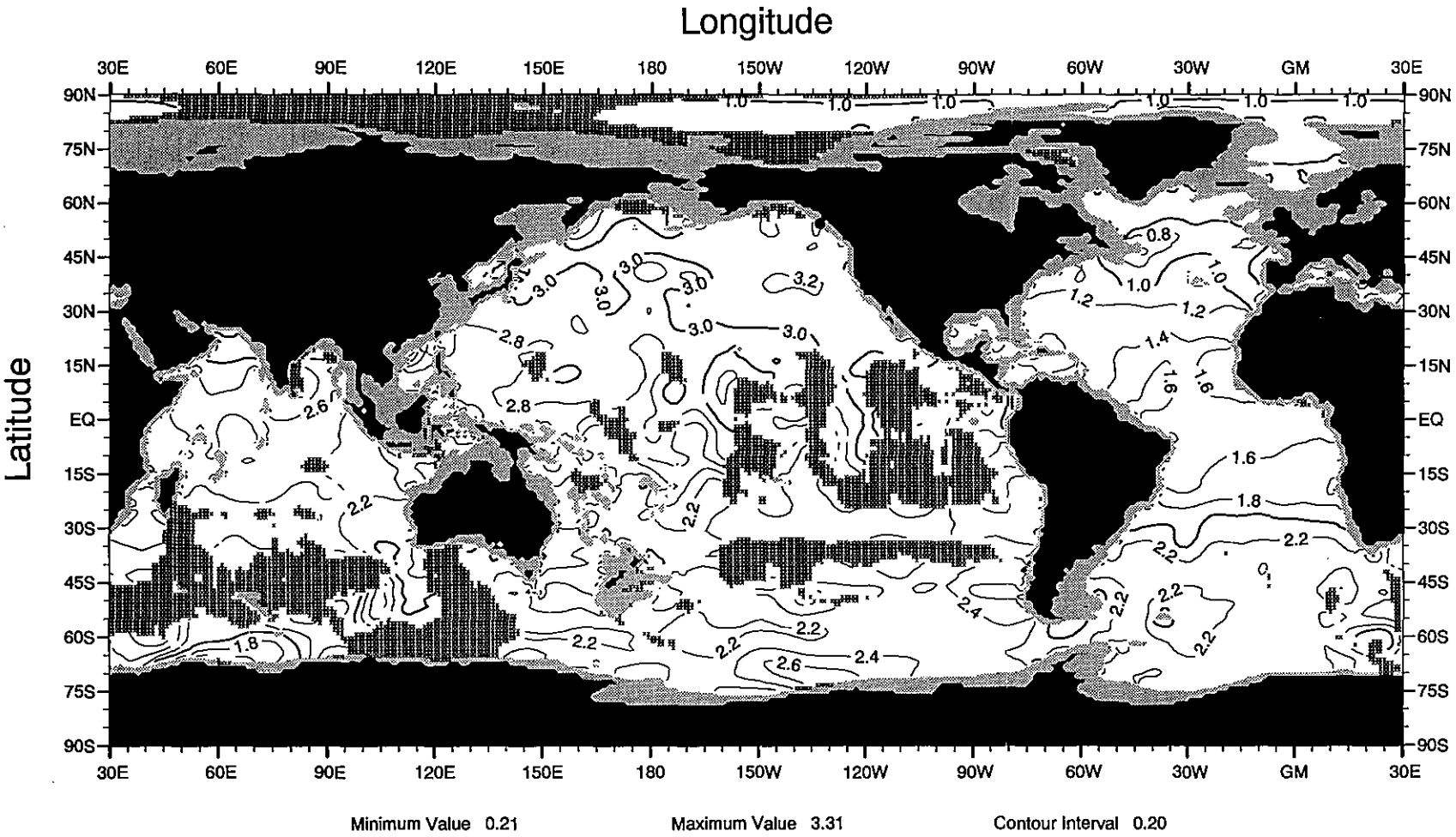

Fig. B16 Annual mean phosphate (μM) at 1500 m depth

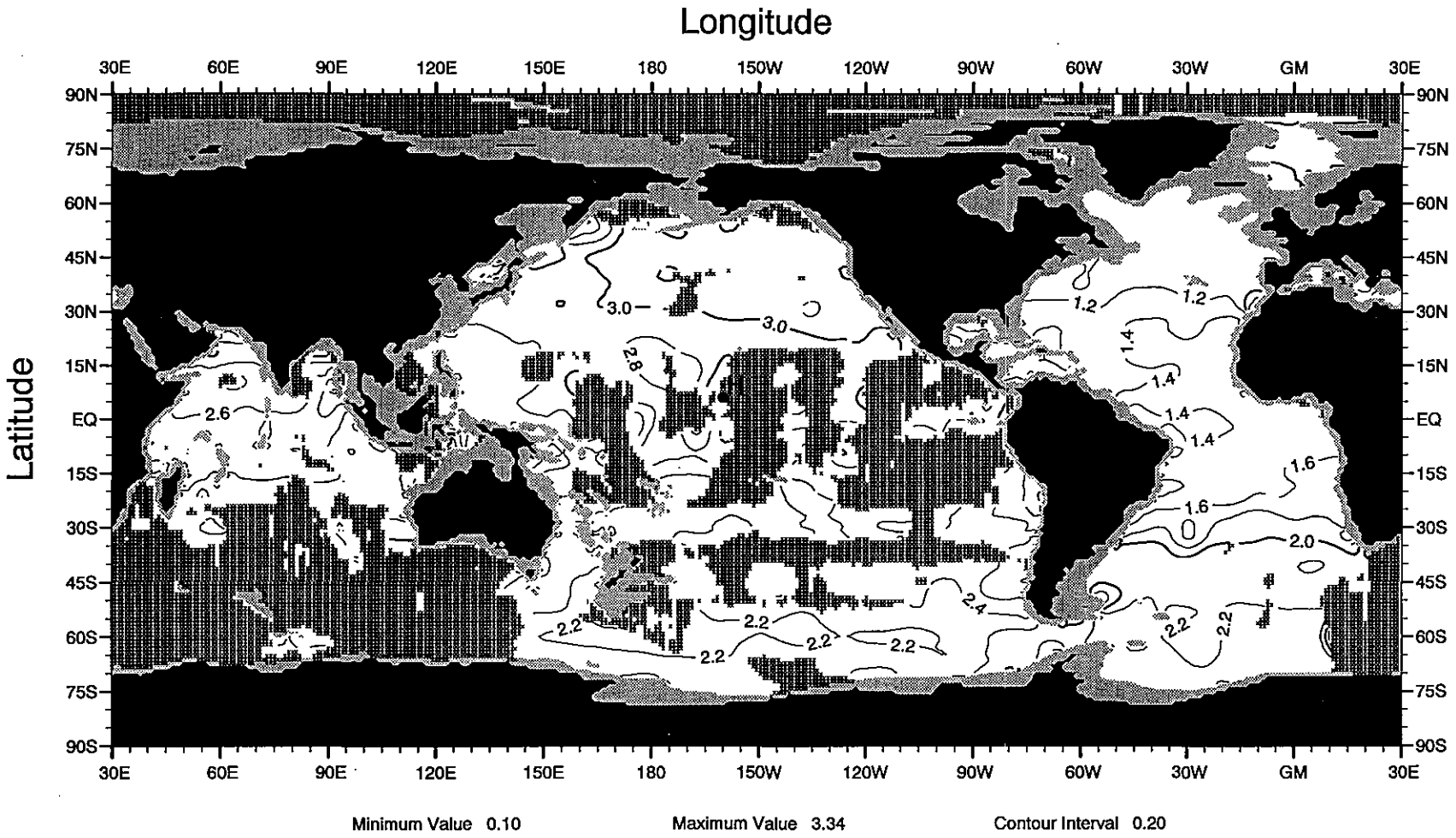

Fig. B17 Annual mean phosphate (μM) at 1750 m depth

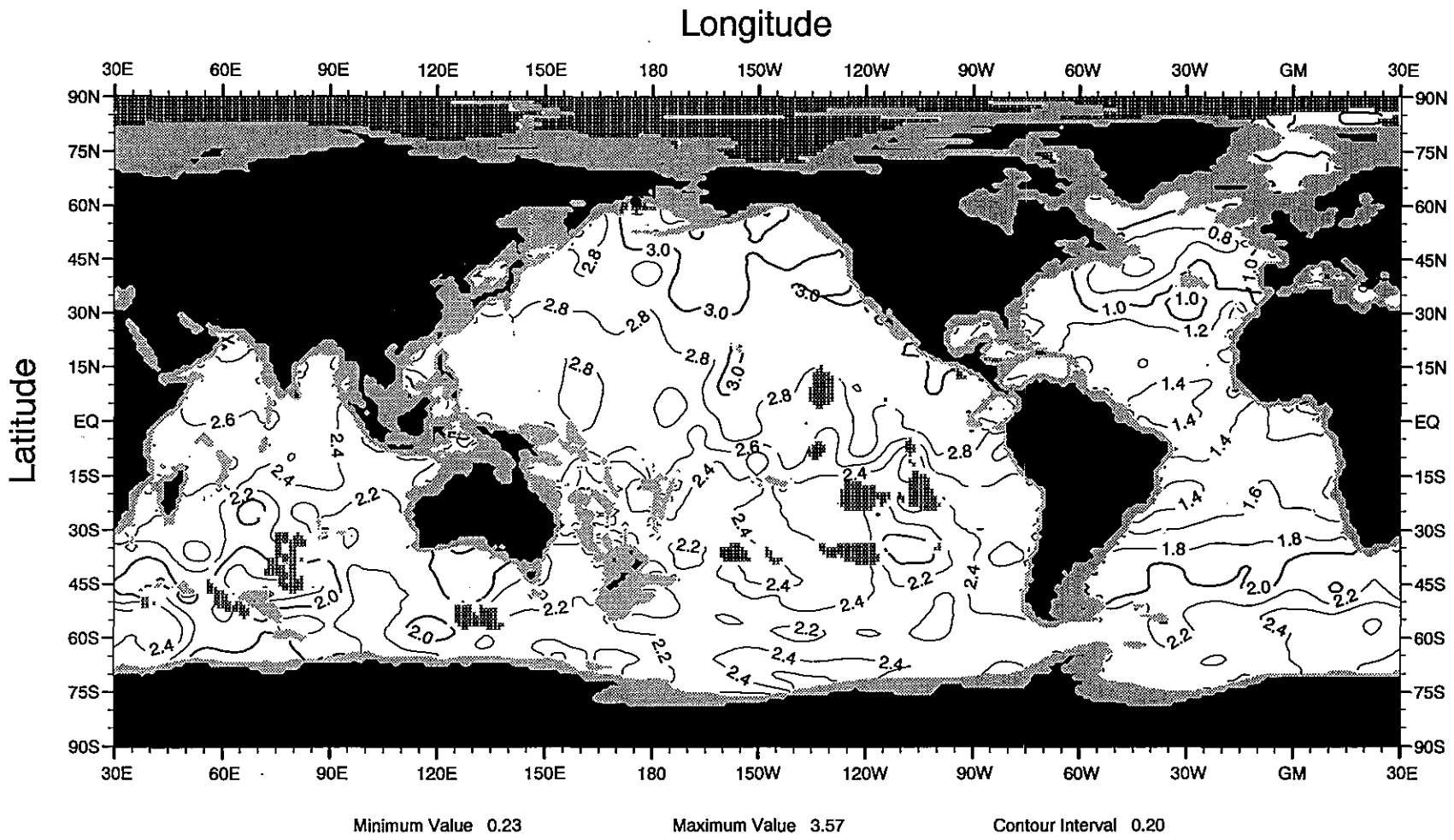

Fig. B18 Annual mean phosphate (μM) at 2000 m depth

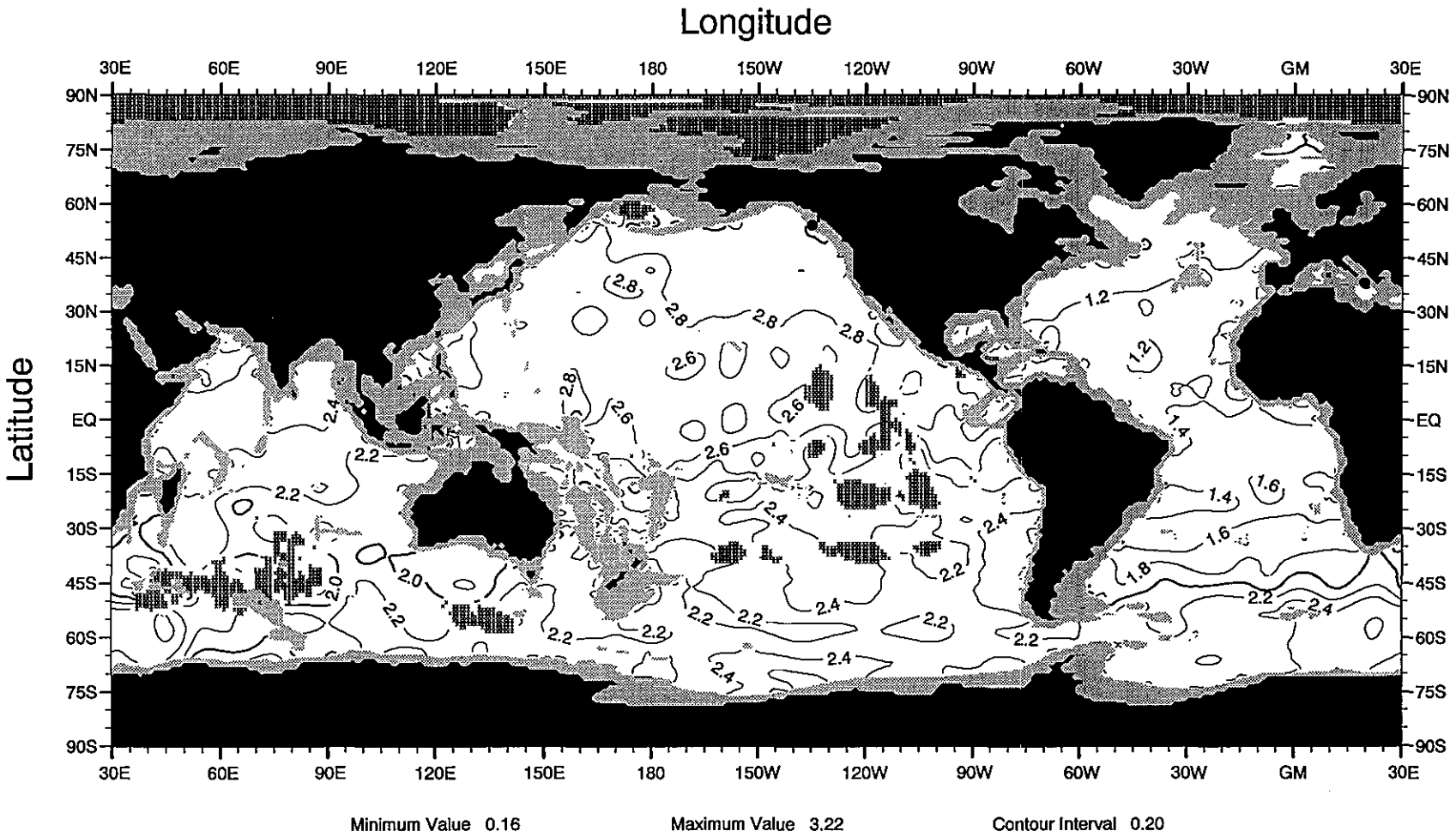

Fig. B19 Annual mean phosphate (μM) at 2500 m depth

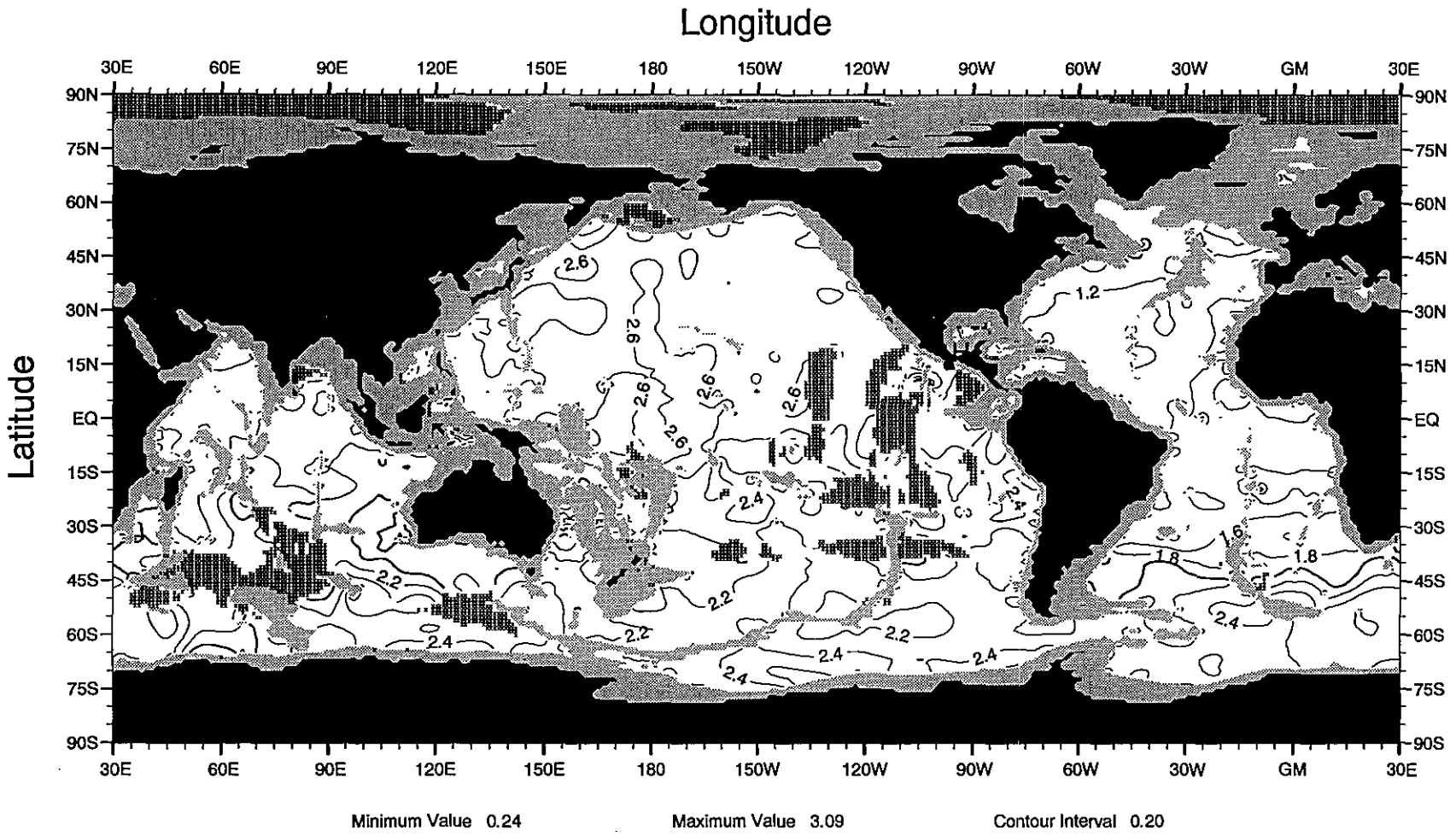

Fig. B20 Annual mean phosphate (μM) at 3000 m depth

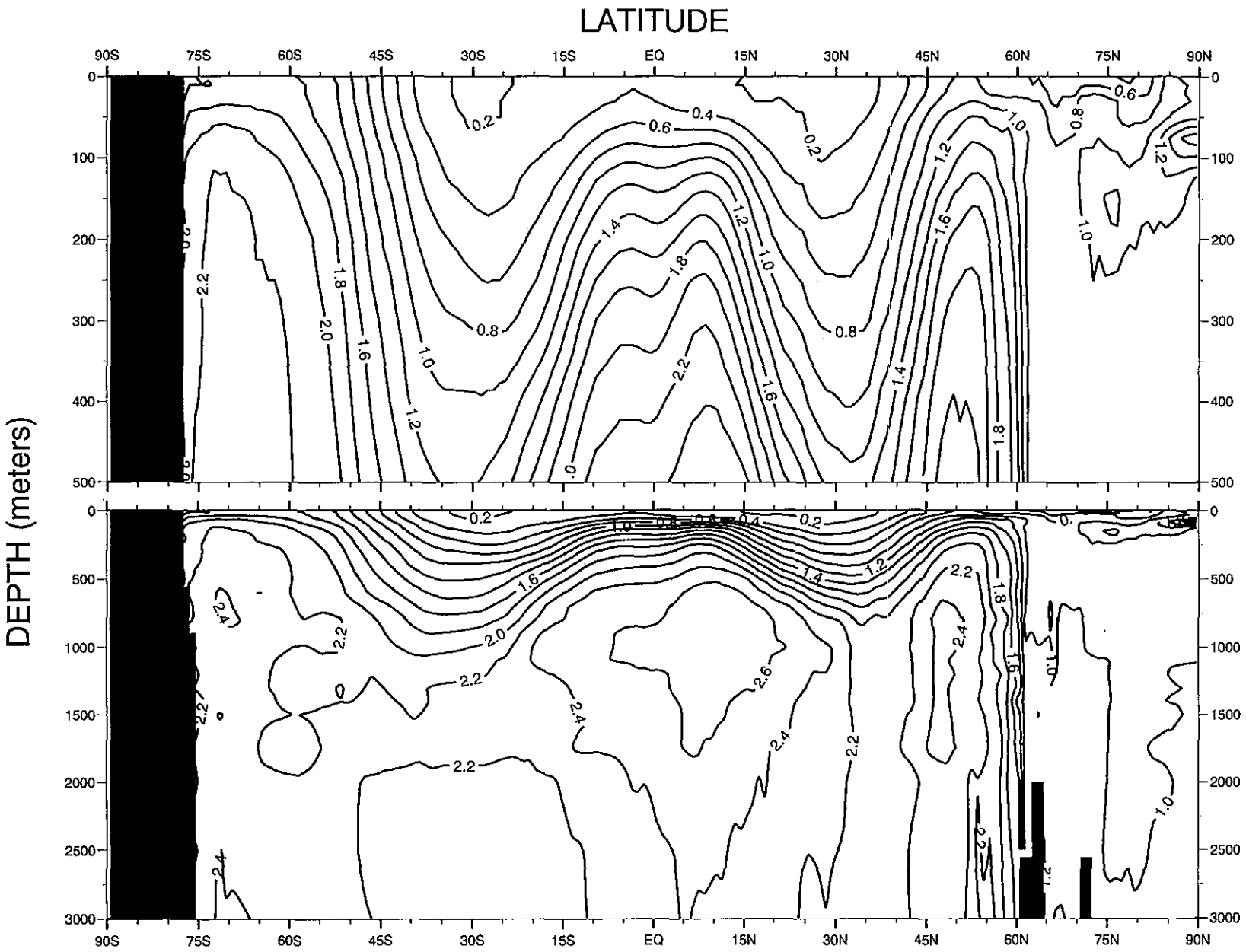

Fig C1. Annual global zonal average (by one-degree squares) of phosphate (μM)

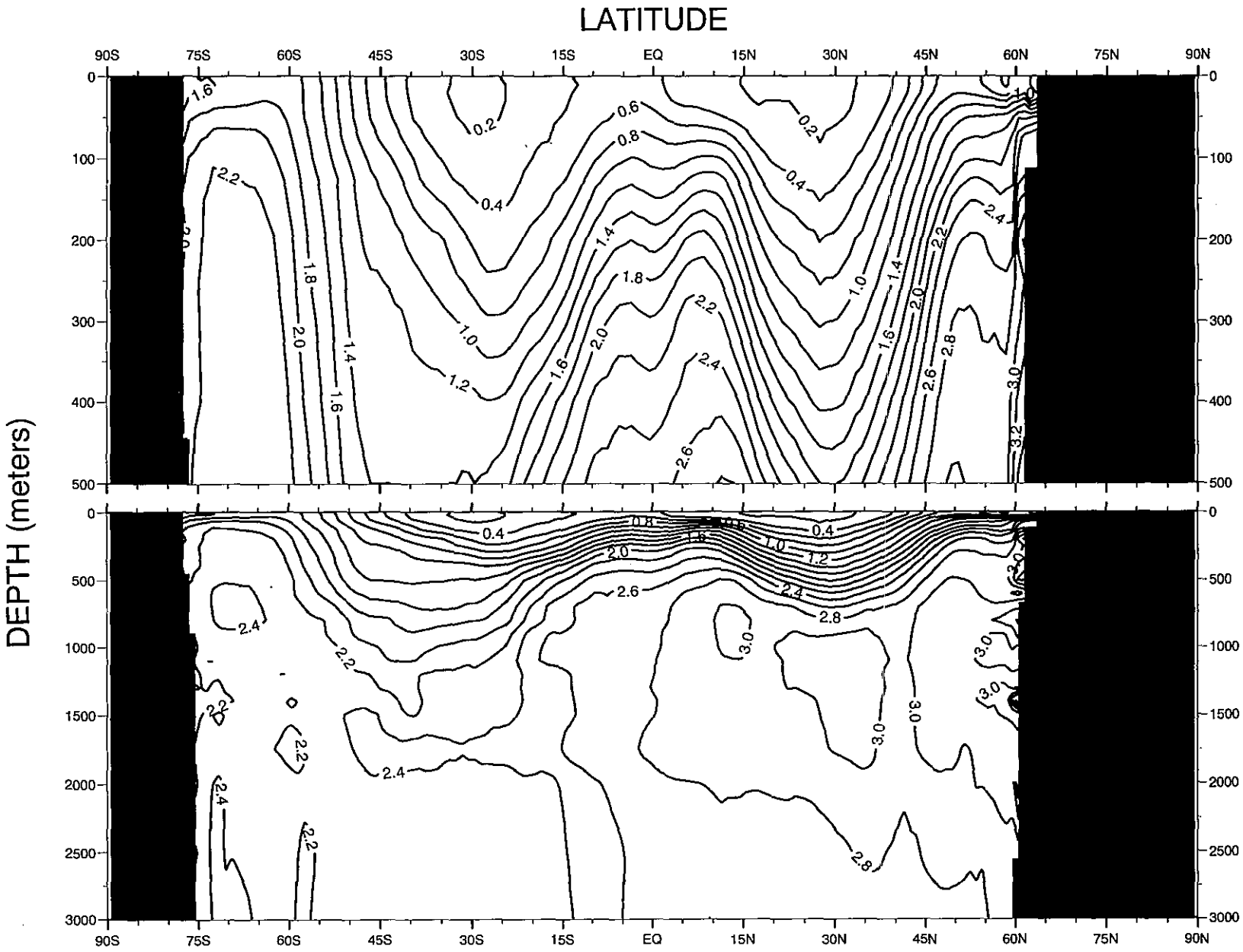

Fig C2. Annual Pacific zonal average (by one-degree squares) of phosphate (μM)

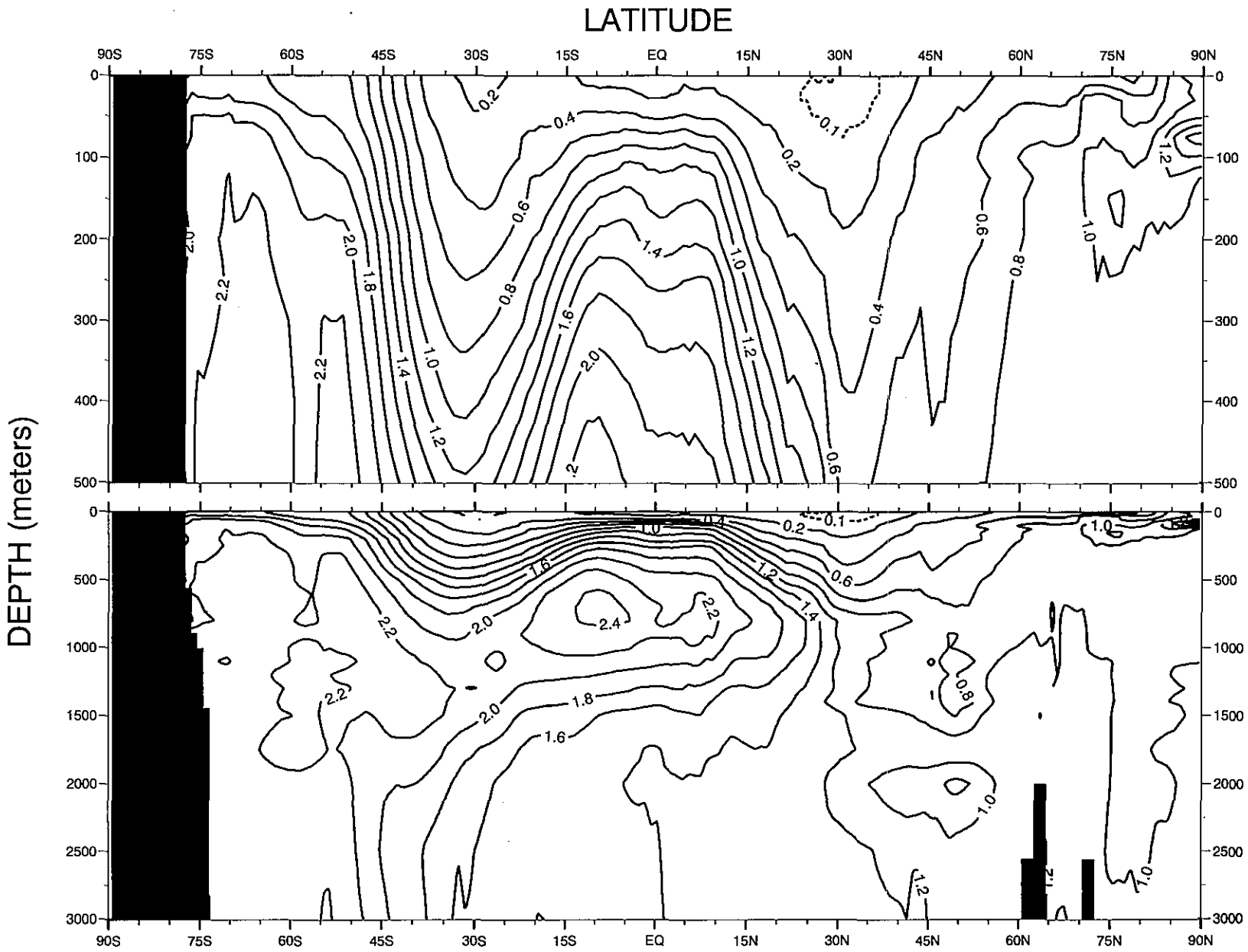

Fig C3. Annual Atlantic zonal average (by one-degree squares) of phosphate (μM)

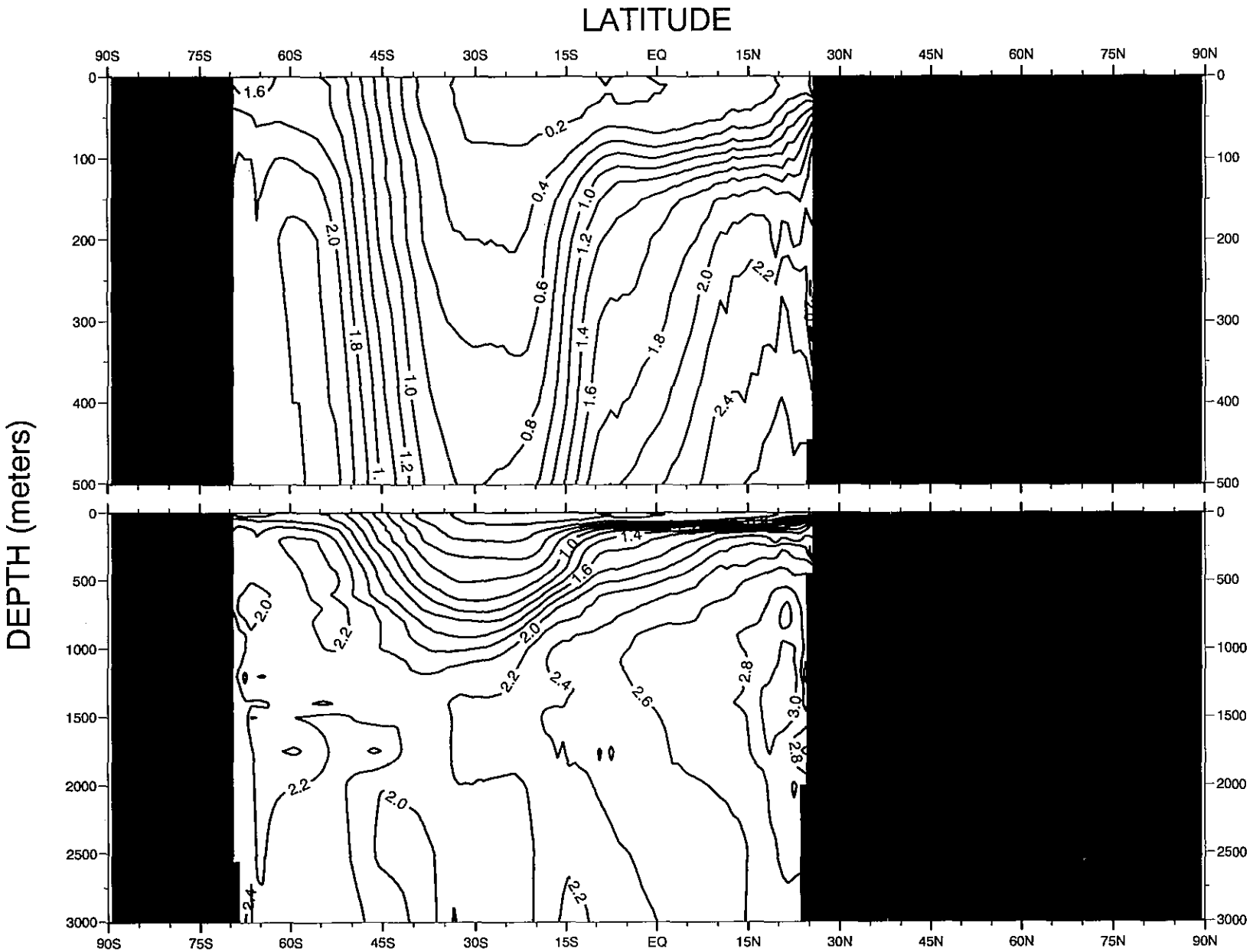

Fig C4. Annual Indian zonal average (by one-degree squares) of phosphate (μM)

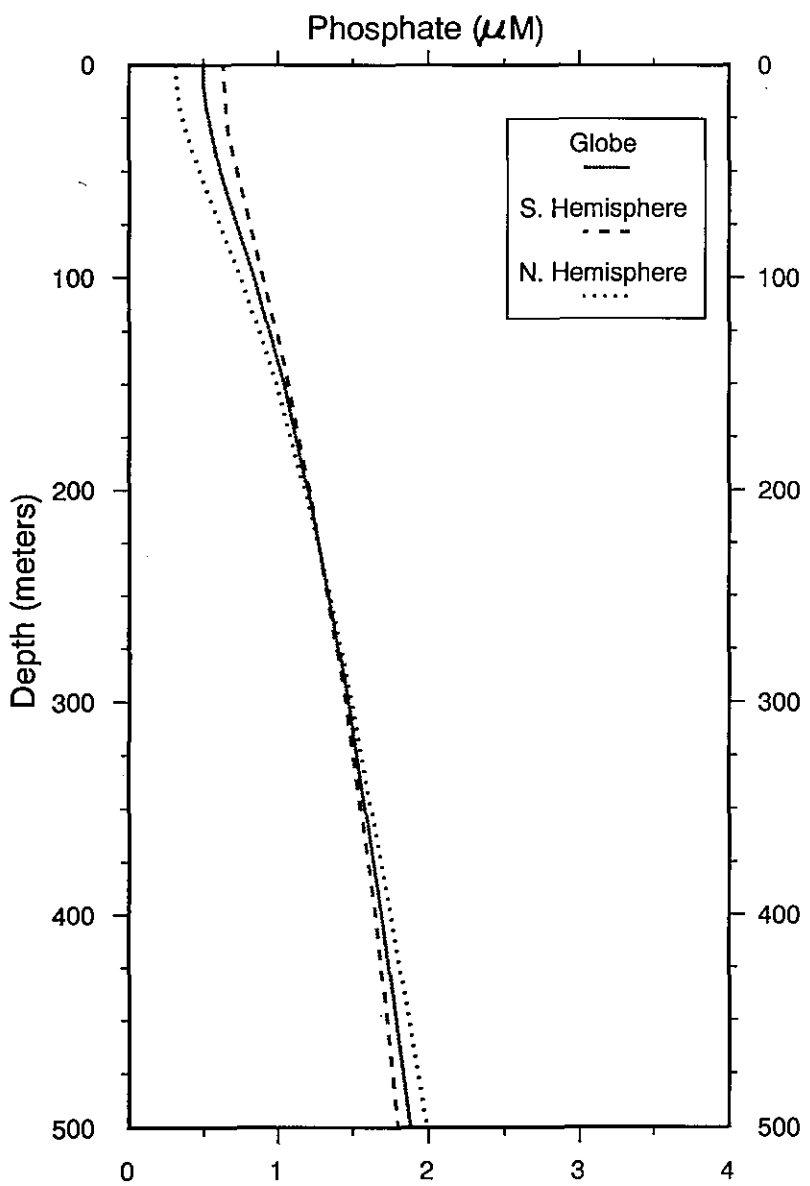

D1a. Annual global phosphate (μM) basin means (0-500 m)

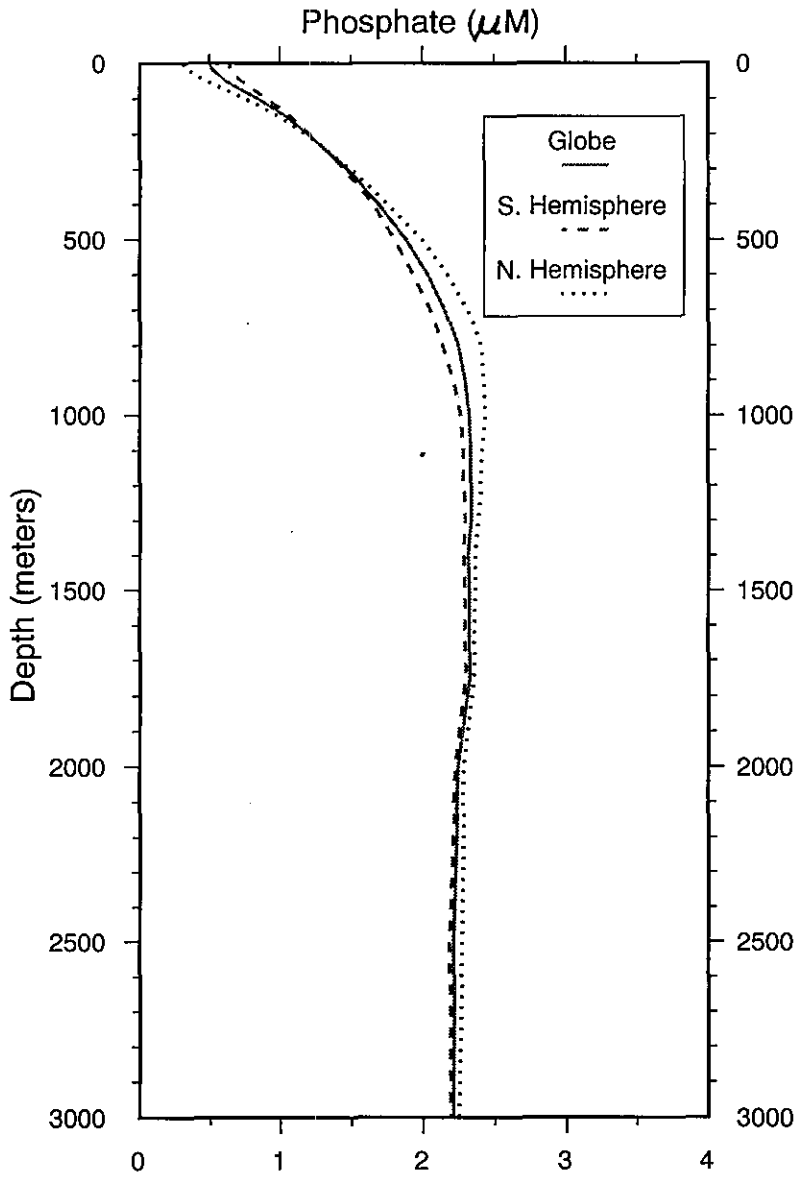

Figure D1b. Annual global phosphate (μM) basin means (0-3000 m)

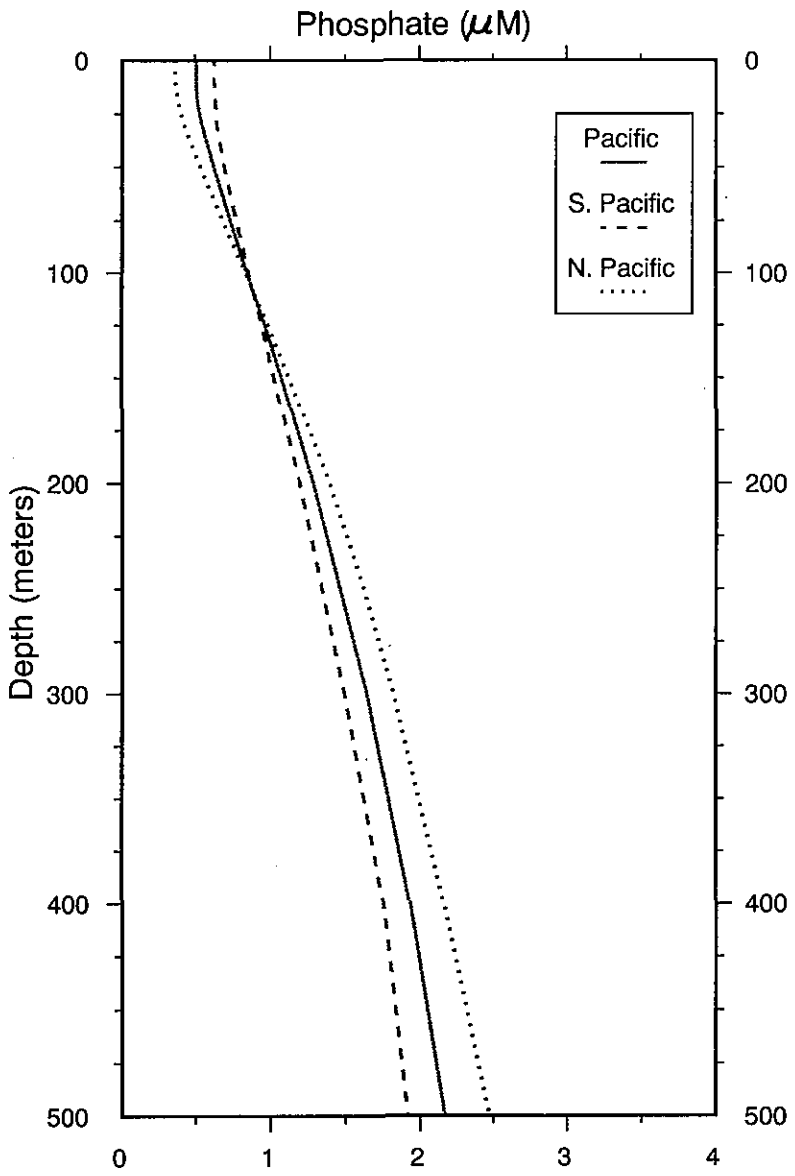

Figure D2a. Annual Pacific phosphate (μM) basin means (0-500 m)

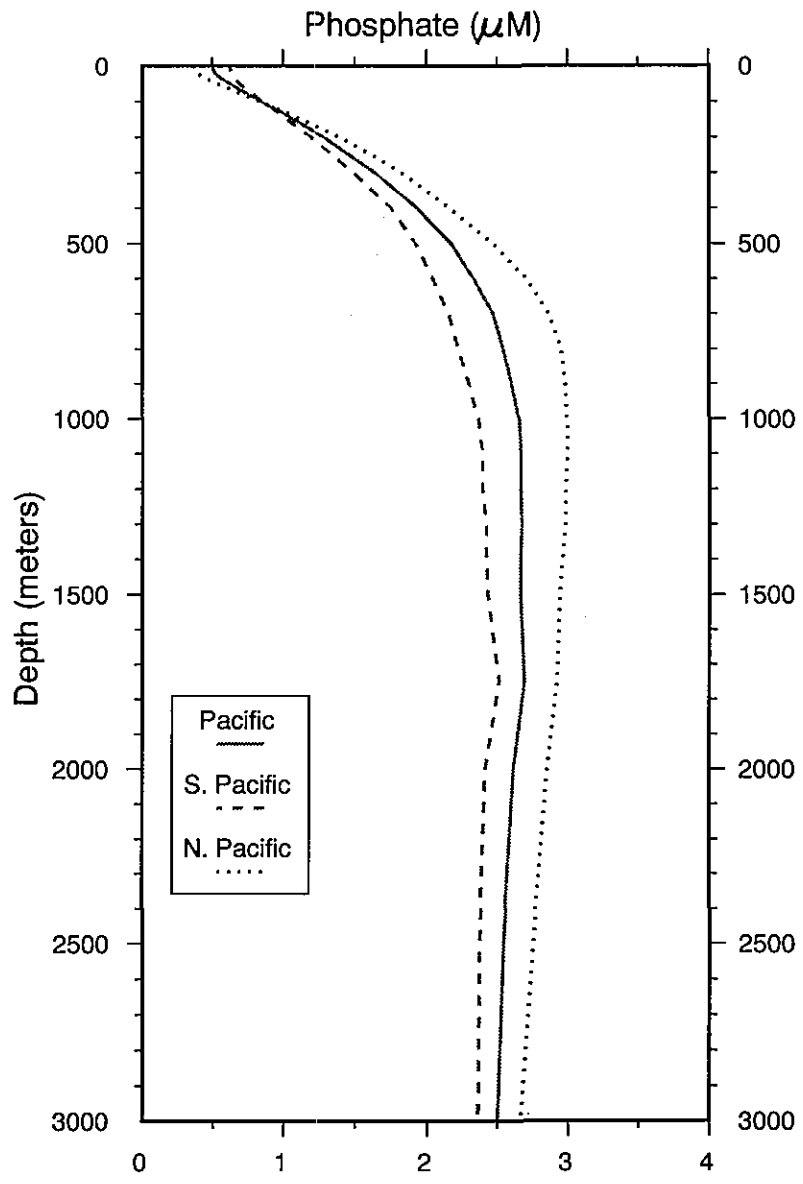

Figure D2b. Annual Pacific phosphate (μM) basin means (0-3000 m)

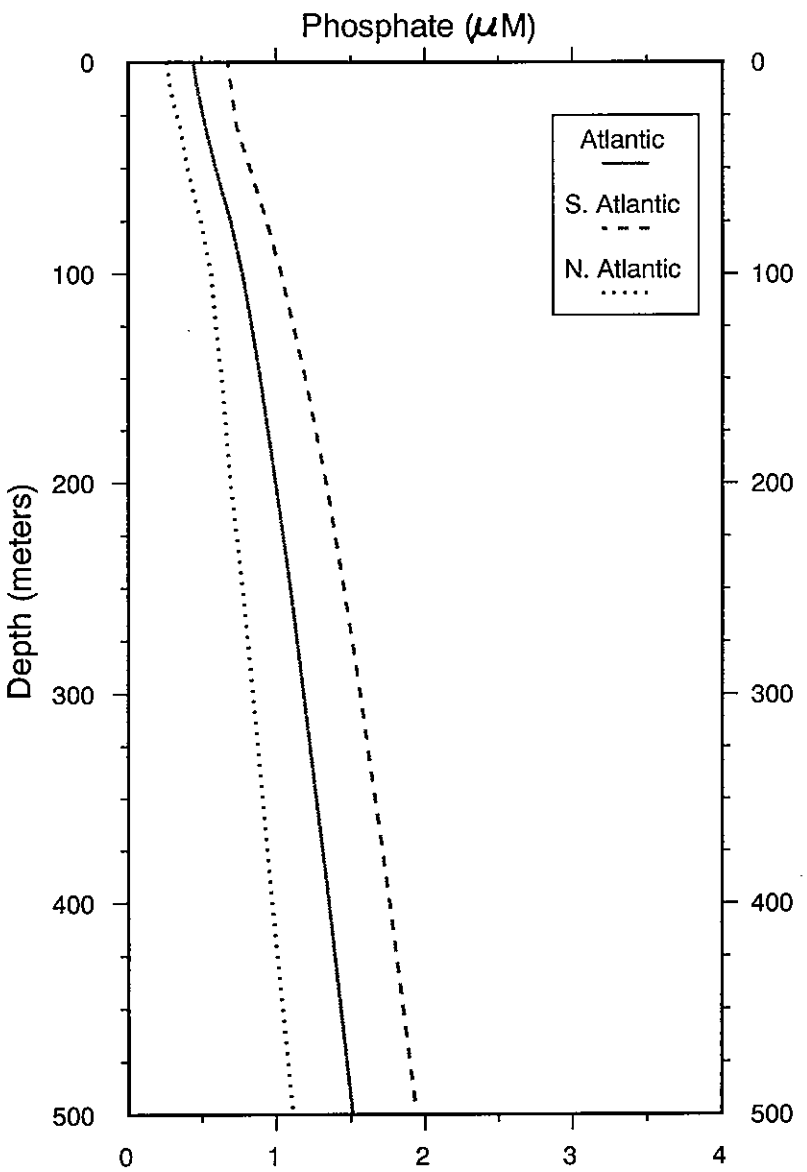

Figure D3a. Annual Atlantic phosphate (μM) basin means (0-500 m)

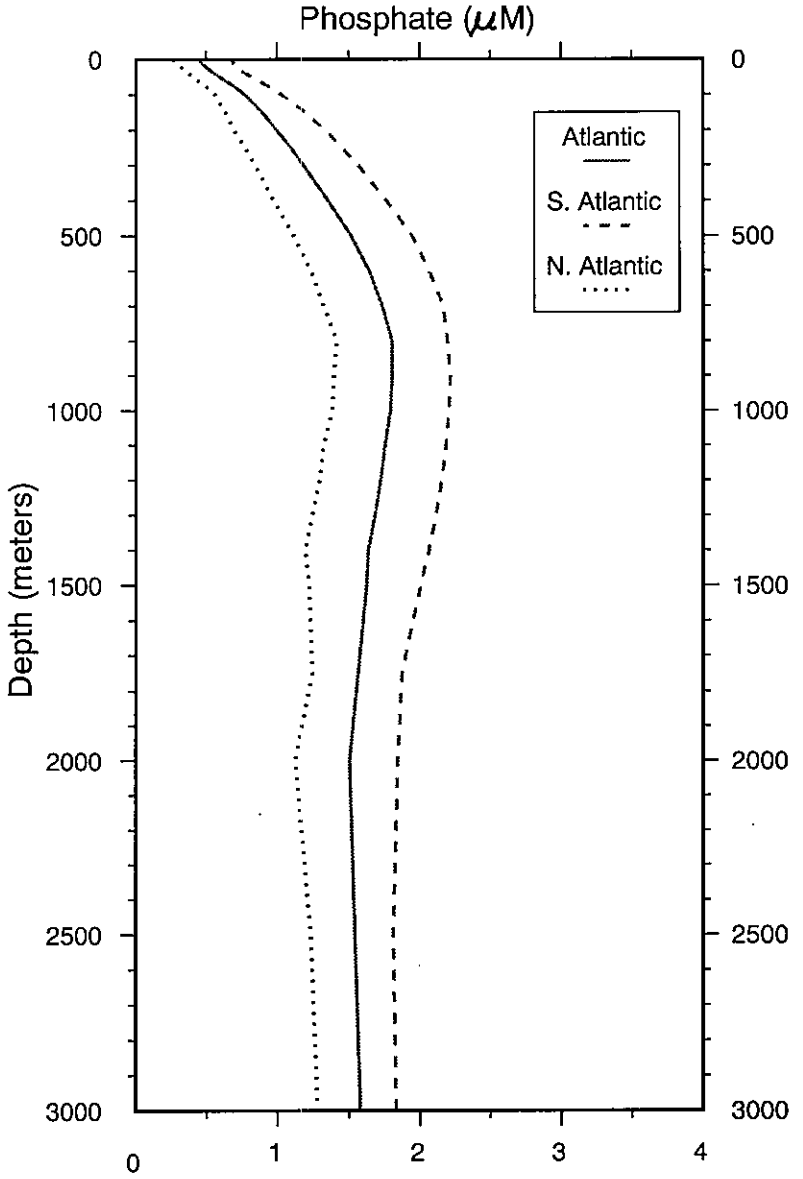

Figure D3b. Annual Atlantic phosphate (μM) basin means (0-3000 m)

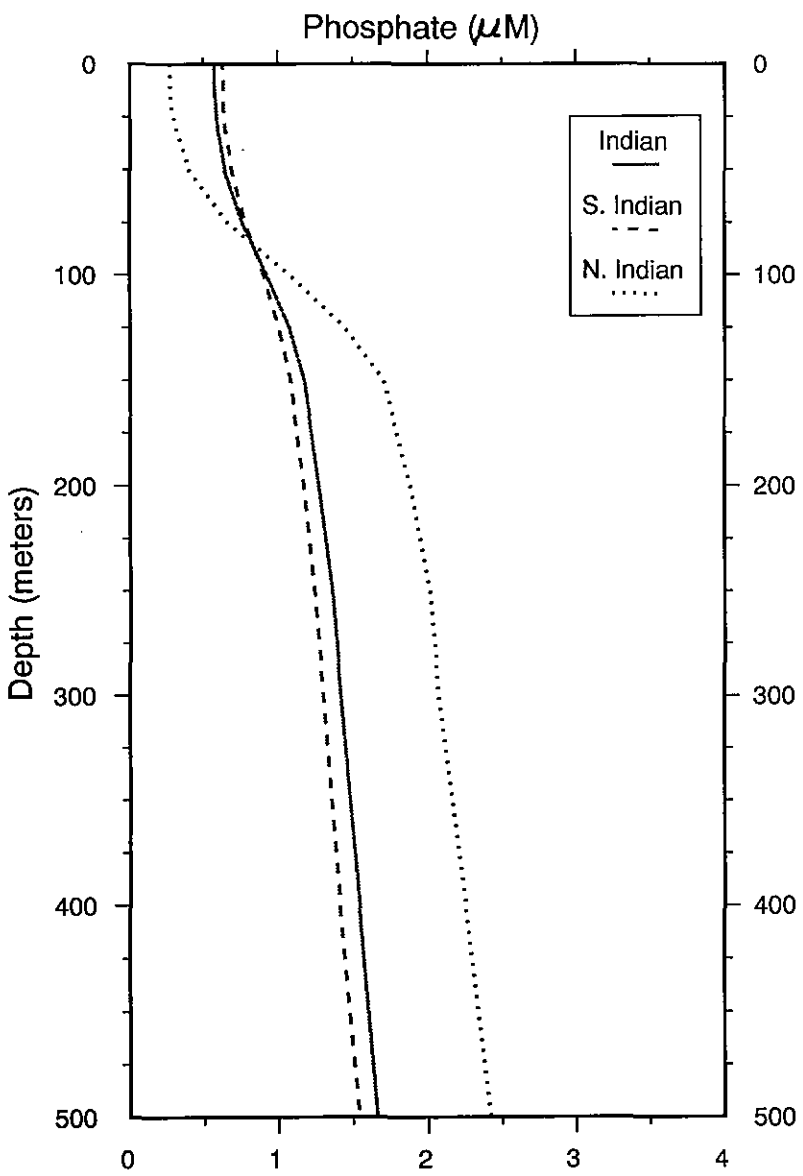

Figure D4a. Annual Indian phosphate (μM) basin means (0-500 m)

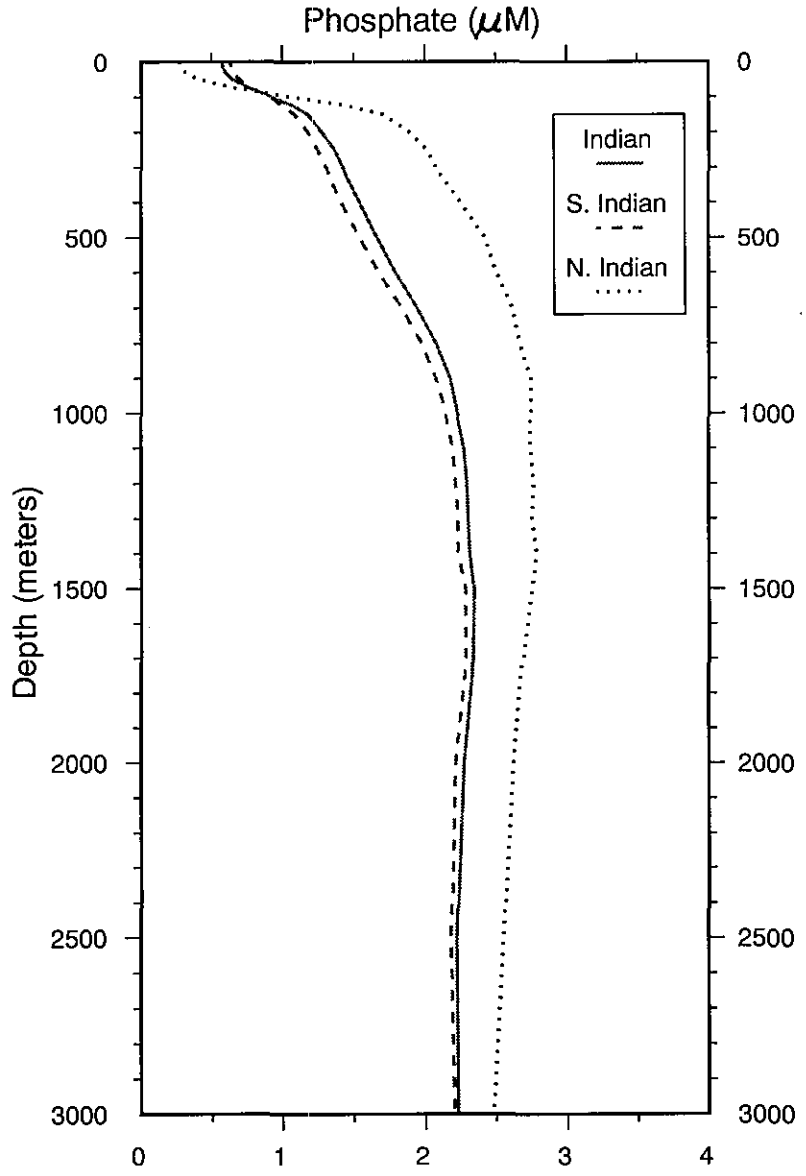

Figure D4b. Annual Indian phosphate (μM) basin means (0-3000 m)

Table D1a. Annual phosphate (μM) basin means and standard errors for the world ocean and Pacific Ocean as a function of depth

		World Ocean		Southern Hemisphere Ocean		Northern Hemisphere Ocean		Pacific Ocean		South Pacific Ocean		North Pacific Ocean	
Standard Level	Depth	Mean	Standard Error	Mean	Standard Error	Mean	Standard Error	Mean	Standard Error	Mean	Standard Error	Mean	Standard Error
1	0	0.50	0.03	0.63	0.04	0.31	0.02	0.50	0.03	0.62	0.05	0.36	0.03
2	10	0.50	0.03	0.64	0.04	0.32	0.02	0.50	0.03	0.62	0.05	0.36	0.03
3	20	0.52	0.03	0.65	0.04	0.34	0.02	0.51	0.03	0.63	0.05	0.38	0.04
4	30	0.55	0.03	0.66	0.04	0.38	0.03	0.54	0.04	0.64	0.05	0.42	0.04
5	50	0.61	0.03	0.72	0.04	0.47	0.04	0.62	0.04	0.69	0.06	0.53	0.06
6	75	0.72	0.03	0.81	0.04	0.61	0.04	0.73	0.05	0.77	0.06	0.68	0.07
7	100	0.84	0.03	0.90	0.05	0.75	0.05	0.84	0.05	0.85	0.07	0.83	0.08
8	125	0.94	0.04	0.99	0.05	0.87	0.06	0.96	0.05	0.94	0.07	0.98	0.08
9	150	1.04	0.04	1.07	0.05	0.99	0.06	1.07	0.05	1.02	0.07	1.12	0.09
10	200	1.20	0.04	1.21	0.05	1.18	0.06	1.28	0.06	1.19	0.07	1.39	0.09
11	250	1.34	0.04	1.33	0.05	1.35	0.07	1.46	0.06	1.34	0.07	1.62	0.09
12	300	1.47	0.04	1.45	0.05	1.49	0.07	1.64	0.05	1.49	0.07	1.82	0.08
13	400	1.69	0.04	1.65	0.04	1.75	0.07	1.93	0.05	1.75	0.06	2.16	0.08
14	500	1.88	0.04	1.80	0.04	1.99	0.07	2.17	0.05	1.92	0.06	2.47	0.06
15	600	2.03	0.04	1.93	0.04	2.17	0.07	2.33	0.04	2.04	0.05	2.70	0.05
16	700	2.15	0.04	2.05	0.03	2.31	0.07	2.47	0.04	2.15	0.05	2.86	0.04
17	800	2.24	0.03	2.13	0.03	2.40	0.07	2.54	0.04	2.22	0.05	2.95	0.03
18	900	2.29	0.03	2.21	0.03	2.42	0.07	2.60	0.04	2.30	0.04	2.98	0.03
19	1000	2.32	0.03	2.26	0.02	2.43	0.07	2.65	0.03	2.36	0.04	2.99	0.03
20	1100	2.33	0.03	2.28	0.02	2.41	0.07	2.66	0.03	2.39	0.04	2.99	0.02
21	1200	2.33	0.03	2.28	0.02	2.40	0.07	2.66	0.03	2.39	0.03	2.98	0.02
22	1300	2.33	0.03	2.29	0.02	2.38	0.08	2.67	0.03	2.42	0.03	2.98	0.02
23	1400	2.31	0.03	2.28	0.02	2.36	0.08	2.66	0.03	2.42	0.03	2.96	0.02
24	1500	2.32	0.03	2.29	0.02	2.36	0.07	2.66	0.03	2.43	0.02	2.94	0.02
25	1750	2.32	0.03	2.29	0.03	2.35	0.07	2.69	0.02	2.51	0.02	2.92	0.02
26	2000	2.24	0.03	2.22	0.02	2.28	0.07	2.61	0.02	2.41	0.02	2.85	0.02
27	2500	2.21	0.03	2.18	0.02	2.27	0.07	2.54	0.02	2.37	0.02	2.75	0.01
28	3000	2.21	0.03	2.19	0.02	2.25	0.06	2.50	0.02	2.36	0.02	2.66	0.01

Table D1b. Annual phosphate (μM) basin means and standard errors for the Atlantic Ocean and Indian Ocean as a function of depth

		Atlantic Ocean		South Atlantic Ocean		North Atlantic Ocean		Indian Ocean		South Indian Ocean		North Indian Ocean	
Standard Level	Depth	Mean	Standard Error	Mean	Standard Error	Mean	Standard Error	Mean	Standard Error	Mean	Standard Error	Mean	Standard Error
1	0	0.44	0.05	0.67	0.09	0.26	0.03	0.57	0.06	0.62	0.07	0.27	0.03
2	10	0.46	0.05	0.69	0.09	0.28	0.03	0.57	0.07	0.63	0.08	0.27	0.03
3	20	0.49	0.05	0.71	0.09	0.31	0.04	0.58	0.07	0.63	0.08	0.28	0.04
4	30	0.52	0.05	0.73	0.09	0.35	0.05	0.59	0.07	0.64	0.08	0.31	0.05
5	50	0.59	0.05	0.82	0.10	0.40	0.04	0.64	0.07	0.69	0.08	0.40	0.06
6	75	0.69	0.06	0.93	0.10	0.49	0.05	0.76	0.07	0.78	0.08	0.66	0.07
7	100	0.77	0.06	1.03	0.10	0.56	0.06	0.92	0.07	0.90	0.08	1.07	0.08
8	125	0.83	0.06	1.11	0.10	0.59	0.06	1.07	0.07	1.00	0.08	1.44	0.08
9	150	0.89	0.06	1.19	0.10	0.63	0.06	1.17	0.07	1.08	0.08	1.70	0.09
10	200	0.99	0.06	1.33	0.10	0.69	0.06	1.27	0.08	1.17	0.08	1.88	0.09
11	250	1.09	0.07	1.45	0.09	0.77	0.07	1.36	0.08	1.24	0.08	2.01	0.09
12	300	1.18	0.07	1.56	0.09	0.84	0.07	1.42	0.08	1.30	0.08	2.07	0.09
13	400	1.35	0.07	1.76	0.08	0.97	0.08	1.54	0.07	1.41	0.08	2.25	0.09
14	500	1.51	0.07	1.94	0.06	1.11	0.08	1.66	0.07	1.54	0.07	2.42	0.08
15	600	1.64	0.07	2.06	0.05	1.23	0.08	1.79	0.07	1.67	0.07	2.50	0.08
16	700	1.73	0.06	2.16	0.04	1.32	0.09	1.94	0.06	1.83	0.06	2.61	0.07
17	800	1.80	0.06	2.19	0.03	1.41	0.08	2.07	0.05	1.97	0.05	2.66	0.06
18	900	1.80	0.06	2.21	0.02	1.39	0.08	2.17	0.05	2.07	0.05	2.74	0.05
19	1000	1.79	0.06	2.20	0.02	1.38	0.08	2.22	0.04	2.14	0.04	2.74	0.05
20	1100	1.75	0.06	2.18	0.02	1.32	0.07	2.27	0.04	2.19	0.03	2.74	0.05
21	1200	1.72	0.06	2.15	0.02	1.29	0.06	2.29	0.04	2.21	0.03	2.76	0.05
22	1300	1.68	0.06	2.11	0.03	1.24	0.06	2.30	0.03	2.23	0.03	2.75	0.05
23	1400	1.63	0.06	2.06	0.04	1.19	0.05	2.31	0.04	2.23	0.03	2.78	0.06
24	1500	1.62	0.05	2.00	0.04	1.22	0.04	2.34	0.03	2.28	0.03	2.75	0.05
25	1750	1.56	0.05	1.87	0.05	1.24	0.04	2.33	0.03	2.28	0.03	2.67	0.04
26	2000	1.50	0.05	1.84	0.06	1.12	0.04	2.27	0.03	2.21	0.03	2.62	0.04
27	2500	1.54	0.05	1.81	0.06	1.23	0.03	2.22	0.03	2.18	0.03	2.55	0.04
28	3000	1.58	0.05	1.83	0.06	1.28	0.03	2.23	0.03	2.20	0.03	2.48	0.04

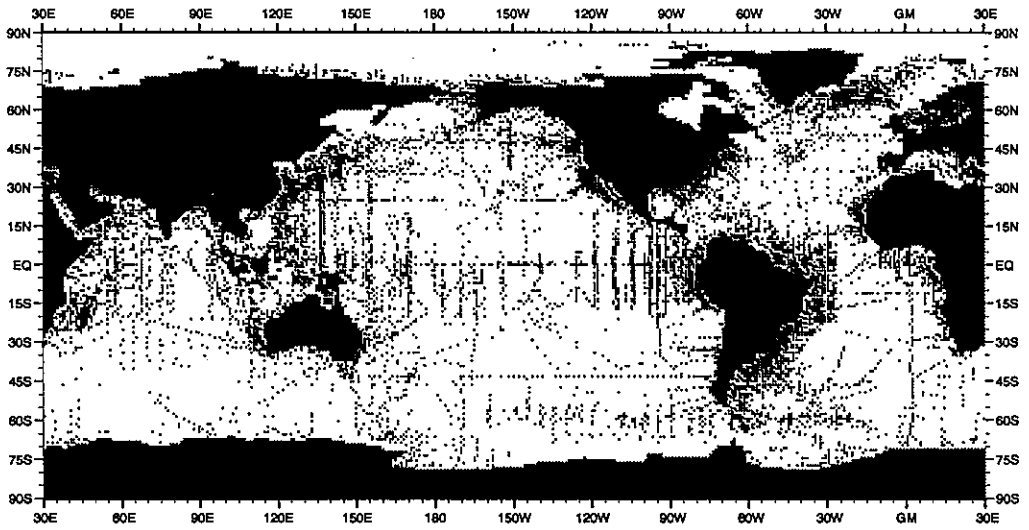

Fig. E1 Distribution of nitrate observations at the surface

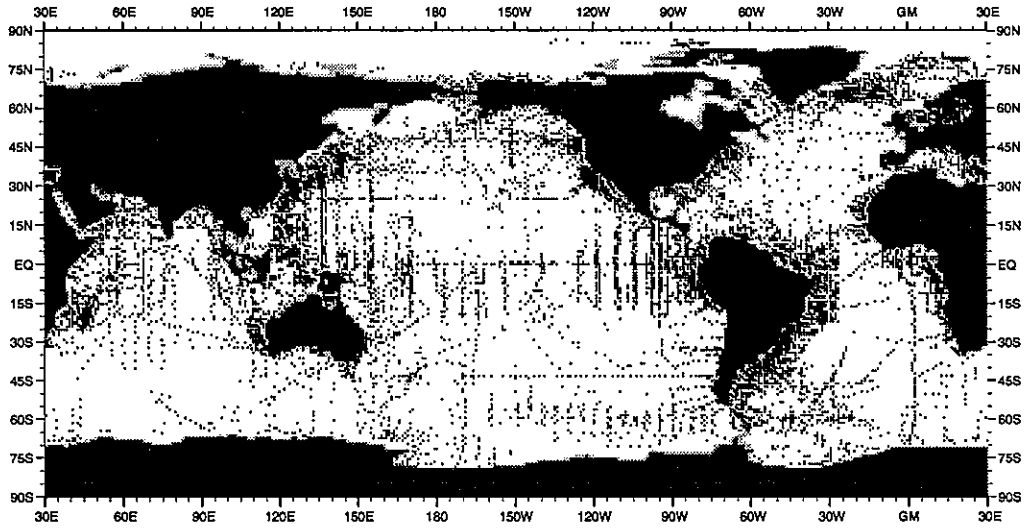

Fig. E2 Distribution of nitrate observations at 30 m depth

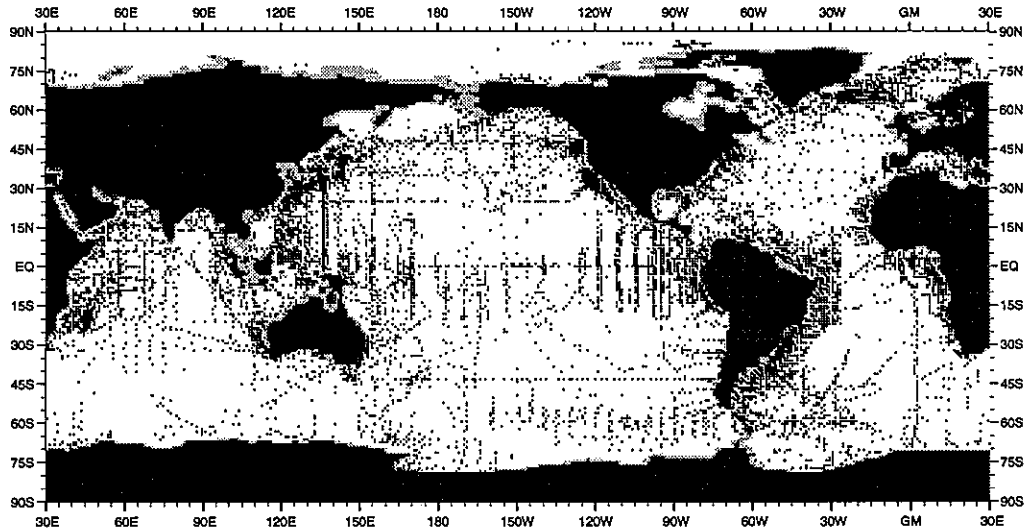

Fig. E3 Distribution of nitrate observations at 50 m depth

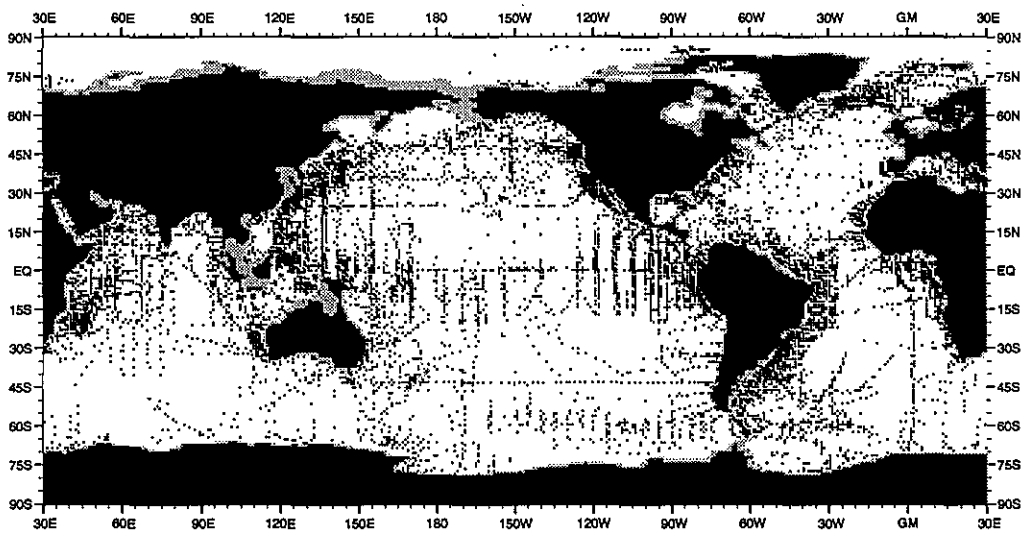

Fig. E4 Distribution of nitrate observations at 75 m depth

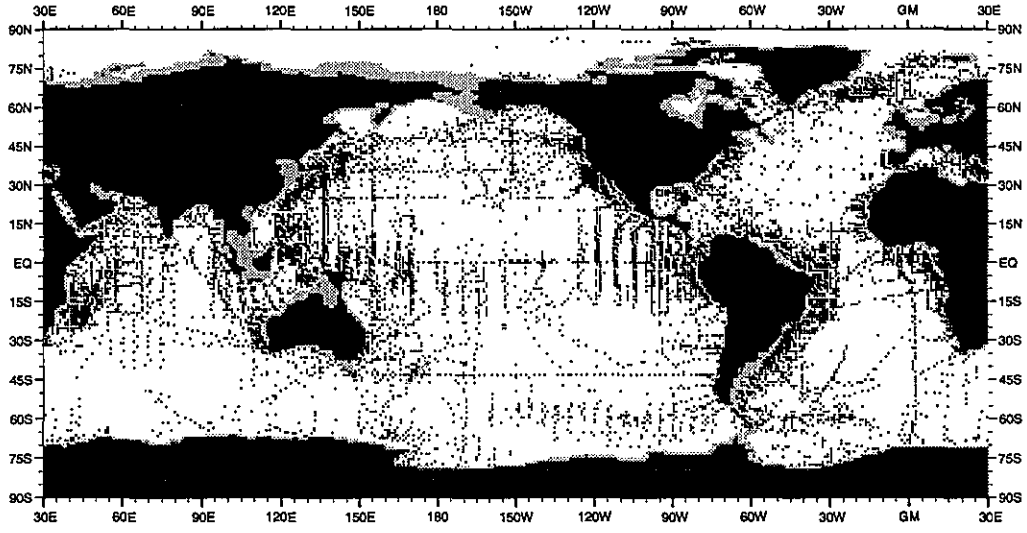

Fig. E5 Distribution of nitrate observations at 100 m depth

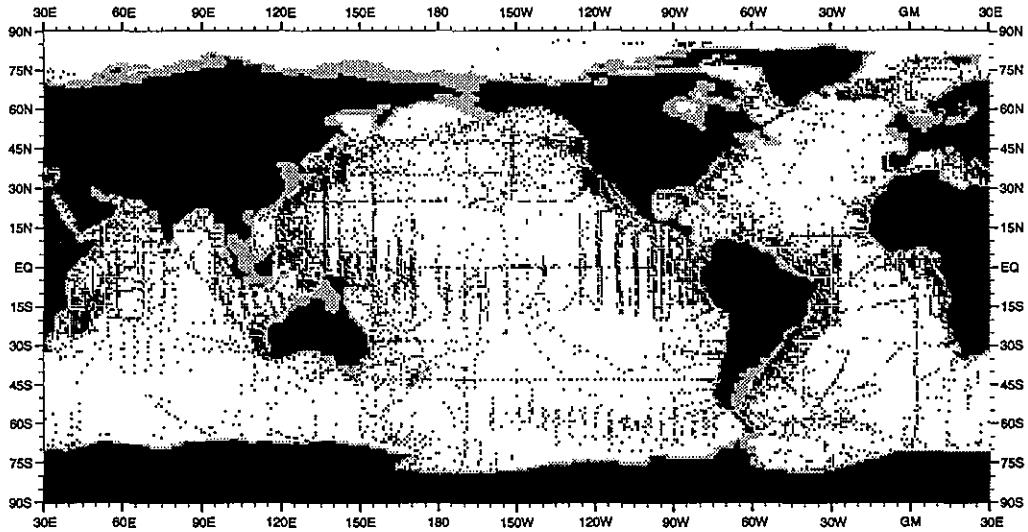

Fig. E6 Distribution of nitrate observations at 125 m depth

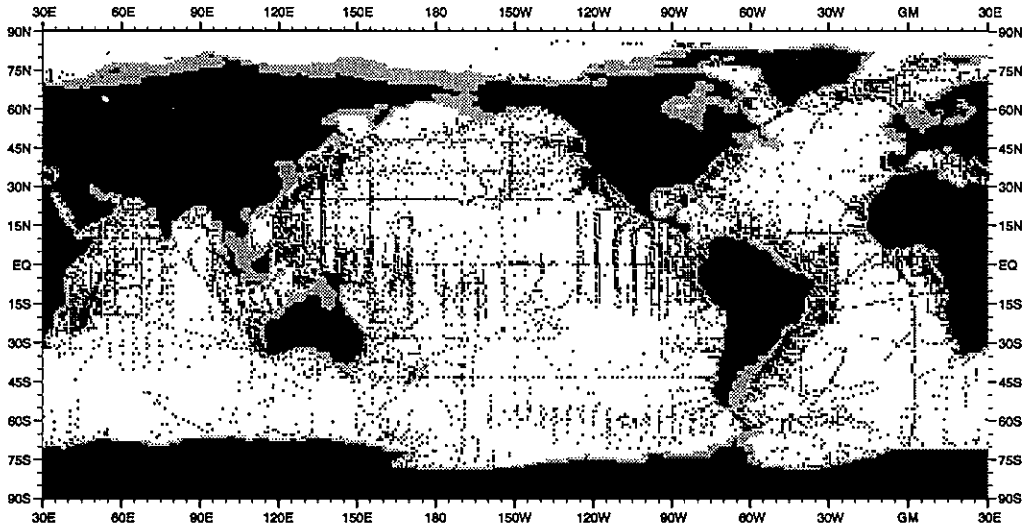

Fig. E7 Distribution of nitrate observations at 150 m depth

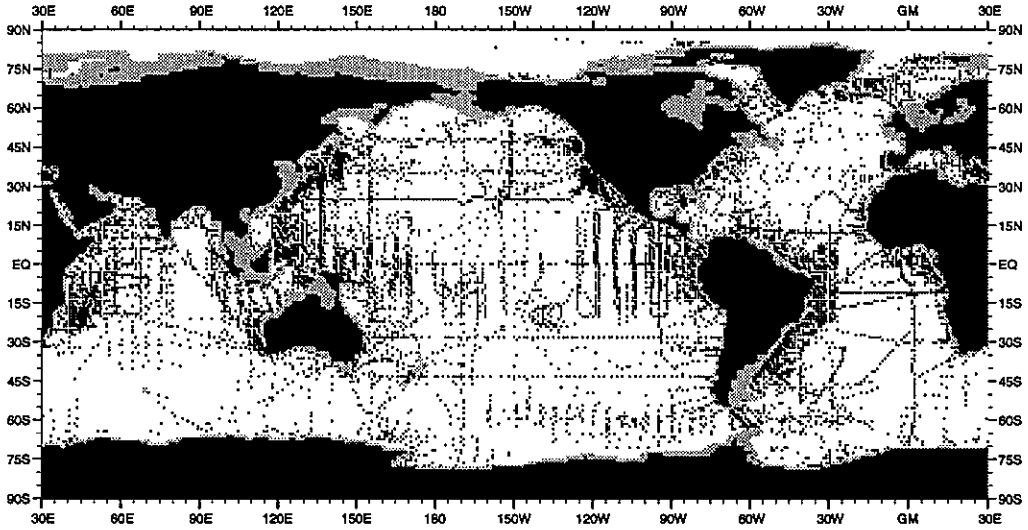

Fig. E8 Distribution of nitrate observations at 250 m depth

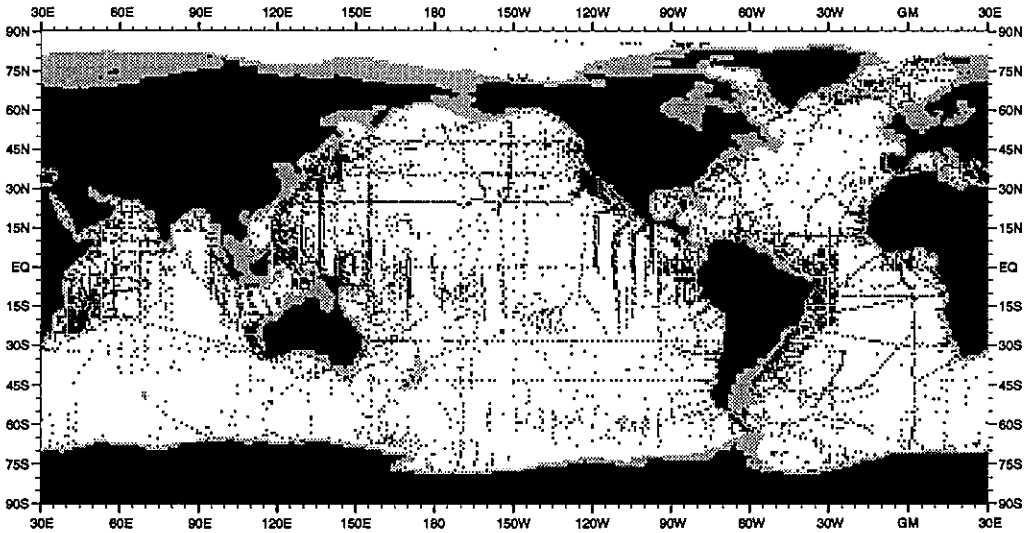

Fig. E9 Distribution of nitrate observations at 400 m depth

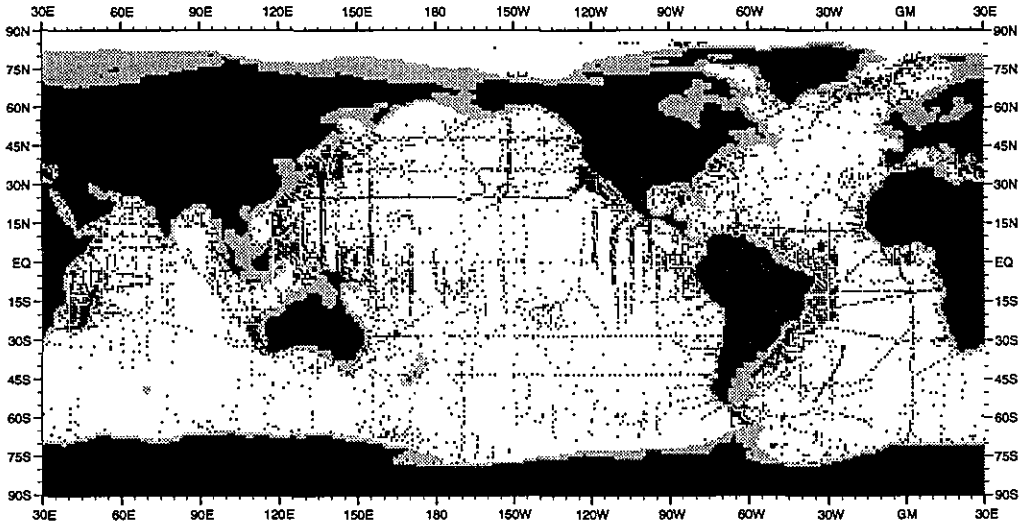

Fig. E10 Distribution of nitrate observations at 500 m depth

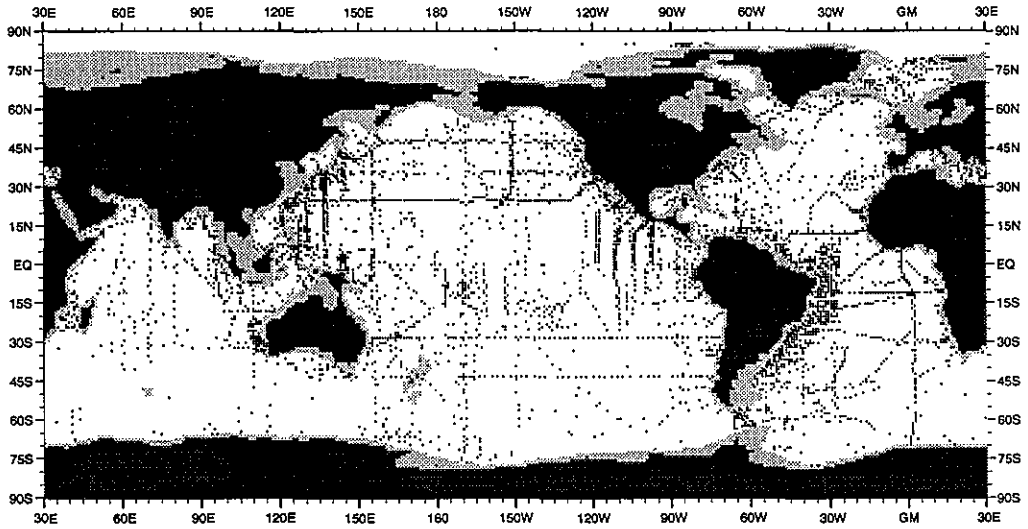

Fig. E11 Distribution of nitrate observations at 700 m depth

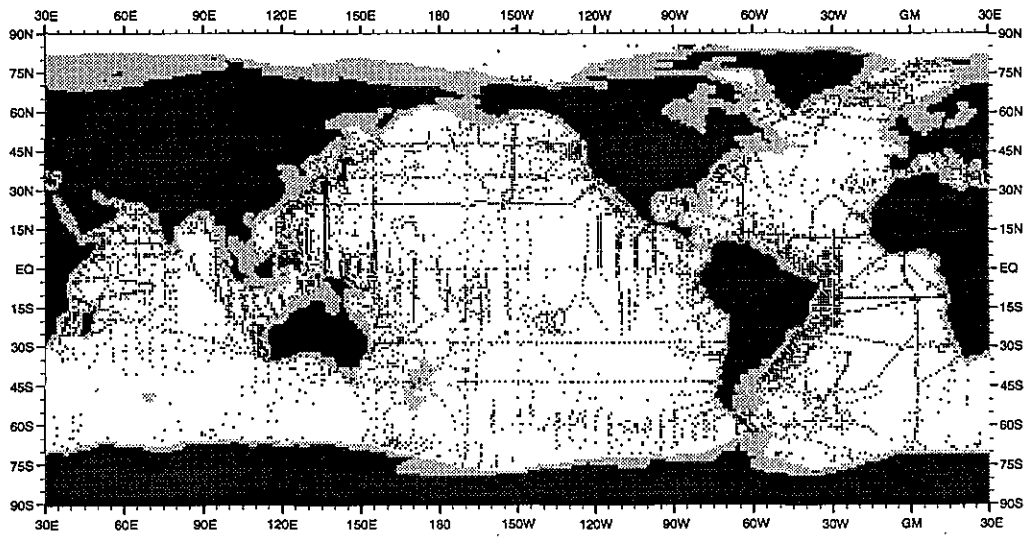

Fig. E12 Distribution of nitrate observations at 900 m depth

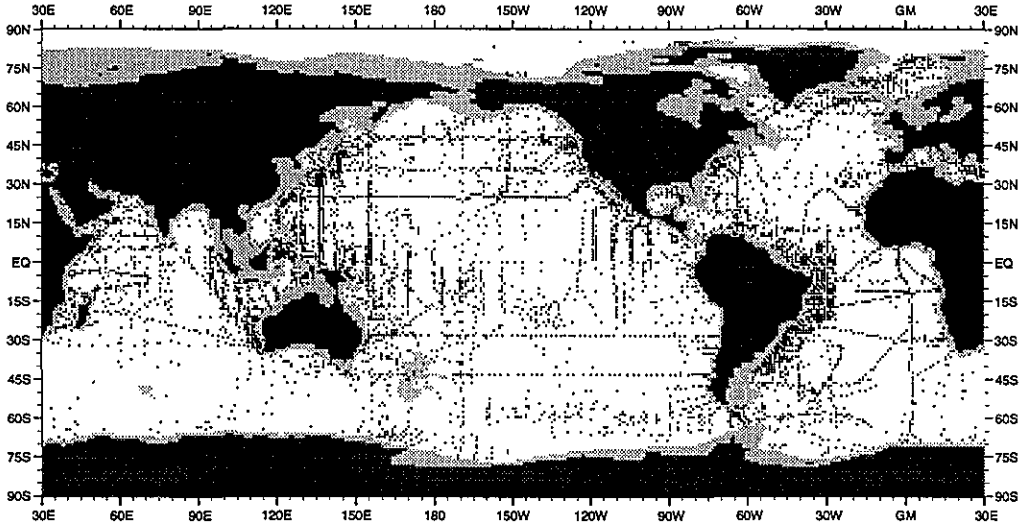

Fig. E13 Distribution of nitrate observations at 1000 m depth

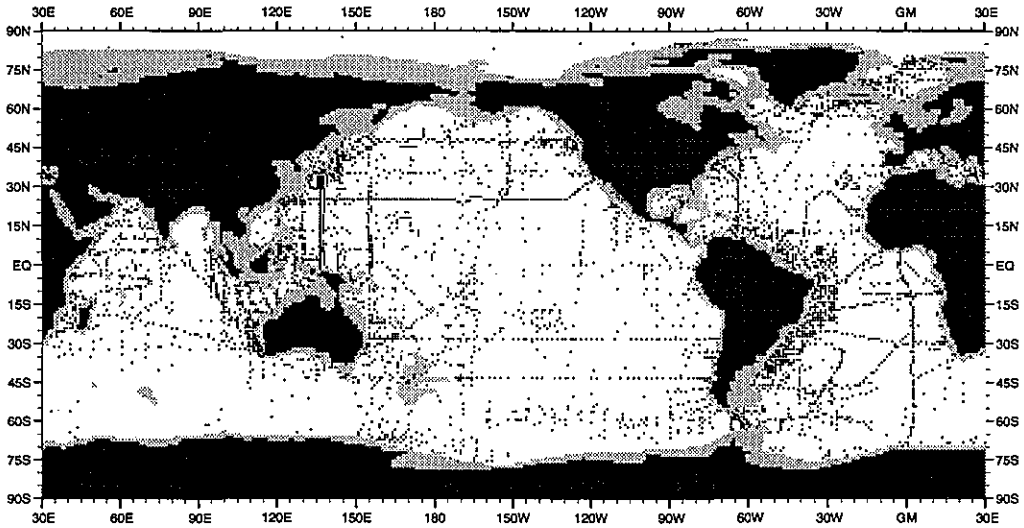

Fig. E14 Distribution of nitrate observations at 1200 m depth

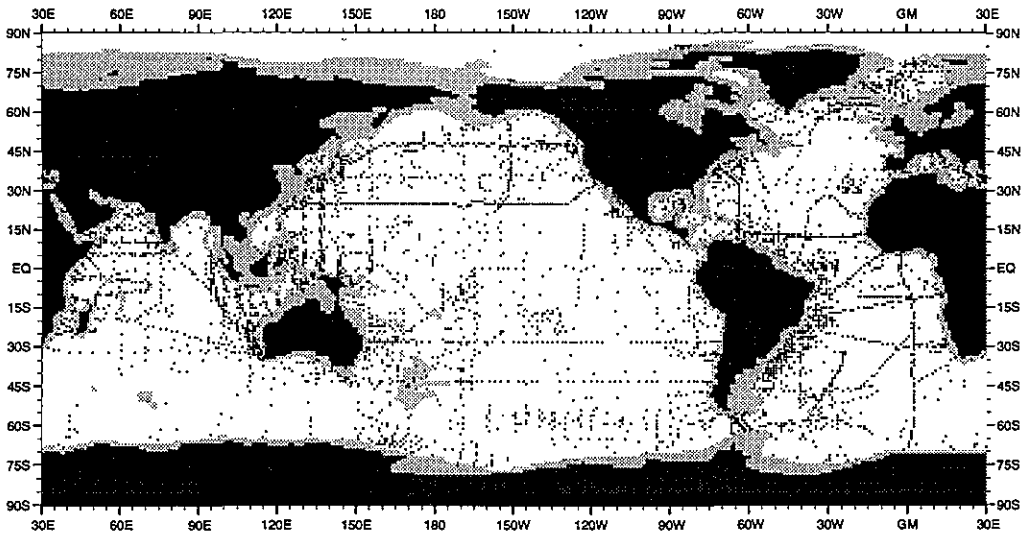

Fig. E15 Distribution of nitrate observations at 1300 m depth

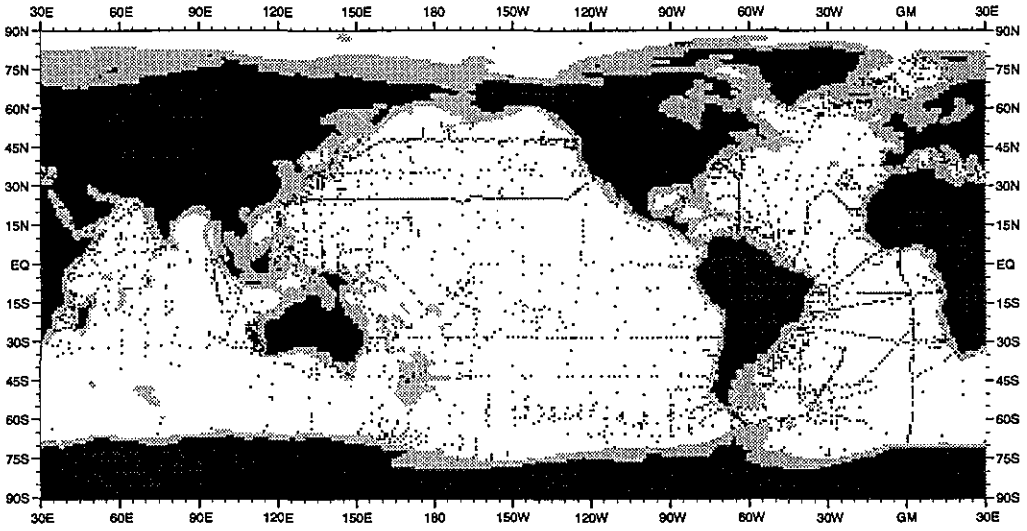

Fig. E16 Distribution of nitrate observations at 1500 m depth

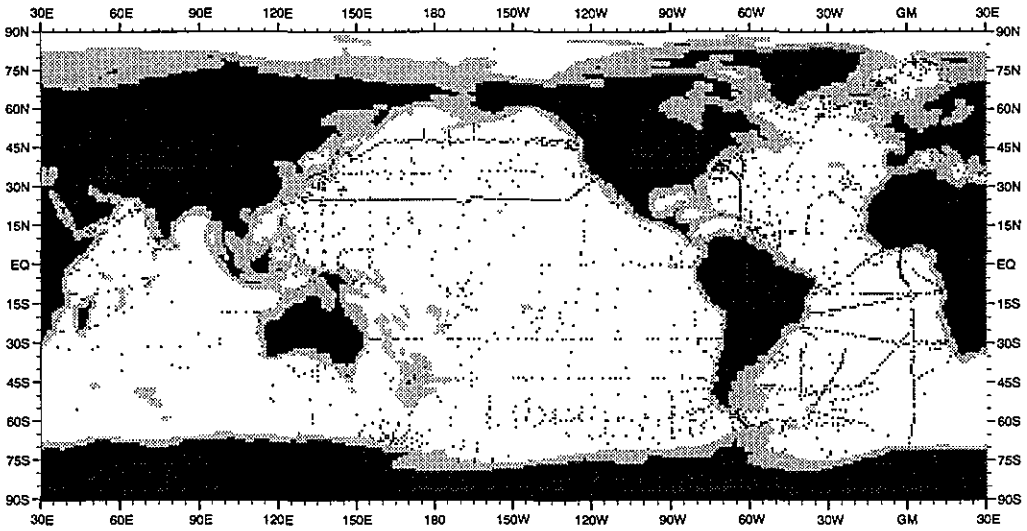

Fig. E17 Distribution of nitrate observations at 1750 m depth

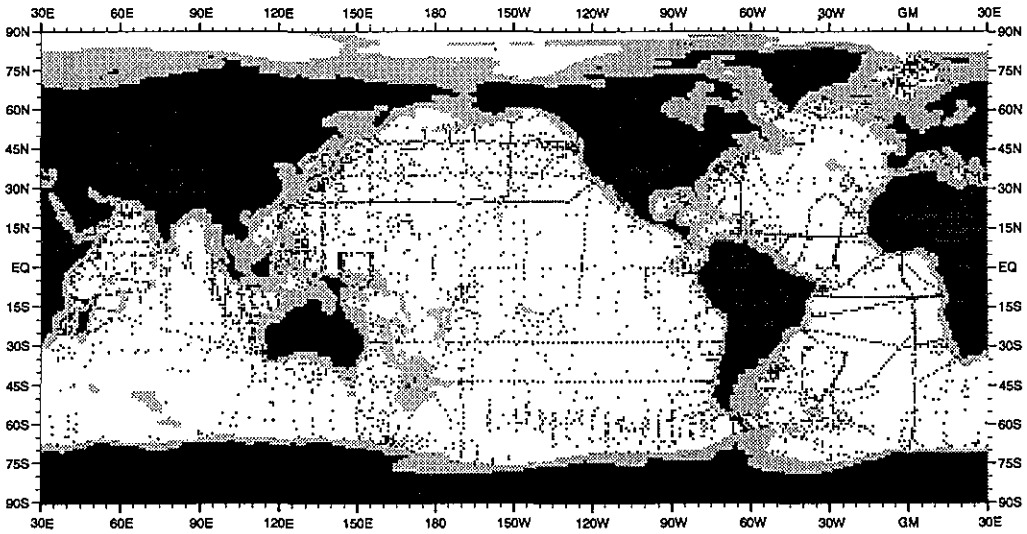

Fig. E18 Distribution of nitrate observations at 2000 m depth

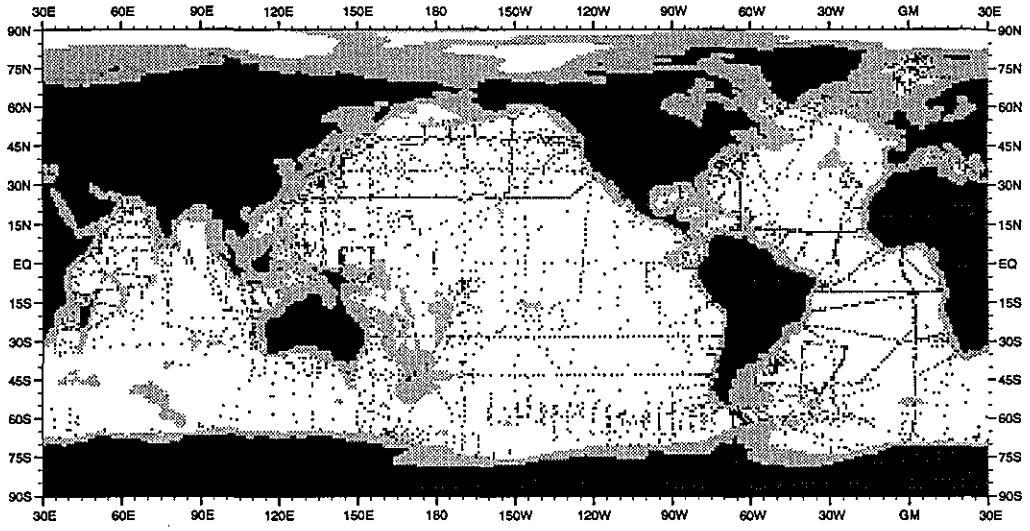

Fig. E19 Distribution of nitrate observations at 2500 m depth

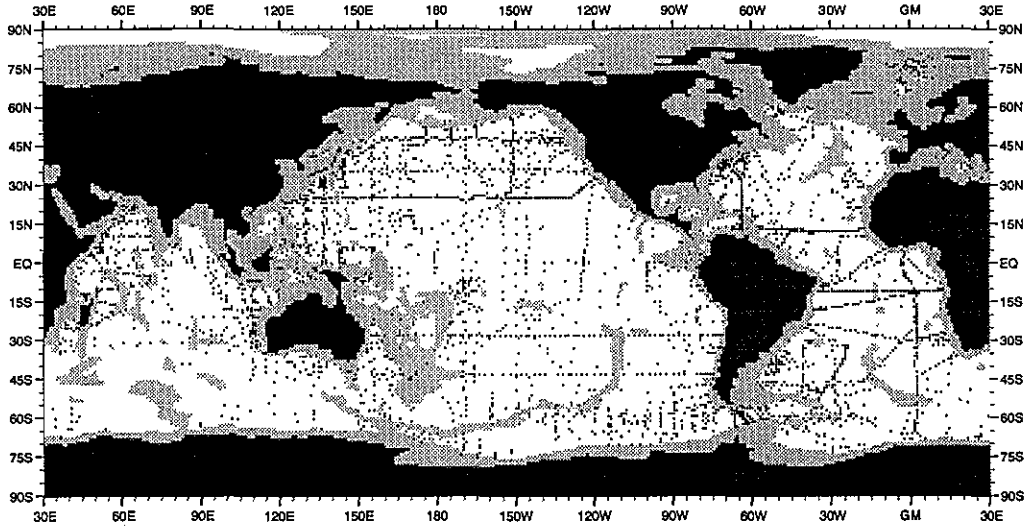

Fig. E20 Distribution of nitrate observations at 3000 m depth

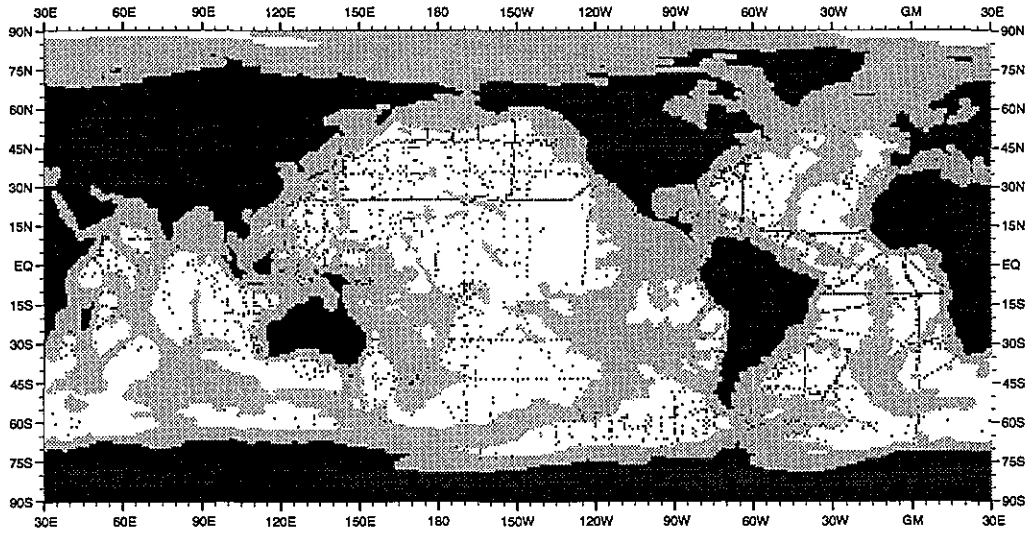

Fig. E21 Distribution of nitrate observations at 4000 m depth

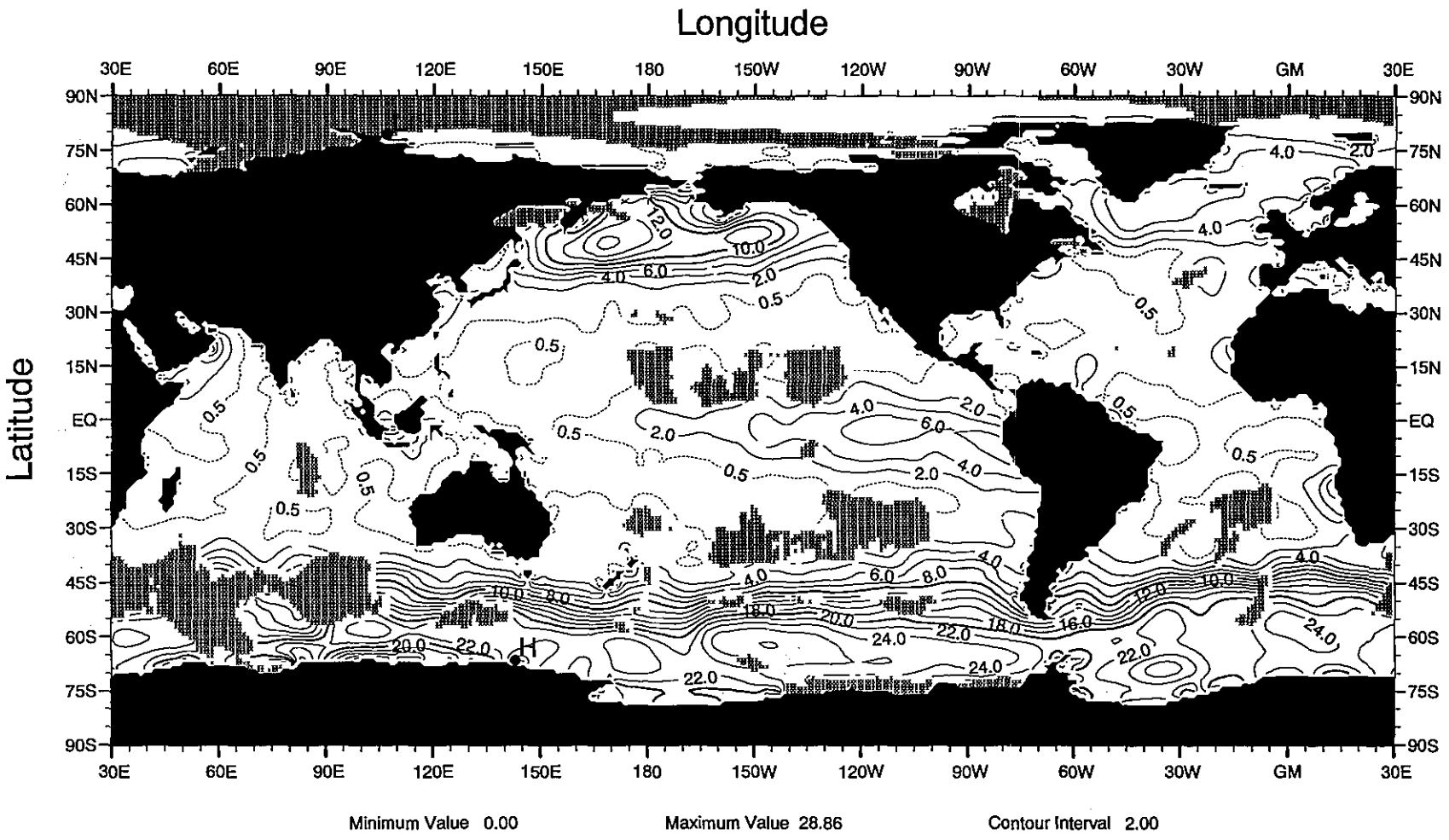

Fig. F1 Annual mean nitrate (μM) at the surface

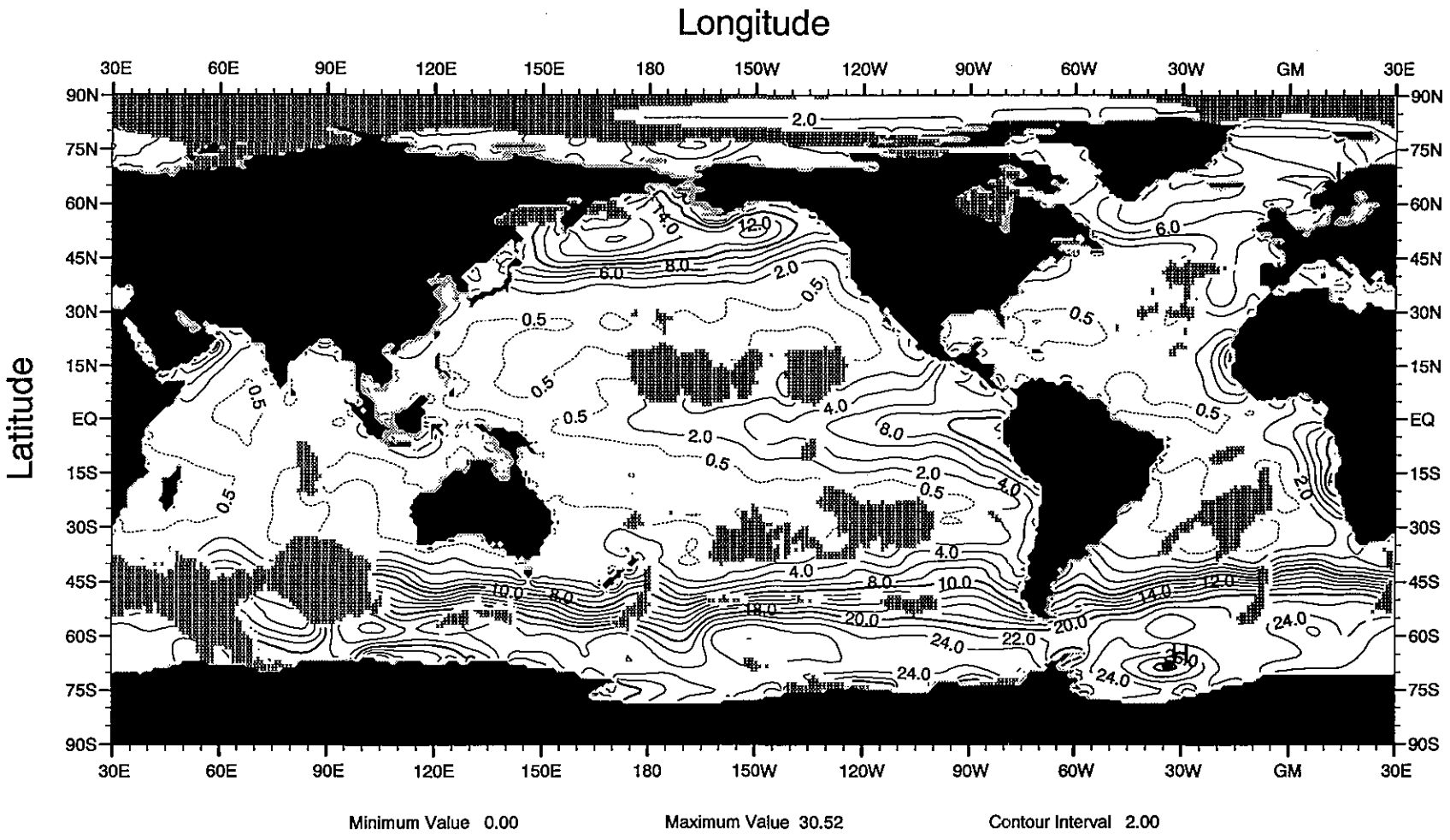

Fig. F2 Annual mean nitrate (μM) at 30 m depth

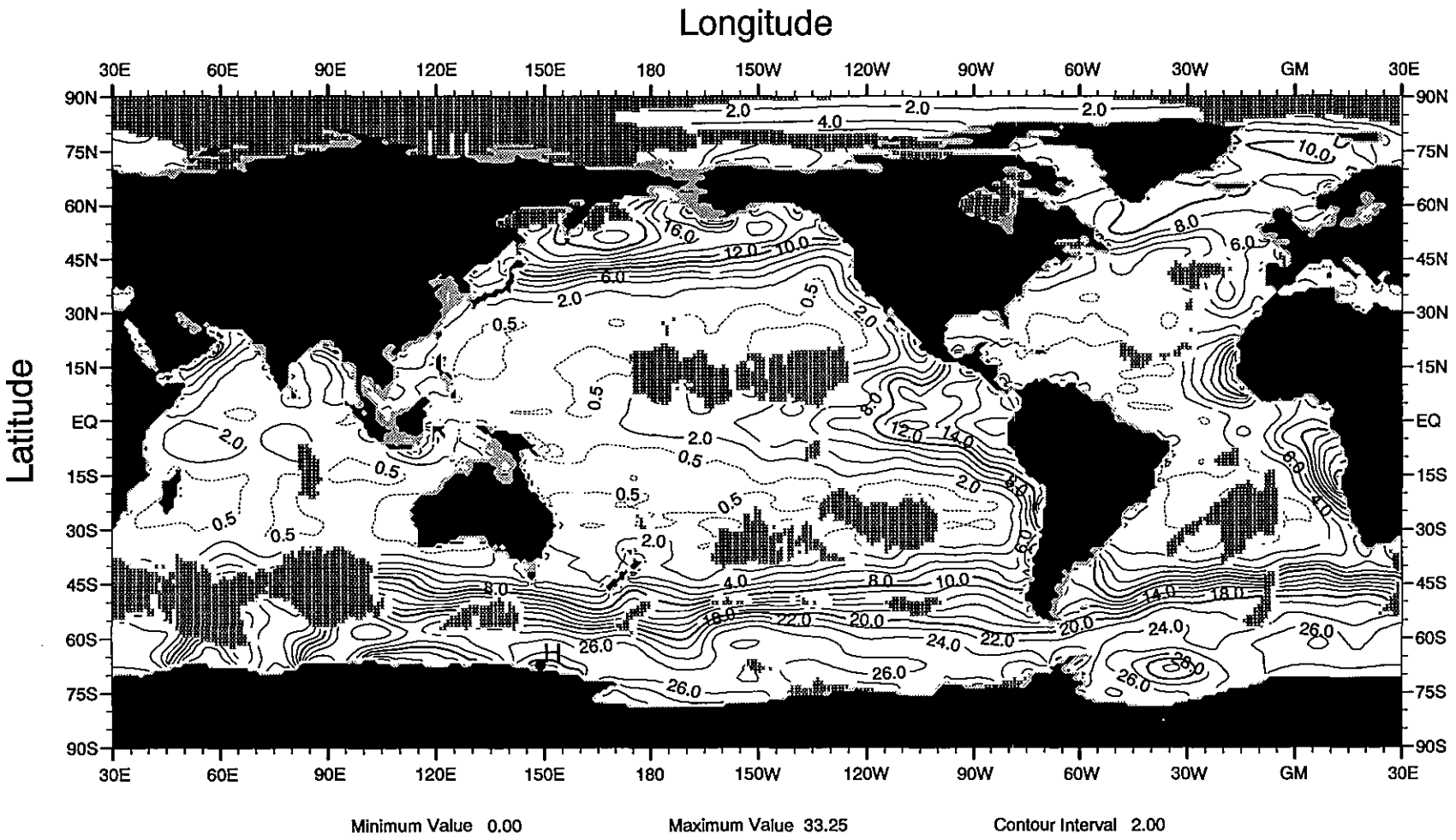

Fig. F3 Annual mean nitrate (μM) at 50 m depth

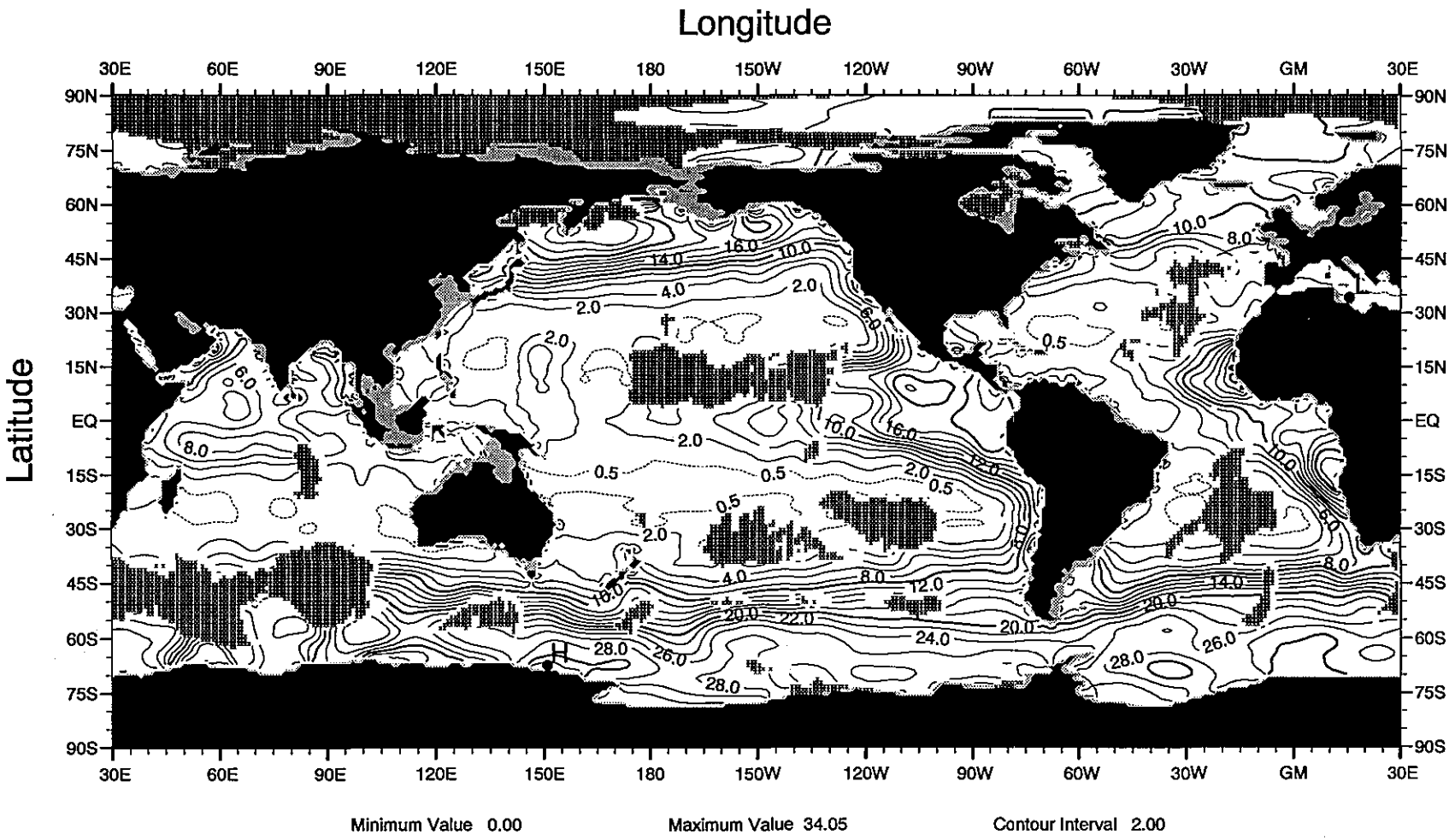

Fig. F4 Annual mean nitrate (μM) at 75 m depth

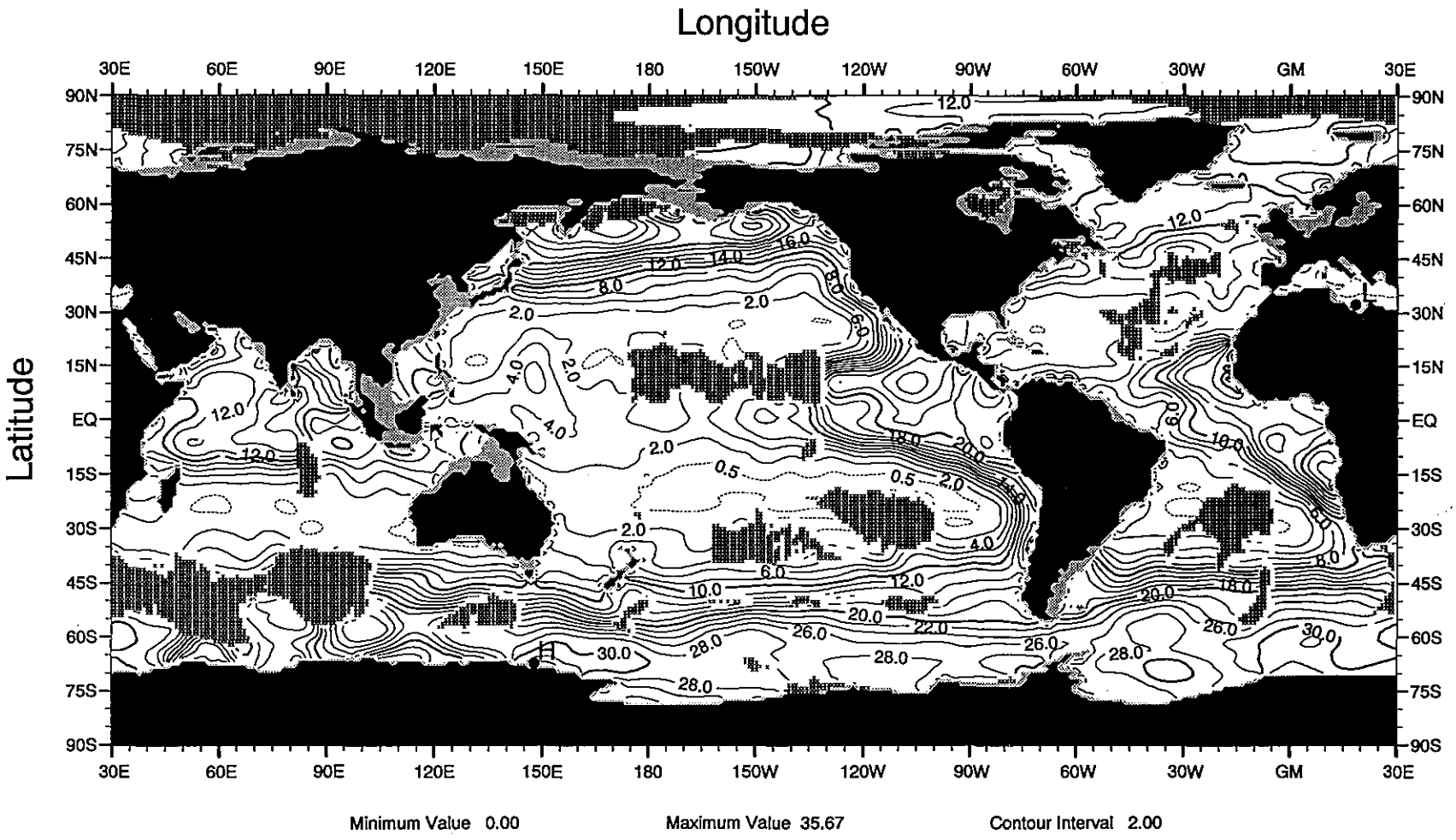

Fig. F5 Annual mean nitrate (μM) at 100 m depth

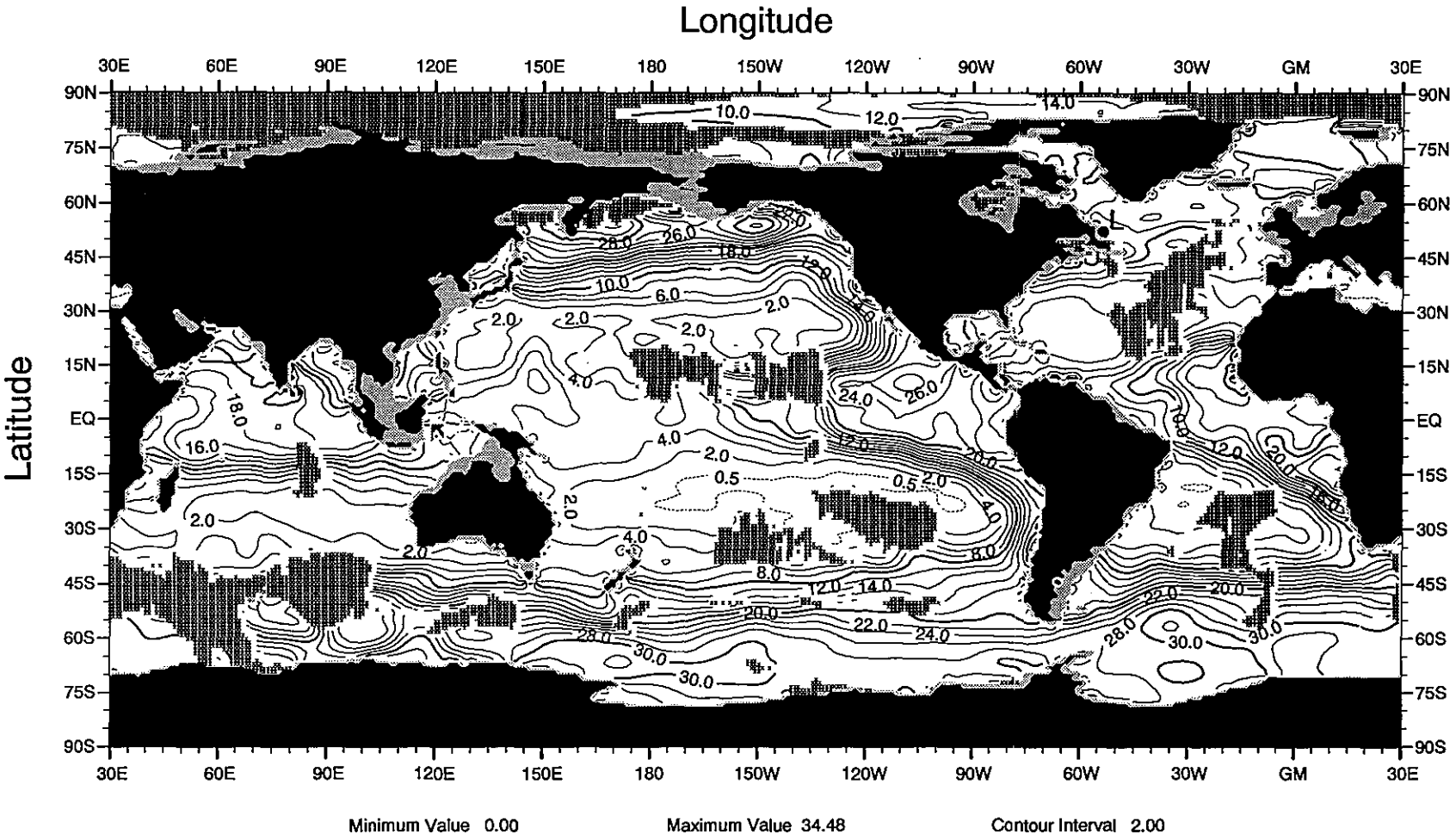

Fig. F6 Annual mean nitrate (μM) at 125 m depth

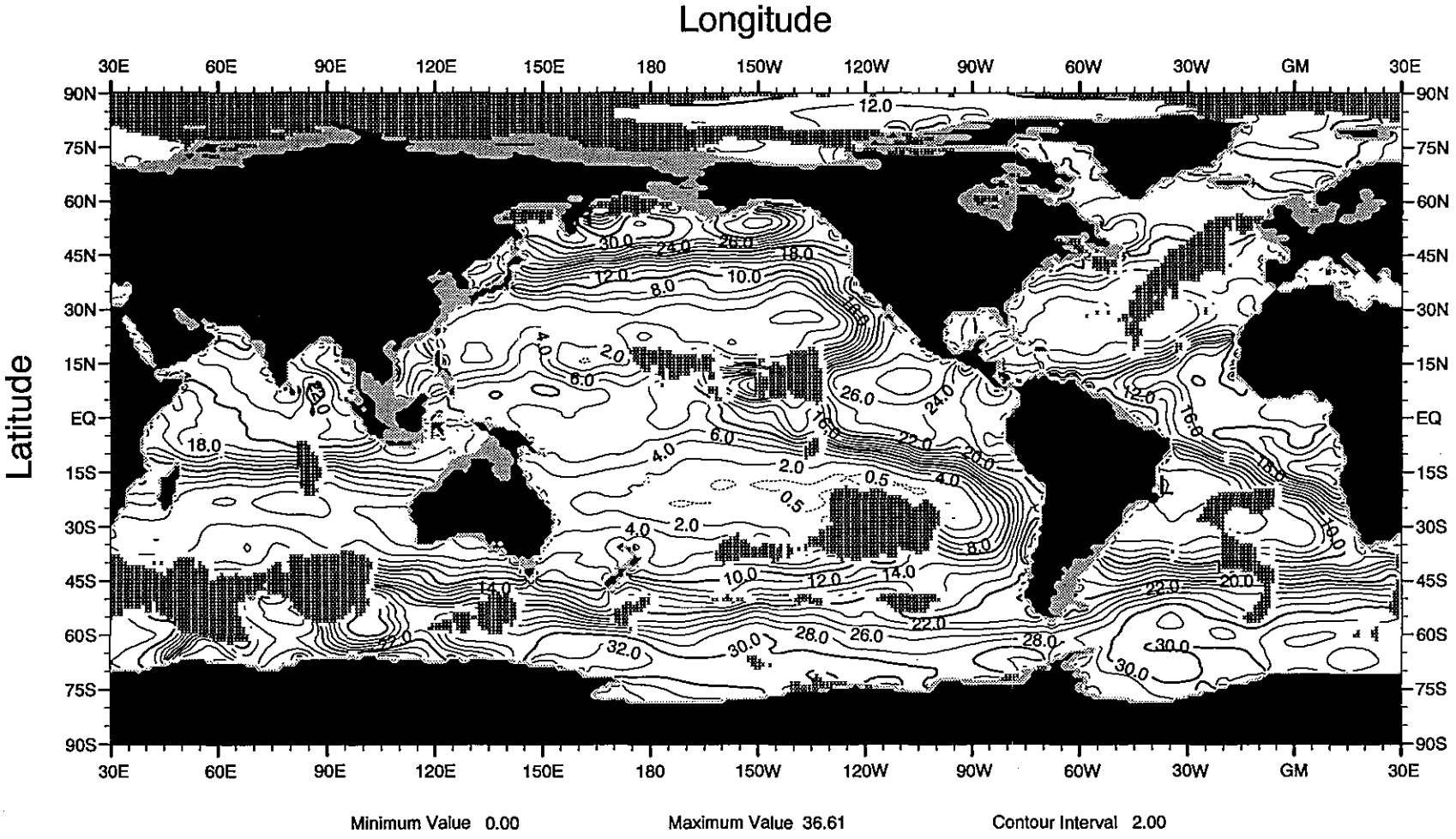

Fig. F7 Annual mean nitrate (μM) at 150 m depth

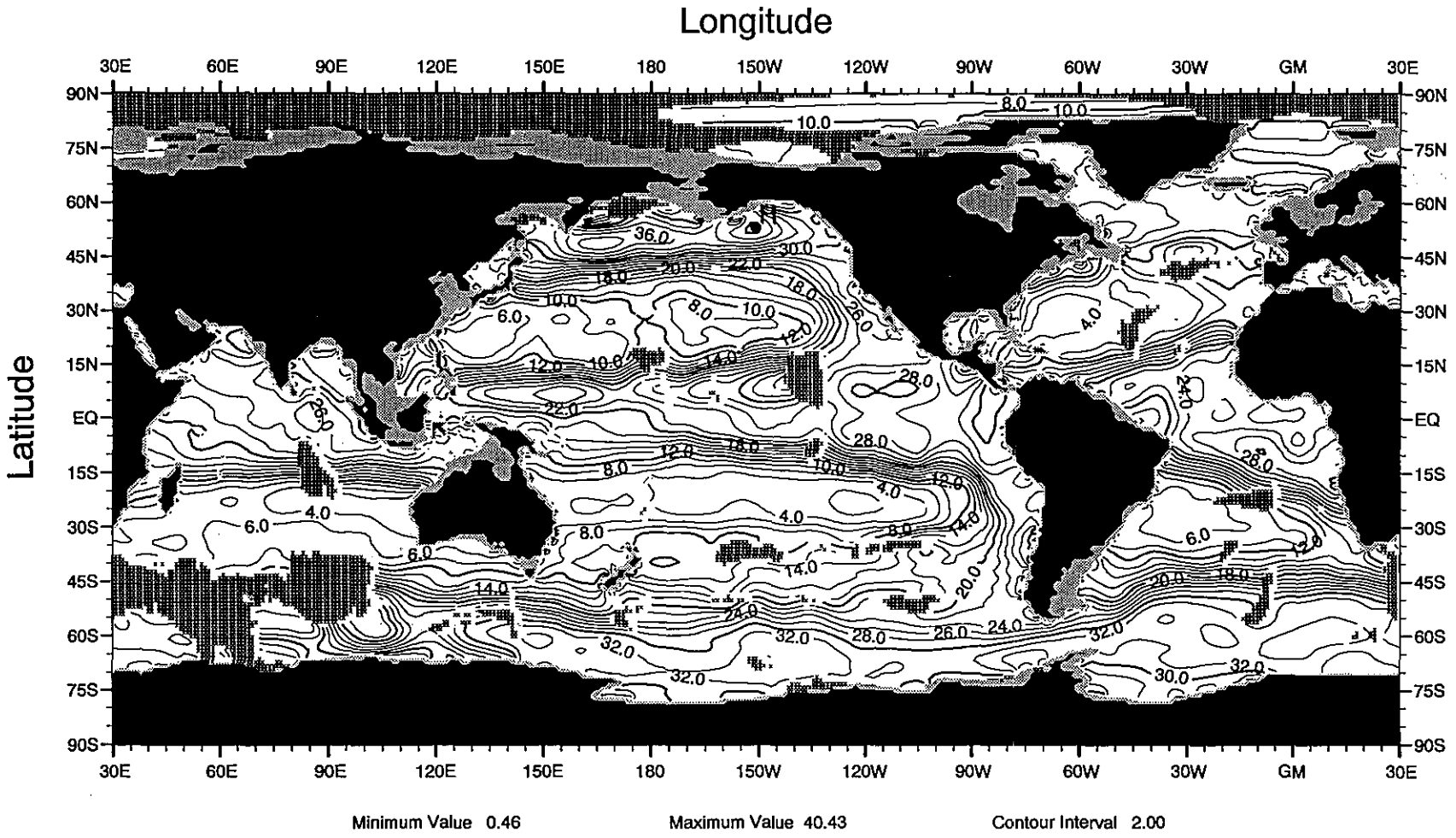

Fig. F8 Annual mean nitrate (μM) at 250 m depth

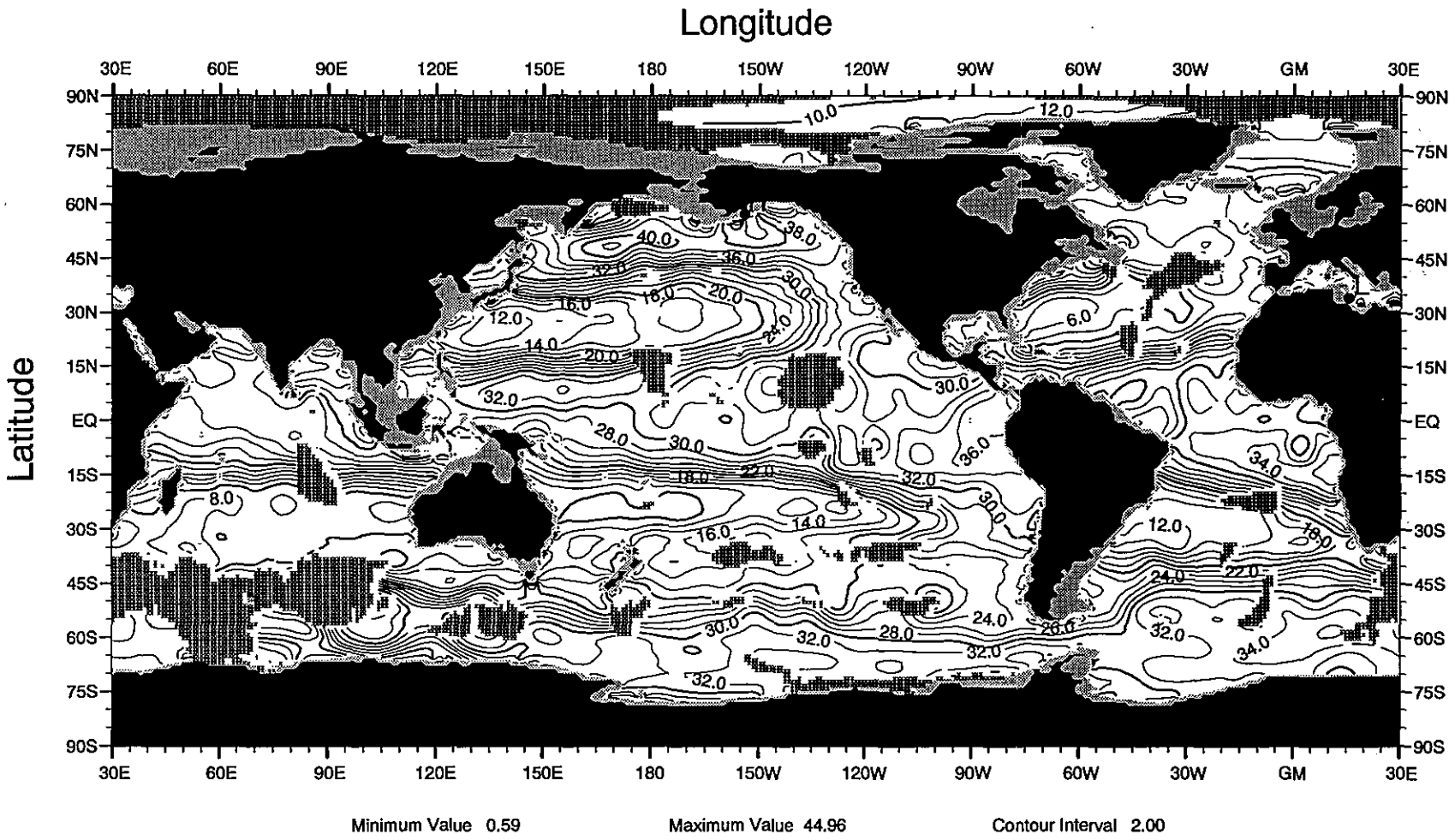

Fig. F9 Annual mean nitrate (μM) at 400 m depth

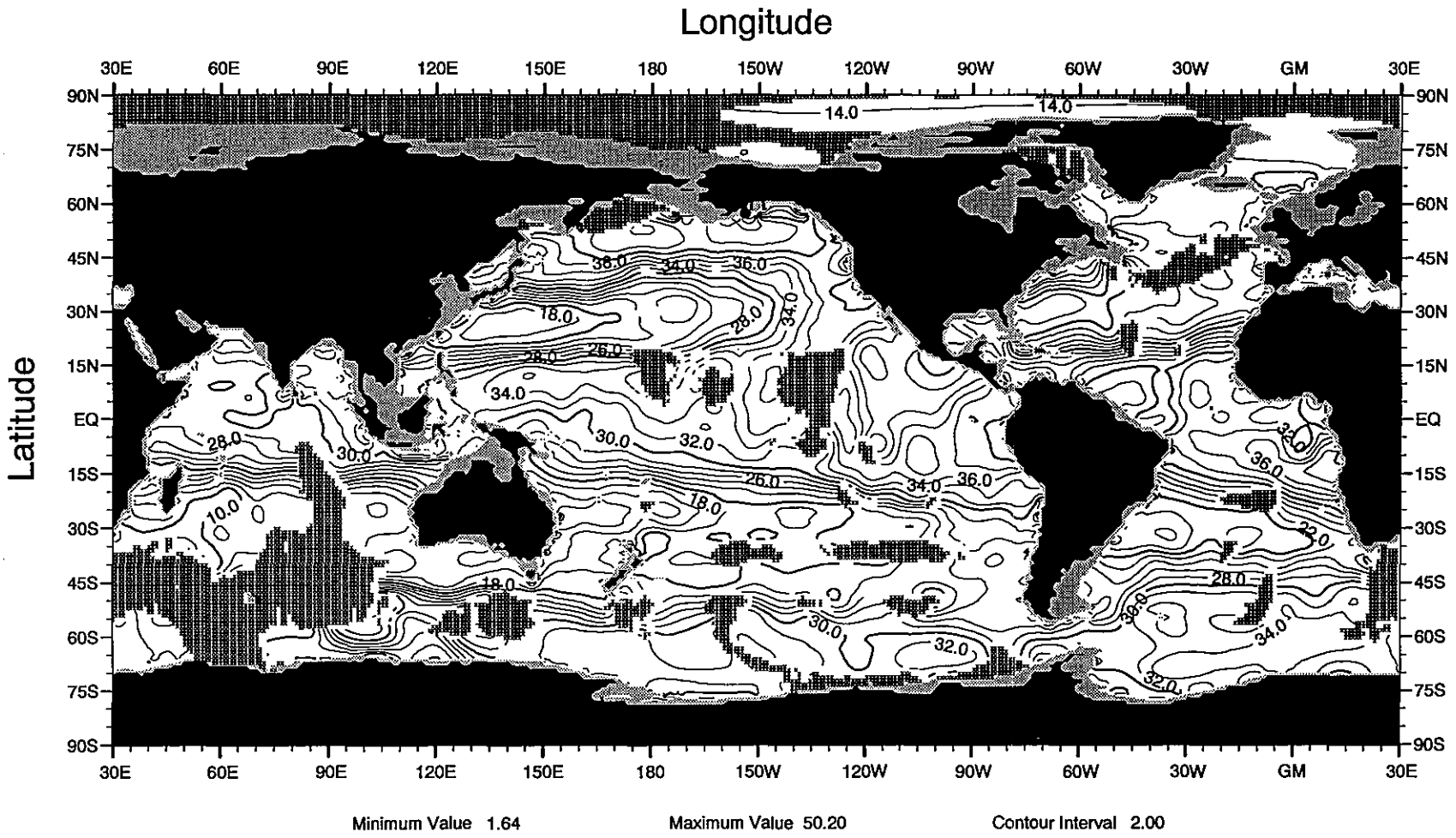

Fig. F10 Annual mean nitrate (μM) at 500 m depth

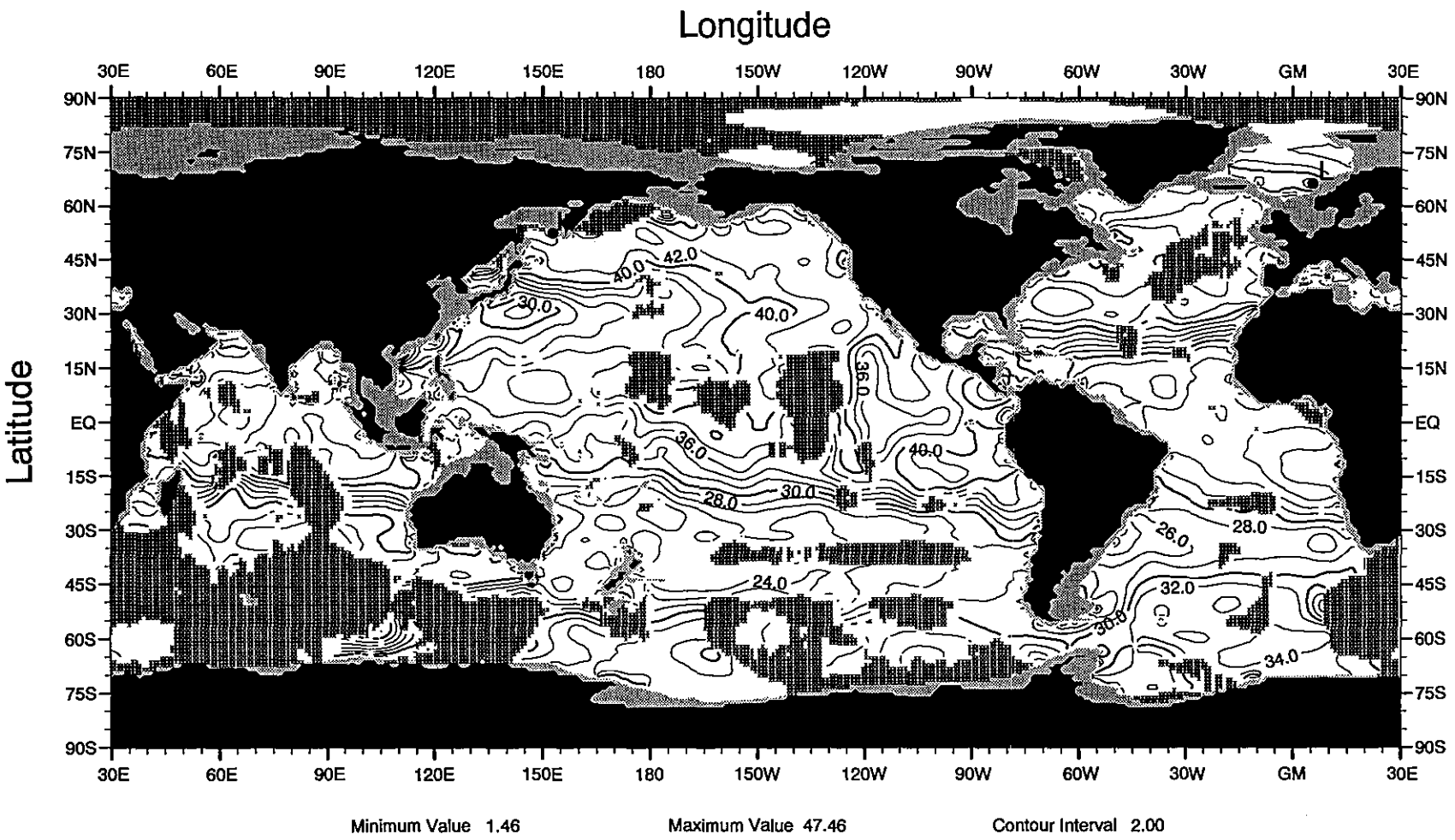

Fig. F11 Annual mean nitrate (μM) at 700 m depth

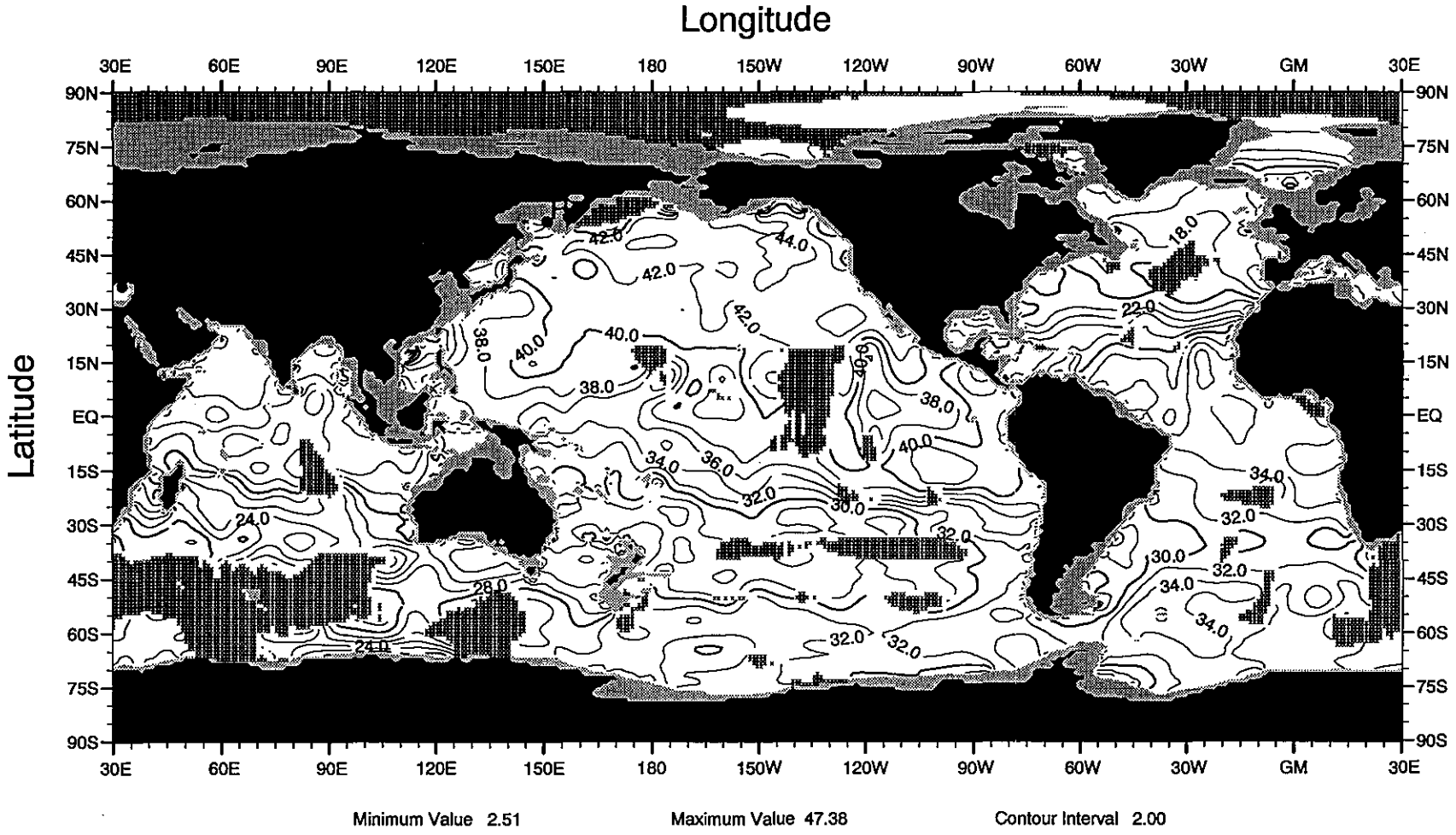

Fig. F12 Annual mean nitrate (μM) at 900 m depth

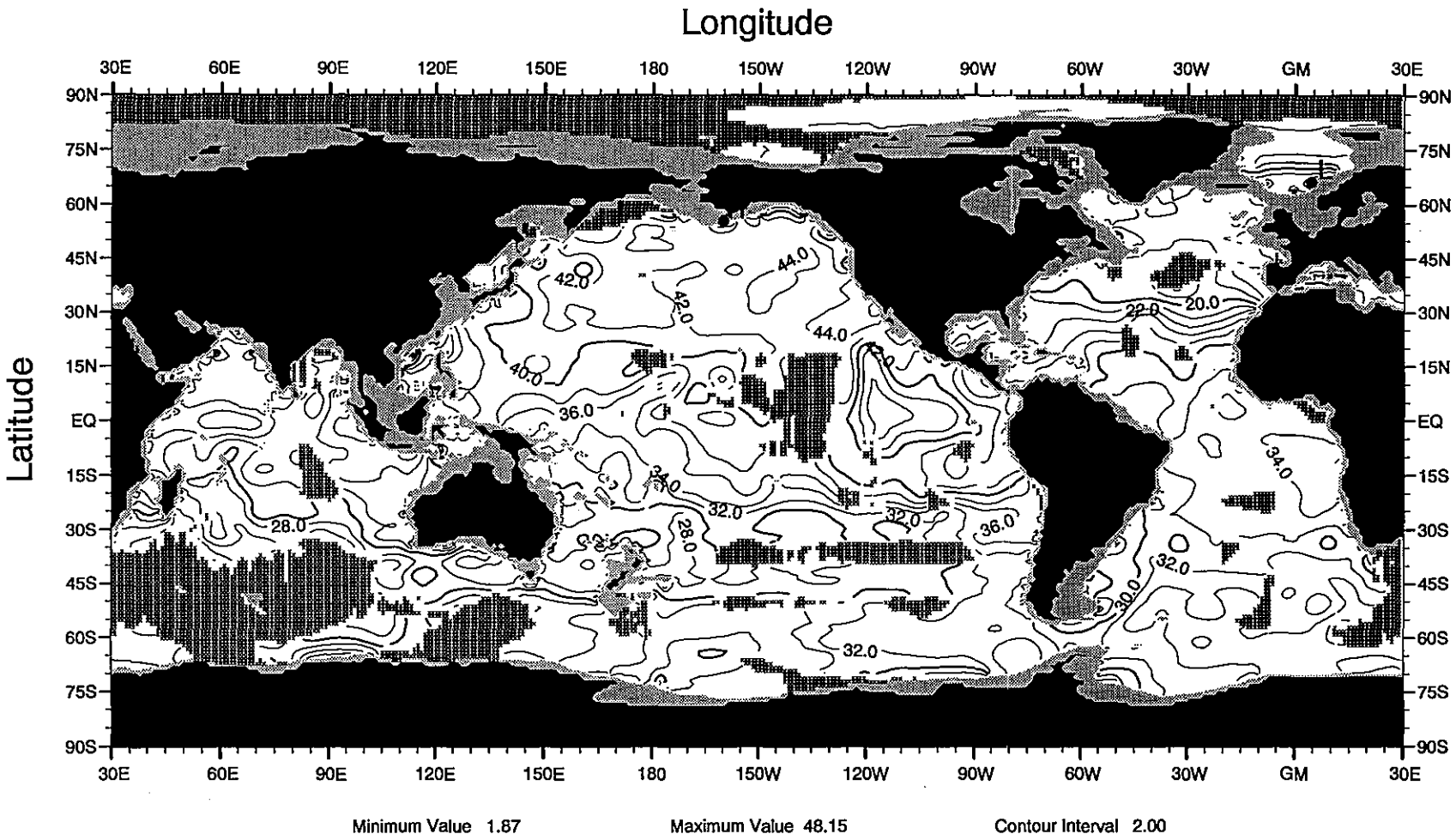

Fig. F13 Annual mean nitrate (μM) at 1000 m depth

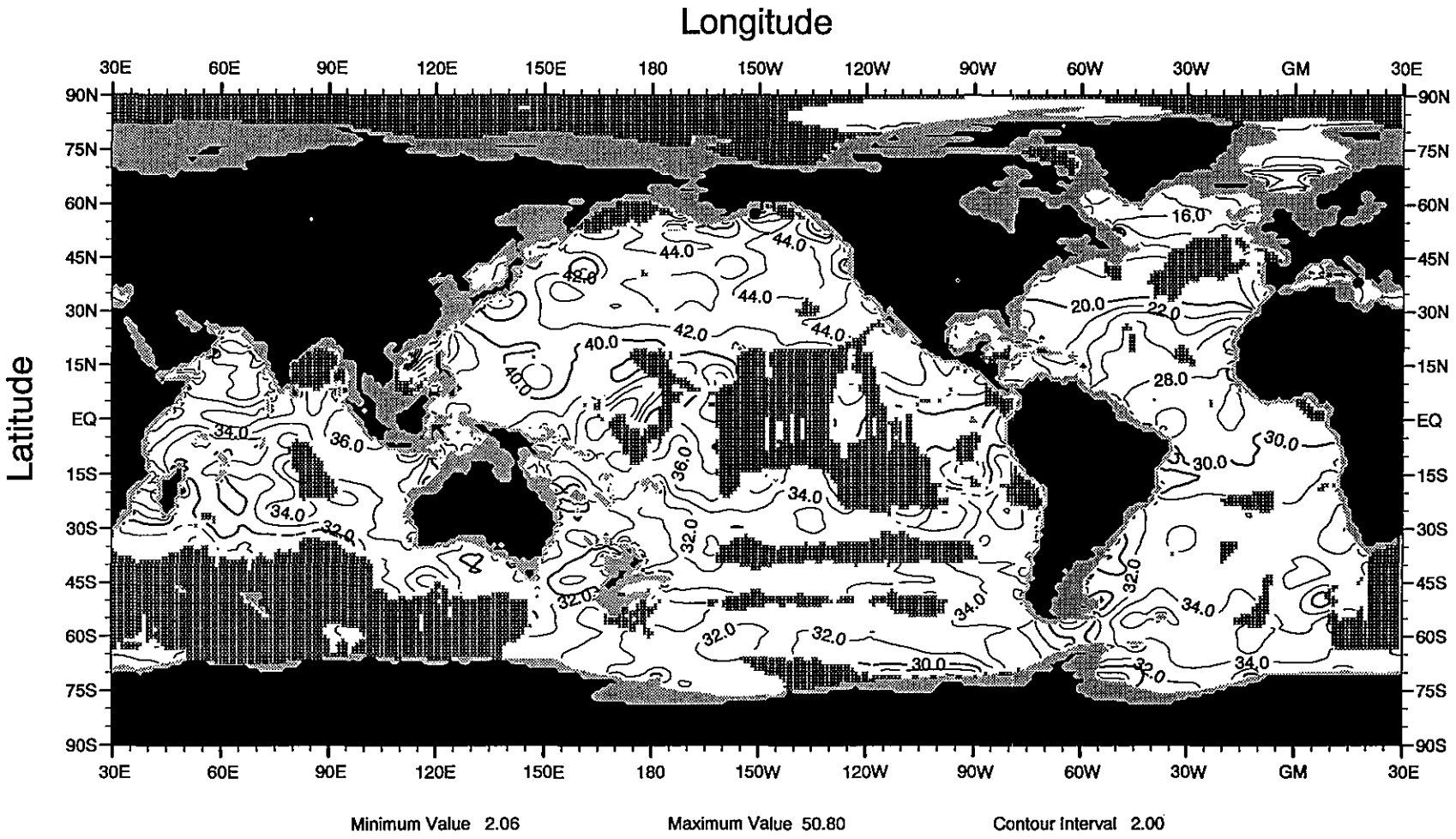

Fig. F14 Annual mean nitrate (μM) at 1200 m depth

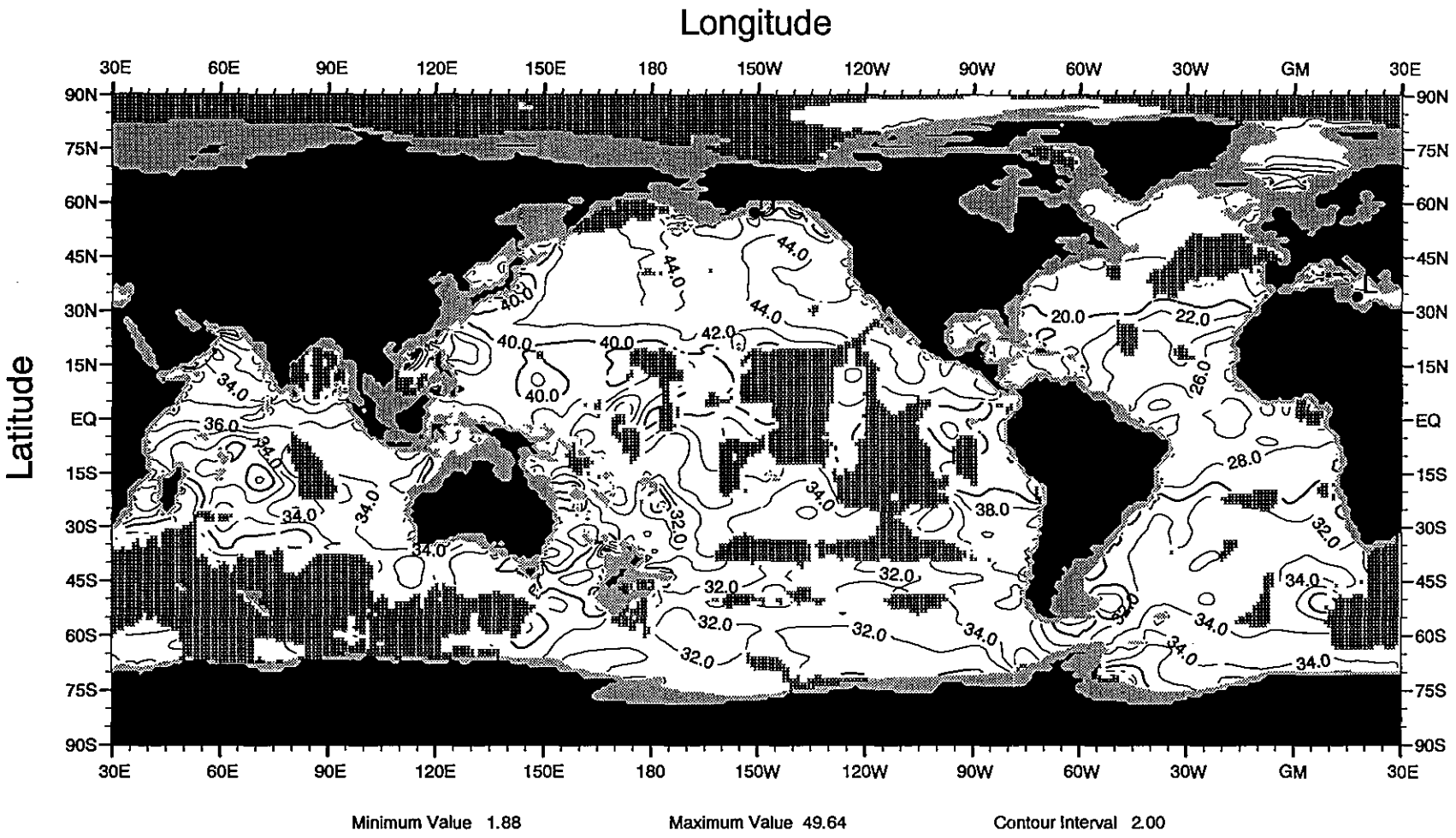

Fig. F15 Annual mean nitrate (μM) at 1300 m depth

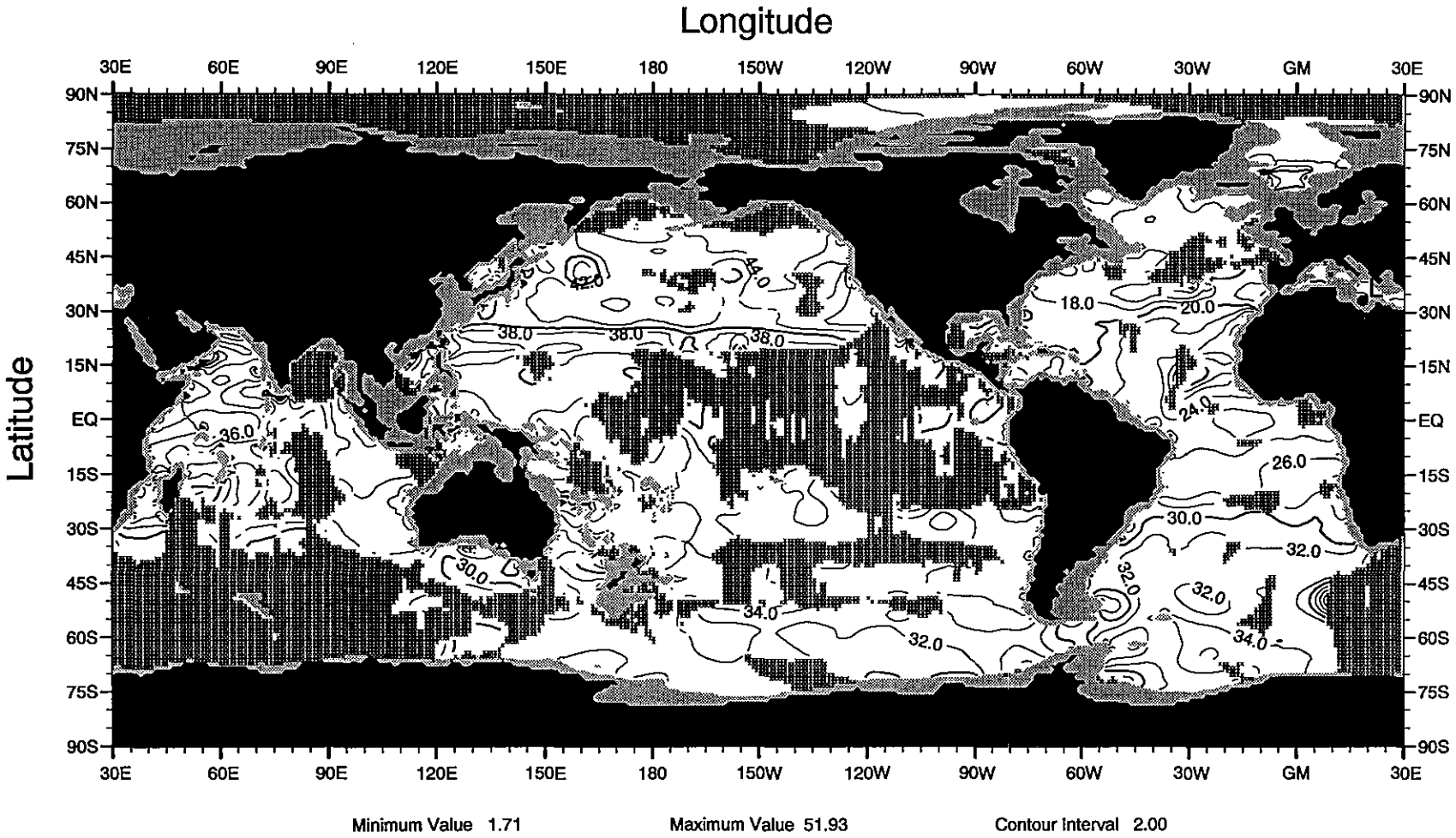

Fig. F16 Annual mean nitrate (μM) at 1500 m depth

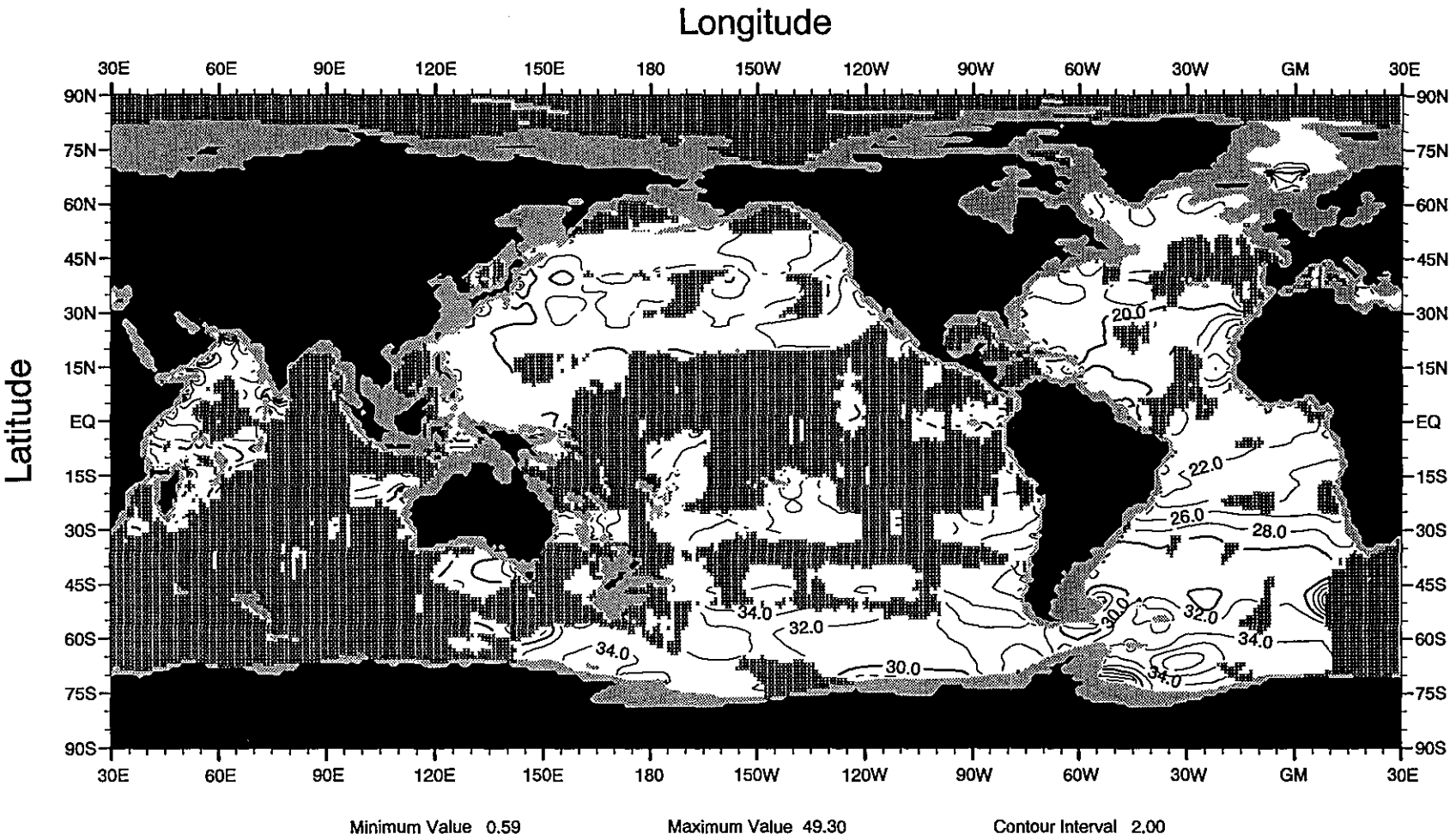

Fig. F17 Annual mean nitrate (μM) at 1750 m depth

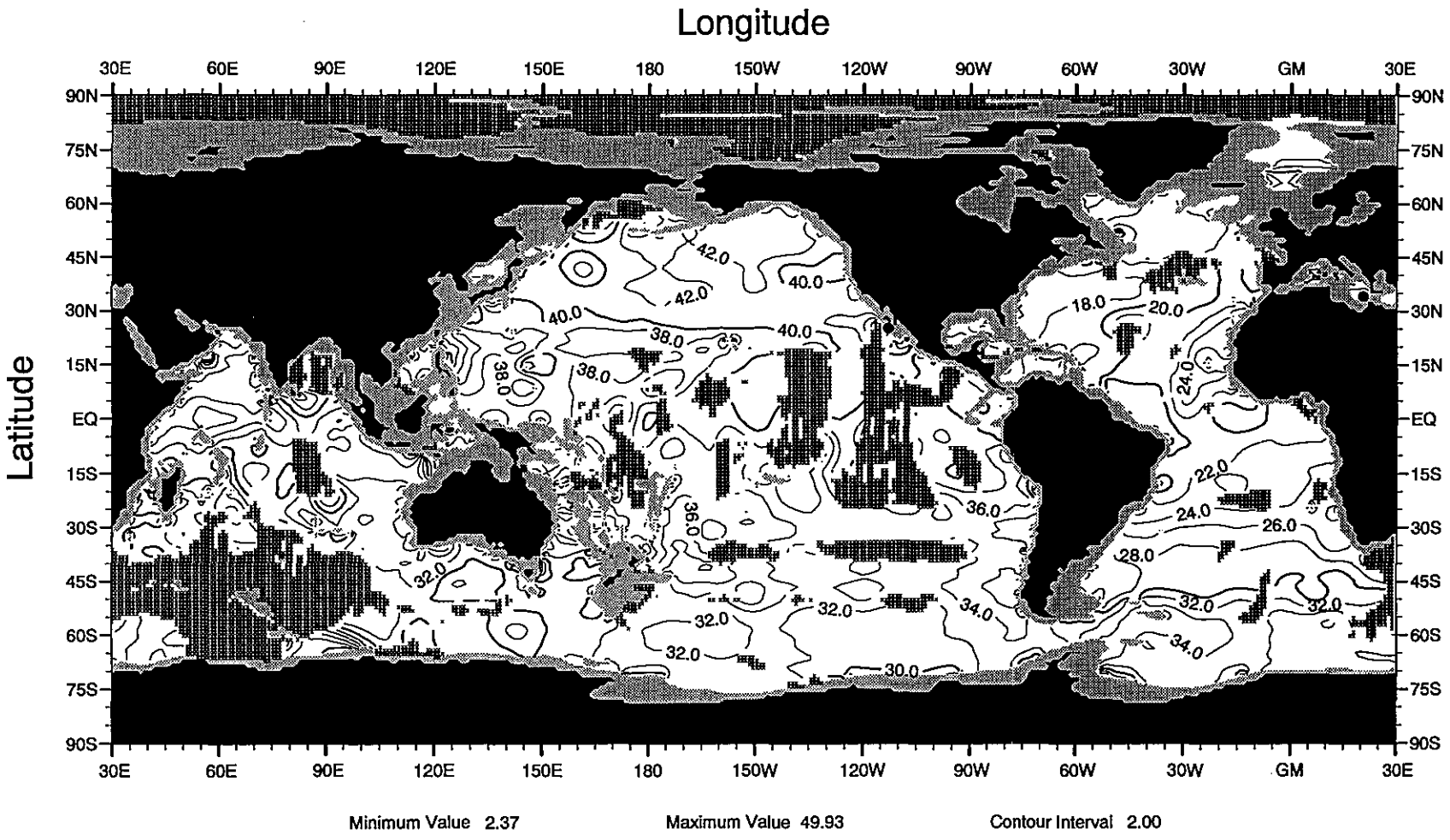

Fig. F18 Annual mean nitrate (μM) at 2000 m depth

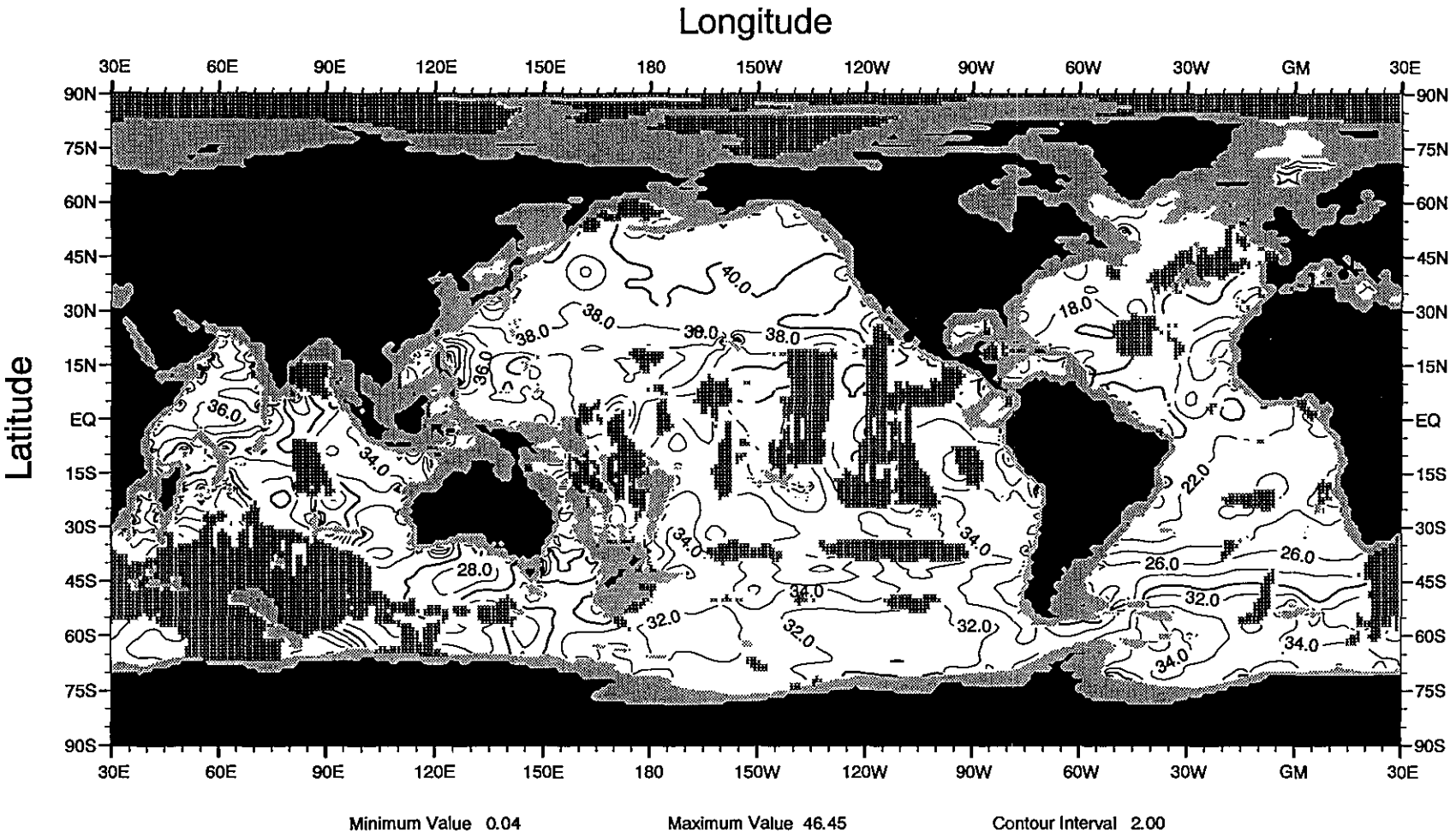

Fig. F19 Annual mean nitrate (μM) at 2500 m depth

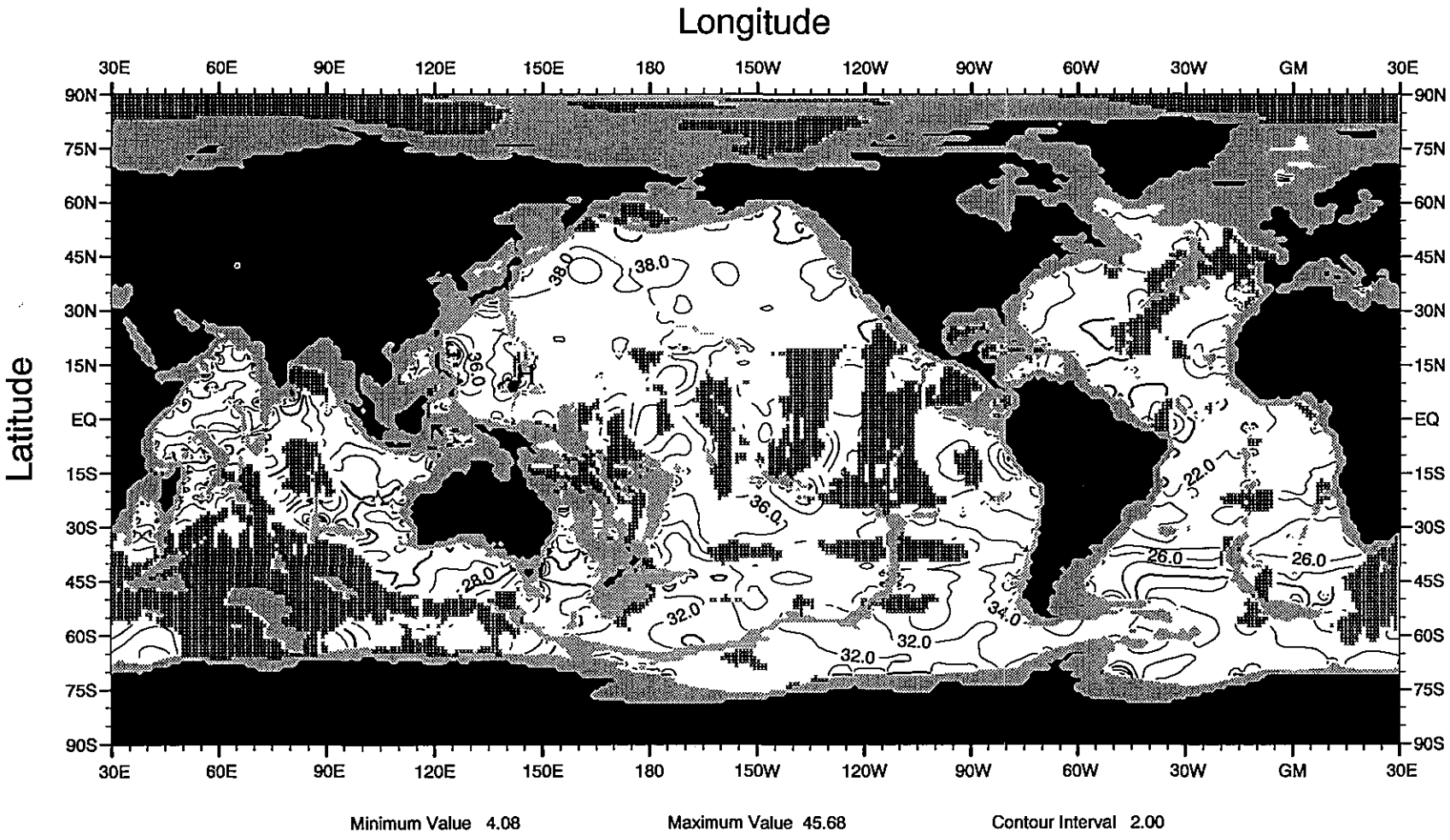

Fig. F20 Annual mean nitrate (μM) at 3000 m depth

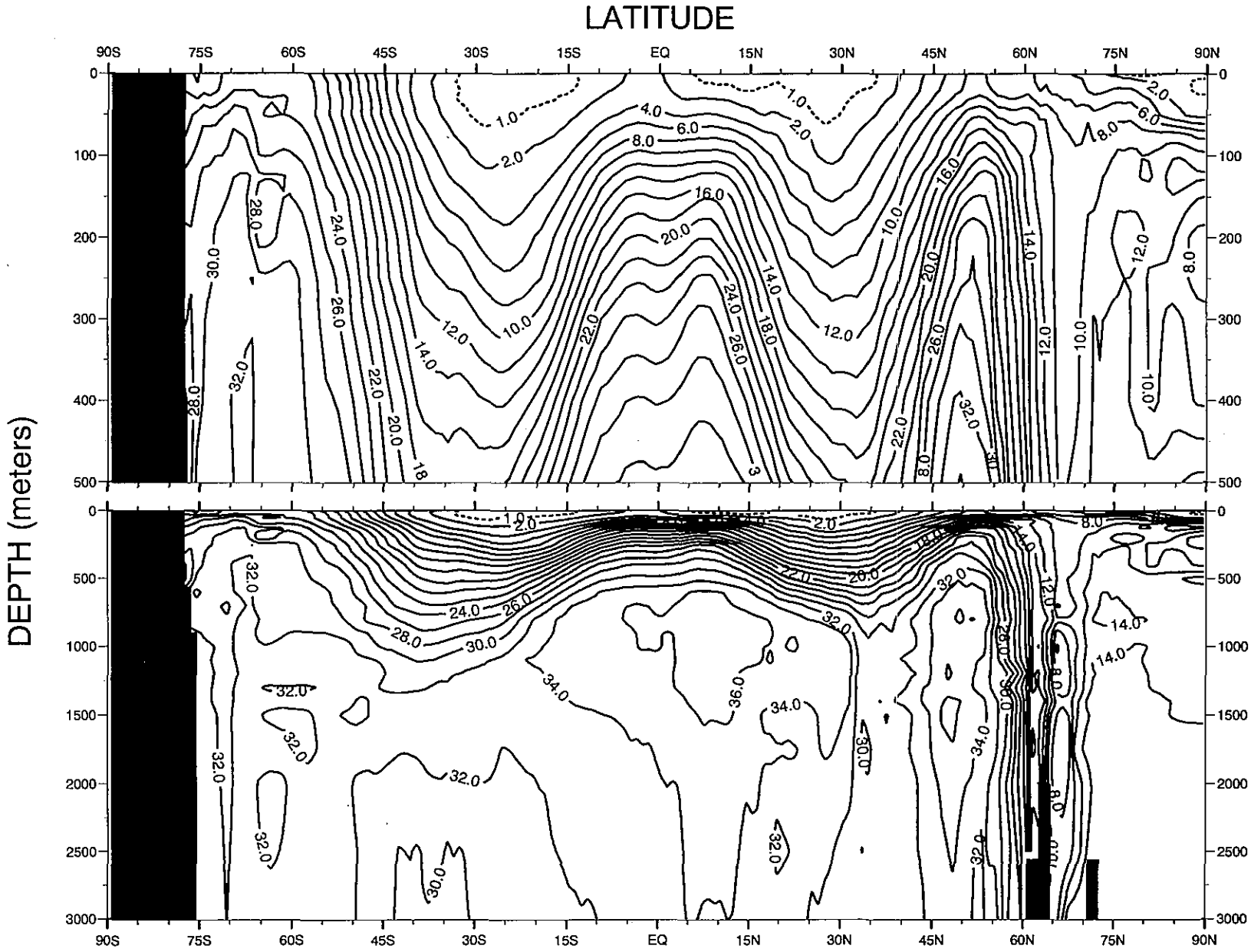

Fig G1. Annual global zonal average (by one-degree squares) of nitrate (μM)

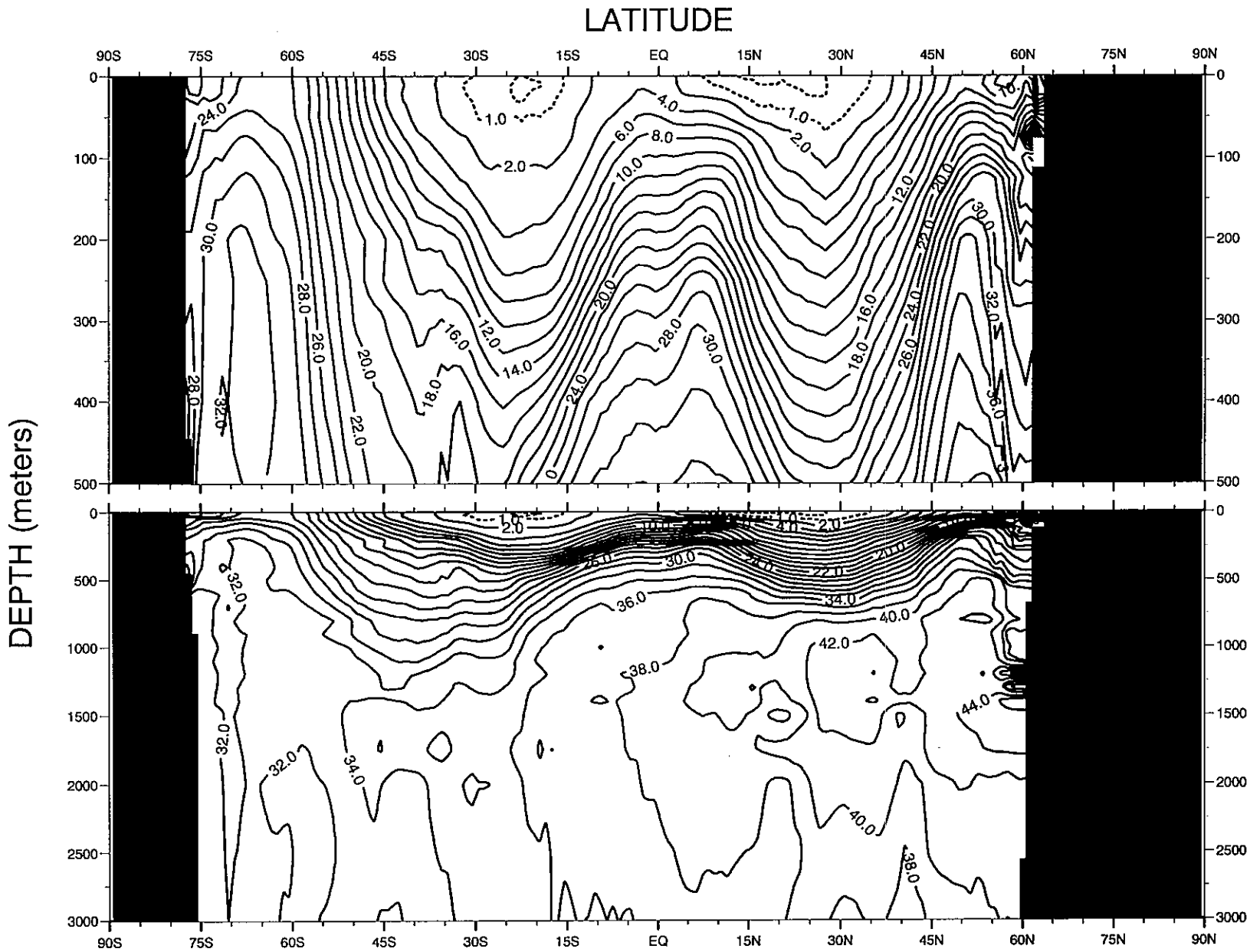

Fig G2. Annual Pacific zonal average (by one-degree squares) of nitrate (μM)

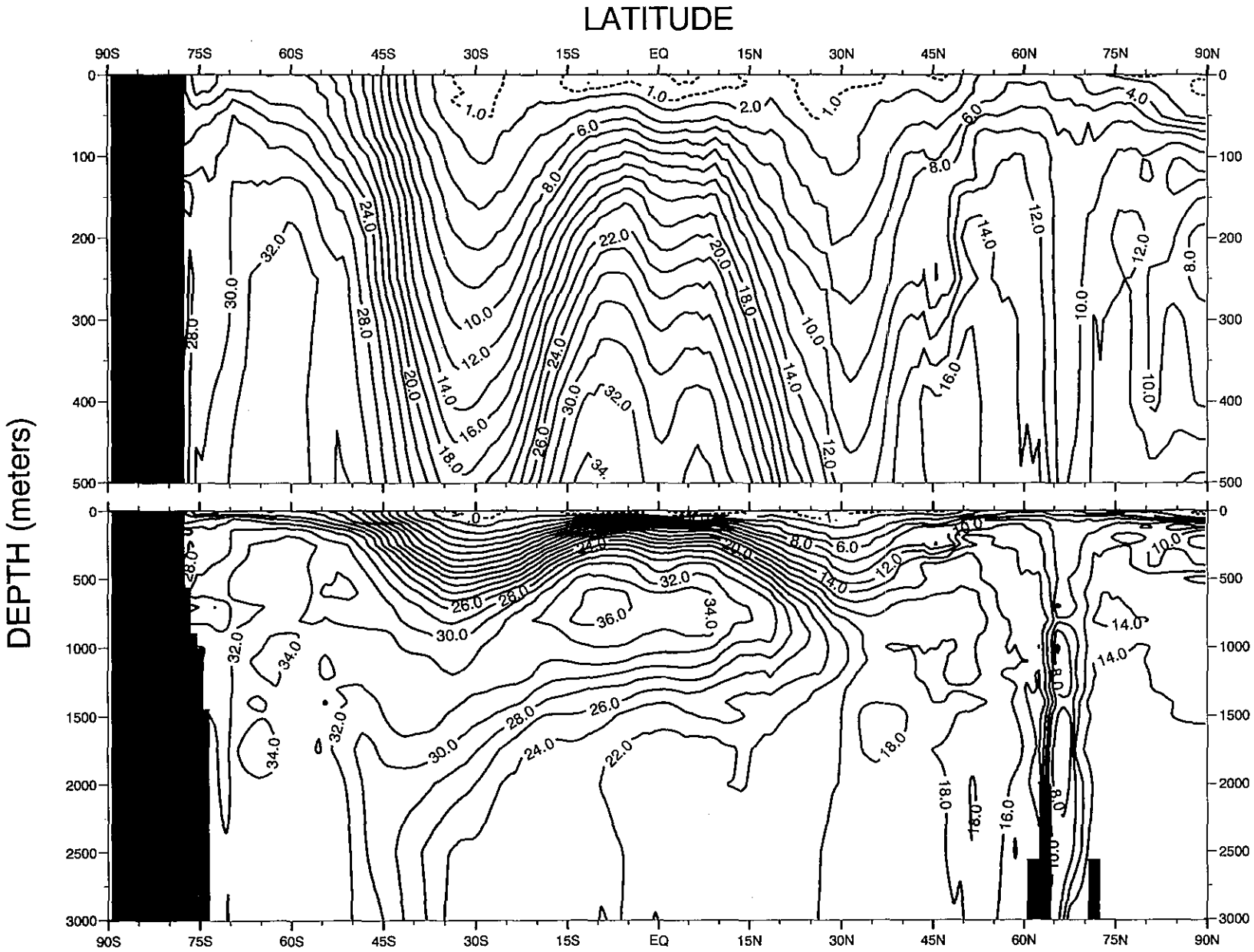

Fig G3. Annual Atlantic zonal average (by one-degree squares) of nitrate (μM)

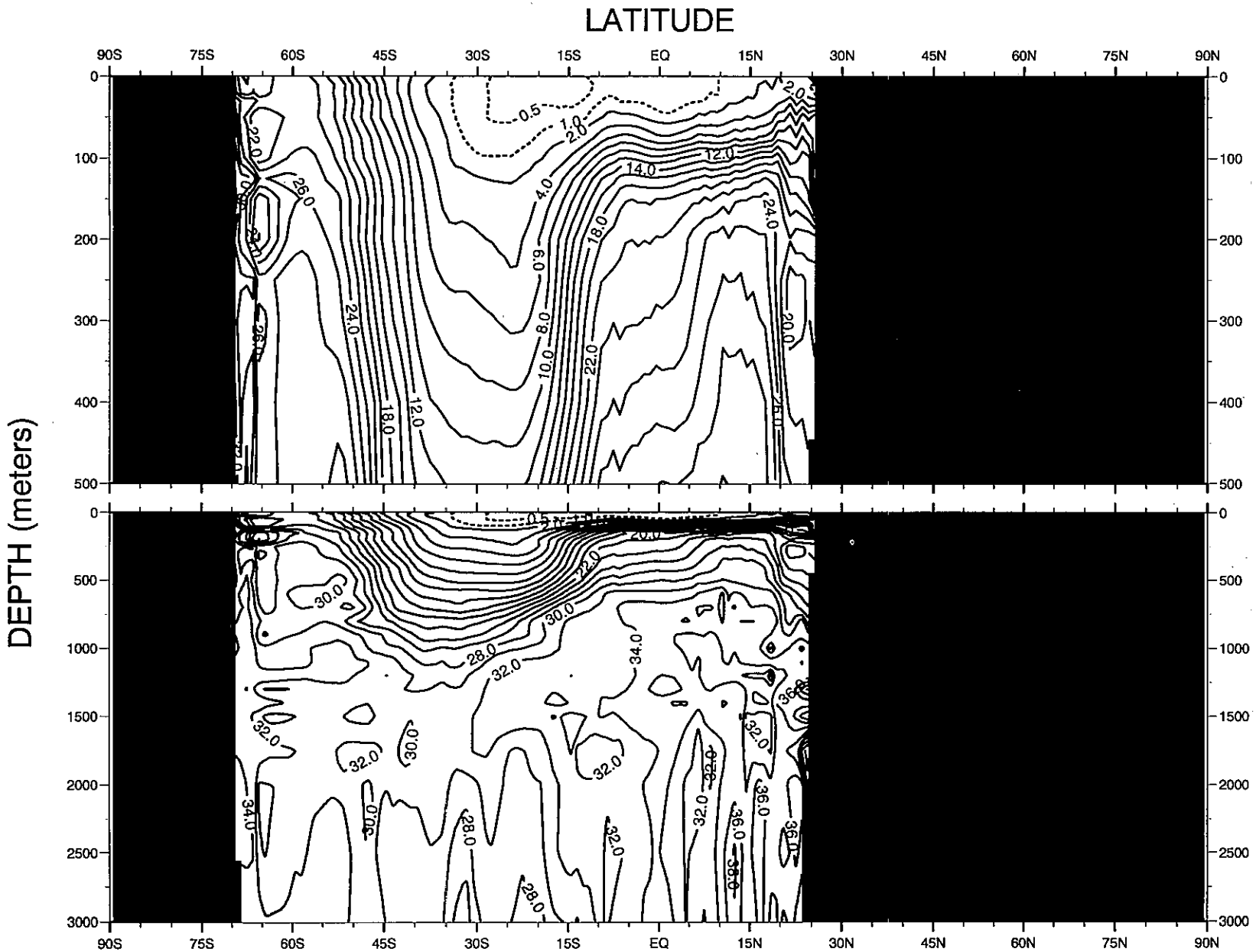

Fig G4. Annual Indian zonal average (by one-degree squares) of nitrate (μM)

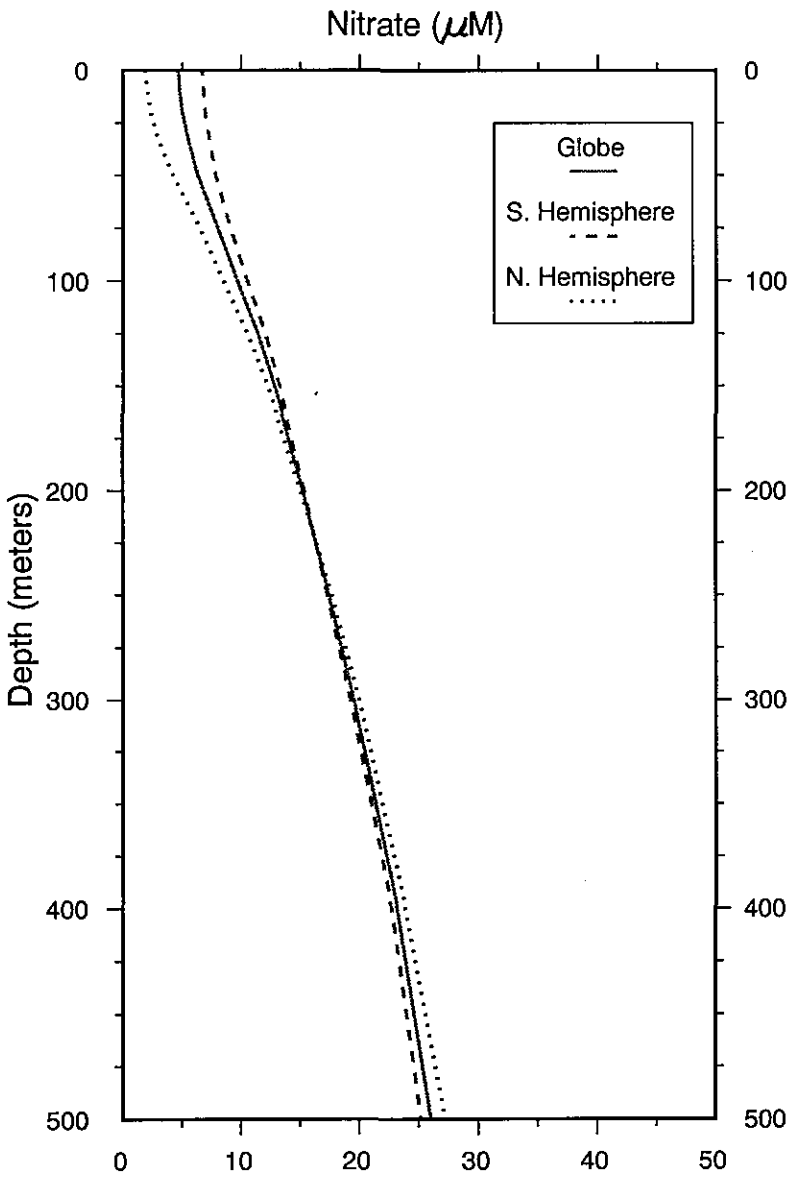

Figure H1a. Annual global nitrate (μM) basin means (0-500 m)

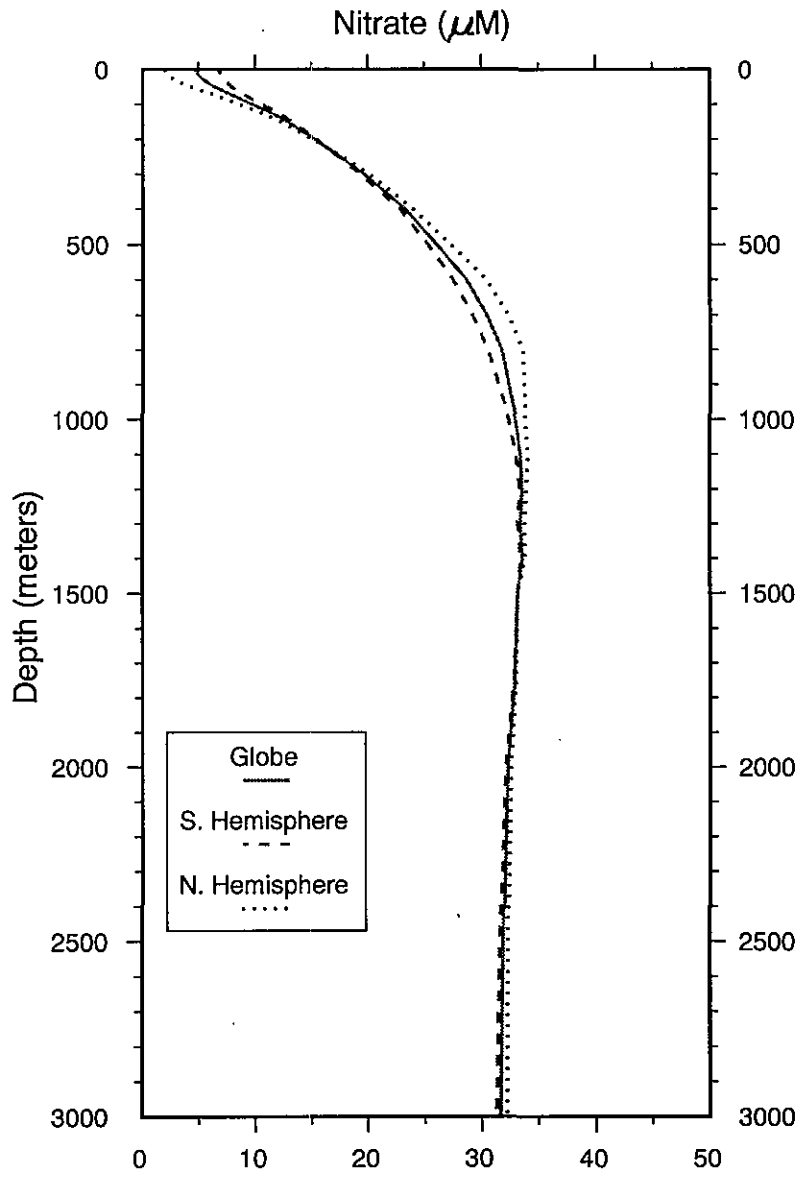

Figure H1b. Annual global nitrate (μM) basin means (0-3000 m)

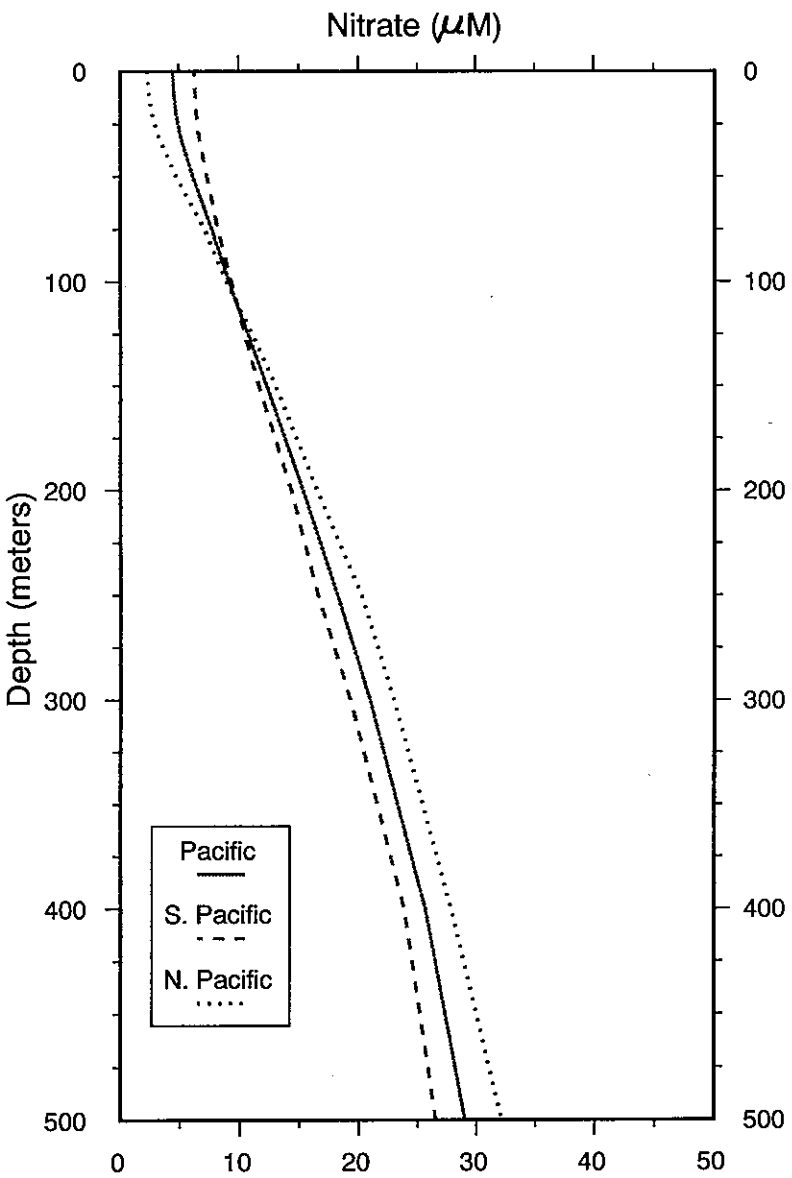

Figure H2a. Annual Pacific nitrate (μM) basin means (0-500 m)

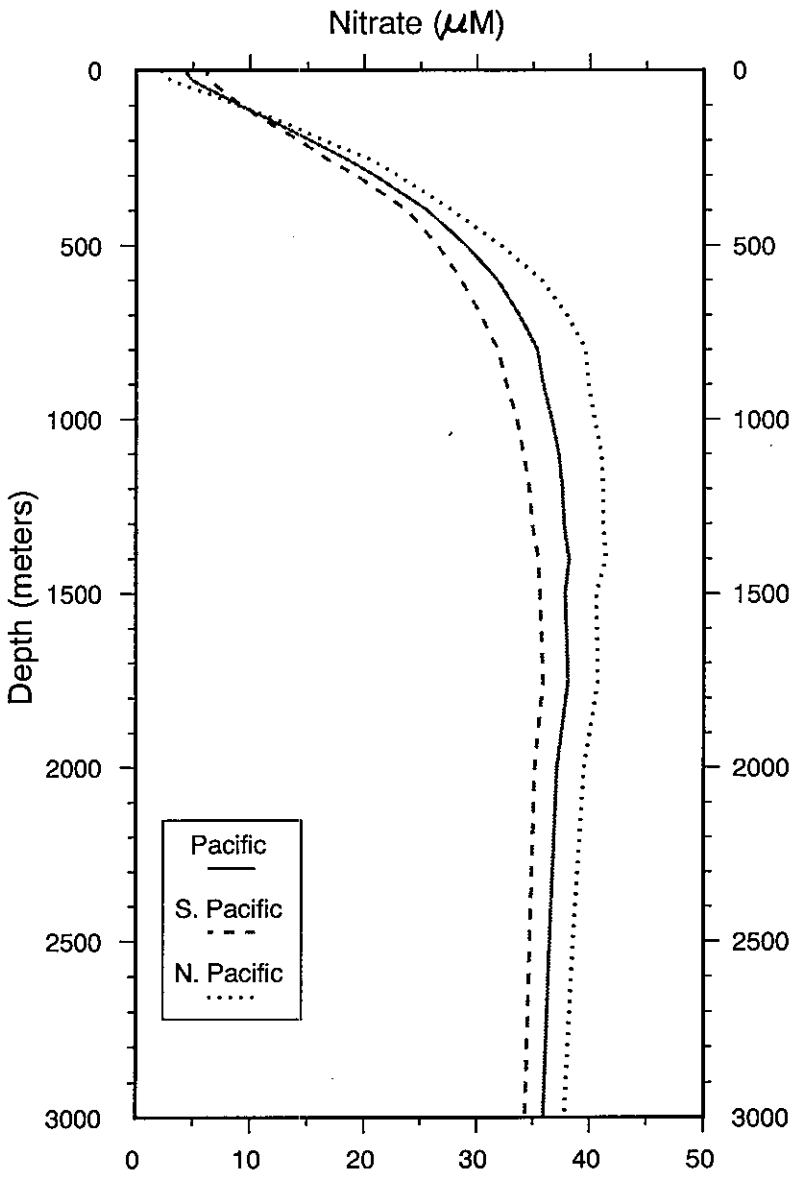

Figure H2b. Annual Pacific nitrate (μM) basin means (0-3000 m)

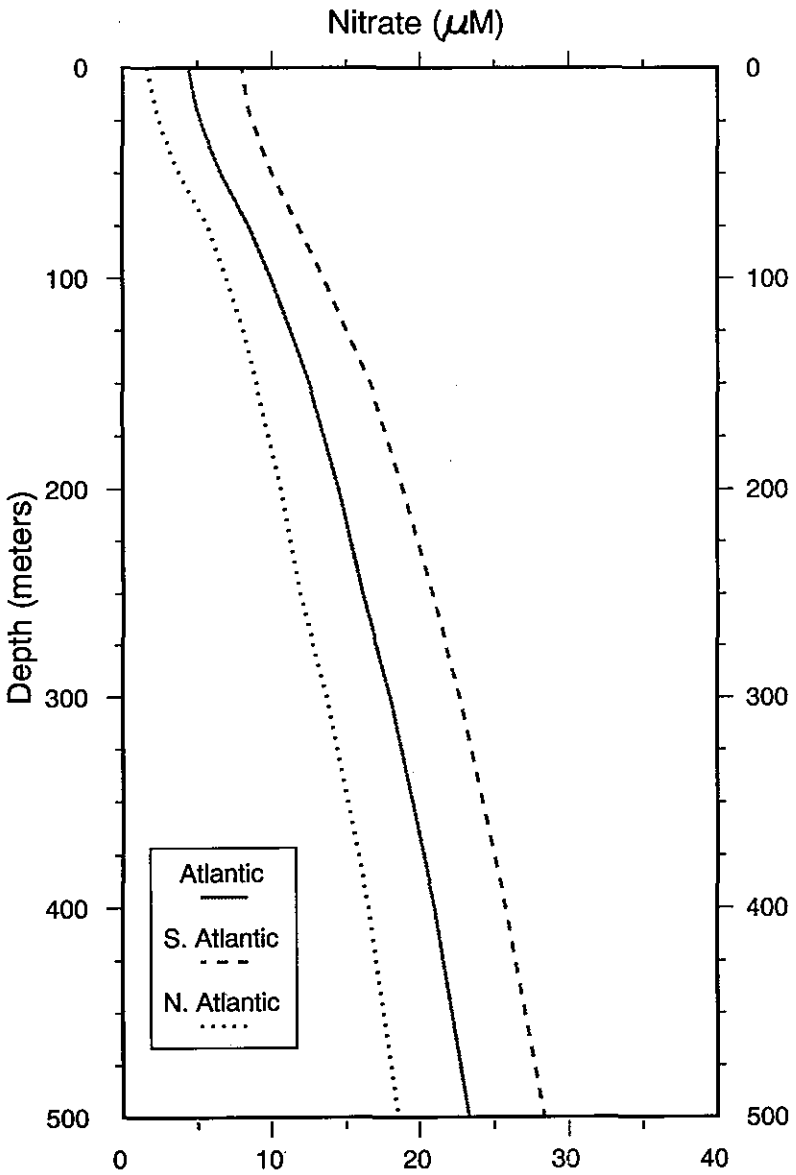

Figure H3a. Annual Atlantic nitrate (μM) basin means (0-500 m)

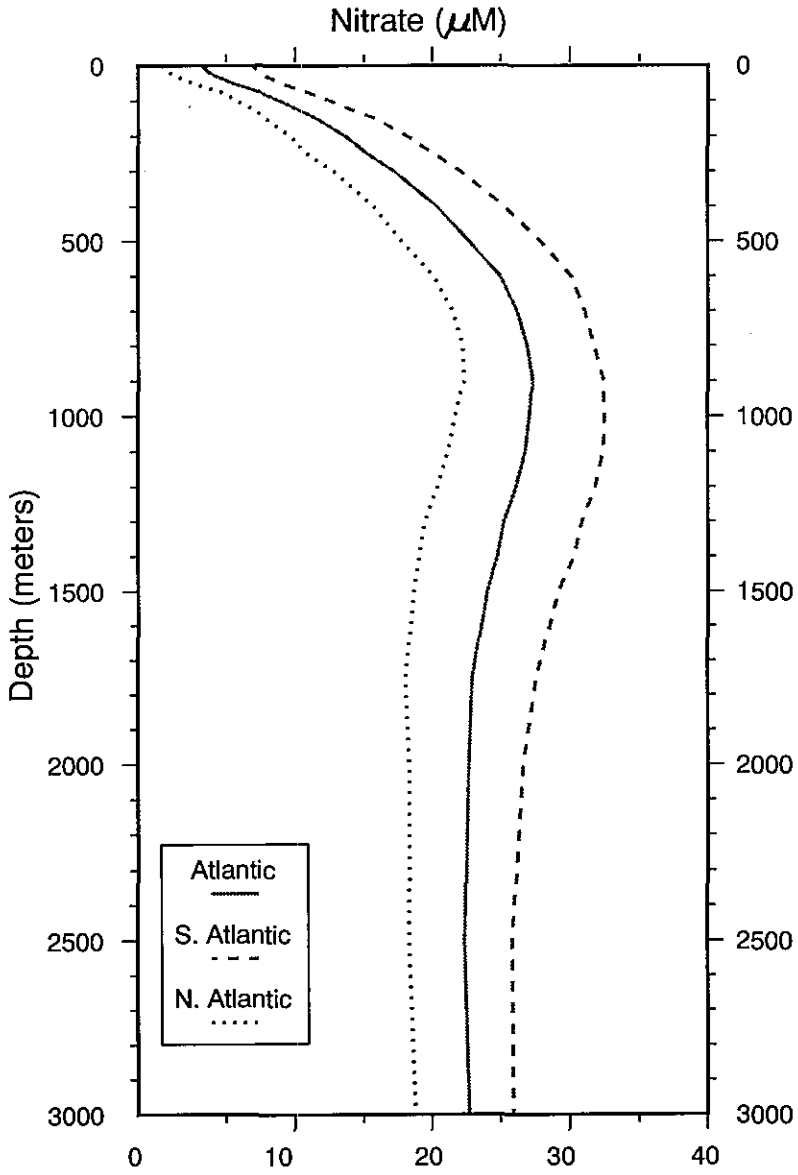

Figure H3b. Annual Atlantic nitrate (μM) basin means (0-3000 m)

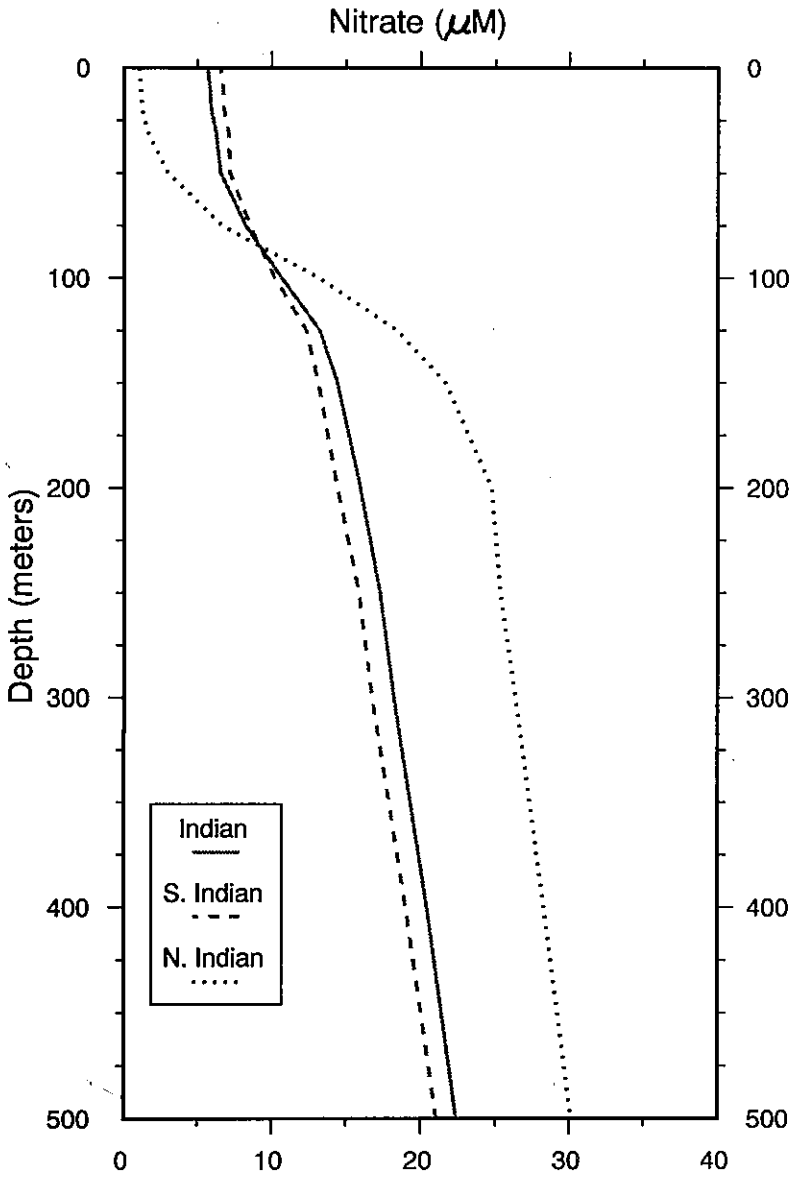

Figure H4a. Annual Indian nitrate (μM) basin means (0-500 m)

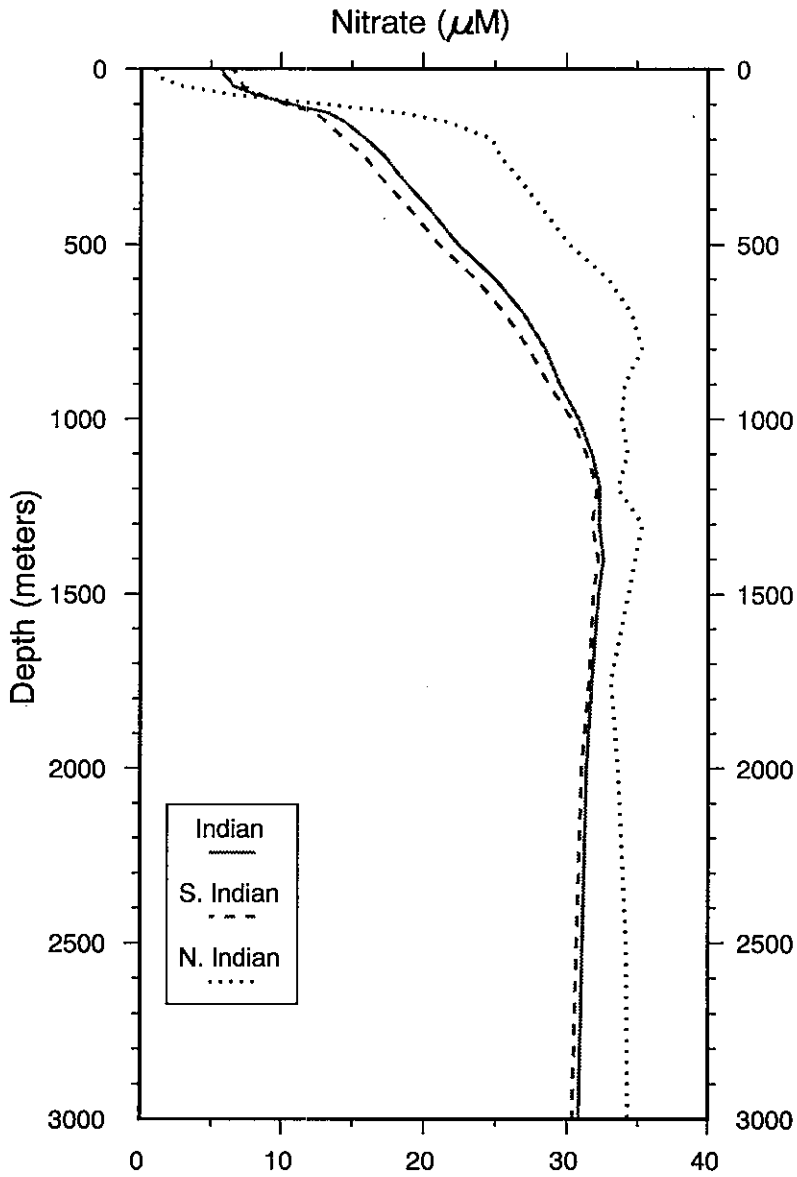

Figure H4b. Annual Indian nitrate (μM) basin means (0-3000 m)

Table H1a. Annual mean nitrate (μM) basin means and standard errors for the world ocean and Pacific Ocean as a function of depth

		World Ocean		Southern Hemisphere Ocean		Northern Hemisphere Ocean		Pacific Ocean		South Pacific Ocean		North Pacific Ocean	
Standard Level	Depth	Mean	Standard Error	Mean	Standard Error	Mean	Standard Error	Mean	Standard Error	Mean	Standard Error	Mean	Standard Error
1	0	4.66	0.37	6.69	0.58	1.90	0.22	4.38	0.50	6.17	0.82	2.25	0.37
2	10	4.81	0.38	6.82	0.60	2.07	0.23	4.47	0.50	6.23	0.83	2.35	0.38
3	20	5.00	0.38	6.95	0.60	2.35	0.24	4.65	0.51	6.35	0.83	2.62	0.40
4	30	5.38	0.39	7.25	0.62	2.82	0.27	5.00	0.52	6.55	0.84	3.15	0.45
5	50	6.32	0.41	7.84	0.63	4.20	0.38	6.06	0.57	7.22	0.88	4.68	0.62
6	75	8.02	0.43	9.10	0.65	6.50	0.49	7.66	0.62	8.17	0.93	7.04	0.80
7	100	9.67	0.46	10.50	0.67	8.49	0.59	9.09	0.68	9.27	0.97	8.88	0.93
8	125	11.38	0.49	12.01	0.69	10.49	0.66	10.65	0.71	10.37	0.98	11.00	1.01
9	150	12.78	0.50	13.18	0.69	12.20	0.70	12.22	0.72	11.58	0.99	13.00	1.03
10	200	15.21	0.50	15.34	0.68	15.02	0.74	15.26	0.71	14.29	0.98	16.46	1.02
11	250	17.43	0.51	17.28	0.68	17.66	0.77	18.20	0.71	16.54	0.96	20.23	1.01
12	300	19.54	0.50	19.24	0.65	19.97	0.78	20.93	0.68	19.27	0.90	22.96	0.97
13	400	23.20	0.48	22.74	0.59	23.89	0.80	25.59	0.60	23.80	0.79	27.80	0.86
14	500	26.02	0.46	25.21	0.54	27.23	0.82	29.04	0.55	26.52	0.70	32.13	0.74
15	600	28.60	0.45	27.44	0.49	30.33	0.83	31.81	0.52	28.60	0.65	35.74	0.58
16	700	30.35	0.43	29.10	0.43	32.23	0.82	33.74	0.49	30.32	0.59	37.94	0.47
17	800	31.69	0.41	30.47	0.37	33.54	0.83	35.35	0.45	31.86	0.53	39.62	0.41
18	900	32.29	0.39	31.40	0.32	33.63	0.83	35.87	0.42	32.60	0.48	39.86	0.38
19	1000	32.92	0.38	32.36	0.27	33.77	0.86	36.62	0.39	33.54	0.44	40.39	0.37
20	1100	33.36	0.38	32.95	0.24	34.00	0.88	37.23	0.38	34.14	0.37	41.01	0.38
21	1200	33.51	0.38	33.30	0.21	33.84	0.91	37.59	0.35	34.65	0.32	41.19	0.37
22	1300	33.33	0.39	33.10	0.24	33.70	0.93	37.71	0.34	34.88	0.33	41.17	0.35
23	1400	33.50	0.40	33.37	0.25	33.70	0.94	38.14	0.33	35.45	0.32	41.42	0.36
24	1500	33.08	0.40	33.08	0.28	33.07	0.93	37.83	0.29	35.57	0.28	40.57	0.36
25	1750	32.84	0.42	32.77	0.31	32.95	0.94	38.06	0.27	35.87	0.26	40.71	0.27
26	2000	32.22	0.40	32.04	0.33	32.51	0.90	37.10	0.27	35.12	0.28	39.49	0.28
27	2500	31.82	0.40	31.56	0.34	32.23	0.87	36.45	0.25	34.71	0.27	38.53	0.27
28	3000	31.62	0.39	31.28	0.35	32.17	0.83	35.91	0.23	34.31	0.28	37.76	0.22

Table H1b. Annual mean nitrate (μM) basin means and standard errors for the Atlantic Ocean and Indian Ocean as a function of depth

		Atlantic Ocean		South Atlantic Ocean		North Atlantic Ocean		Indian Ocean		South Indian Ocean		North Indian Ocean	
Standard Level	Depth	Mean	Standard Error	Mean	Standard Error	Mean	Standard Error	Mean	Standard Error	Mean	Standard Error	Mean	Standard Error
1	0	4.40	0.68	7.98	1.34	1.59	0.23	5.67	0.91	6.54	1.04	1.05	0.33
2	10	4.65	0.69	8.17	1.37	1.89	0.25	5.83	0.94	6.72	1.08	1.11	0.37
3	20	4.95	0.69	8.42	1.37	2.20	0.27	5.91	0.95	6.79	1.09	1.23	0.40
4	30	5.42	0.71	8.93	1.40	2.63	0.31	6.23	0.98	7.09	1.12	1.57	0.50
5	50	6.58	0.76	10.03	1.46	3.79	0.44	6.54	0.93	7.19	1.07	2.97	0.77
6	75	8.44	0.80	11.78	1.50	5.69	0.57	8.28	0.92	8.57	1.07	6.70	0.90
7	100	9.93	0.85	13.50	1.53	6.93	0.67	10.67	0.93	10.22	1.07	13.16	1.04
8	125	11.25	0.88	15.02	1.55	8.06	0.70	13.26	1.01	12.34	1.14	18.41	1.15
9	150	12.51	0.92	16.64	1.56	8.94	0.76	14.44	1.03	13.15	1.12	21.65	1.24
10	200	14.51	0.94	18.87	1.50	10.62	0.84	15.98	1.08	14.42	1.14	24.74	1.23
11	250	16.14	0.97	20.84	1.45	11.90	0.95	17.31	1.10	15.89	1.19	25.33	1.30
12	300	18.01	0.96	22.69	1.34	13.71	1.04	18.22	1.08	16.78	1.15	26.35	1.36
13	400	20.98	0.95	25.78	1.15	16.51	1.17	20.40	1.03	19.01	1.10	28.27	1.26
14	500	23.28	0.93	28.34	0.91	18.52	1.23	22.36	0.97	21.02	1.02	30.12	1.15
15	600	25.47	0.91	30.44	0.76	20.74	1.28	24.94	0.89	23.58	0.91	32.91	1.18
16	700	26.68	0.86	31.40	0.58	22.14	1.26	26.94	0.82	25.65	0.83	34.56	0.96
17	800	27.36	0.82	32.04	0.49	22.83	1.22	28.45	0.67	27.30	0.67	35.31	0.73
18	900	27.75	0.82	32.70	0.34	22.92	1.22	29.46	0.55	28.70	0.58	34.04	0.72
19	1000	27.55	0.81	32.82	0.26	22.31	1.12	30.79	0.42	30.29	0.44	33.87	0.79
20	1100	27.24	0.78	32.69	0.23	21.80	0.99	31.76	0.37	31.35	0.40	34.28	0.56
21	1200	26.61	0.76	32.14	0.30	21.05	0.90	32.31	0.30	32.11	0.31	33.59	0.76
22	1300	25.72	0.74	31.22	0.40	20.14	0.77	32.26	0.35	31.77	0.35	35.33	0.67
23	1400	25.26	0.72	30.64	0.50	19.77	0.67	32.56	0.28	32.19	0.29	34.81	0.56
24	1500	24.55	0.72	29.57	0.57	19.35	0.70	32.20	0.37	31.86	0.39	34.33	0.99
25	1750	23.52	0.68	28.02	0.69	18.79	0.57	31.76	0.26	31.55	0.27	33.09	0.79
26	2000	23.26	0.65	27.09	0.71	19.05	0.59	31.37	0.36	31.03	0.36	33.60	1.02
27	2500	22.99	0.63	26.35	0.73	19.06	0.55	31.09	0.41	30.66	0.39	34.16	1.30
28	3000	23.31	0.63	26.41	0.77	19.47	0.46	30.80	0.45	30.34	0.45	34.29	1.22

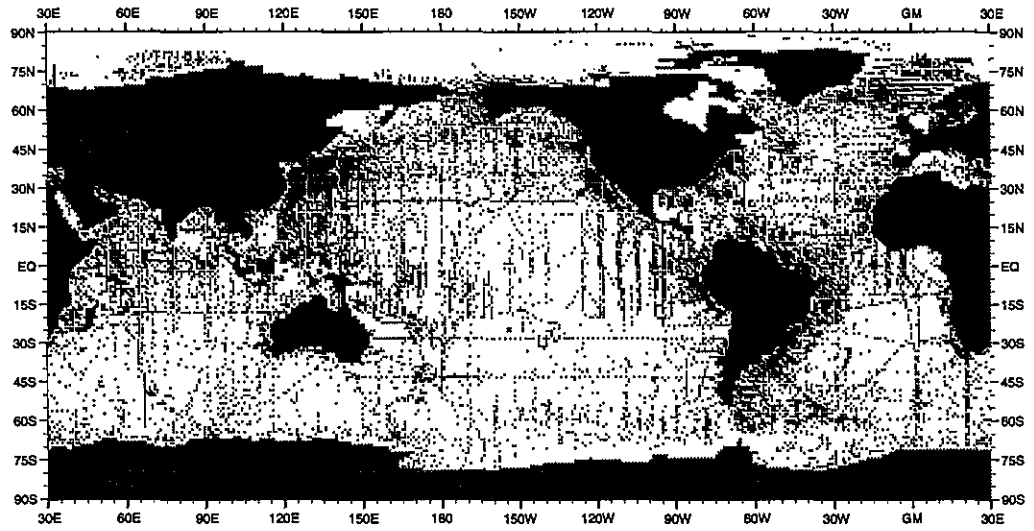

Fig. I1 Distribution of silicate observations at the surface

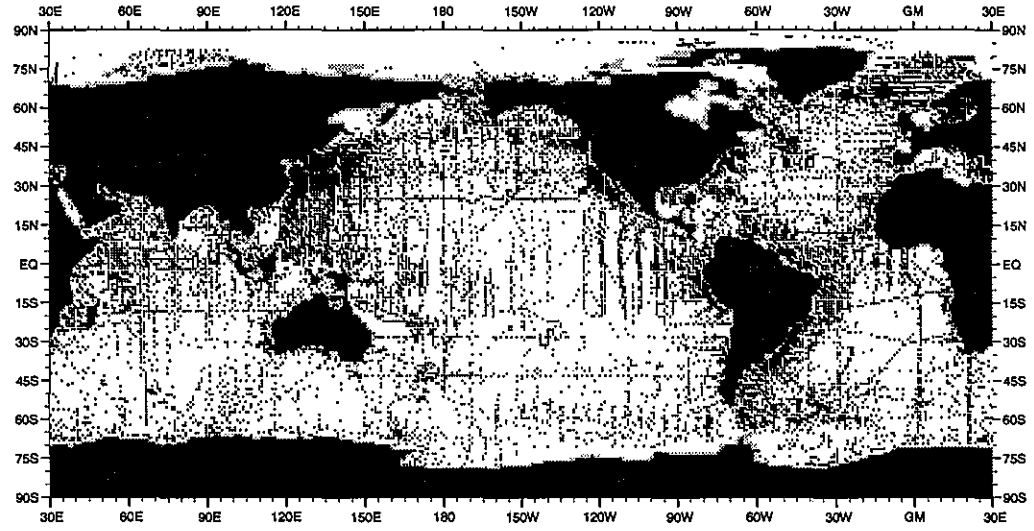

Fig. I2 Distribution of silicate observations at 30 m depth

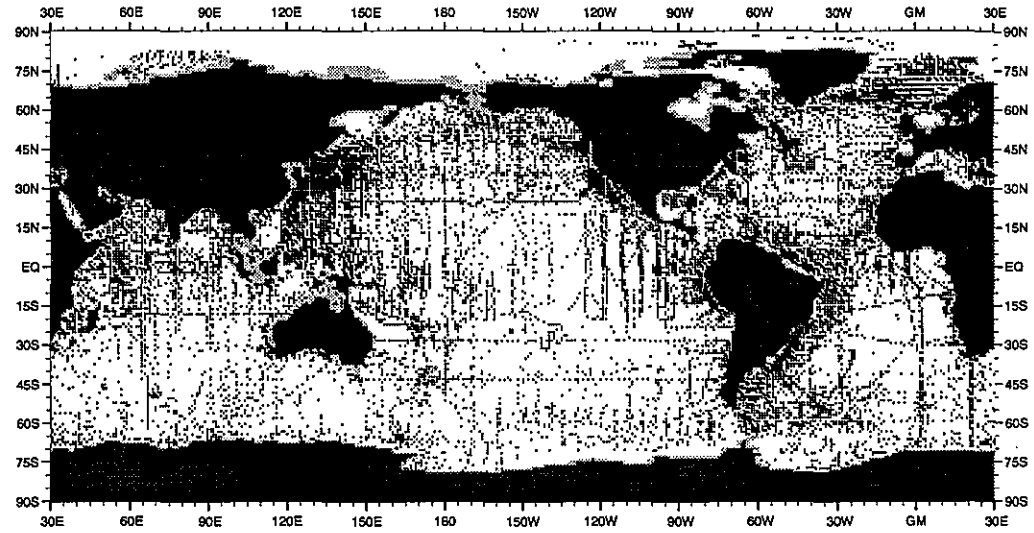

Fig. I3 Distribution of silicate observations at 50 m depth

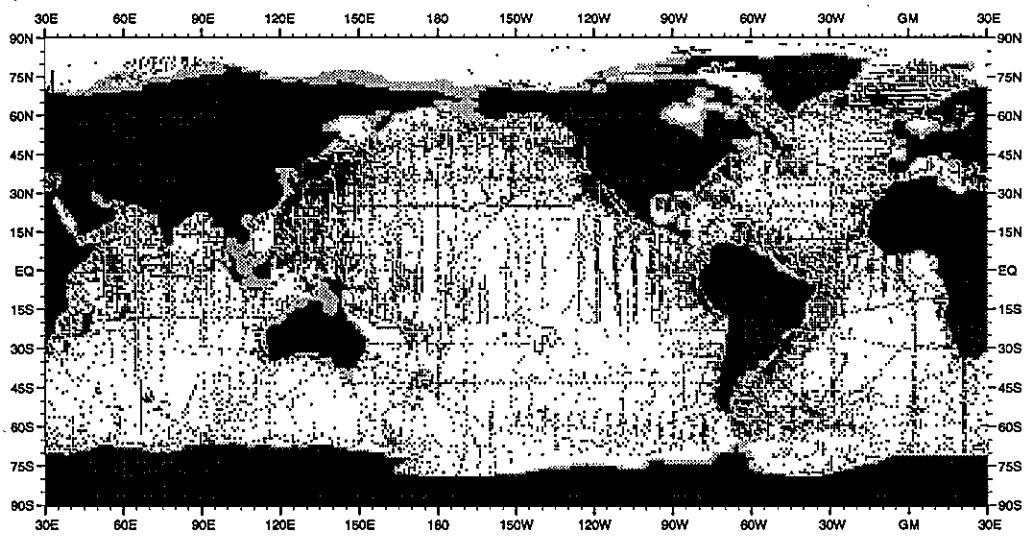

Fig. I4 Distribution of silicate observations at 75 m depth

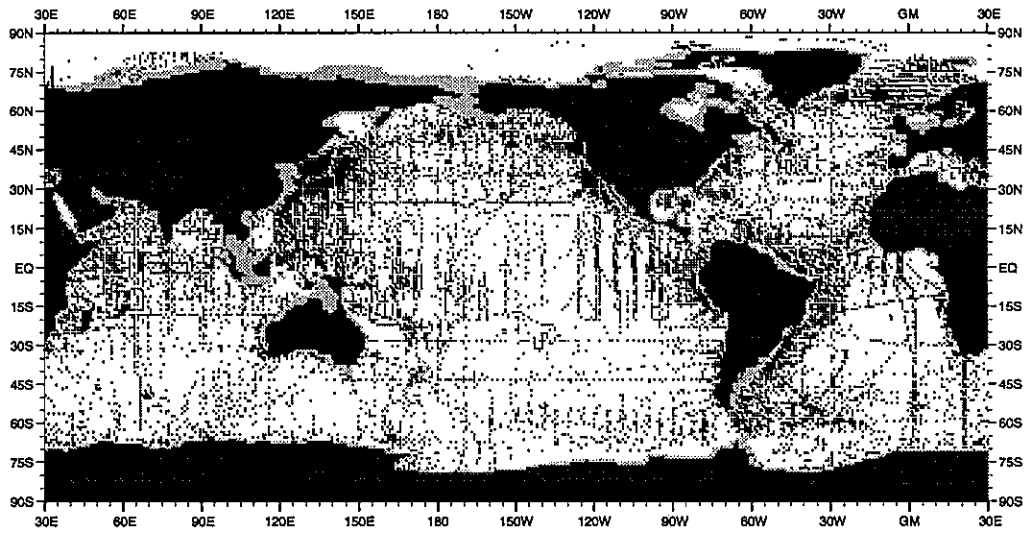

Fig. I5 Distribution of silicate observations at 100 m depth

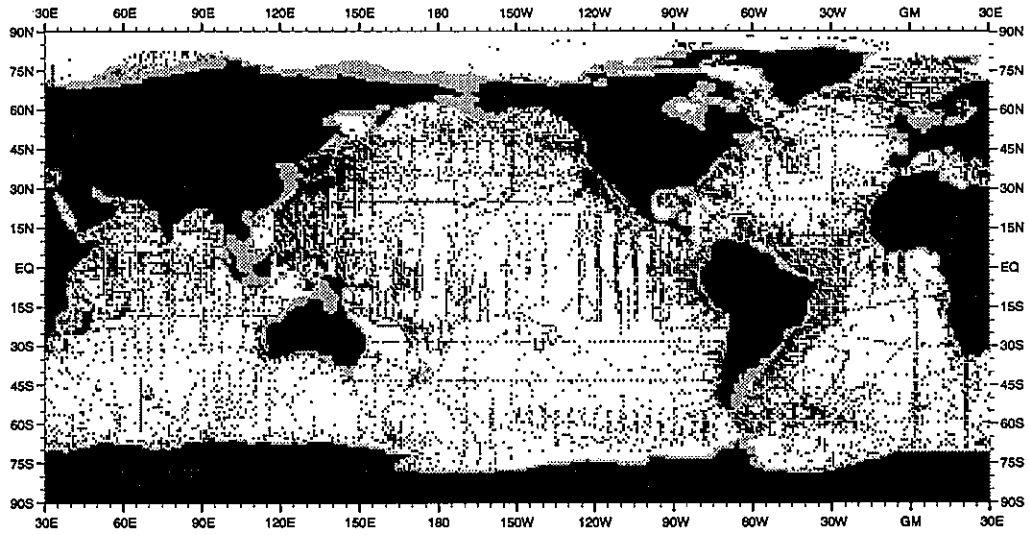

Fig. I6 Distribution of silicate observations at 125 m depth

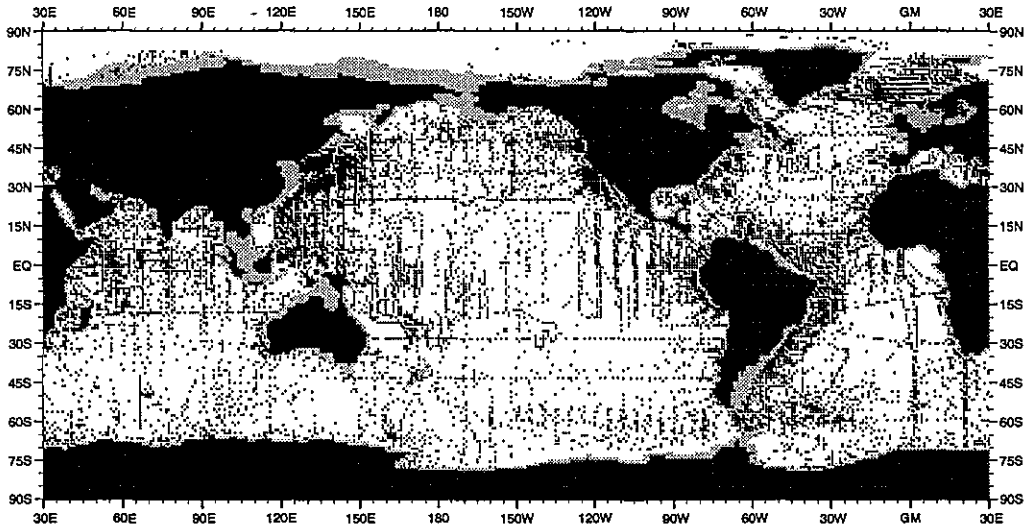

Fig. I7 Distribution of silicate observations at 150 m depth

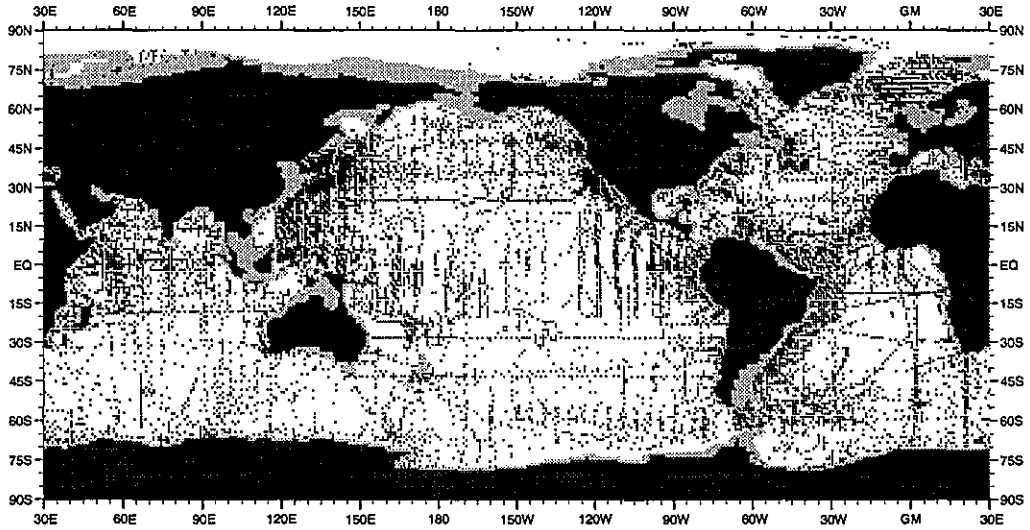

Fig. I8 Distribution of silicate observations at 250 m depth

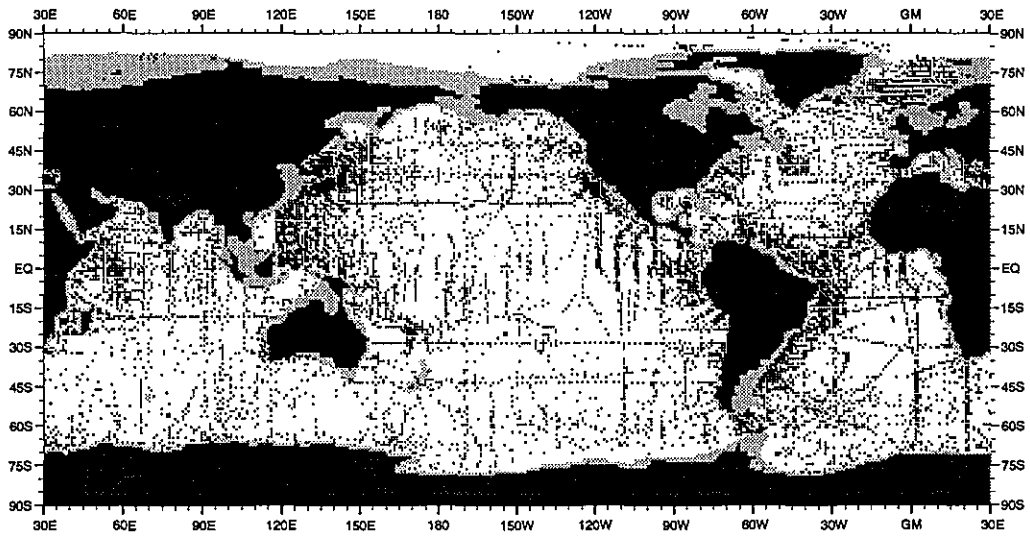

Fig. I9 Distribution of silicate observations at 400 m depth

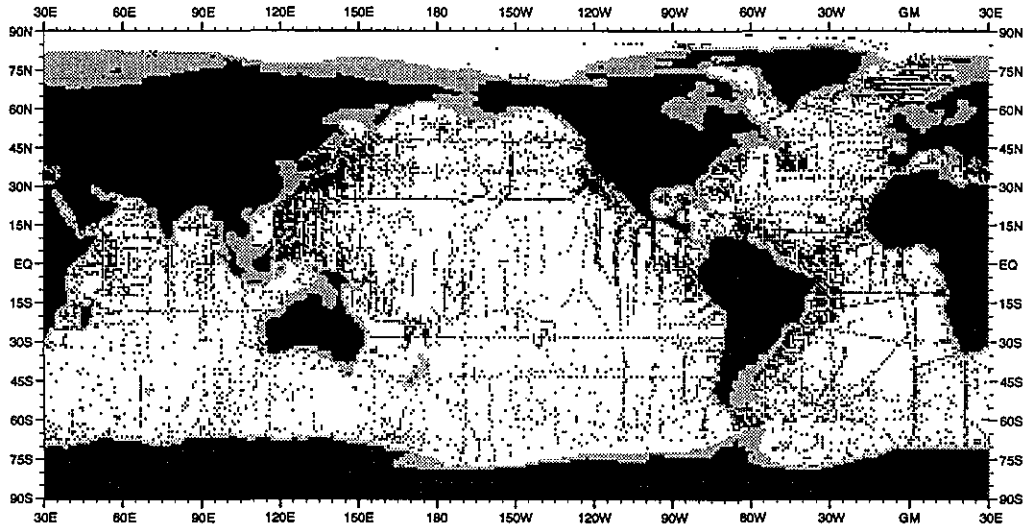

Fig. I10 Distribution of silicate observations at 500 m depth

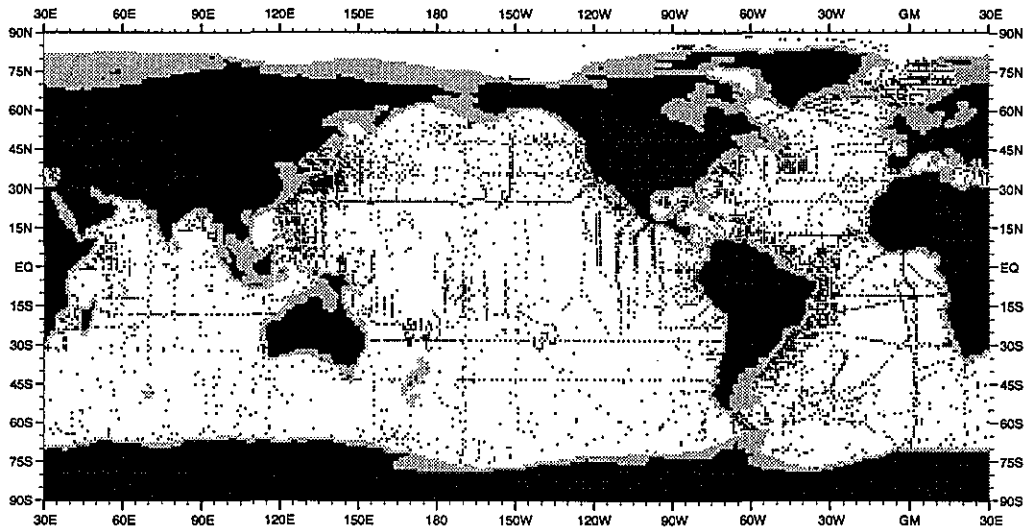

Fig. I11 Distribution of silicate observations at 700 m depth

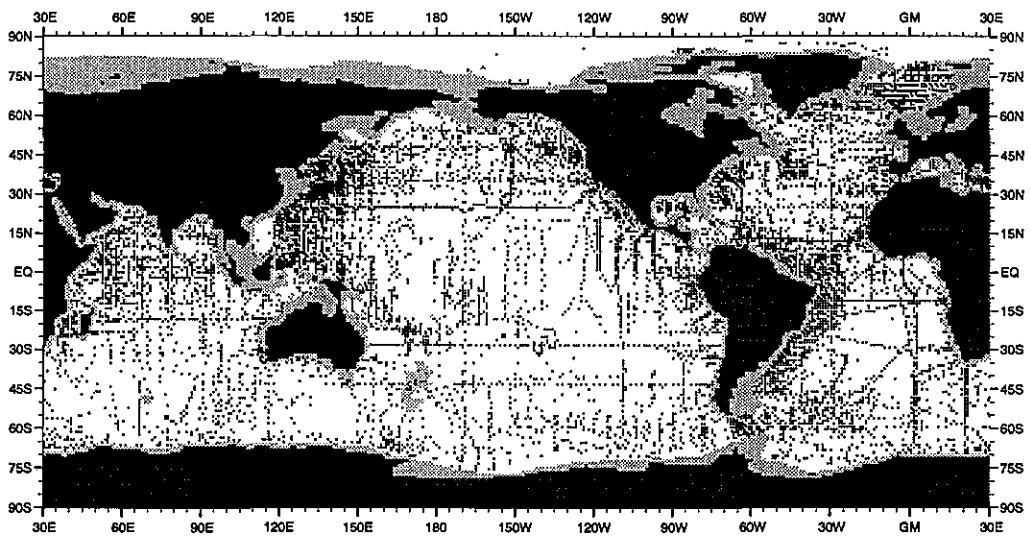

Fig. I12 Distribution of silicate observations at 900 m depth

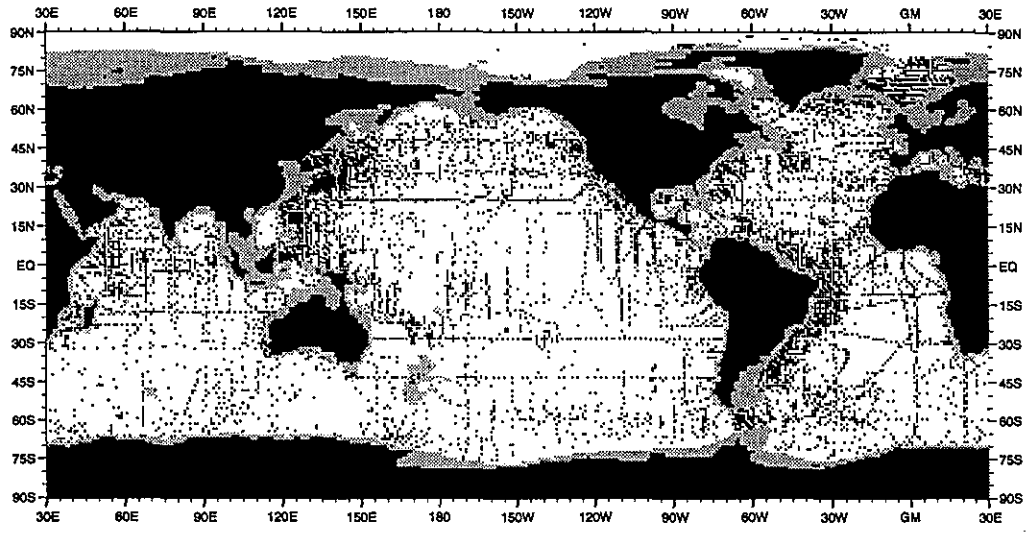

Fig. I13 Distribution of silicate observations at 1000 m depth

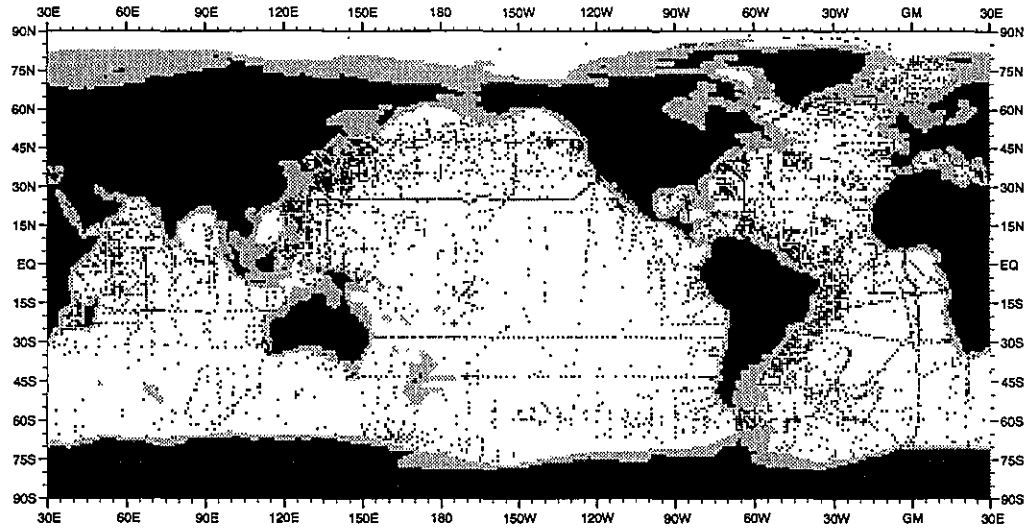

Fig. I14 Distribution of silicate observations at 1200 m depth

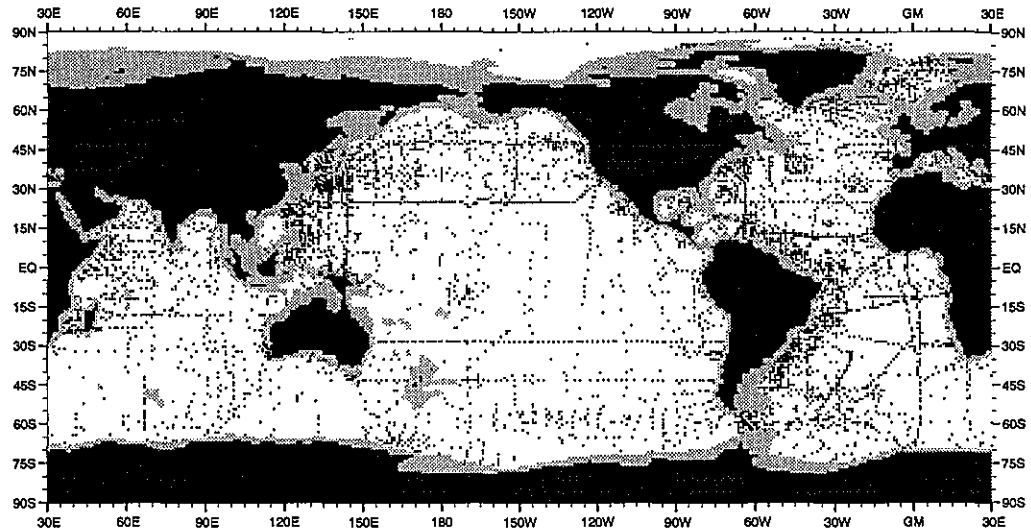

Fig. I15 Distribution of silicate observations at 1300 m depth

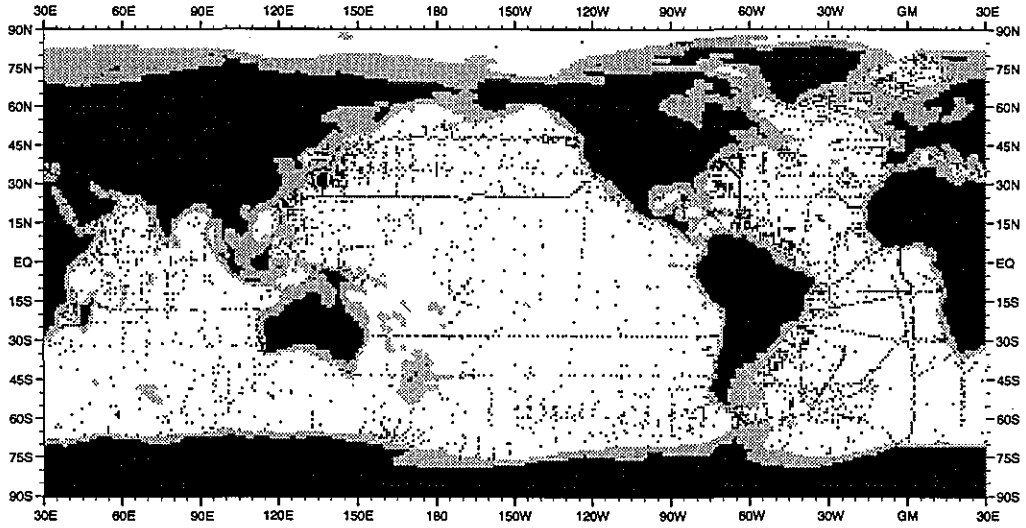

Fig. I16 Distribution of silicate observations at 1500 m depth

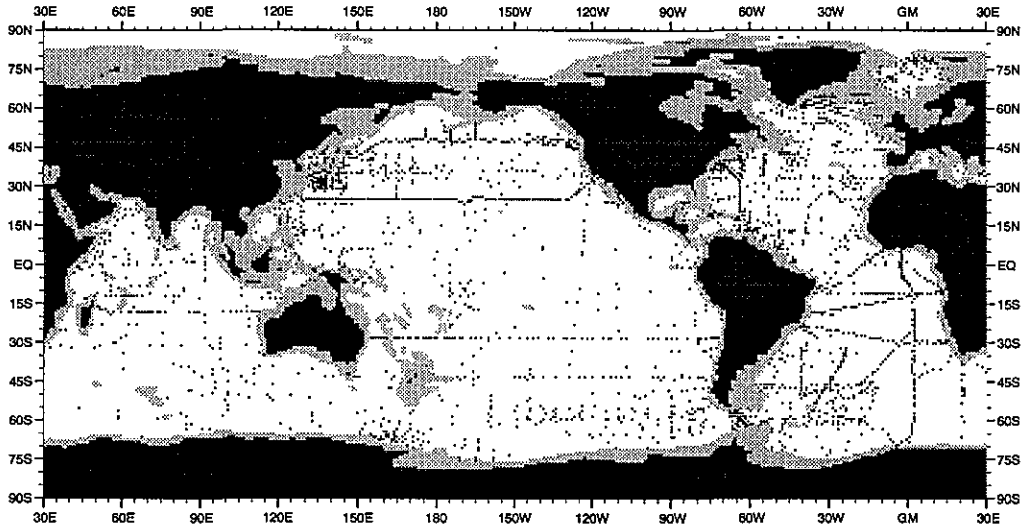

Fig. I17 Distribution of silicate observations at 1750 m depth

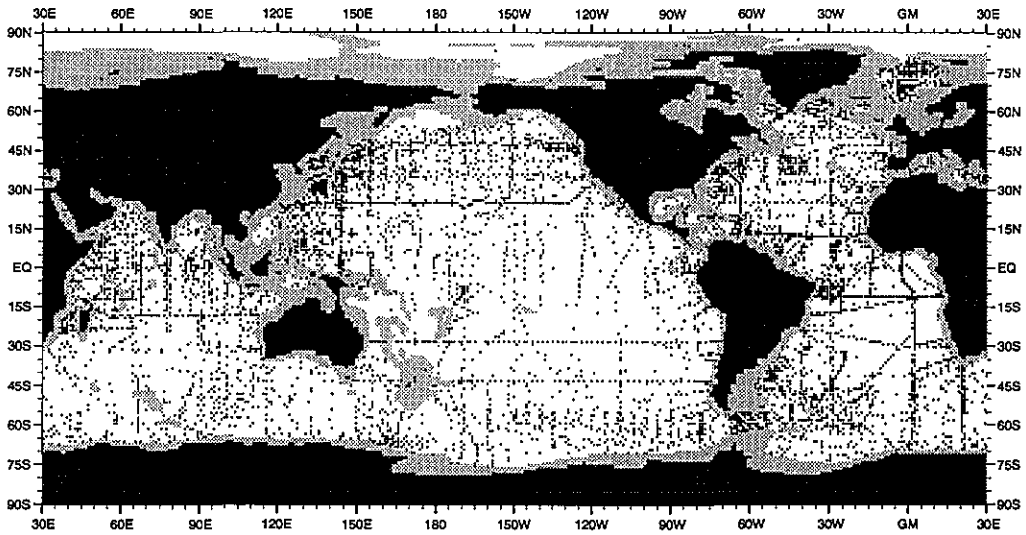

Fig. I18 Distribution of silicate observations at 2000 m depth

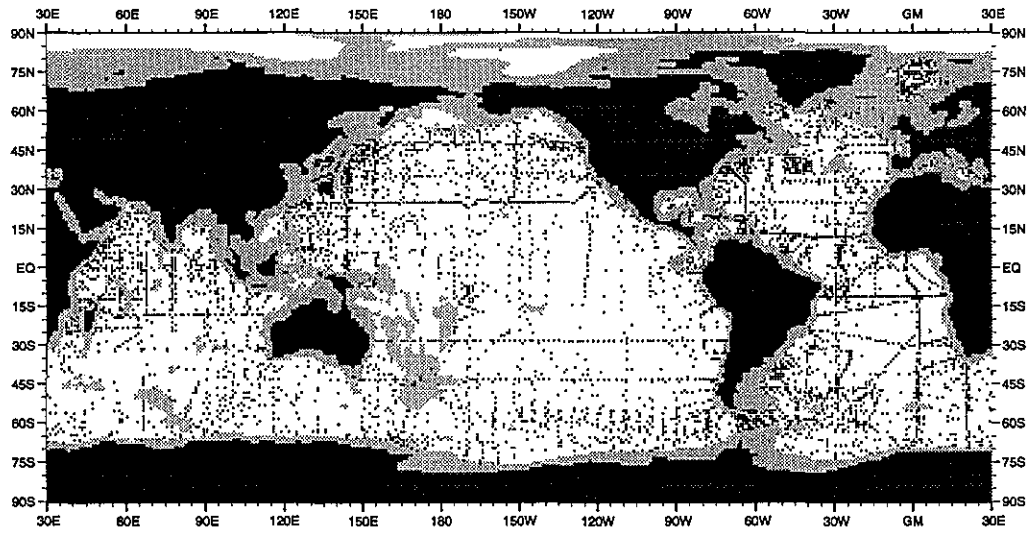

Fig. I19 Distribution of silicate observations at 2500 m depth

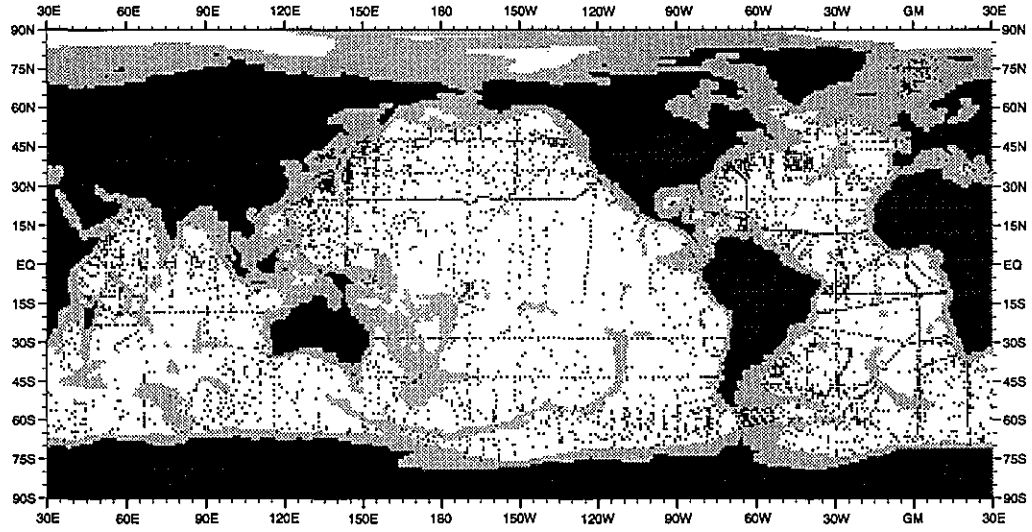

Fig. I20 Distribution of silicate observations at 3000 m depth

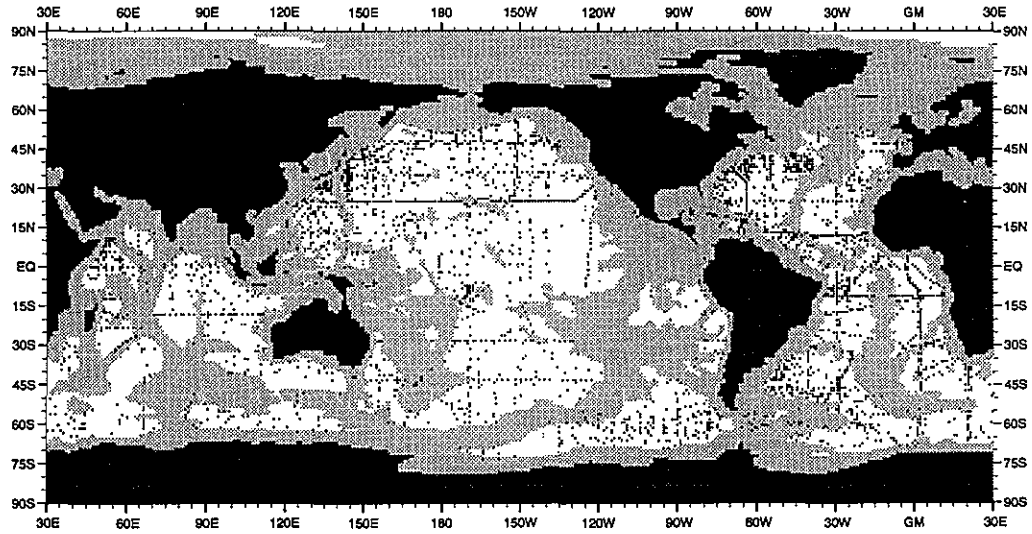

Fig. I21 Distribution of silicate observations at 4000 m depth

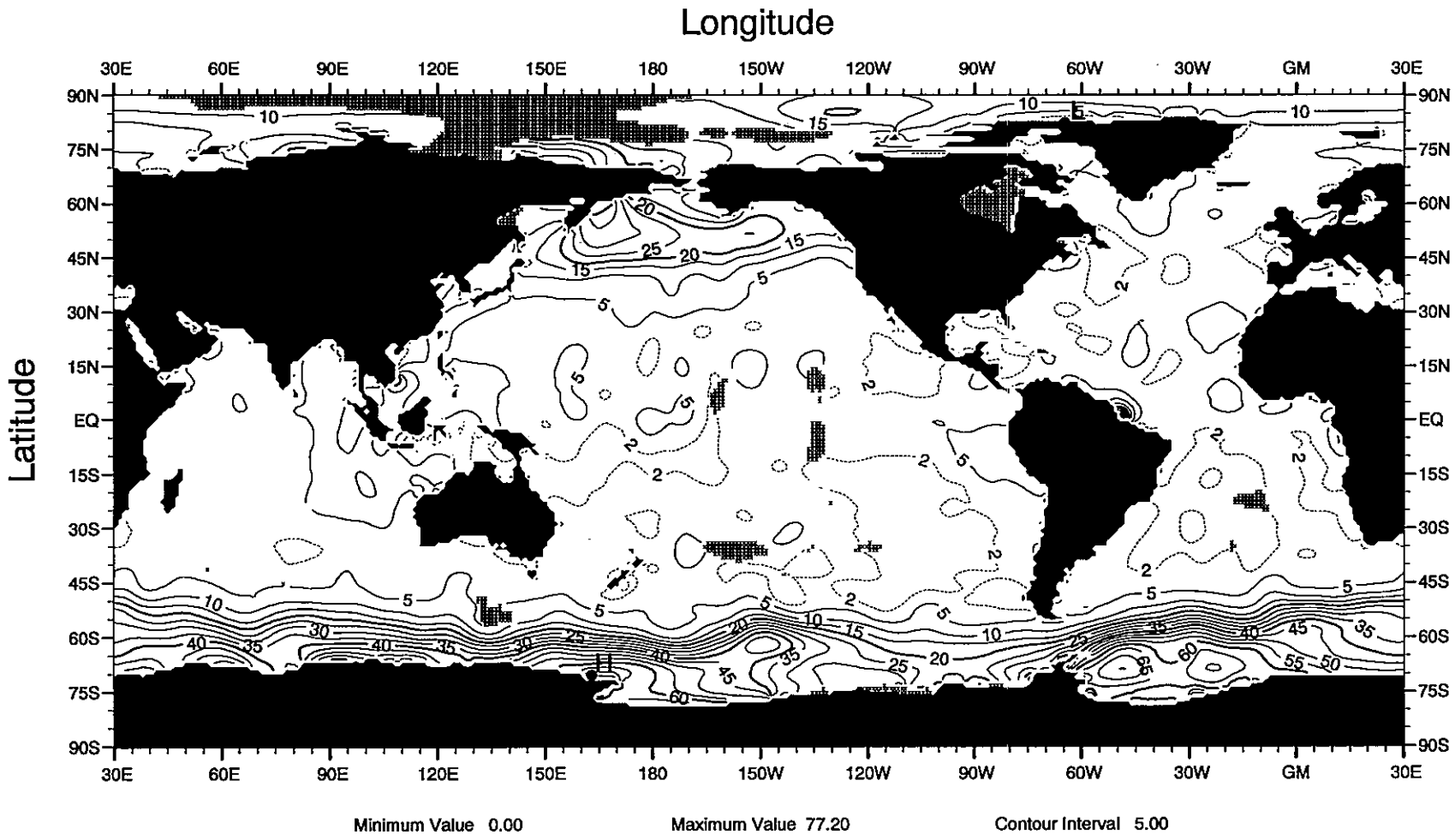

Fig. J1 Annual mean silicate (μM) at the surface

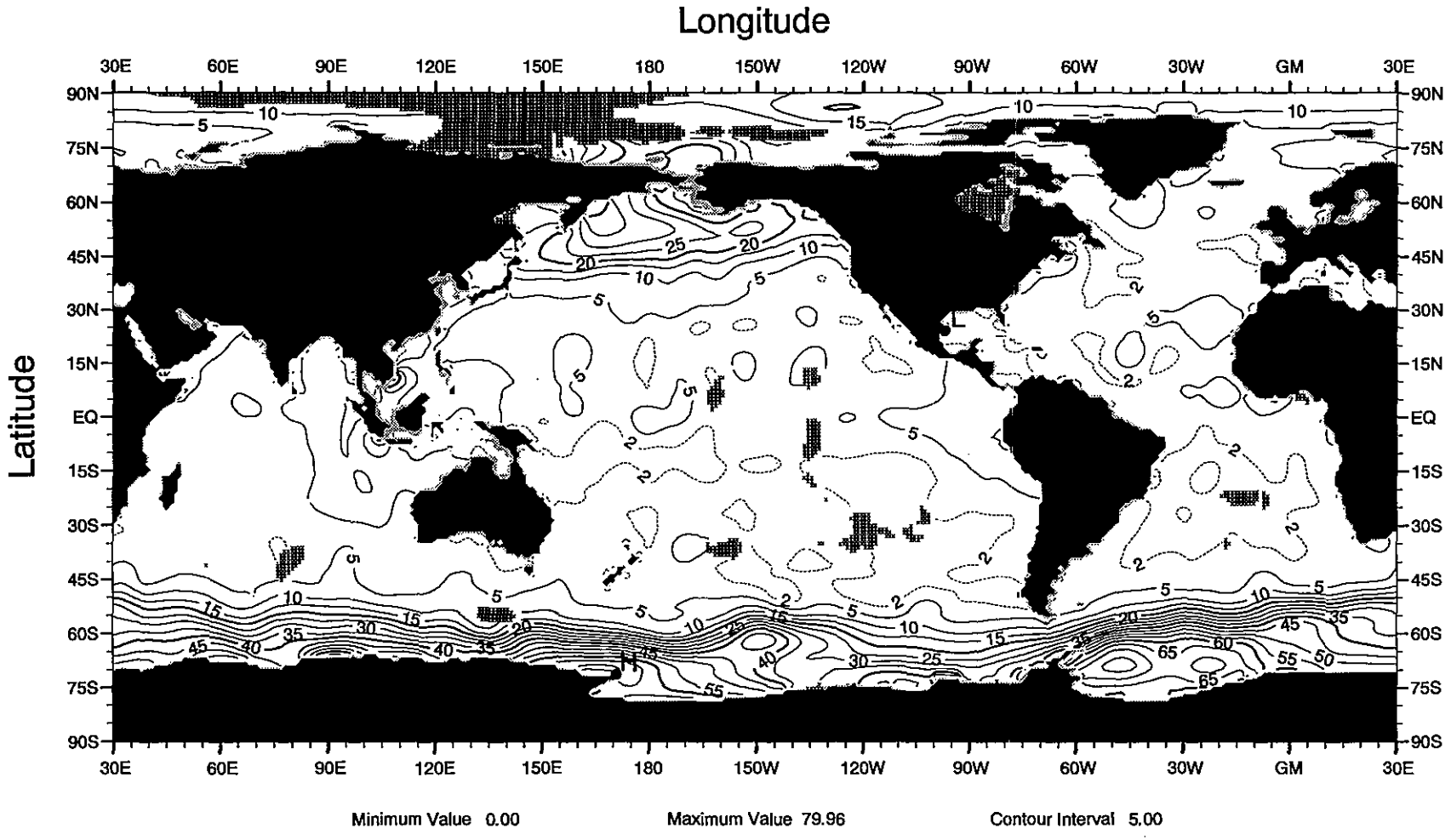

Fig. J2 Annual mean silicate (μM) at 30 m depth

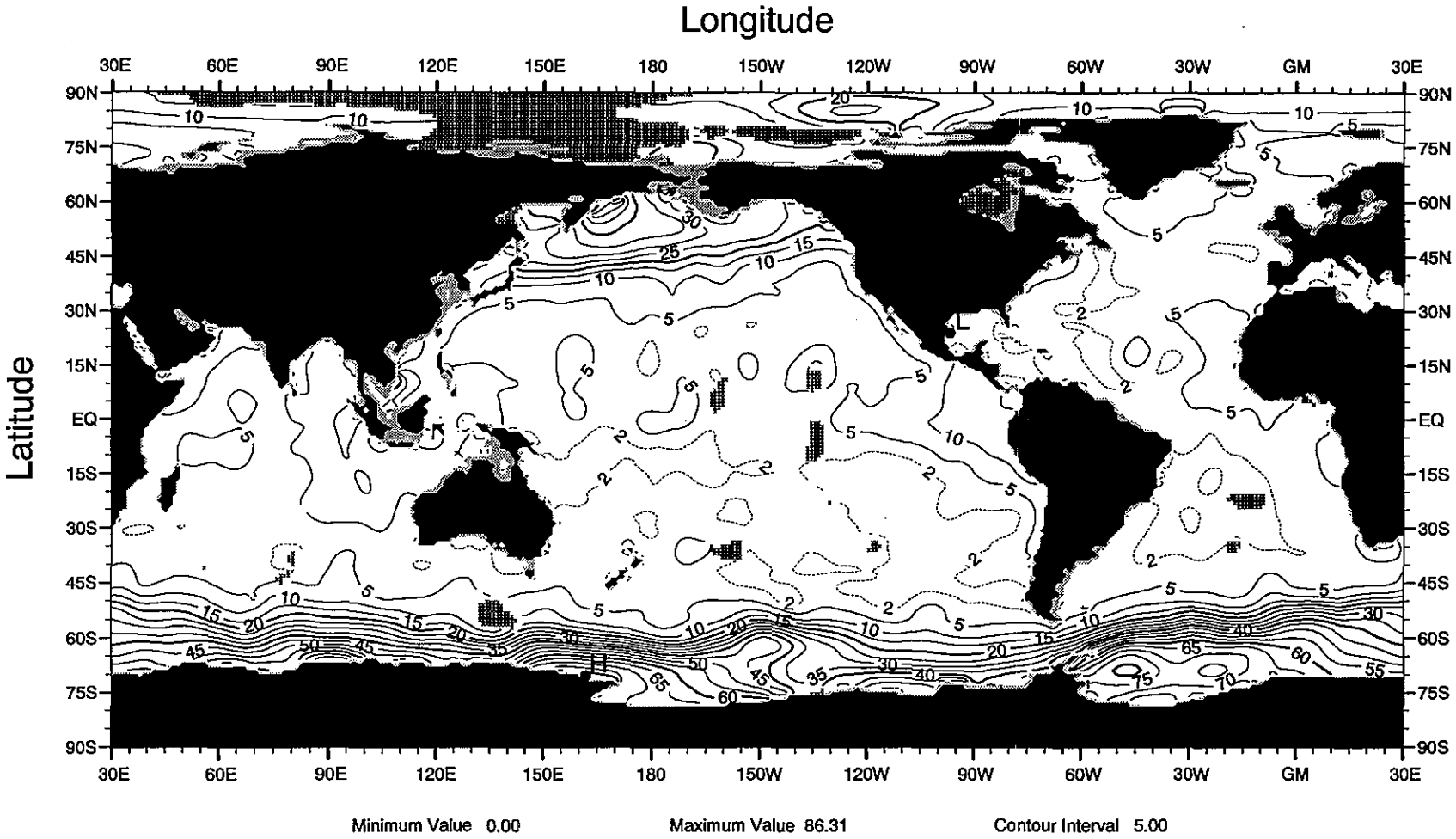

Fig. J3 Annual mean silicate (μM) at 50 m depth

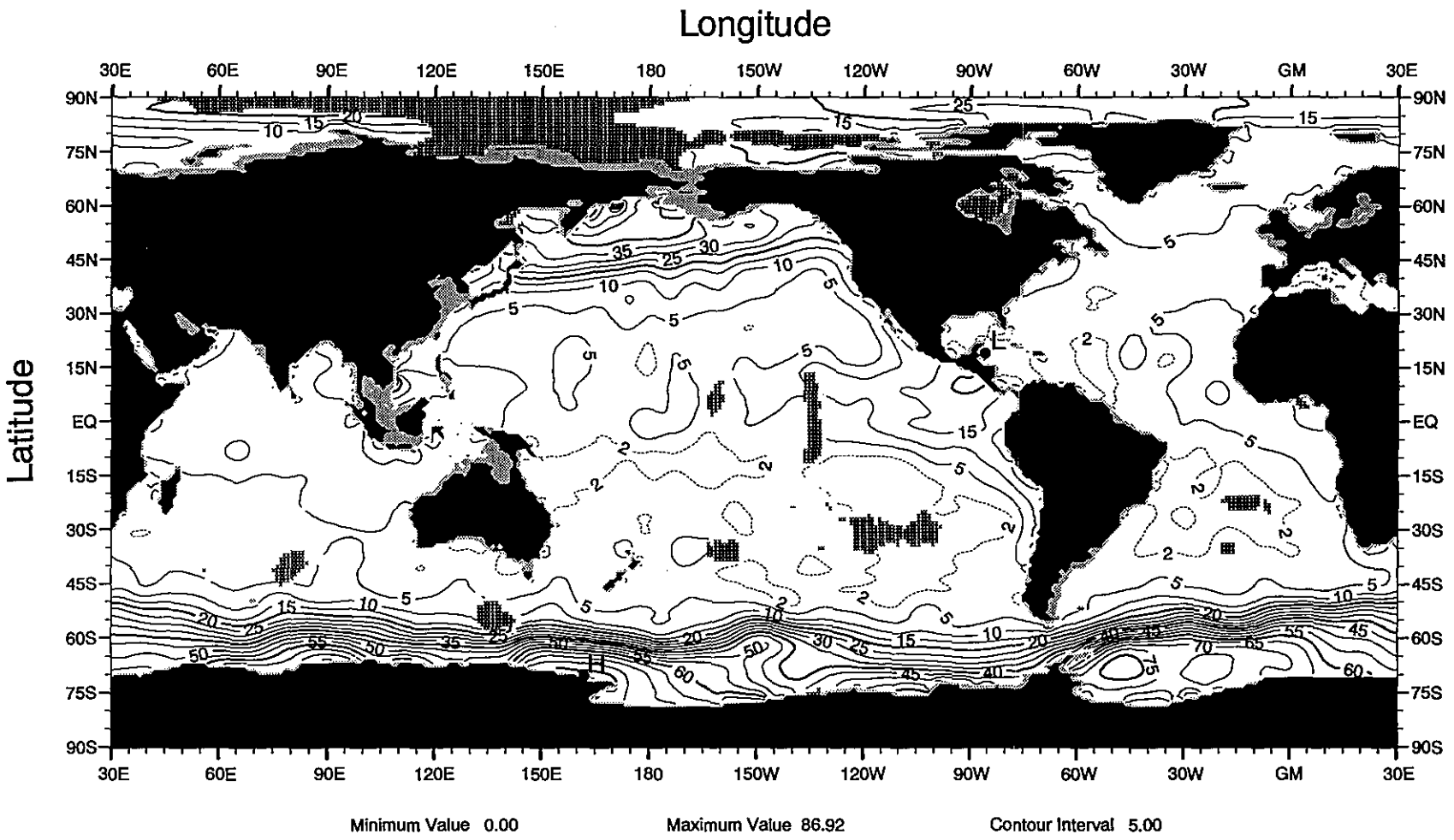

Fig. J4 Annual mean silicate (μM) at 75 m depth

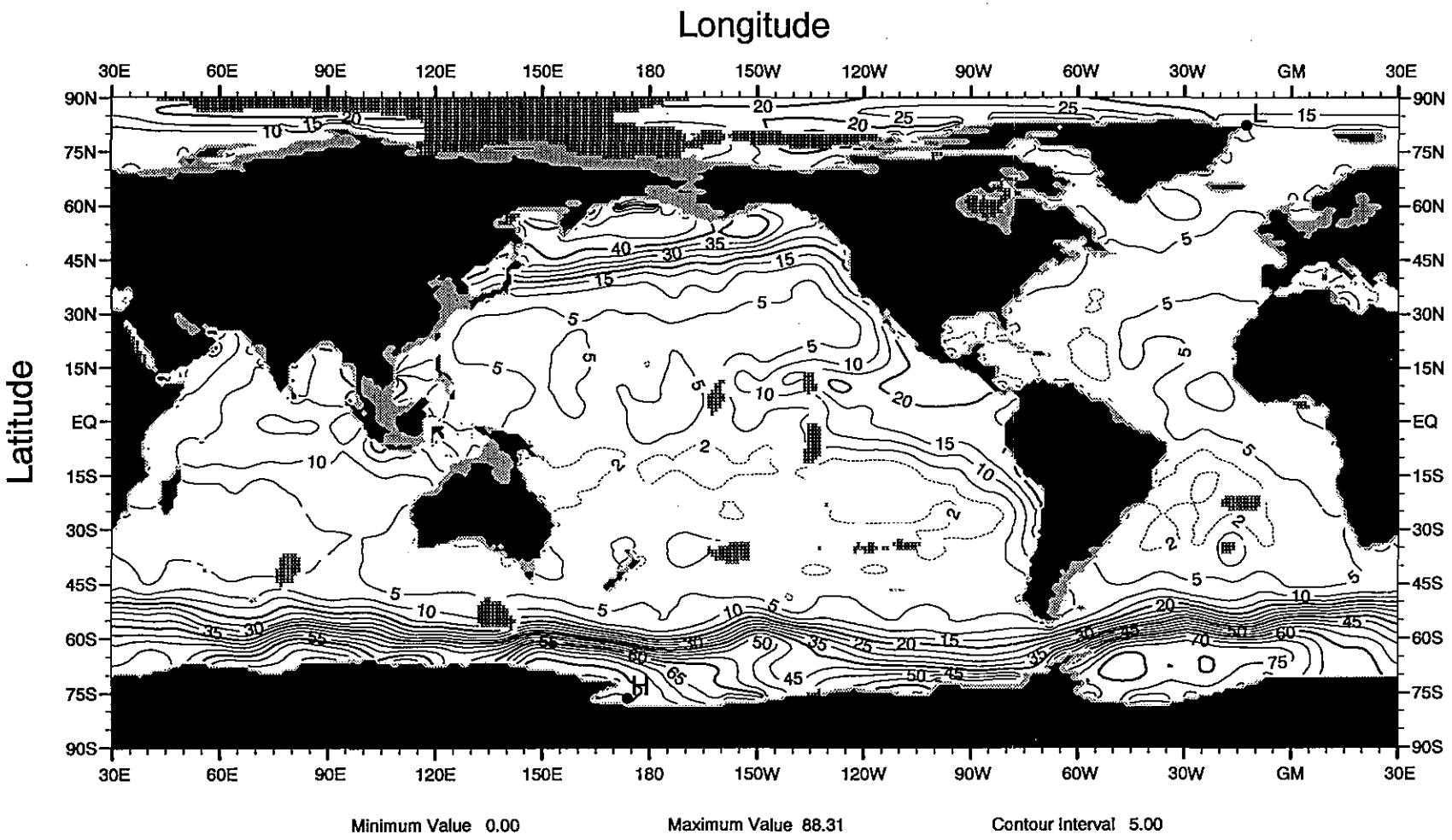

Fig. J5 Annual mean silicate (μM) at 100 m depth

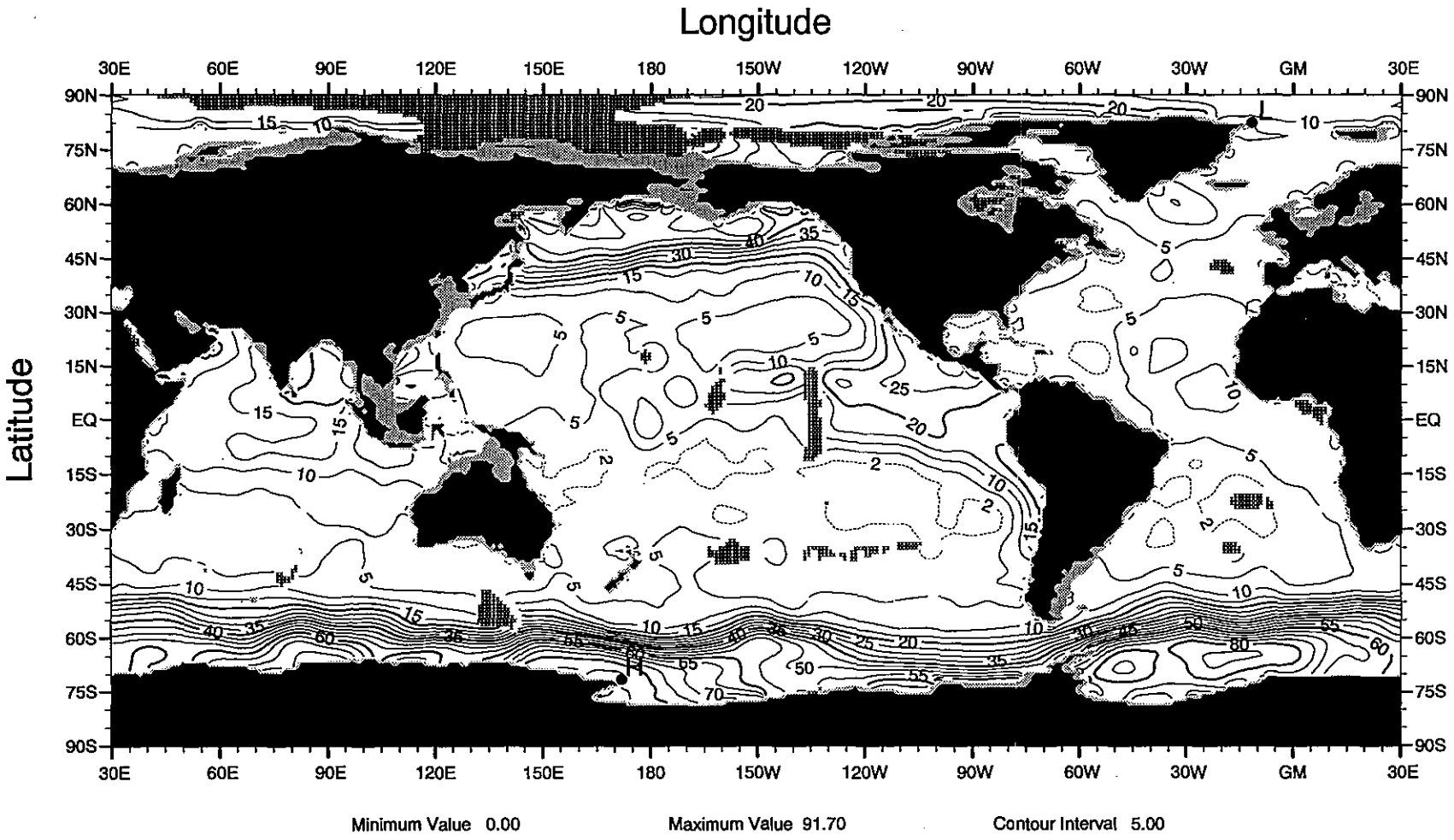

Fig. J6 Annual mean silicate (μM) at 125 m depth

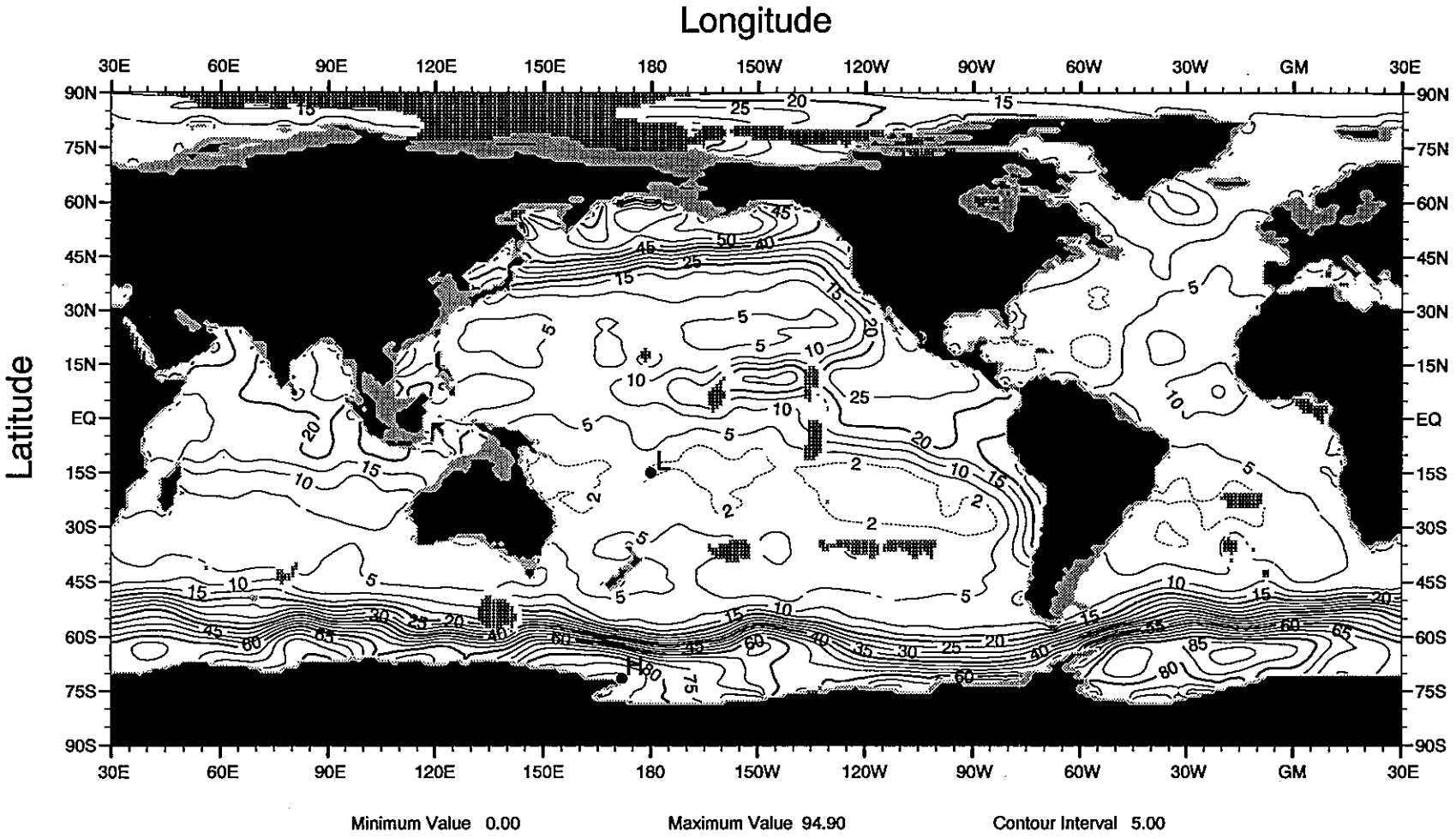

Fig. J7 Annual mean silicate (μM) at 150 m depth

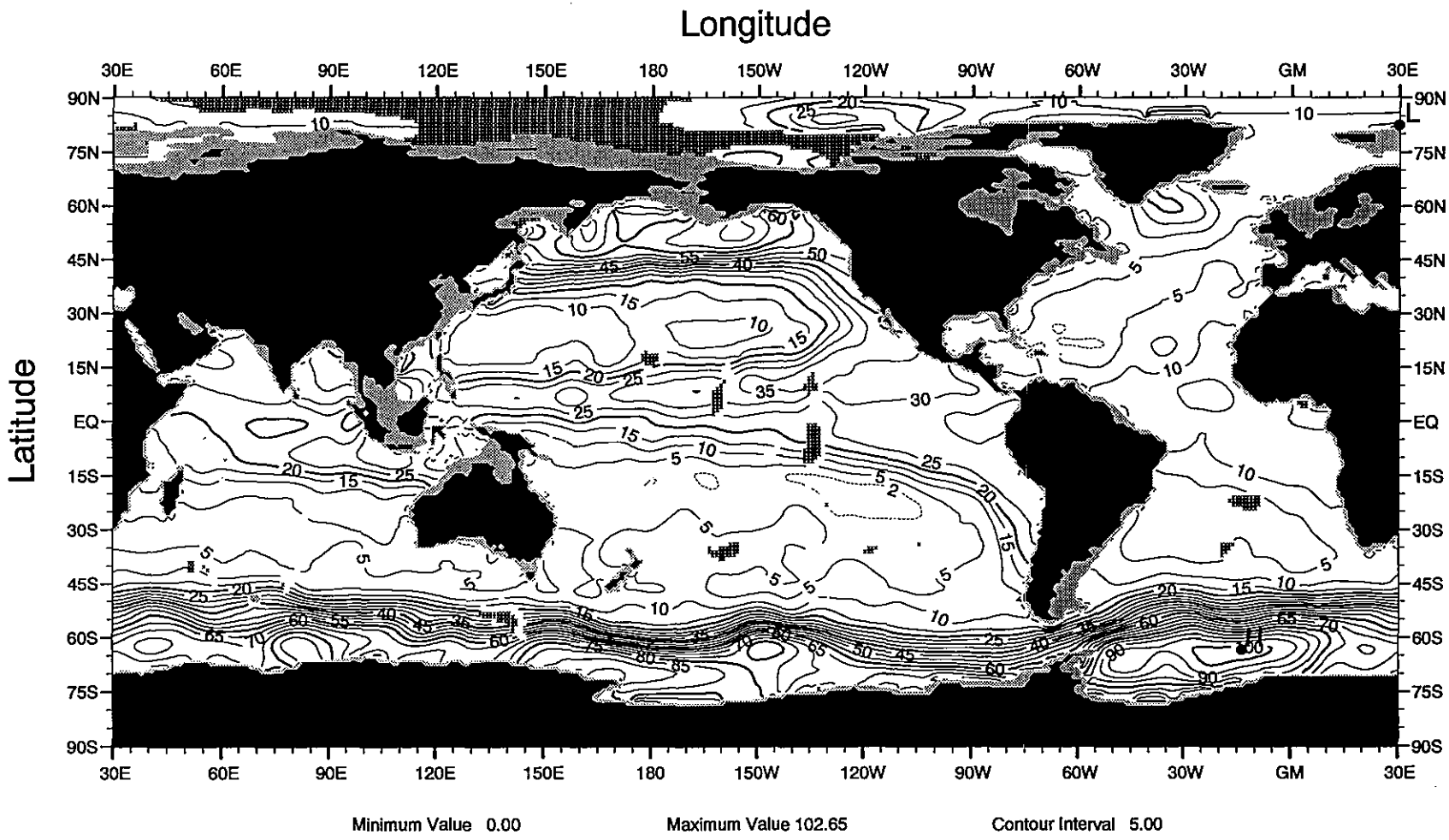

Fig. J8 Annual mean silicate (μM) at 250 m depth

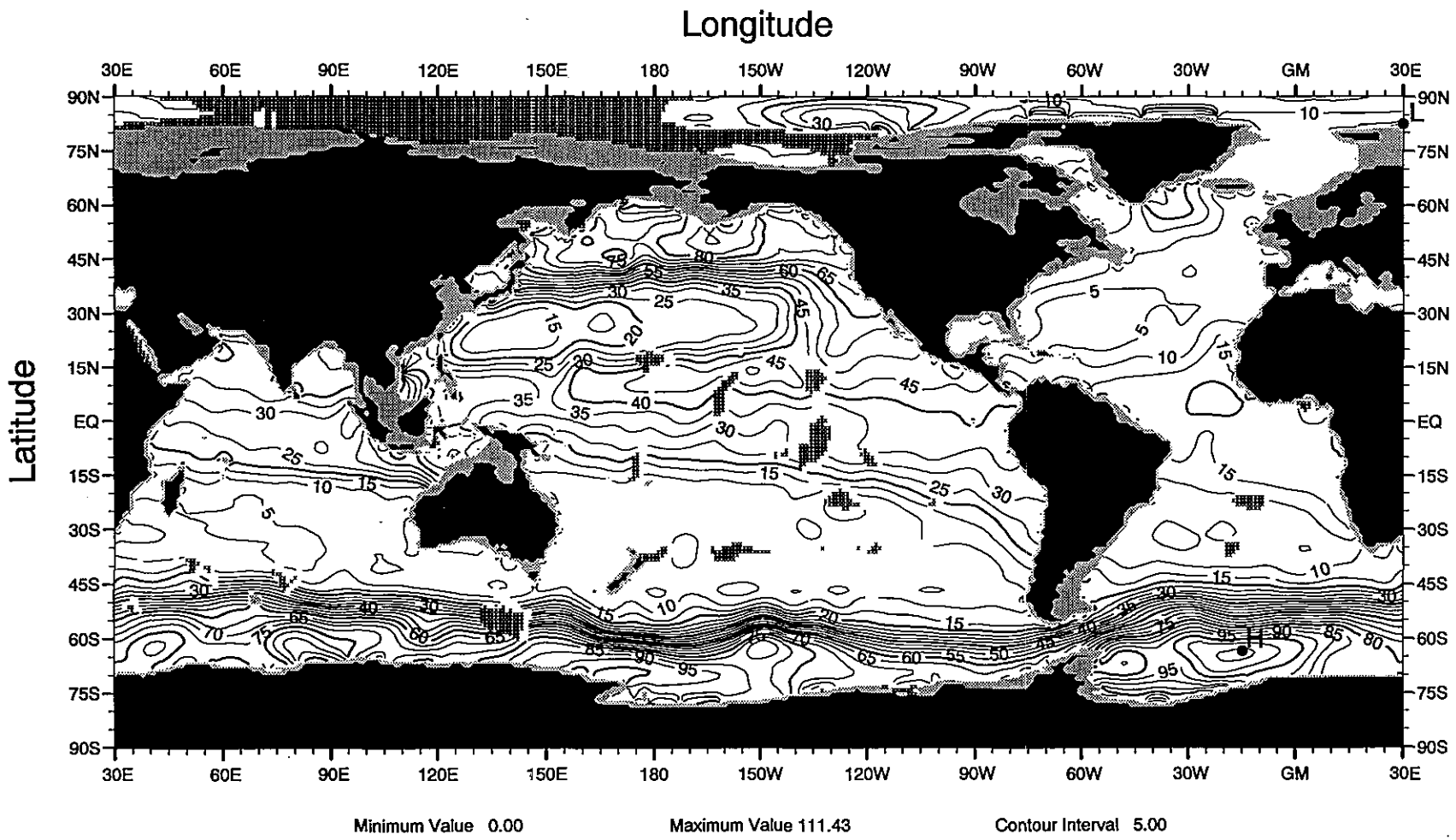

Fig. J9 Annual mean silicate (μM) at 400 m depth

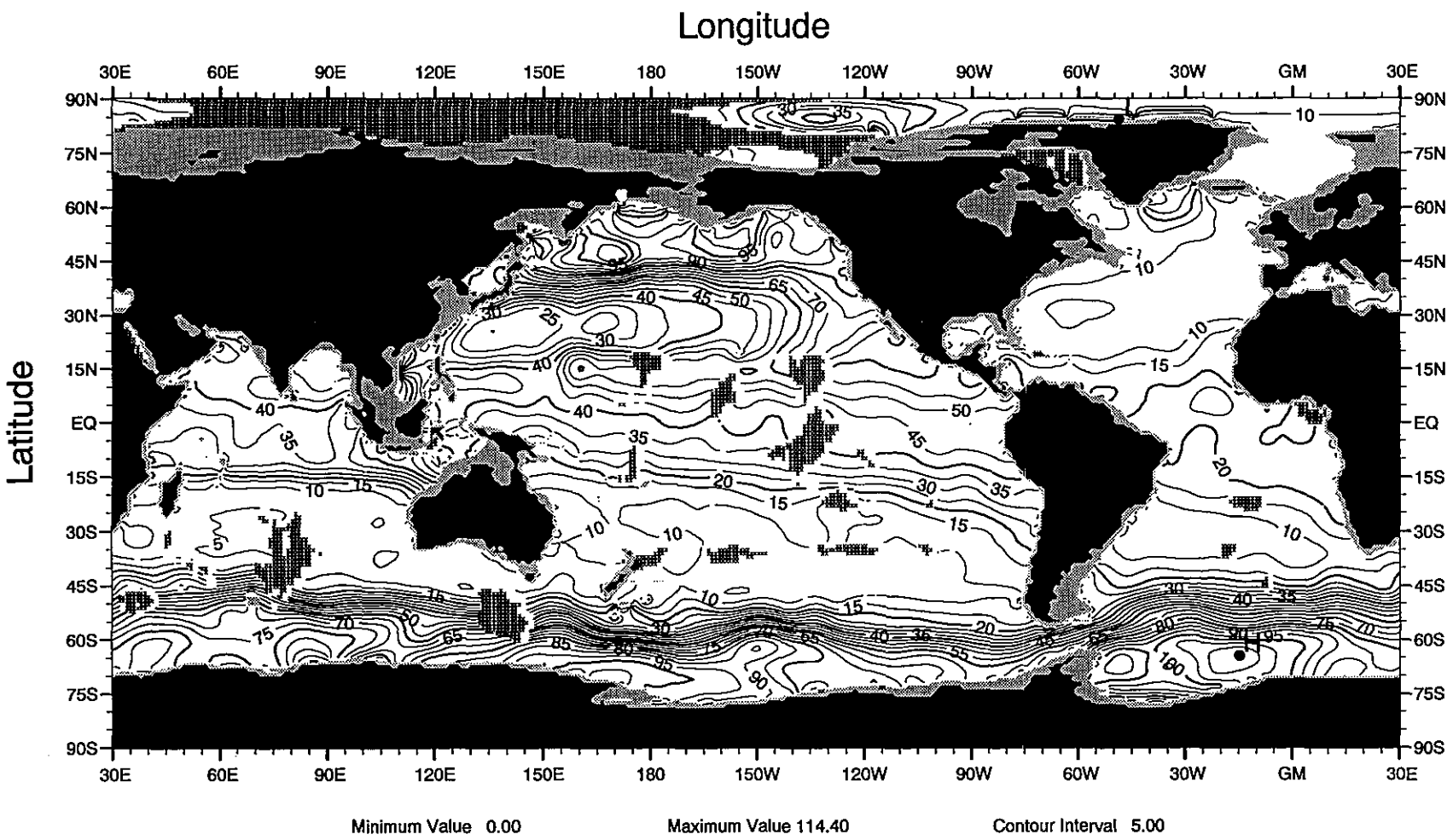

Fig. J10 Annual mean silicate (μM) at 500 m depth

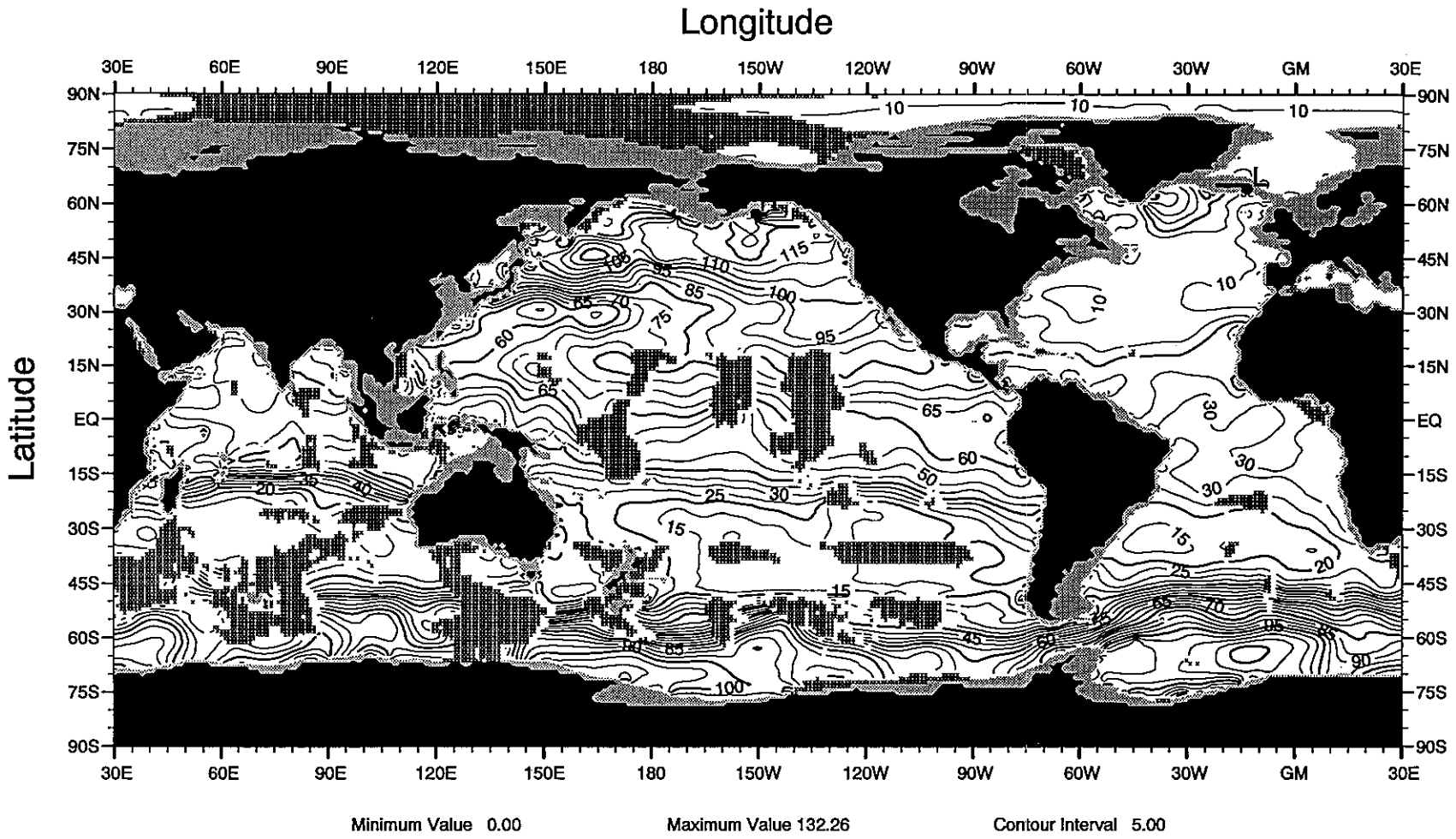

Fig. J11 Annual mean silicate (μM) at 700 m depth

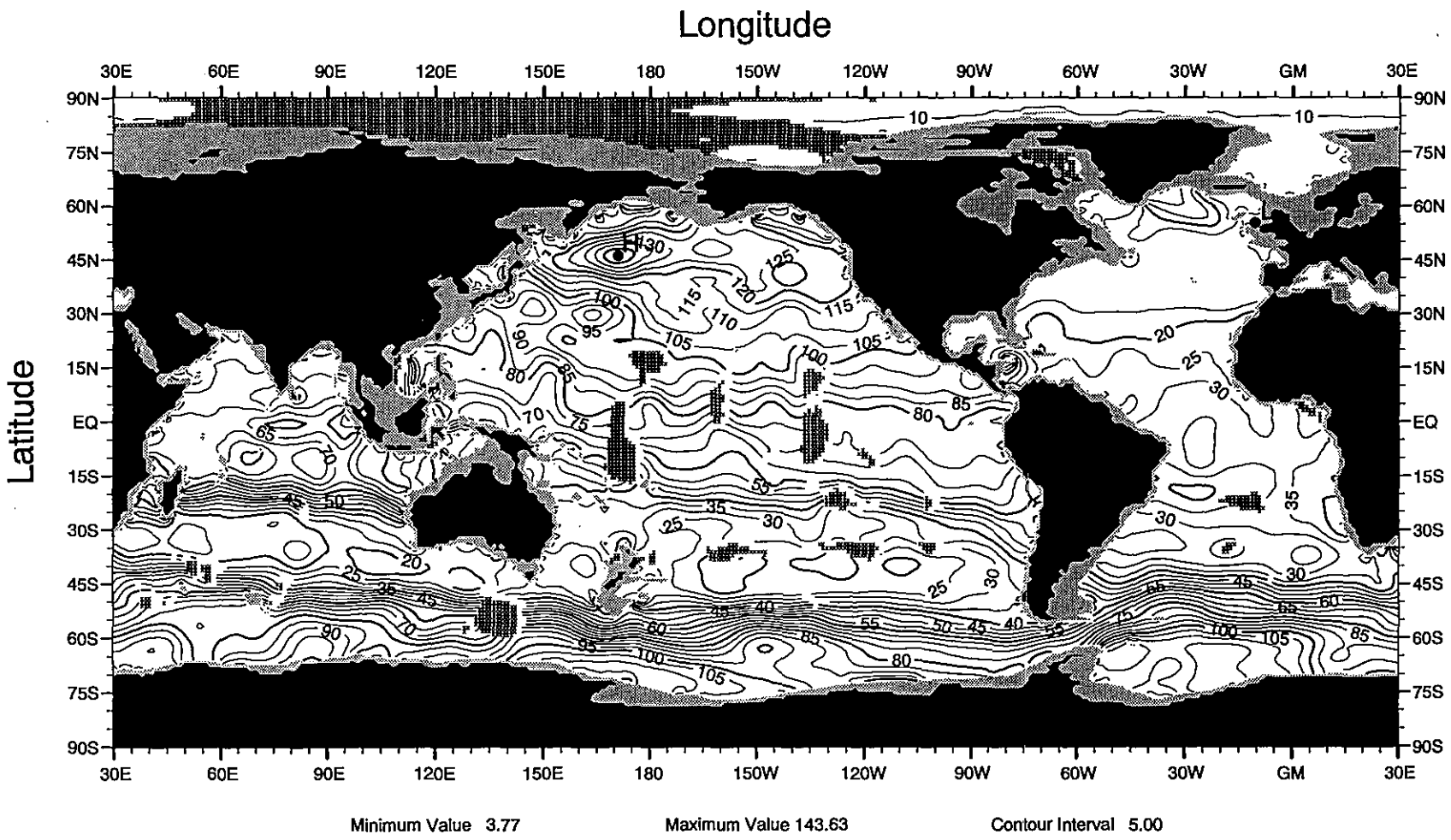

Fig. J12 Annual mean silicate (μM) at 900 m depth

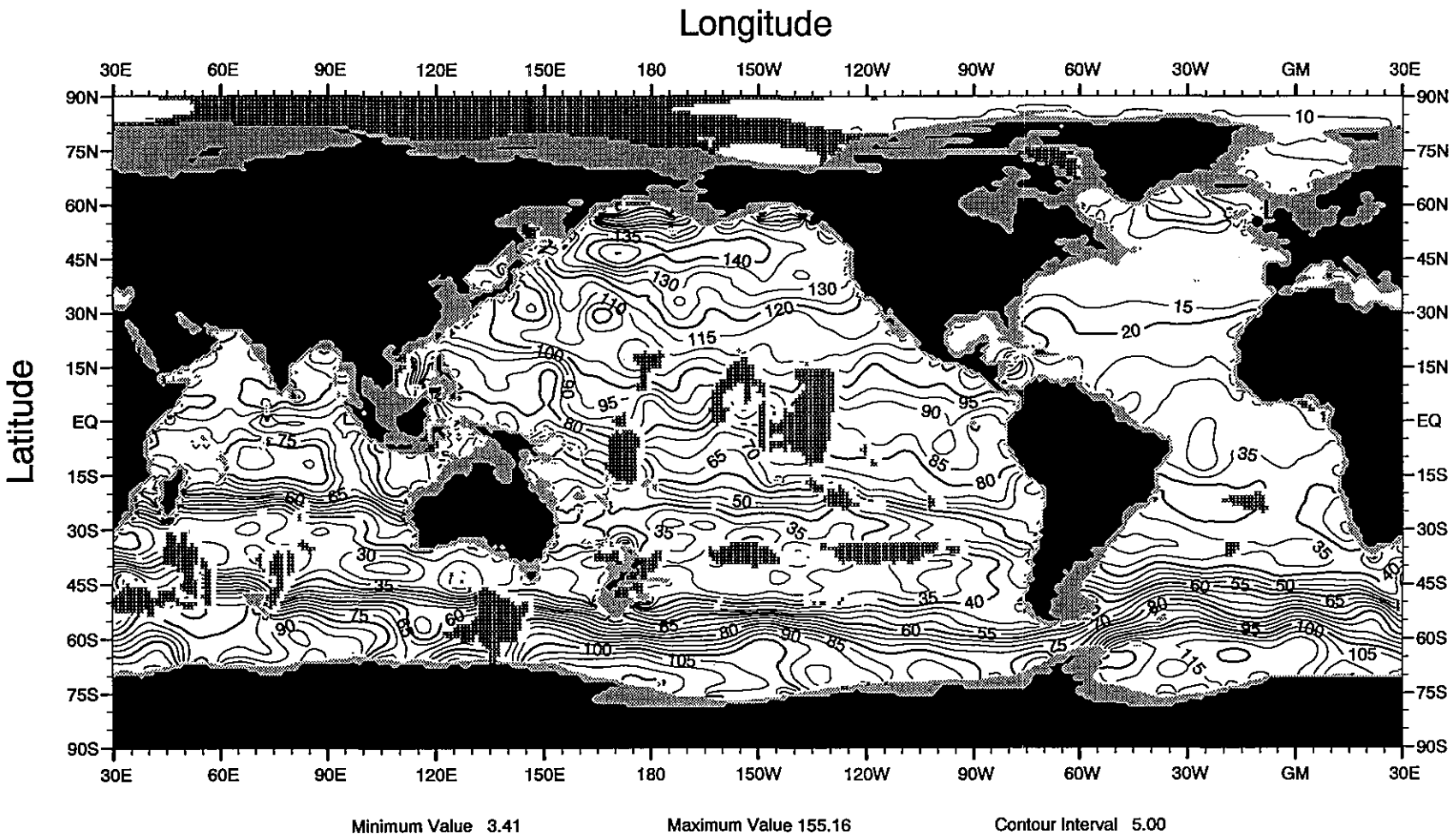

Fig. J13 Annual mean silicate (μM) at 1000 m depth

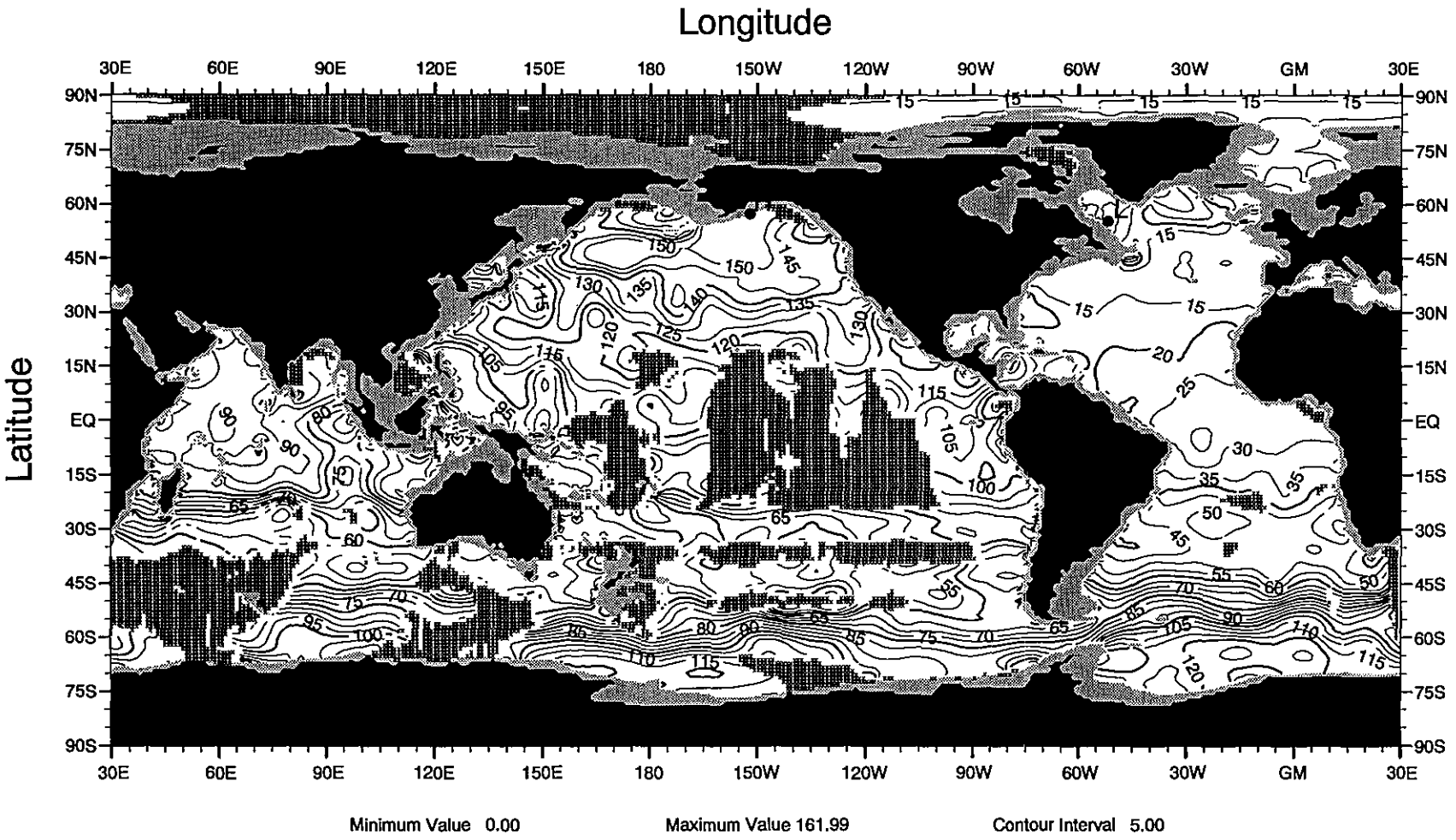

Fig. J14 Annual mean silicate (μM) at 1200 m depth

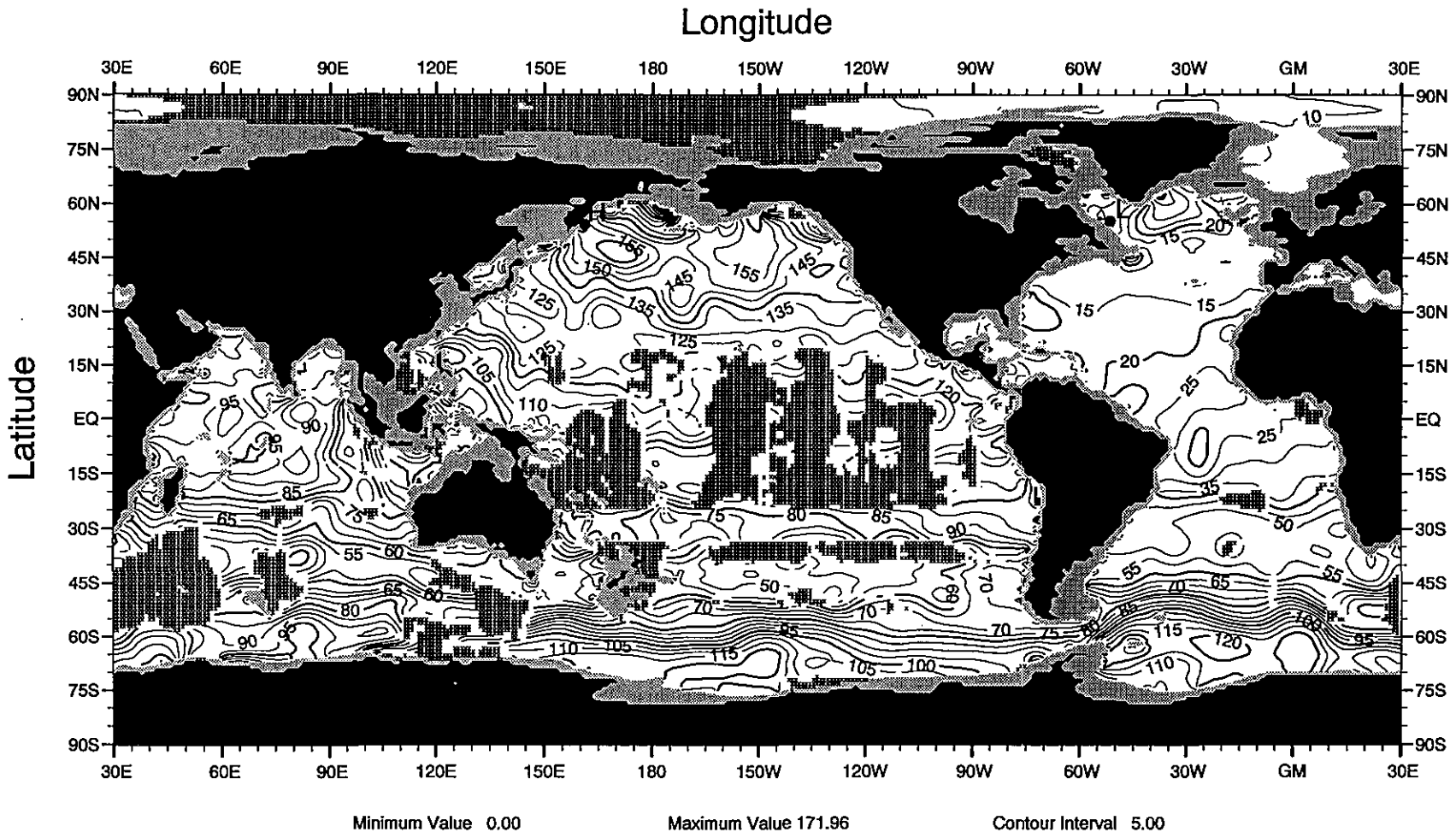

Fig. J15 Annual mean silicate (μM) at 1300 m depth

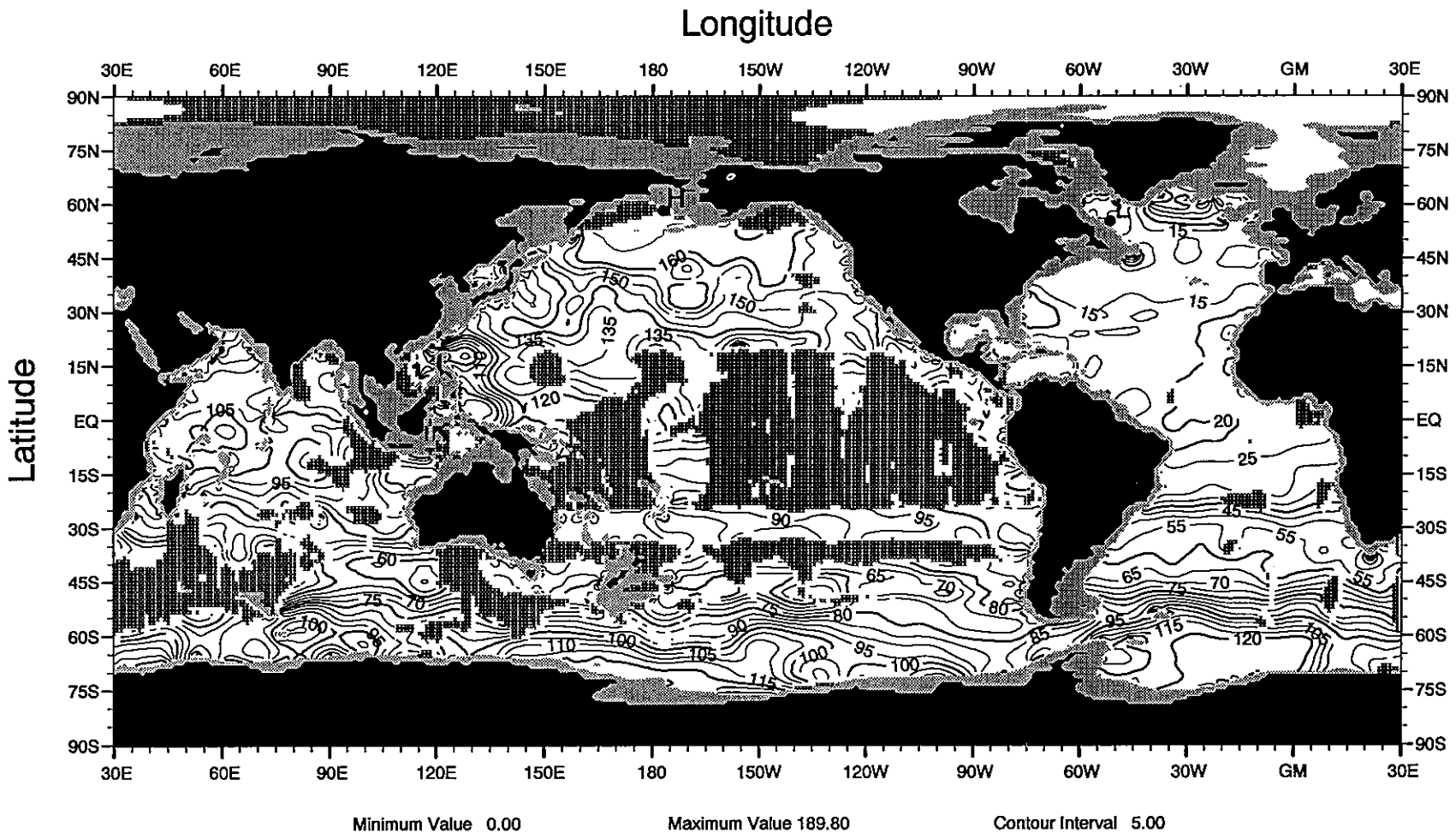

Fig. J16 Annual mean silicate (μM) at 1500 m depth

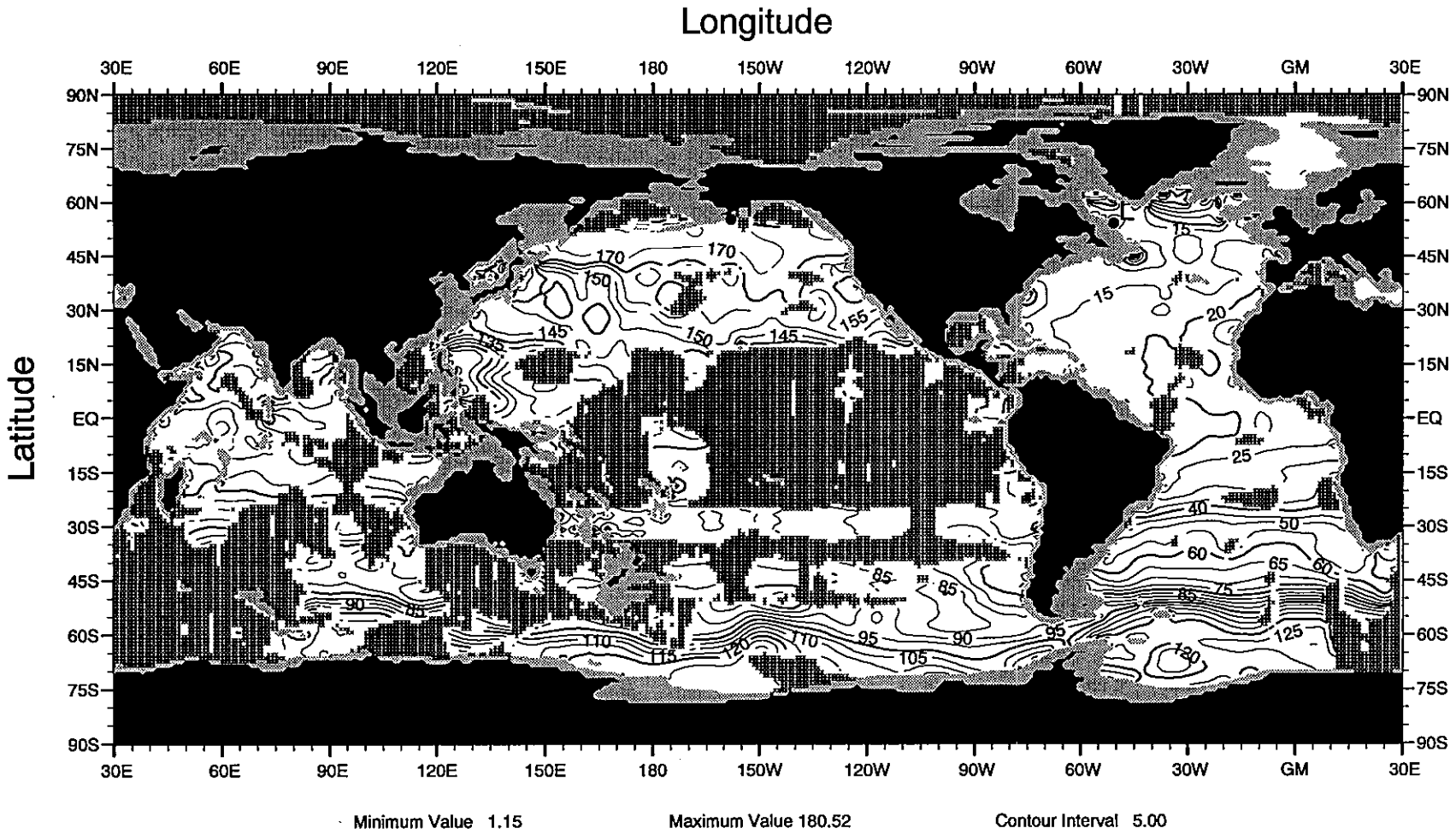

Fig. J17 Annual mean silicate (μM) at 1750 m depth

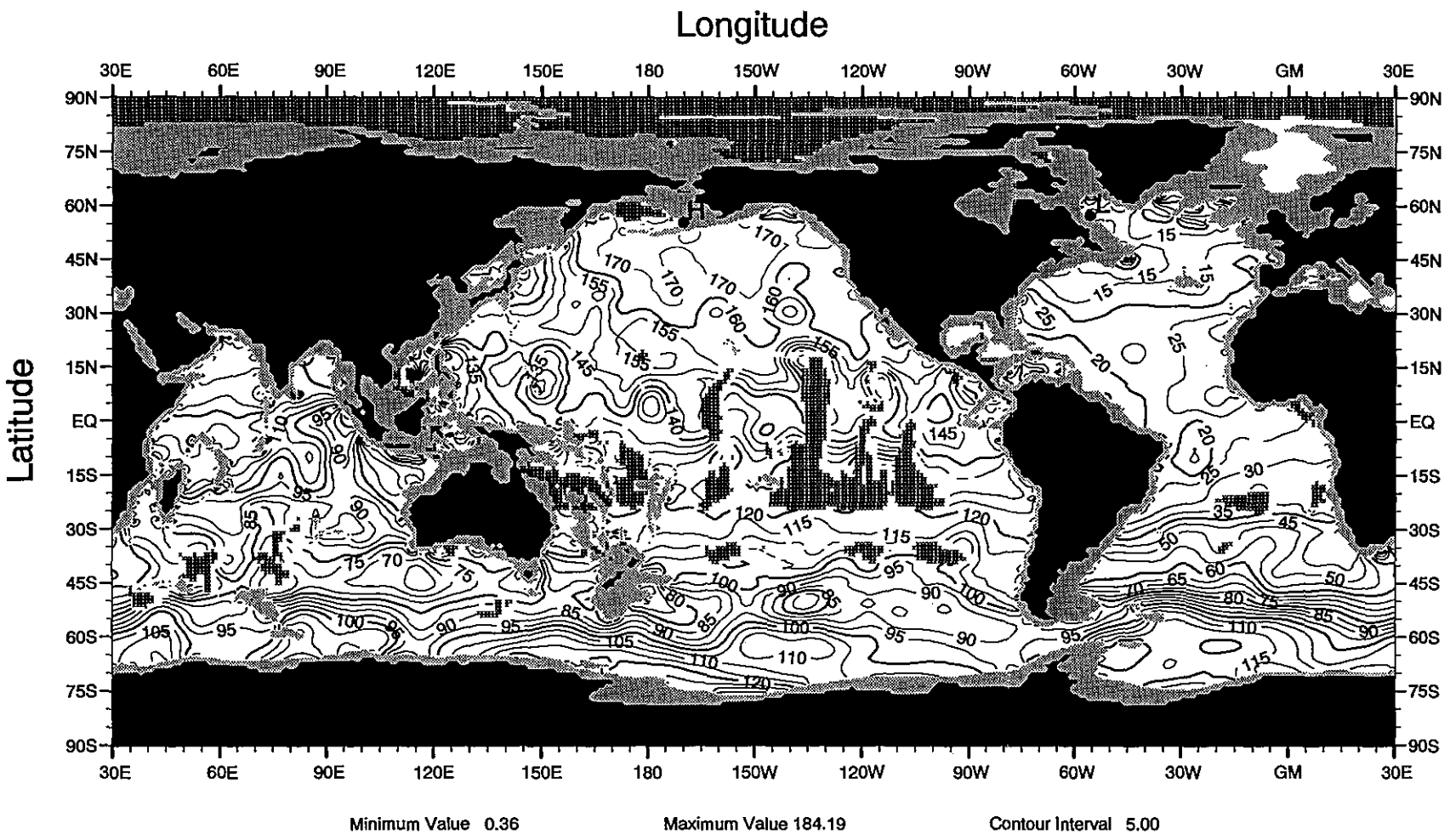

Fig. J18 Annual mean silicate (μM) at 2000 m depth

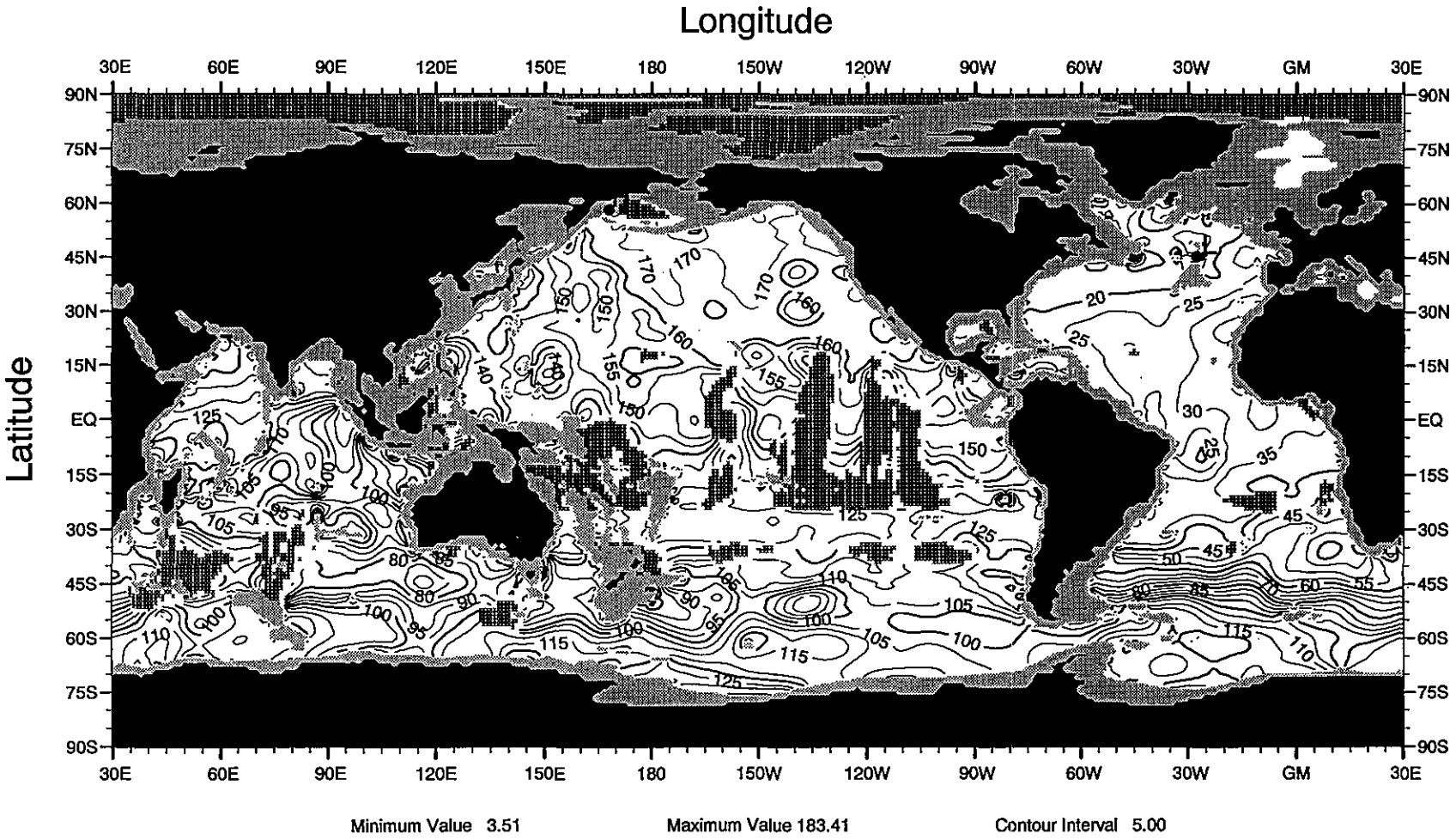

Fig. J19 Annual mean silicate (μM) at 2500 m depth

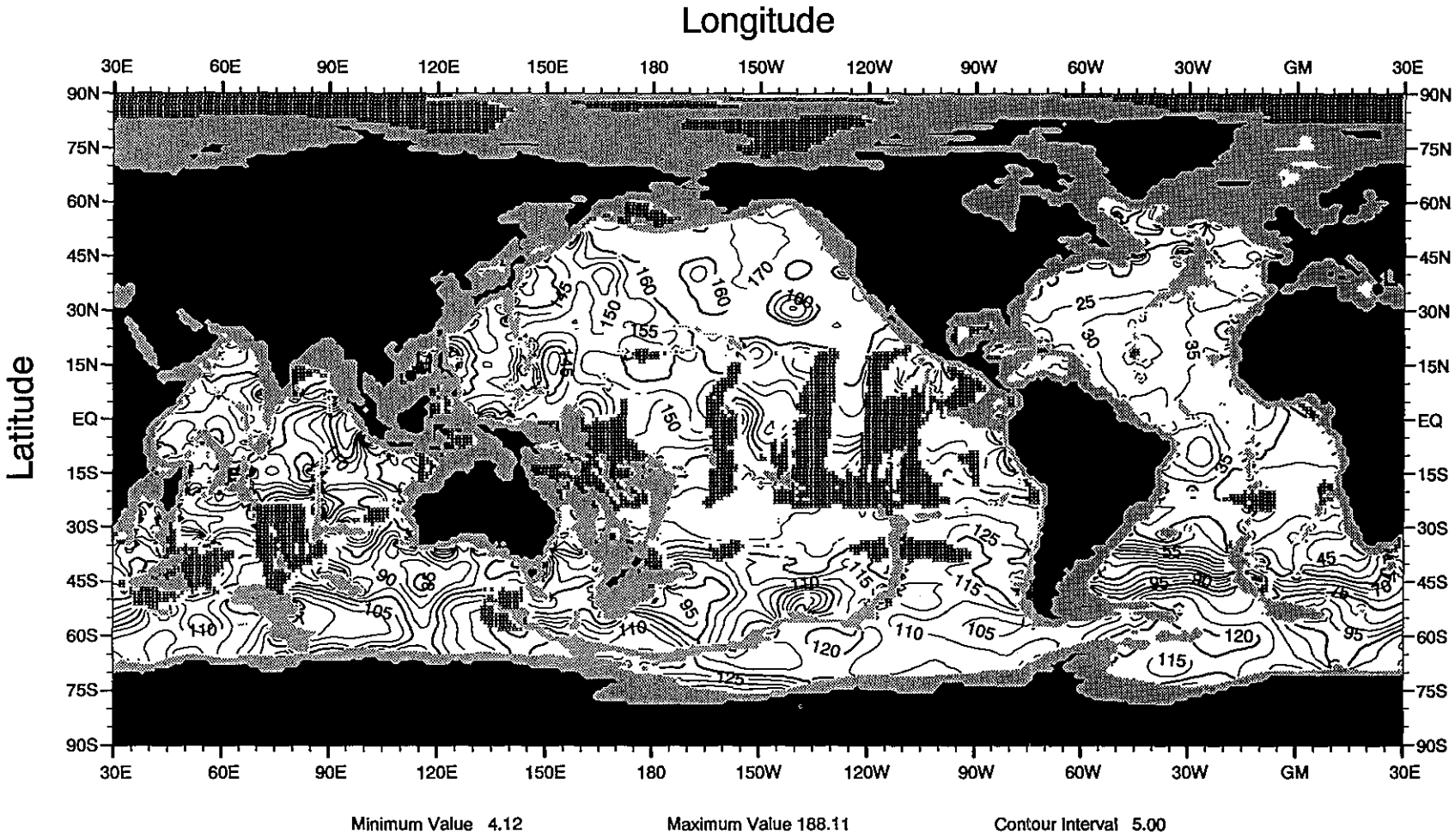

Fig. J20 Annual mean silicate (μM) at 3000 m depth

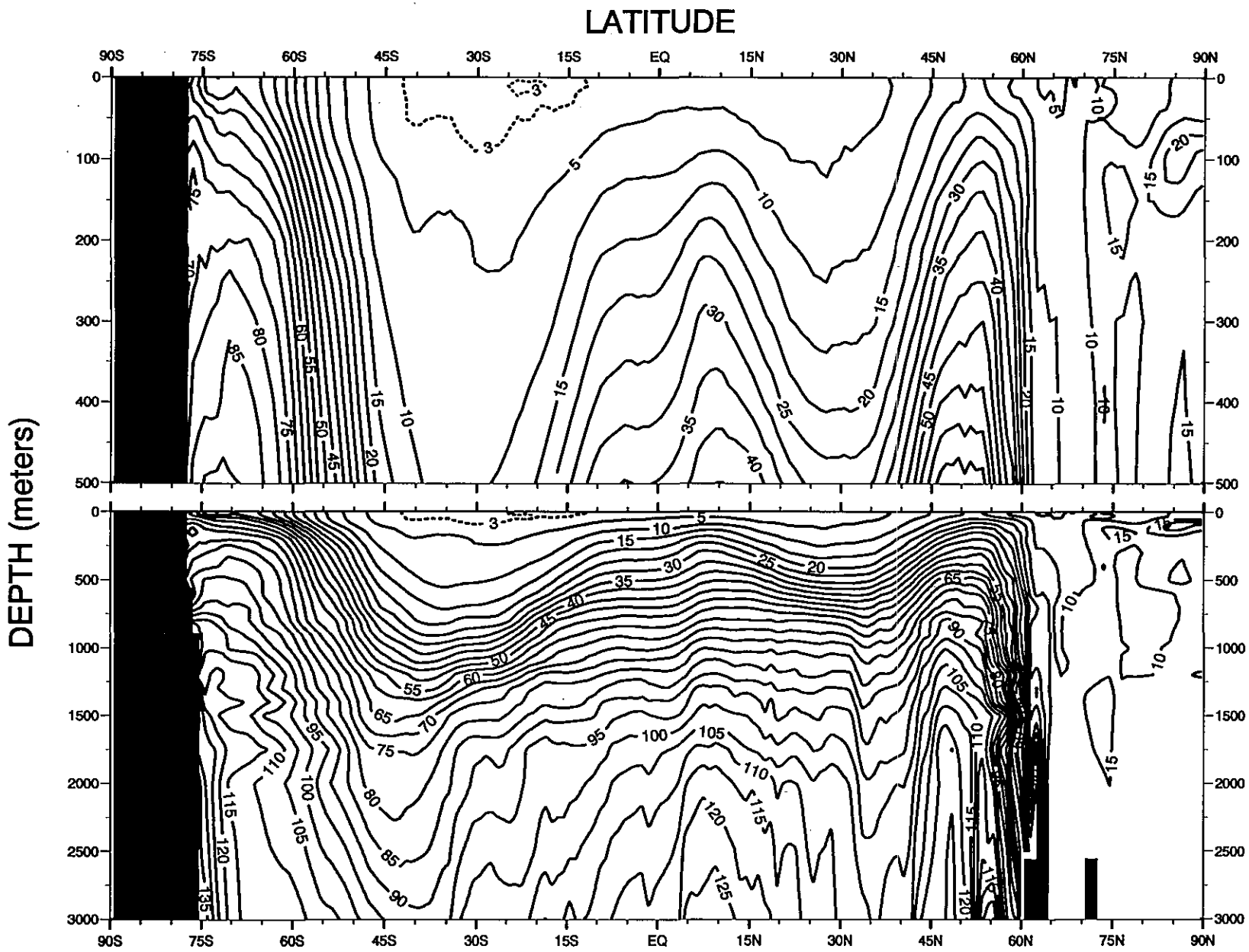

Fig K1. Annual global zonal average (by one-degree squares) of silicate (μM)

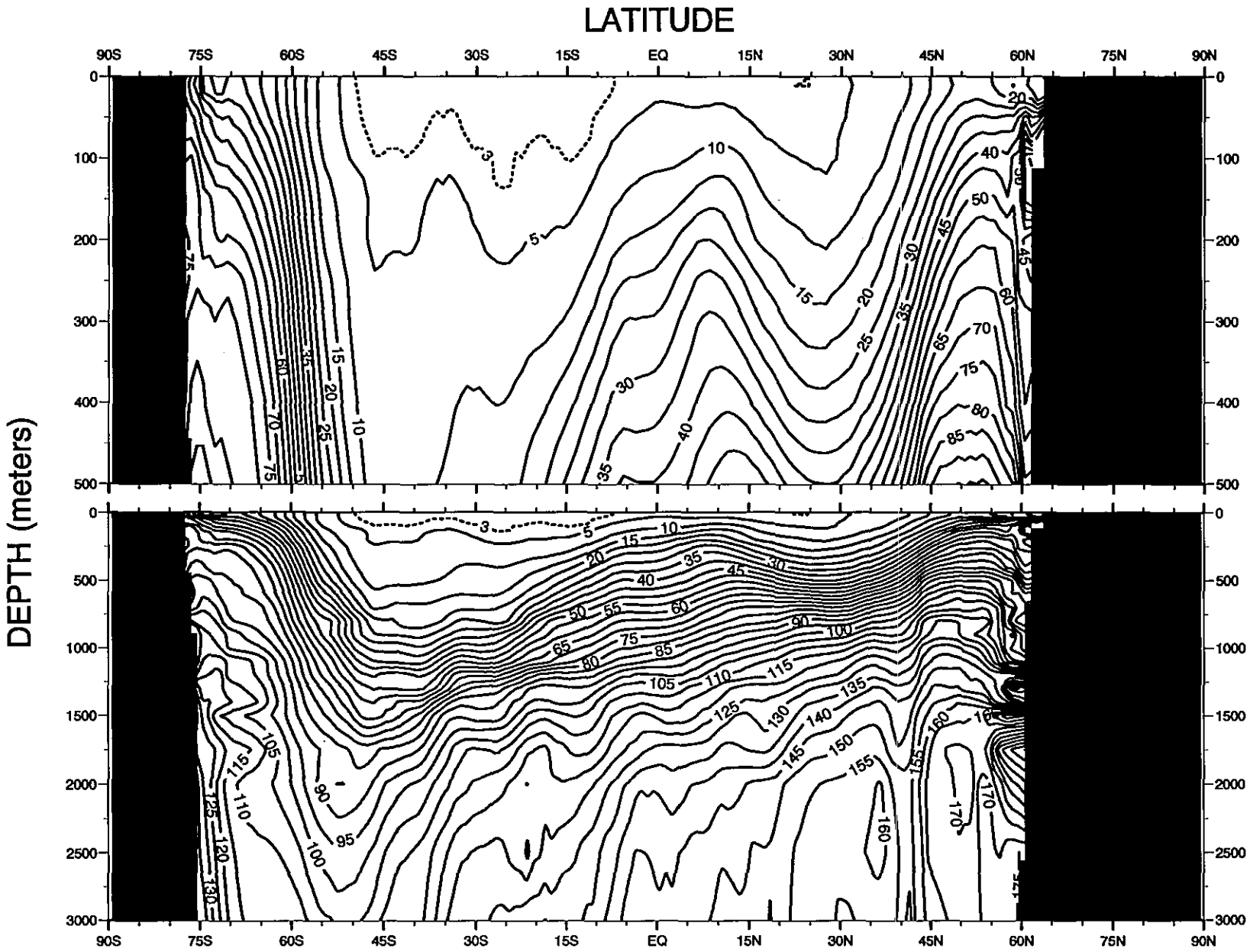

Fig K2. Annual Pacific zonal average (by one-degree squares) of silicate (μM)

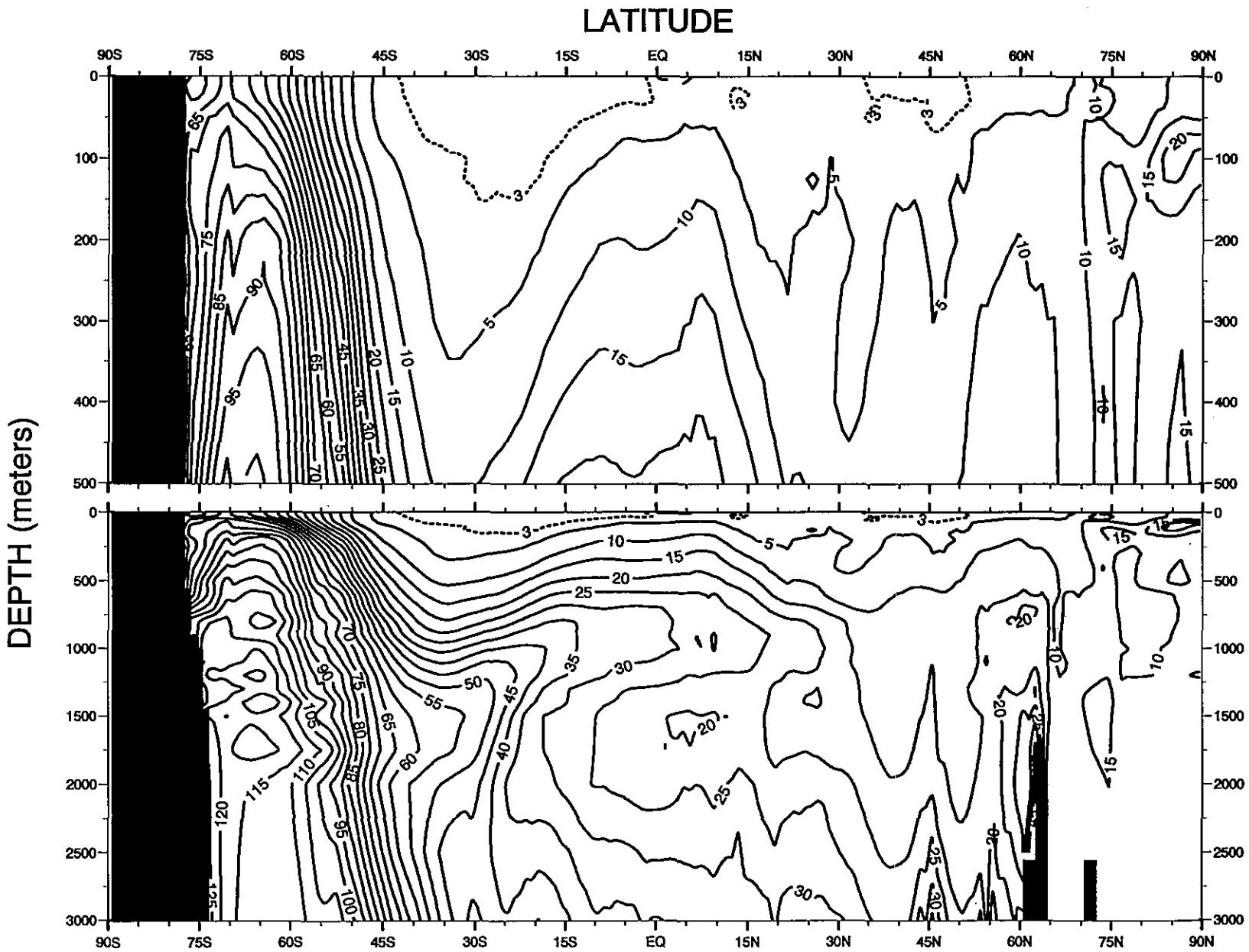

Fig K3. Annual Atlantic zonal average (by one-degree squares) of silicate (μM)

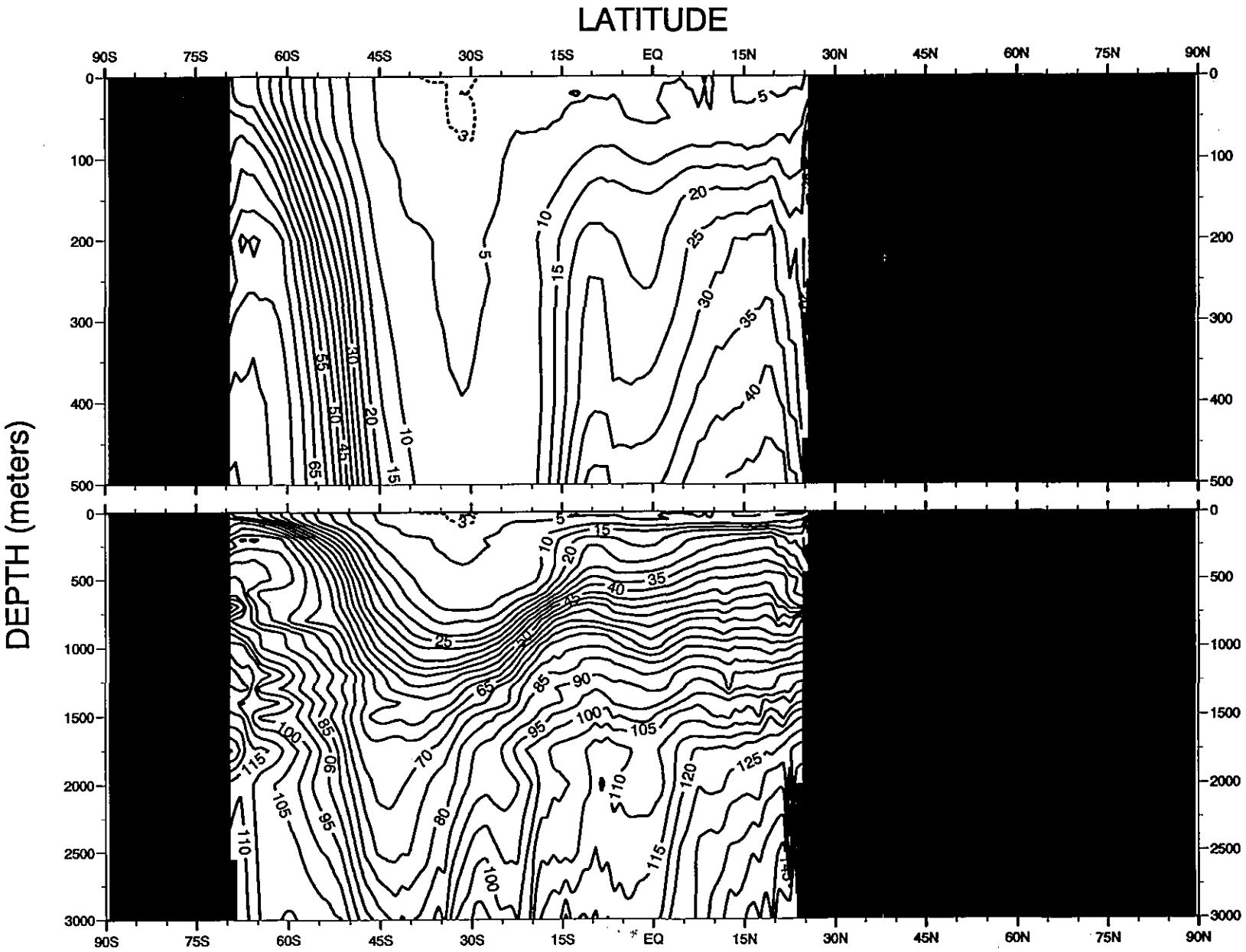

Fig K4. Annual Indian zonal average (by one-degree squares) of silicate (μM)

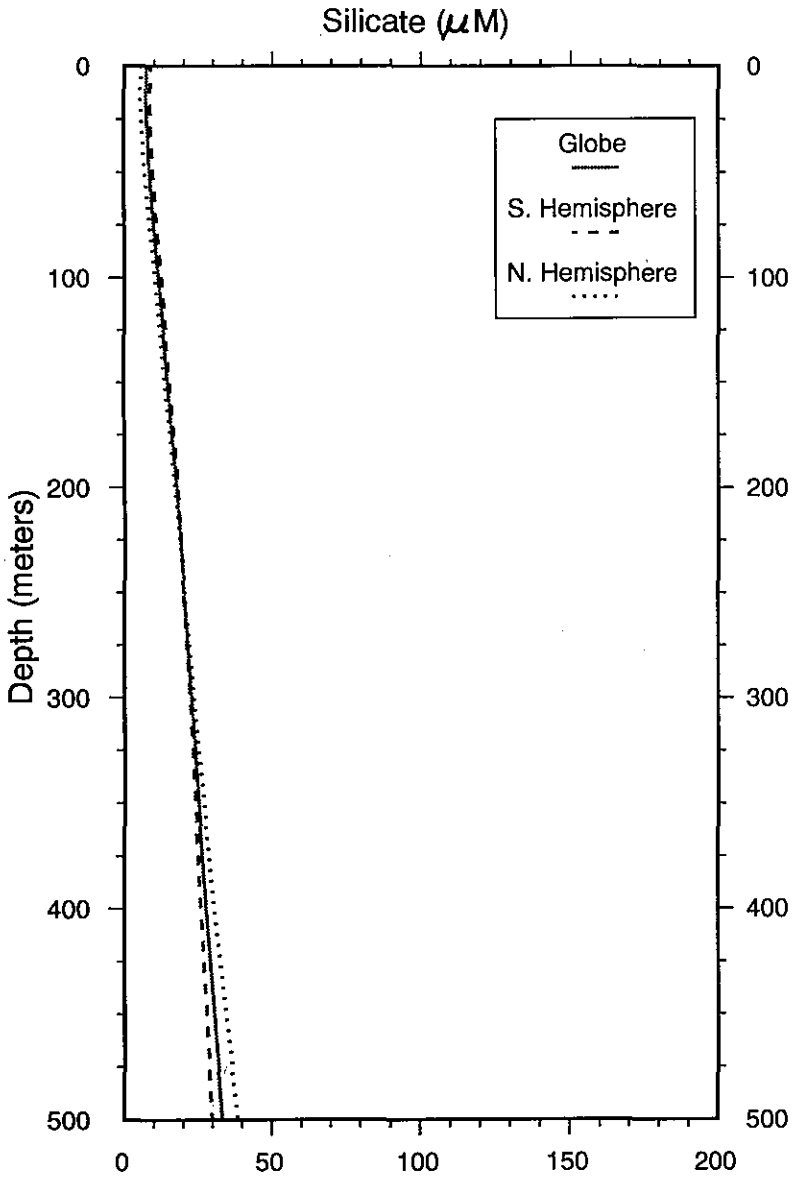

Figure L1a. Annual global silicate (μM) basin means (0-500 m)

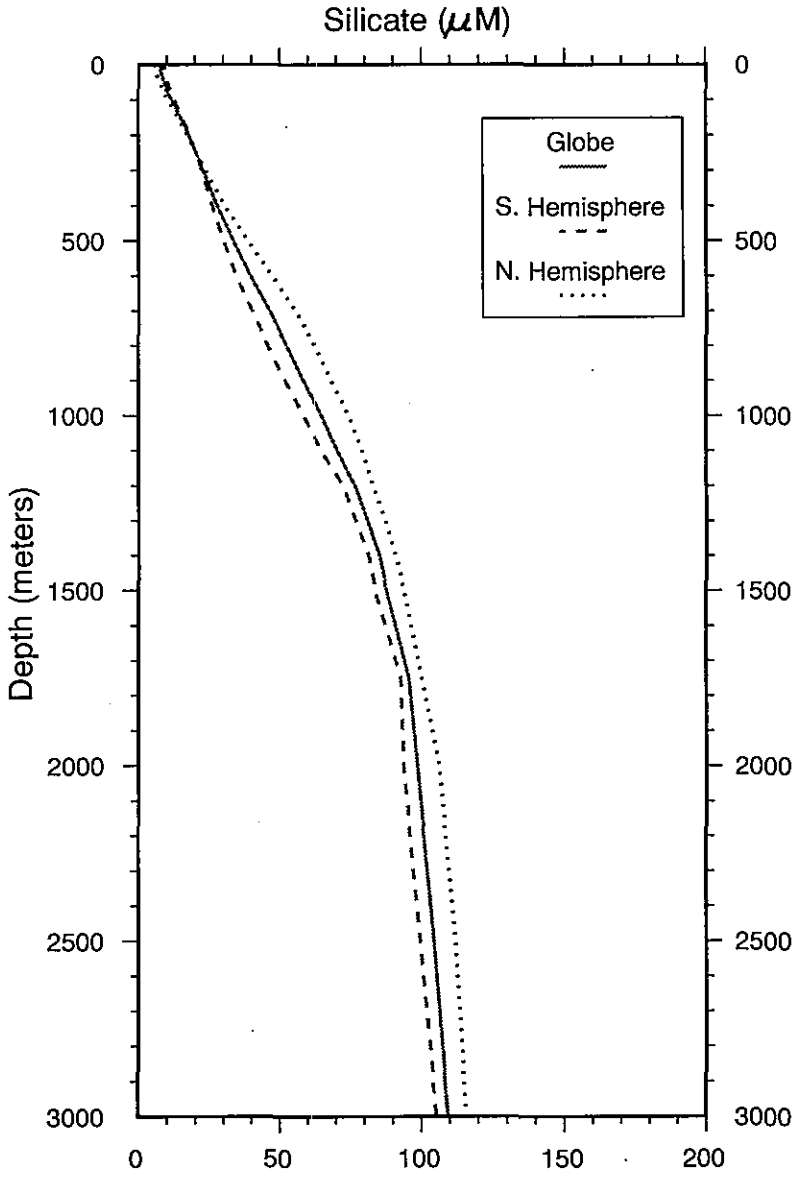

Figure L1b. Annual global silicate (μM) basin means (0-3000 m)

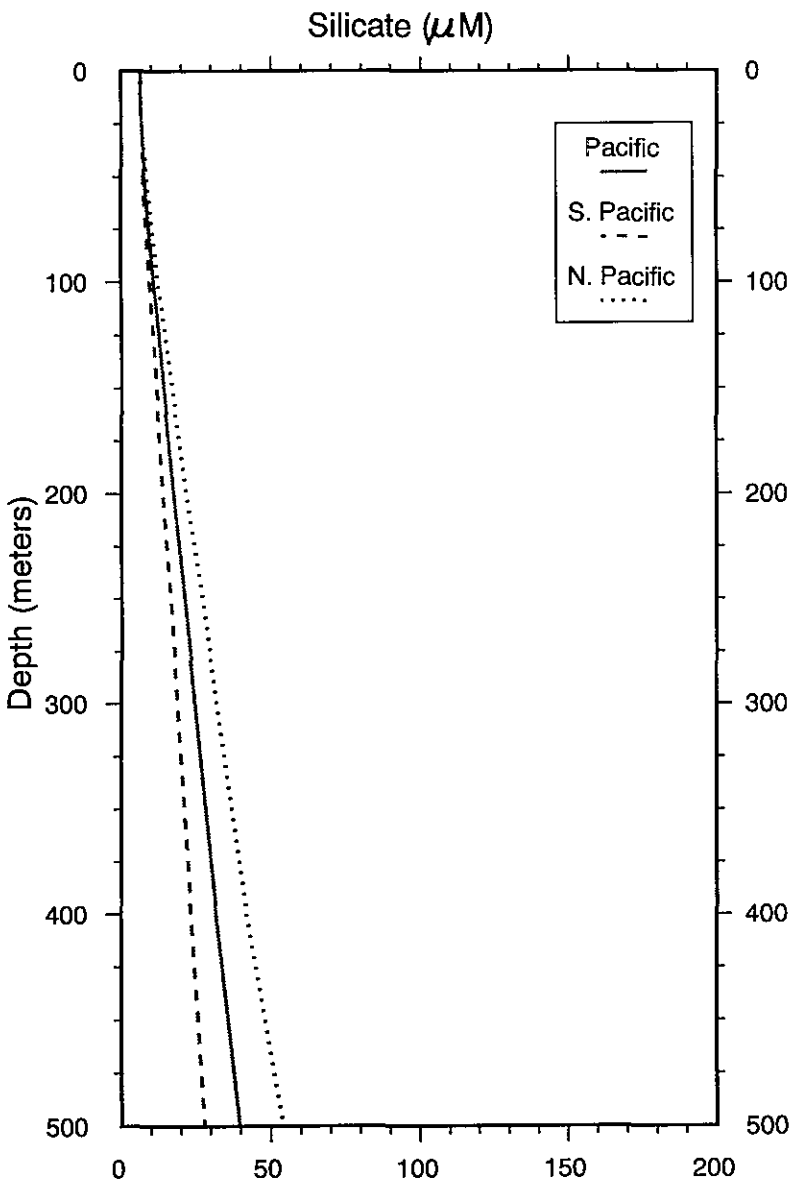

Figure L2a. Annual Pacific silicate (μM) basin means (0-500 m)

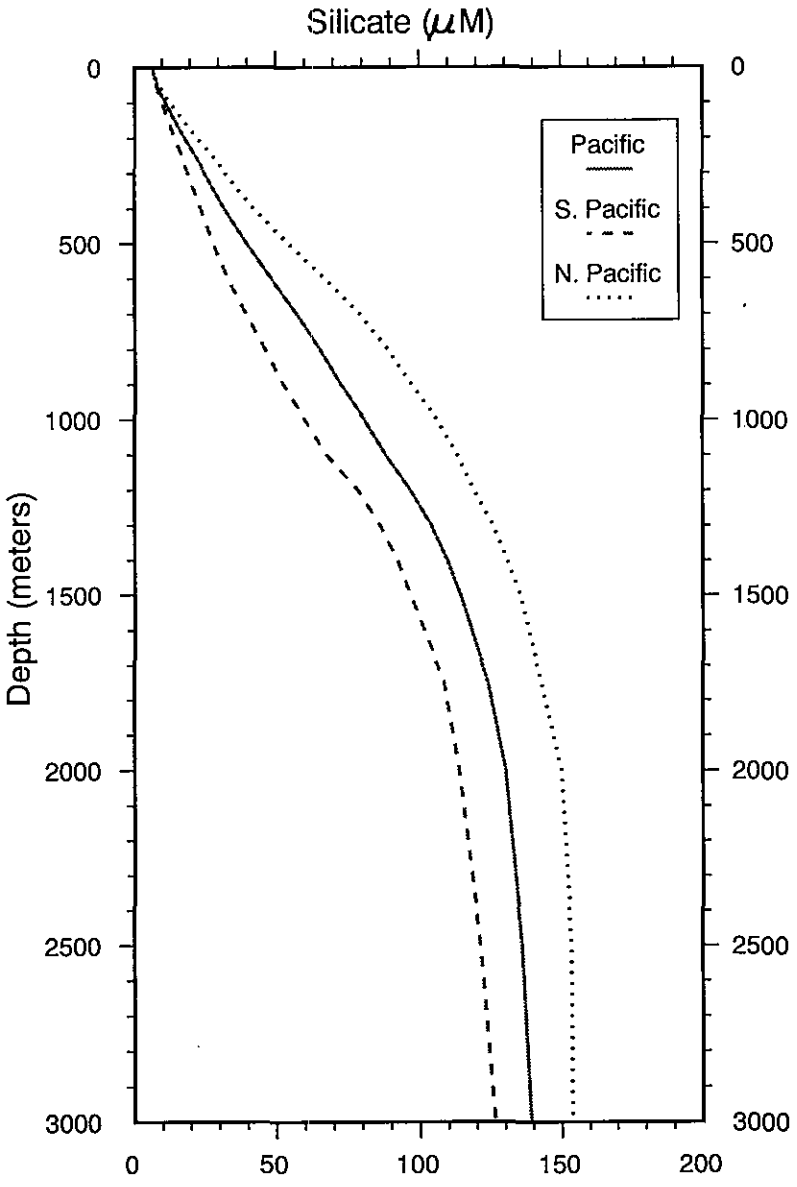

Figure L2b. Annual Pacific silicate (μM) basin means (0-3000 m)

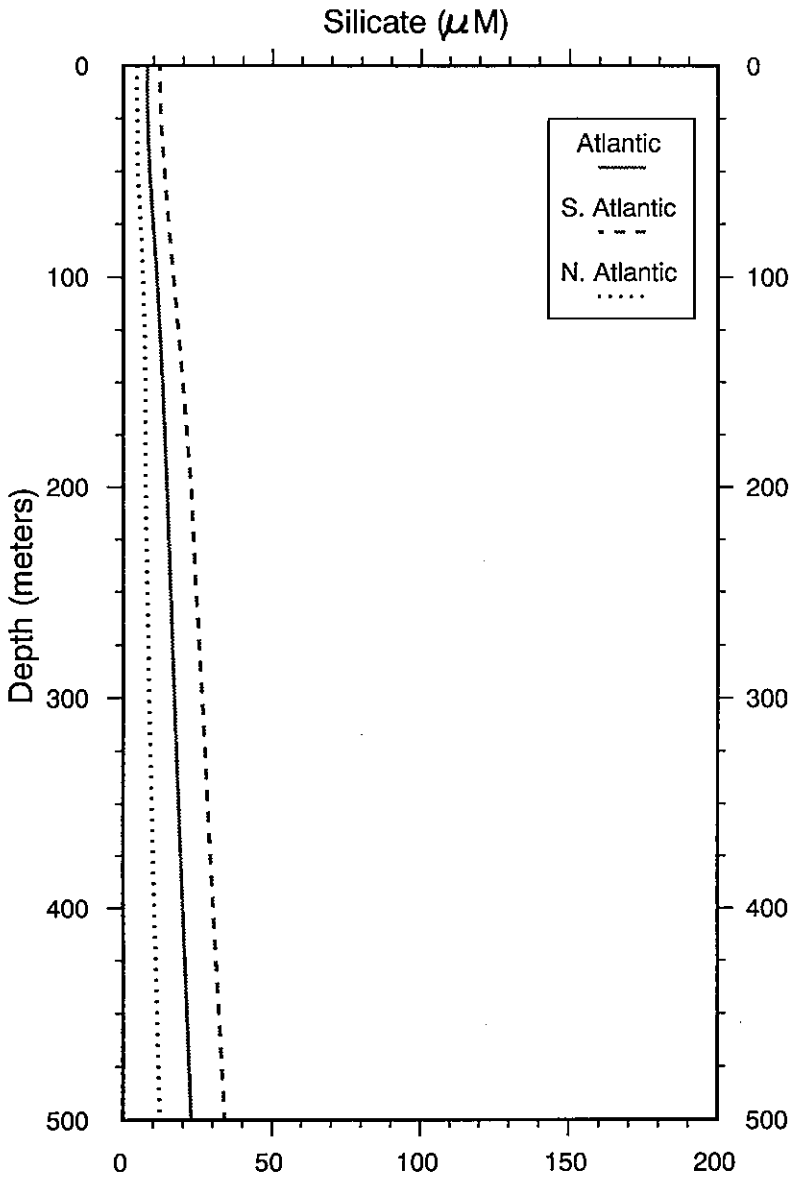

Figure L3a. Annual Atlantic silicate (μM) basin means (0-500 m)

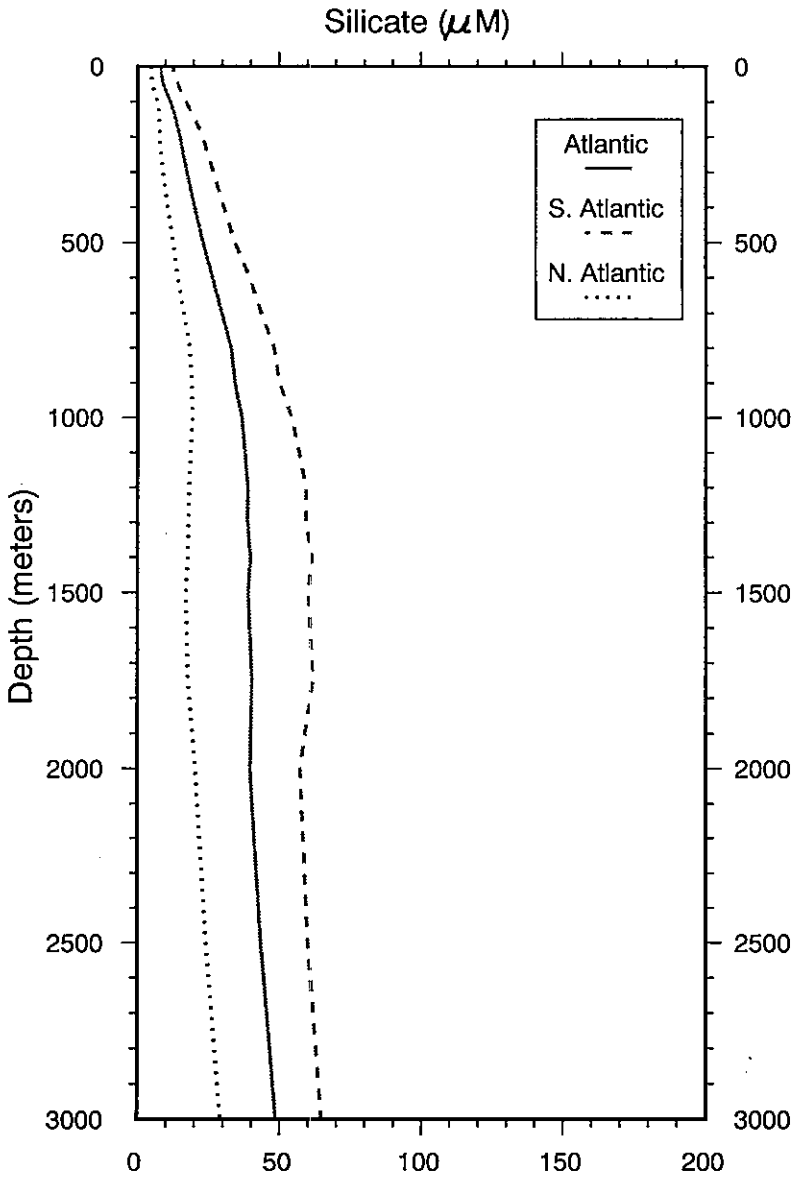

Figure L3b. Annual Atlantic silicate (μM) basin means (0-3000 m)

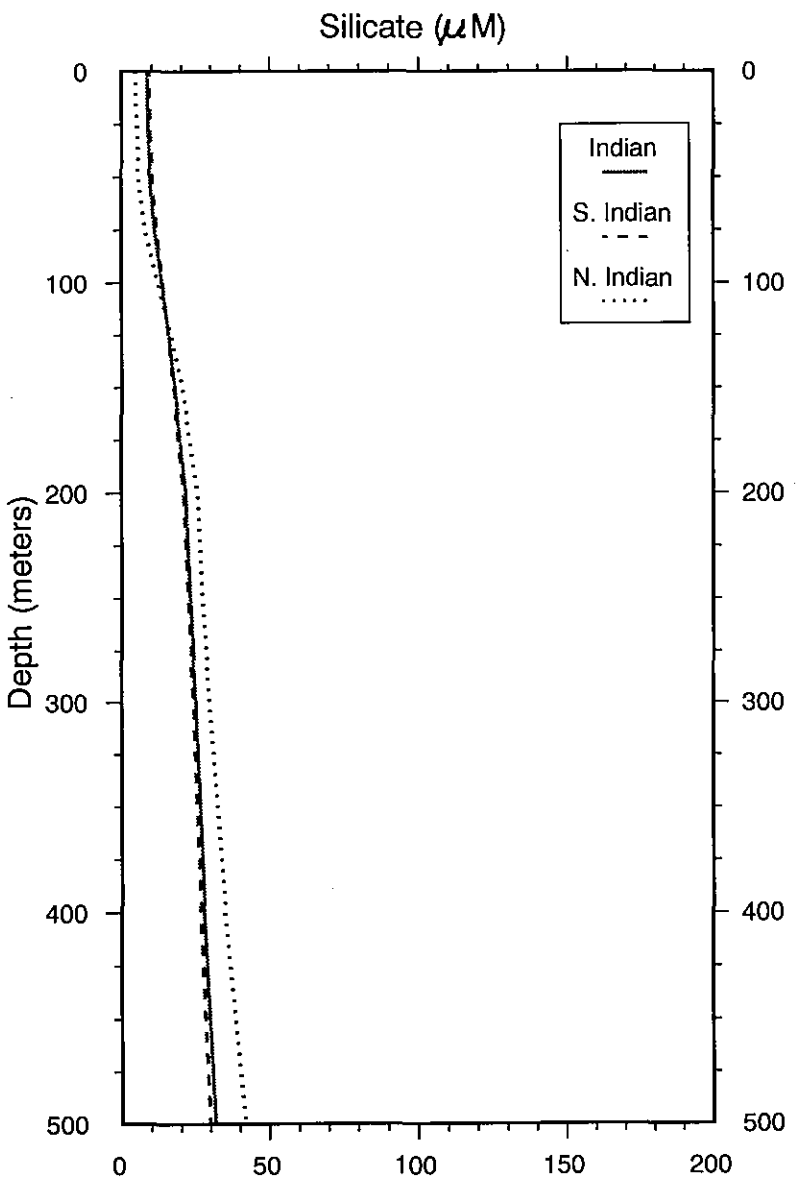

Figure L4a. Annual Indian silicate (μM) basin means (0-500 m)

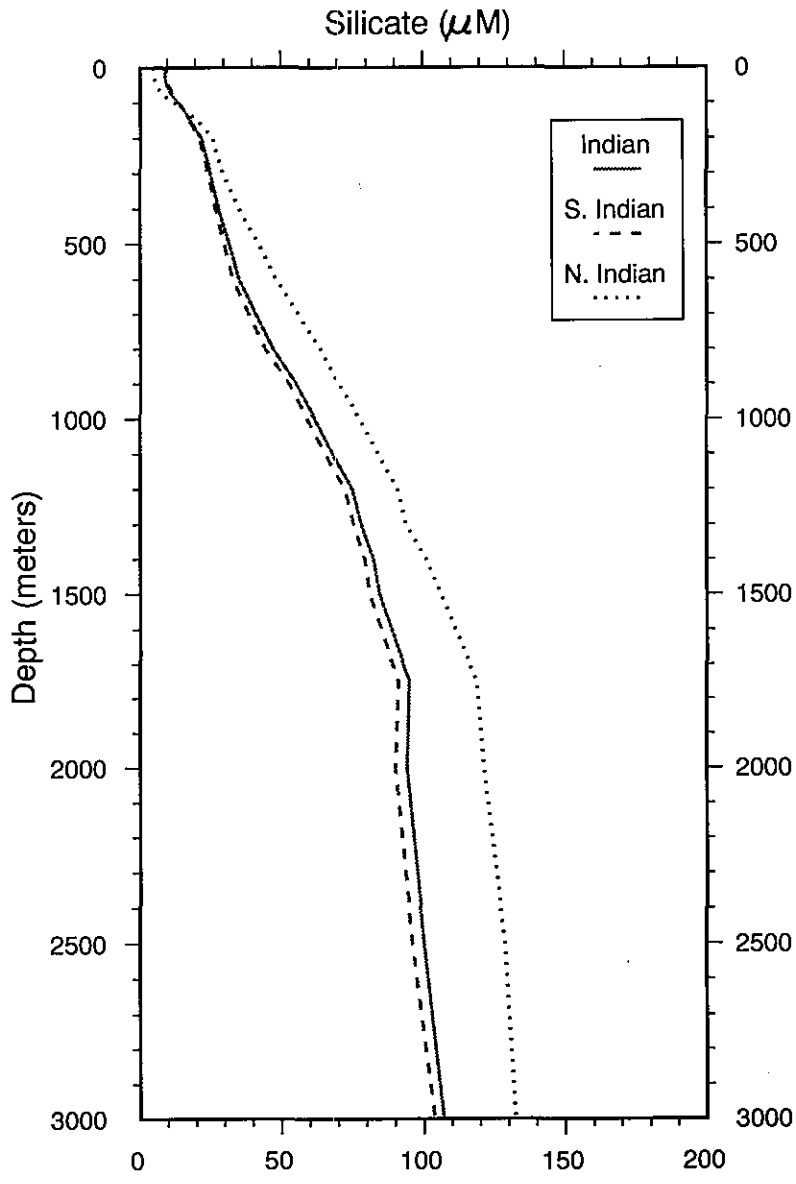

Figure L4b. Annual Indian silicate (μM) basin means (0-3000 m)

Table L1a. Annual silicate (μM) basin means and standard errors for the world ocean and Pacific Ocean as a function of depth

		World Ocean		Southern Hemisphere Ocean		Northern Hemisphere Ocean		Pacific Ocean		South Pacific Ocean		North Pacific Ocean	
Standard Level	Depth	Mean	Standard Error	Mean	Standard Error	Mean	Standard Error	Mean	Standard Error	Mean	Standard Error	Mean	Standard Error
1	0	7.5	0.6	8.7	1.0	5.7	0.4	6.6	0.7	6.6	1.1	6.6	0.7
2	10	7.4	0.6	8.8	1.0	5.6	0.4	6.6	0.7	6.7	1.1	6.5	0.7
3	20	7.6	0.6	8.9	1.0	5.8	0.5	6.8	0.7	6.8	1.2	6.8	0.7
4	30	7.8	0.6	9.1	1.0	6.1	0.5	7.1	0.7	7.0	1.2	7.2	0.8
5	50	8.6	0.7	9.8	1.1	7.0	0.6	8.1	0.9	7.6	1.3	8.7	1.0
6	75	10.0	0.7	11.0	1.2	8.5	0.7	9.4	0.9	8.5	1.4	10.5	1.1
7	100	11.6	0.8	12.5	1.3	10.3	0.8	10.9	1.0	9.5	1.5	12.5	1.3
8	125	13.2	0.9	14.0	1.3	12.1	0.9	12.6	1.1	10.8	1.7	14.8	1.4
9	150	14.7	0.9	15.3	1.4	13.8	1.0	14.2	1.2	11.8	1.8	17.2	1.5
10	200	17.7	1.0	18.1	1.6	17.1	1.1	17.6	1.3	14.0	1.9	22.0	1.6
11	250	20.3	1.1	20.1	1.6	20.4	1.3	21.4	1.4	16.6	2.1	27.3	1.7
12	300	22.8	1.2	22.2	1.7	23.6	1.4	24.9	1.5	19.0	2.1	32.1	1.8
13	400	27.7	1.3	25.9	1.8	30.4	1.7	31.8	1.7	23.5	2.2	42.0	2.0
14	500	33.4	1.4	29.8	1.8	38.6	2.1	39.7	1.9	27.9	2.3	54.2	2.2
15	600	39.4	1.5	34.3	1.8	47.1	2.5	48.3	2.1	33.0	2.3	67.0	2.2
16	700	46.1	1.6	39.9	1.8	55.5	2.8	57.1	2.2	39.3	2.4	78.9	2.2
17	800	52.5	1.7	45.8	1.8	62.6	3.2	65.2	2.4	45.9	2.5	88.7	2.2
18	900	58.3	1.8	51.8	1.8	68.2	3.4	72.4	2.3	52.4	2.4	96.9	2.0
19	1000	64.7	1.9	58.4	1.7	74.4	3.8	80.7	2.4	60.0	2.3	105.9	2.1
20	1100	70.2	2.0	64.5	1.7	78.9	4.1	88.1	2.3	67.7	2.2	113.2	2.0
21	1200	76.5	2.0	72.3	1.7	82.9	4.3	96.7	2.2	78.5	2.1	118.9	2.1
22	1300	80.9	2.1	76.8	1.7	87.2	4.6	103.9	2.1	86.0	2.1	125.7	1.9
23	1400	85.0	2.2	81.3	1.8	90.7	4.8	109.5	2.0	92.2	1.9	130.6	2.0
24	1500	87.7	2.3	83.6	1.9	93.9	5.1	114.1	2.1	96.6	1.9	135.3	2.2
25	1750	95.5	2.4	92.6	2.1	100.0	5.3	123.9	1.8	108.3	1.6	142.8	1.8
26	2000	98.5	2.6	93.6	2.2	106.2	5.6	130.1	1.9	113.7	1.8	149.9	1.8
27	2500	104.3	2.6	99.5	2.4	111.8	5.6	135.9	1.8	121.2	1.7	153.4	1.6
28	3000	109.3	2.6	105.3	2.4	115.7	5.6	139.1	1.6	126.4	1.7	153.7	1.5

Table L1b. Annual silicate (μM) basin means and standard errors for the Atlantic Ocean and Indian Ocean as a function of depth

		Atlantic Ocean		South Atlantic Ocean		North Atlantic Ocean		Indian Ocean		South Indian Ocean		North Indian Ocean	
Standard Level	Depth	Mean	Standard Error	Mean	Standard Error	Mean	Standard Error	Mean	Standard Error	Mean	Standard Error	Mean	Standard Error
1	0	8.1	1.3	12.4	2.8	4.7	0.5	8.6	1.2	9.3	1.4	4.7	0.5
2	10	8.0	1.3	12.3	2.8	4.5	0.5	8.7	1.2	9.4	1.4	4.8	0.5
3	20	8.1	1.4	12.5	2.9	4.6	0.6	8.8	1.2	9.5	1.5	5.0	0.6
4	30	8.3	1.4	12.7	2.9	4.7	0.6	9.0	1.3	9.7	1.5	5.2	0.6
5	50	8.8	1.5	13.8	3.2	4.8	0.5	9.5	1.4	10.2	1.6	5.7	0.8
6	75	10.1	1.6	15.2	3.4	5.8	0.6	11.2	1.5	11.8	1.8	7.9	0.8
7	100	11.3	1.8	16.8	3.6	6.7	0.8	13.6	1.7	13.9	2.0	12.2	1.2
8	125	12.3	1.9	18.3	3.8	7.1	0.9	15.8	1.8	15.7	2.2	16.6	1.4
9	150	13.2	2.0	19.9	4.0	7.4	0.9	17.9	2.0	17.4	2.3	20.4	1.4
10	200	14.7	2.2	22.7	4.4	7.5	0.7	21.6	2.3	20.9	2.7	25.7	1.6
11	250	15.9	2.3	24.5	4.4	8.1	0.7	23.2	2.4	22.4	2.8	27.2	1.8
12	300	17.2	2.4	26.4	4.6	8.7	0.7	25.0	2.5	24.2	2.9	29.6	1.9
13	400	19.9	2.5	30.1	4.6	10.3	0.8	28.0	2.7	26.8	3.1	35.0	1.9
14	500	22.9	2.6	34.1	4.6	12.3	0.9	31.7	2.8	29.9	3.2	41.9	2.0
15	600	26.2	2.7	39.3	4.7	13.9	1.1	35.1	2.7	32.9	3.1	48.1	1.6
16	700	29.4	2.7	43.3	4.6	16.2	1.1	41.0	2.7	38.5	3.1	55.6	1.6
17	800	32.8	2.8	47.8	4.5	18.1	1.2	46.9	2.6	44.1	2.9	63.6	1.6
18	900	34.1	2.7	49.8	4.2	18.9	1.2	55.0	2.8	52.5	3.2	70.1	1.9
19	1000	36.6	2.9	54.1	4.2	19.1	1.2	61.8	2.6	59.1	2.9	77.6	2.0
20	1100	37.6	3.0	56.7	4.3	18.6	1.1	68.1	2.6	65.5	2.9	84.1	1.7
21	1200	38.7	3.2	59.2	4.5	18.1	1.0	74.9	2.4	72.4	2.6	90.7	1.8
22	1300	38.7	3.2	59.1	4.5	17.9	1.0	78.0	2.2	75.4	2.4	93.9	2.0
23	1400	39.6	3.5	61.2	4.9	17.6	1.0	82.3	2.2	79.3	2.3	100.9	2.2
24	1500	38.8	3.4	60.1	4.9	16.9	1.0	84.4	2.2	81.0	2.3	106.1	1.7
25	1750	40.1	3.7	61.5	5.3	17.6	1.0	95.1	2.4	91.3	2.4	118.8	2.2
26	2000	39.5	3.3	57.0	4.9	20.2	1.1	94.1	2.3	90.1	2.1	121.3	3.9
27	2500	43.3	3.4	59.8	4.8	24.0	1.2	100.1	2.5	96.1	2.3	128.7	4.2
28	3000	48.6	3.5	64.6	5.0	28.9	1.3	107.1	2.4	103.8	2.3	132.4	4.3

Table M1. Area, volume, and percent volume contribution of each standard level to total basin volume mean, for the world ocean as a function of depth

Standard Level	Depth (m)	World Ocean			Southern Hemisphere Ocean			Northern Hemisphere Ocean		
		Area (10^4km^2)	Volume (10^4km^3)	% Volume	Area (10^4km^2)	Volume (10^4km^3)	% Volume	Area (10^4km^2)	Volume (10^4km^3)	% Volume
1	0	35013	175	0.14	20176	101	0.13	14837	74	0.14
2	10	34934	349	0.27	20149	201	0.26	14786	148	0.28
3	20	34854	349	0.27	20121	201	0.26	14733	147	0.28
4	30	34765	521	0.40	20102	302	0.39	14663	220	0.42
5	50	34354	773	0.60	19967	449	0.58	14386	324	0.62
6	75	34162	854	0.66	19928	498	0.65	14234	356	0.68
7	100	33735	843	0.65	19799	495	0.64	13936	348	0.67
8	125	33665	842	0.65	19790	495	0.64	13875	347	0.67
9	150	33496	1256	0.97	19757	741	0.96	13738	515	0.99
10	200	33182	1659	1.28	19690	985	1.28	13491	675	1.30
11	250	33104	1655	1.28	19677	984	1.28	13427	671	1.29
12	300	32879	2466	1.91	19612	1471	1.91	13267	995	1.91
13	400	32692	3269	2.53	19545	1955	2.53	13147	1315	2.52
14	500	32418	3242	2.51	19409	1941	2.52	13009	1301	2.50
15	600	32267	3227	2.50	19346	1935	2.51	12920	1292	2.48
16	700	32114	3211	2.49	19287	1929	2.50	12826	1283	2.46
17	800	31910	3191	2.47	19197	1920	2.49	12714	1271	2.44
18	900	31803	3180	2.46	19143	1914	2.48	12661	1266	2.43
19	1000	31494	3149	2.44	19008	1901	2.46	12486	1249	2.40
20	1100	31390	3139	2.43	18966	1897	2.46	12424	1242	2.39
21	1200	31203	3120	2.41	18882	1888	2.45	12322	1232	2.37
22	1300	31067	3107	2.40	18824	1882	2.44	12243	1224	2.35
23	1400	30981	3098	2.40	18778	1878	2.43	12203	1220	2.34
24	1500	30721	5376	4.16	18644	3263	4.23	12076	2113	4.06
25	1750	30438	7610	5.89	18498	4624	5.99	11941	2985	5.73
26	2000	29694	11135	8.62	18142	6803	8.82	11552	4332	8.32
27	2500	28546	14273	11.05	17547	8773	11.37	10999	5500	10.56
28	3000	26476	13238	10.24	16290	8145	10.56	10186	5093	9.78
29	3500	23056	11528	8.92	14019	7009	9.09	9037	4518	8.68
30	4000	18419	9209	7.13	10854	5427	7.03	7565	3783	7.26
31	4500	12569	6285	4.86	6850	3425	4.44	5719	2859	5.49
32	5000	6828	3414	2.64	3172	1586	2.06	3657	1828	3.51
33	5500	1911	478	0.37	506	126	0.16	1406	351	0.67

Table M2. Area, volume, and percent volume contribution of each standard level to total basin volume mean, for the Pacific Ocean as a function of depth

Standard Level	Depth (m)	Pacific Ocean			South Pacific Ocean			North Pacific Ocean		
		Area (10^4km^2)	Volume (10^4km^3)	% Volume	Area (10^4km^2)	Volume (10^4km^3)	% Volume	Area (10^4km^2)	Volume (10^4km^3)	% Volume
1	0	17388	87	0.13	9459	47	0.13	7929	40	0.12
2	10	17346	173	0.26	9438	94	0.27	7908	79	0.24
3	20	17306	173	0.25	9417	94	0.27	7889	79	0.24
4	30	17248	259	0.38	9400	141	0.40	7847	118	0.36
5	50	17101	385	0.57	9339	210	0.59	7762	175	0.54
6	75	16994	425	0.62	9309	233	0.66	7685	192	0.59
7	100	16879	422	0.62	9277	232	0.65	7602	190	0.58
8	125	16866	422	0.62	9274	232	0.65	7591	190	0.58
9	150	16861	632	0.93	9273	348	0.98	7588	285	0.88
10	200	16794	840	1.24	9249	462	1.30	7544	377	1.16
11	250	16779	839	1.23	9245	462	1.30	7534	377	1.16
12	300	16718	1254	1.84	9218	691	1.95	7500	562	1.73
13	400	16666	1667	2.45	9193	919	2.59	7473	747	2.30
14	500	16570	1657	2.44	9133	913	2.57	7436	744	2.29
15	600	16518	1652	2.43	9098	910	2.56	7420	742	2.28
16	700	16452	1645	2.42	9060	906	2.55	7392	739	2.27
17	800	16360	1636	2.41	9008	901	2.54	7353	735	2.26
18	900	16309	1631	2.40	8969	897	2.53	7339	734	2.26
19	1000	16182	1618	2.38	8893	889	2.51	7289	729	2.24
20	1100	16125	1613	2.37	8867	887	2.50	7258	726	2.23
21	1200	16054	1605	2.36	8824	882	2.49	7230	723	2.22
22	1300	15996	1600	2.35	8790	879	2.48	7206	721	2.22
23	1400	15955	1596	2.35	8763	876	2.47	7193	719	2.21
24	1500	15858	2775	4.08	8699	1522	4.29	7159	1253	3.85
25	1750	15730	3933	5.78	8612	2153	6.07	7119	1780	5.47
26	2000	15407	5778	8.50	8409	3153	8.89	6998	2624	8.07
27	2500	14976	7488	11.01	8130	4065	11.46	6846	3423	10.53
28	3000	14075	7037	10.35	7534	3767	10.62	6540	3270	10.06
29	3500	12476	6238	9.18	6471	3236	9.12	6005	3002	9.23
30	4000	10069	5034	7.41	4793	2397	6.76	5276	2638	8.11
31	4500	7035	3517	5.17	2813	1406	3.96	4222	2111	6.49
32	5000	4073	2036	3.00	1246	623	1.76	2827	1413	4.35
33	5500	1277	319	0.47	173	43	0.12	1104	276	0.85

Table M3. Area, volume, and percent volume contribution of each standard level to total basin volume mean, for the Atlantic Ocean as a function of depth

		Atlantic Ocean			South Atlantic Ocean			North Atlantic Ocean		
Standard Level	Depth (m)	Area (10^4km^2)	Volume (10^4km^3)	% Volume	Area (10^4km^2)	Volume (10^4km^3)	% Volume	Area (10^4km^2)	Volume (10^4km^3)	% Volume
1	0	10212	51	0.15	4489	22	0.13	5723	29	0.18
2	10	10180	102	0.30	4486	45	0.26	5694	57	0.35
3	20	10152	102	0.30	4486	45	0.26	5667	57	0.35
4	30	10125	152	0.45	4484	67	0.38	5642	85	0.52
5	50	9934	224	0.66	4447	100	0.57	5487	123	0.76
6	75	9858	246	0.73	4443	111	0.63	5415	135	0.84
7	100	9624	241	0.71	4394	110	0.63	5230	131	0.81
8	125	9569	239	0.71	4389	110	0.62	5180	130	0.80
9	150	9415	353	1.05	4361	164	0.93	5054	190	1.17
10	200	9206	460	1.36	4342	217	1.24	4864	243	1.50
11	250	9145	457	1.35	4335	217	1.23	4811	241	1.49
12	300	9012	676	2.00	4319	324	1.84	4693	352	2.17
13	400	8895	890	2.64	4293	429	2.44	4602	460	2.84
14	500	8802	880	2.61	4266	427	2.43	4536	454	2.80
15	600	8724	872	2.58	4253	425	2.42	4470	447	2.76
16	700	8655	866	2.56	4240	424	2.41	4415	441	2.73
17	800	8563	856	2.54	4213	421	2.40	4350	435	2.69
18	900	8521	852	2.52	4206	421	2.39	4315	431	2.67
19	1000	8414	841	2.49	4193	419	2.39	4221	422	2.61
20	1100	8378	838	2.48	4184	418	2.38	4194	419	2.59
21	1200	8297	830	2.46	4160	416	2.37	4136	414	2.56
22	1300	8237	824	2.44	4151	415	2.36	4085	409	2.52
23	1400	8207	821	2.43	4148	415	2.36	4059	406	2.51
24	1500	8127	1422	4.21	4131	723	4.11	3996	699	4.32
25	1750	8020	2005	5.94	4109	1027	5.85	3911	978	6.04
26	2000	7766	2912	8.63	4064	1524	8.67	3702	1388	8.58
27	2500	7348	3674	10.88	3961	1981	11.27	3386	1693	10.46
28	3000	6693	3347	9.91	3707	1853	10.55	2986	1493	9.22
29	3500	5793	2897	8.58	3263	1632	9.29	2530	1265	7.81
30	4000	4592	2296	6.80	2627	1314	7.48	1965	983	6.07
31	4500	3182	1591	4.71	1787	894	5.09	1395	697	4.31
32	5000	1688	844	2.50	877	438	2.50	812	406	2.51
33	5500	386	96	0.29	84	21	0.12	301	75	0.47

Table M4. Area, volume, and percent volume contribution of each standard level to total basin volume mean, for the Indian Ocean as a function of depth

		Indian Ocean			South Indian Ocean			North Indian Ocean		
Standard Level	Depth (m)	Area (10^4km^2)	Volume (10^4km^3)	% Volume	Area (10^4km^2)	Volume (10^4km^3)	% Volume	Area (10^4km^2)	Volume (10^4km^3)	% Volume
1	0	7411	37	0.13	6240	31	0.13	1171	6	0.17
2	10	7409	74	0.27	6240	62	0.26	1169	12	0.35
3	20	7402	74	0.27	6235	62	0.26	1167	12	0.35
4	30	7398	111	0.40	6235	94	0.39	1164	17	0.52
5	50	7332	165	0.60	6198	139	0.58	1134	26	0.75
6	75	7325	183	0.67	6193	155	0.64	1131	28	0.84
7	100	7249	181	0.66	6145	154	0.64	1104	28	0.82
8	125	7247	181	0.66	6143	154	0.64	1104	28	0.82
9	150	7236	271	0.99	6140	230	0.95	1097	41	1.22
10	200	7198	360	1.31	6115	306	1.27	1083	54	1.60
11	250	7197	360	1.31	6114	306	1.27	1083	54	1.60
12	300	7166	537	1.95	6092	457	1.89	1074	81	2.38
13	400	7147	715	2.60	6075	608	2.52	1072	107	3.17
14	500	7063	706	2.57	6025	603	2.50	1037	104	3.07
15	600	7041	704	2.56	6011	601	2.49	1030	103	3.05
16	700	7022	702	2.55	6002	600	2.49	1020	102	3.02
17	800	7002	700	2.54	5991	599	2.48	1011	101	2.99
18	900	6989	699	2.54	5983	598	2.48	1006	101	2.98
19	1000	6912	691	2.51	5935	593	2.46	977	98	2.89
20	1100	6900	690	2.51	5928	593	2.46	972	97	2.88
21	1200	6865	686	2.49	5909	591	2.45	956	96	2.83
22	1300	6846	685	2.49	5894	589	2.44	952	95	2.82
23	1400	6831	683	2.48	5880	588	2.44	951	95	2.81
24	1500	6748	1181	4.29	5827	1020	4.22	922	161	4.77
25	1750	6700	1675	6.08	5789	1447	5.99	911	228	6.74
26	2000	6533	2450	8.90	5680	2130	8.82	853	320	9.46
27	2500	6234	3117	11.32	5467	2733	11.32	767	384	11.35
28	3000	5716	2858	10.38	5058	2529	10.47	659	329	9.75
29	3500	4792	2396	8.71	4290	2145	8.88	502	251	7.43
30	4000	3760	1880	6.83	3436	1718	7.11	324	162	4.80
31	4500	2353	1176	4.27	2250	1125	4.66	103	51	1.52
32	5000	1067	534	1.94	1049	525	2.17	18	9	0.27
33	5560	249	62	0.23	249	62	0.26	0	0	0.00

Table M5a. Number of independent points (N_I) used in the standard error computation for the world ocean and Pacific Ocean.

Standard Level	Depth (m)	World Ocean N_I	Southern Hemisphere N_I	Northern Hemisphere N_I	Pacific Ocean N_I	South Pacific Ocean N_I	North Pacific Ocean N_I
1	0	361.8	208.5	153.3	179.7	97.8	81.9
2	10	361.0	208.2	152.8	179.3	97.5	81.7
3	20	360.2	207.9	152.3	178.8	97.3	81.5
4	30	359.3	207.7	151.5	178.2	97.1	81.1
5	50	355.0	206.3	148.7	176.7	96.5	80.2
6	75	353.0	205.9	147.1	175.6	96.2	79.4
7	100	348.6	204.6	144.0	174.4	95.9	78.6
8	125	347.9	204.5	143.4	174.3	95.8	78.5
9	150	346.1	204.2	142.0	174.2	95.8	78.4
10	200	342.9	203.5	139.4	173.6	95.6	78.0
11	250	342.1	203.3	138.8	173.4	95.5	77.9
12	300	339.8	202.7	137.1	172.8	95.3	77.5
13	400	337.8	202.0	135.9	172.2	95.0	77.2
14	500	335.0	200.6	134.4	171.2	94.4	76.8
15	600	333.5	199.9	133.5	170.7	94.0	76.7
16	700	331.9	199.3	132.6	170.0	93.6	76.4
17	800	329.8	198.4	131.4	169.1	93.1	76.0
18	900	328.7	197.8	130.8	168.5	92.7	75.8
19	1000	325.5	196.4	129.0	167.2	91.9	75.3
20	1100	324.4	196.0	128.4	166.6	91.6	75.0
21	1200	322.5	195.1	127.3	165.9	91.2	74.7
22	1300	321.1	194.5	126.5	165.3	90.8	74.5
23	1400	320.2	194.1	126.1	164.9	90.6	74.3
24	1500	317.5	192.7	124.8	163.9	89.9	74.0
25	1750	314.6	191.2	123.4	162.6	89.0	73.6
26	2000	306.9	187.5	119.4	159.2	86.9	72.3
27	2500	295.0	181.3	113.7	154.8	84.0	70.7
28	3000	273.6	168.3	105.3	145.5	77.9	67.6
29	3500	238.3	144.9	93.4	128.9	66.9	62.1
30	4000	190.3	112.2	78.2	104.1	49.5	54.5
31	4500	129.9	70.8	59.1	72.7	29.1	43.6
32	5000	70.6	32.8	37.8	42.1	12.9	29.2
33	5500	19.8	5.2	14.5	13.2	1.8	11.4

Table M5b. Number of independent points (N_I) used in the standard error computation for the Atlantic Ocean and Indian Ocean.

Standard Level	Depth (m)	Atlantic Ocean N_I	South Atlantic Ocean N_I	North Atlantic Ocean N_I	Indian Ocean N_I	South Indian Ocean N_I	North Indian Ocean N_I
1	0	105.5	46.4	59.1	76.6	64.5	12.1
2	10	105.2	46.4	58.8	76.6	64.5	12.1
3	20	104.9	46.4	58.6	76.5	64.4	12.1
4	30	104.6	46.3	58.3	76.5	64.4	12.0
5	50	102.7	46.0	56.7	75.8	64.1	11.7
6	75	101.9	45.9	56.0	75.7	64.0	11.7
7	100	99.5	45.4	54.1	74.9	63.5	11.4
8	125	98.9	45.4	53.5	74.9	63.5	11.4
9	150	97.3	45.1	52.2	74.8	63.4	11.3
10	200	95.1	44.9	50.3	74.4	63.2	11.2
11	250	94.5	44.8	49.7	74.4	63.2	11.2
12	300	93.1	44.6	48.5	74.1	63.0	11.1
13	400	91.9	44.4	47.6	73.9	62.8	11.1
14	500	91.0	44.1	46.9	73.0	62.3	10.7
15	600	90.2	44.0	46.2	72.8	62.1	10.6
16	700	89.4	43.8	45.6	72.6	62.0	10.5
17	800	88.5	43.5	45.0	72.4	61.9	10.4
18	900	88.1	43.5	44.6	72.2	61.8	10.4
19	1000	86.9	43.3	43.6	71.4	61.3	10.1
20	1100	86.6	43.2	43.3	71.3	61.3	10.0
21	1200	85.7	43.0	42.7	70.9	61.1	9.9
22	1300	85.1	42.9	42.2	70.8	60.9	9.8
23	1400	84.8	42.9	41.9	70.6	60.8	9.8
24	1500	84.0	42.7	41.3	69.7	60.2	9.5
25	1750	82.9	42.5	40.4	69.2	59.8	9.4
26	2000	80.3	42.0	38.3	67.5	58.7	8.8
27	2500	75.9	40.9	35.0	64.4	56.5	7.9
28	3000	69.2	38.3	30.9	59.1	52.3	6.8
29	3500	59.9	33.7	26.1	49.5	44.3	5.2
30	4000	47.5	27.2	20.3	38.9	35.5	3.4
31	4500	32.9	18.5	14.4	24.3	23.3	1.1
32	5000	17.4	9.1	8.4	11.0	10.8	0.0
33	5500	4.0	0.9	3.1	2.6	2.6	0.0

Table M6. Volume means of phosphate, nitrate, and silicate for the major ocean basins and the volume of each basin (0-3000 m)

Basin	Volume ($10^4 km^3$)	Phosphate (μM)	Nitrate (μM)	Silicate (μM)
Globe	91690	2.07	29.22	73.0
Southern Hemisphere	55497	2.04	29.01	69.5
Northern Hemisphere	36193	2.11	29.54	78.4
Pacific	47321	2.37	33.04	93.9
South Pacific	25884	2.17	30.89	79.3
North Pacific	21436	2.61	35.63	111.6
Atlantic	24358	1.51	22.83	34.3
South Atlantic	12344	1.86	27.29	50.8
North Atlantic	12014	1.14	18.24	17.4
Indian	20049	2.04	27.95	70.8
South Indian	17308	1.97	27.41	68.3
North Indian	2741	2.45	31.40	86.4